

**Development of agarose gel electrophoresis as a novel method
to monitor lignin degradation**

Christopher A. Holt

Submitted in accordance with the requirements for the degree of Doctor of
Philosophy

The University of Leeds
School of Chemical and Process Engineering

November 2019

The candidate confirms that the work submitted is his own and that appropriate credit has been given where reference has been made to the work of others.

This copy has been supplied on the understanding that it is copyright material and that no quotation from the thesis may be published without proper acknowledgement.

The right of Christopher A. Holt to be identified as Author of this work has been asserted by him in accordance with the Copyright, Designs and Patents Act 1988.

© 2019 The University of Leeds and Christopher A. Holt

Acknowledgements

I would firstly like to thank ESPRC for funding the project through the Bioenergy CDT. I would also like to thank Biome Bioplastics for co-funding the project. I would especially like to thank Prof. John Blacker his supervision, and for always making time for me during the PhD. Special thanks to Krisztina Kovacs-Schreiner for all the help with the project. Additionally, thanks to everyone involved in the LIGPoly project. I would like to thank Prof. Stéphanie Baumberger and everyone at INRA Versailles for the fantastic placement, and Prof. Tim Bugg for facilitating it. I would like to thank everyone involved with the Bioenergy CDT, especially Emily Bryan-Kinns, James McKay and Prof. Jenny Jones. Thanks to Iram Razaq for help with the pyrolysis-GC/MS work, Aaron Brown for help with the HTC work and Dr Andy Ross for allowing use of the equipment. I would also like to thank everyone past and present part of iPRD, especially Ahmed Abdelrazak and Alvaro Cruz Izquierdo. Thanks to Prof. Bruce Turnbull and Dr Michael Webb for allowing me to carry out lab work in the School of Chemistry's biochemistry labs and everyone part of the labs for all their help during my PhD. I would like to thank my parents for all their help and support along with my sister Vicky and Danny. Special thanks to Júlia for all her support and help. Thanks to all involved in my education, in particular John Miller. Finally, thanks to everyone I have played football with during my PhD, hope to be back on the pitch soon!

Abstract

Lignin represents the sole bulk alternative source of sustainable aromatic platform chemicals that are otherwise produced by the petrochemical industry (Gillet et al., 2017). Currently there is no high-throughput analytical technique that can be used to quantify or assess the degradation of polymeric lignin. This has significantly held back research within this field, as information about polymeric lignin is crucial if a process is to be developed to efficiently valorise it. The aim of this project was to use agarose gel electrophoresis to develop a novel technique to quantify and assess changes in the structure of polymeric lignin. Another aim was to utilise agarose gel electrophoresis to assess the quantity of low molecular weight aromatic products produced by lignin degradation. Agarose gel electrophoresis has, for the first time, been shown in this study to separate effectively polymeric lignin from low molecular weight components. Electrophoretic variables such as pH, voltage, gel-type, buffer, level and edge-effects have been explored and optima determined. Migrating bands have been characterized and confirmed by multiple methods, as lignin. Band visualisation and quantification techniques have been developed to quantify and assess the polymeric fraction of a lignin sample. Purified samples of lignin have been prepared by cutting bands from the gel and extracting into solution. The method has been shown to separate Kraft, protobind and organosolv lignins corresponding to their respective molecular weight to charge (m/z) distribution, and the results were closely comparable to laborious analyses using Gel Permeation Chromatography (GPC). Electrophoresis with 1% agarose gel in sodium borate buffer at pH 8.75 was found to be highly effective in assessing the concentration and m/z distribution of polymeric lignin after biological, chemical

and hydrothermal degradation. Trace profiles of the imaged bands show possible differences in the mechanisms of degradation and indicate lignin shape as another mobility factor. High throughput methods were developed with 40 simultaneous lanes. The method was also shown to be successful in separating low molecular weight products from polymeric lignin, and therefore has the potential to be used to assess the production of platform chemicals.

Table of contents

Acknowledgements	I
Abstract	III
Table of contents	V
List of tables	IX
List of figures	X
List of abbreviations	XVII
Chapter 1	1
1.1 Introduction	1
1.1.1 Climate change and sustainability	1
1.1.2 Need for renewable aromatics.....	1
1.2 Introduction to lignocellulose	2
1.2.1 Cellulose structure and characteristics.....	3
1.2.2 Hemicellulose structure and characteristics	3
1.2.3 Lignin structure and characteristics	4
1.2.4 Overall lignocellulose structure.....	7
1.3 Sources of lignin	8
1.3.1 Crude biomass	8
1.3.2 Lignocellulosic biorefineries	9
1.3.3 Paper and pulp industries	9
1.4 Products from lignin	10
1.5 Degradation of lignin.....	11
1.5.1 Chemical degradation	11
1.5.2 Thermochemical degradation	12
1.5.3 Biological degradation.....	13
1.5.4 Bacterial production of metabolites via lignin depolymerisation 20	
1.5.5 Routes for process development in lignin valorisation.....	24
1.6 Methods to determine lignin content	26
1.7 Molecular weight determination of lignin.....	27
1.8 Research rationale, aims and objectives	29
1.8.1 Research rationale and purpose.....	29
1.8.2 Project aims.....	29

1.8.3	Project objectives.....	29
Chapter 2	31
2.1	Materials	31
2.2	General method for precipitation, acetylation and GPC	32
2.3	General method for gel electrophoresis	33
2.3.1	Gel recipe.....	33
2.3.2	Gel production method and electrophoresis sample preparation.....	33
2.3.3	Loading of gel lanes with multichannel pipette	34
2.4	ImageJ analysis method	35
2.4.1	Calculation of distance migrated	41
Chapter 3	44
3.1	Introduction.....	44
3.2	Methods and Results	47
3.2.1	Preparation of the initial TAE gel.....	47
3.2.2	Optimisation of the electrophoretic conditions.....	48
3.2.3	Effect of pH	51
3.2.4	Effect of buffer strength	55
3.2.5	Initial extraction, electrophoresis and imaging of lignin experiment	57
3.2.6	Purification of lignin from gel	59
3.2.7	GPC Analysis.....	61
3.2.8	MALDI-TOF Analysis of Lignin standards.....	65
3.2.9	¹ H NMR of gel extracted lignin	66
3.2.10	Pyrolysis GC/MS.....	68
3.3	Conclusions	79
Chapter 4	81
4.1	Introduction.....	81
4.2	Methods.....	82
4.3	Results and Discussion.....	83
4.3.1	Investigation of surfactant electrophoresis of lignin.....	83
4.3.2	Electrophoresis and imaging of lignin with different buffers ..	92
4.4	Conclusions	96
Chapter 5	97
5.1	Introduction.....	97

5.2	Methods.....	98
5.3	Results and discussion	100
5.3.1	Electrophoresis using unlevelled gels	100
5.3.2	Electrophoresis using levelled gels	106
5.3.3	Electrophoresis using levelled gels loaded using a multichannel pipette	110
5.4	Conclusions.....	113
Chapter 6.....		115
6.1	Introduction	115
6.2	Methods.....	117
6.2.1	Absorbance of lignin measurements	117
6.2.2	Fluorescence of lignin measurements.....	117
6.2.3	GPC of lignin standards	117
6.2.4	Preparation of lignin standards for gel electrophoresis.....	117
6.2.5	Gel electrophoresis of lignin standards	118
6.3	Results and Discussion	119
6.3.1	Absorbance and fluorescence measurements of lignin	119
6.3.2	Preparation of lignin standards for GPC and subsequent comparison with gel electrophoresis.	121
6.3.3	GPC of Protobind and organosolv lignin	128
6.3.4	Electrophoresis of lignin standards.....	132
6.3.5	Comparison of gel electrophoresis to GPC	136
6.4	Conclusions.....	137
Chapter 7.....		139
7.1	Introduction	139
7.2	Methods.....	141
7.2.1	Control sample - pre-degradation tests	141
7.2.2	Bacterial lignin degradation.....	141
7.2.3	Proteinase K and heat treatment of bacterially degraded lignin 142	
7.2.4	Microwave treatment of bacterially degraded lignin.....	142
7.2.5	Hydrothermal Carbonisation (HTC) degradation of lignin....	142
7.2.6	Laccase degradation of lignin	143
7.2.7	Hydrogen peroxide degradation of lignin.....	143
7.2.8	Quantification of lignin degradation	144

7.3	Results and discussion	145
7.3.1	Pre-degradation tests	145
7.3.2	<i>Pseudomonas putida</i> KT2440 degradation of lignin.....	146
7.3.3	<i>Rhodococcus jostii</i> RHA1 degradation of lignin.....	150
7.3.4	Quantification of bacterial lignin degradation.....	153
7.3.5	Quantification and analysis of hydrothermal carbonisation of lignin.....	157
7.3.6	Quantification and analysis of enzymatic degradation of lignin 162	
7.3.7	Quantification and analysis of hydrogen peroxide degradation of lignin.....	168
7.4	Conclusions	173
Chapter 8	176
8.1	Introduction.....	176
8.2	Methods.....	177
8.2.1	Samples investigated	177
8.2.2	Electrophoresis method.....	177
8.2.3	Low molecular weight product sampling and analysis	177
8.2.4	Extraction of electrophoresis eluent for NMR	178
8.3	Results and discussion	180
8.3.1	Low molecular weight product UV analysis	180
8.3.2	NMR of extracted low molecular weight products	182
8.4	Conclusions	184
Chapter 9	186
9.1	Discussion of research outcomes.....	186
9.1.1	Need for a high throughput technique to analyse lignin	186
9.1.2	Electrophoresis to analyse lignin.....	186
9.1.3	Electrophoresis to measure lignin concentration.....	188
9.1.4	Electrophoresis to assess lignin mass to charge changes..	192
9.1.5	Quantification of low molecular weight compounds from lignin degradation	193
9.2	Originality and overall impact of this work.....	194
9.3	Future research	194
9.4	Overall Conclusions	197
References	199

List of tables

Table 3-1 List of the Mn and Mw values for molecular weight for standard Alkali lignin, Alkali lignin purified from the entirety, the top half and the bottom half lignin band on the gel.	63
Table 3-2 Values for Mn and Mw for molecular weight of L6 standard and L6 extracted from the whole band on a gel.....	65
Table 3-3 List of the top 10 identified peaks from the agarose sample at the end of the pyrolysis GC/MS.....	70
Table 3-4 List of the top 10 identified peaks from the Alkali lignin standard at the end of the pyrolysis GC/MS.....	72
Table 3-5 List of the top 10 identified peaks from the gel extracted Alkali lignin sample at the end of the pyrolysis GC/MS.....	73
Table 3-6 List of the top 10 identified peaks from the L6 standard sample at the end of the pyrolysis GC/MS.....	75
Table 3-7 List of the top 10 identified peaks from the L6 precipitated sample at the end of the pyrolysis GC/MS.....	76
Table 3-8 List of the top 10 identified peaks from the gel extracted L6 sample at the end of the pyrolysis GC/MS.....	78
Table 5-1 Electrophoresis conditions and gel information.....	98
Table 6-1 Molecular weight data for precipitated and non-precipitated acetylated lignin 5 samples	124
Table 6-2 Mn and Mw values for Kraft, organosolv and protobind samples.	131

List of figures

Figure 1-1 Repeating cellobiose disaccharide unit of cellulose polymer	3
Figure 1-2 Example structure of hemicellulose polymer.....	4
Figure 1-3 The main monolignols used to synthesise lignin A= p-coumaryl alcohol, B= sinapyl alcohol and C= coniferyl alcohol.	5
Figure 1-4 Example structure of part of a lignin polymer	6
Figure 1-5: Example structure of lignocellulose. Sourced from (Brandt A et al, 2013).....	7
Figure 1-6 Diagram displaying the proposed lignin degradation paths taken by bacteria. Reproduced from (Bugg T.D.H et al, 2011). ...	20
Figure 1-7 Chemical structure of common metabolites produced from lignin degradation by microorganisms. A= vanillin, B= vanillic acid, C= protocatechuic acid, D= ferulic acid, E= p-hydroxybenzoic acid and F= p-coumaric acid (Sainsbury P. D. et al, 2013).	21
Figure 1-8 Diagram displaying the simplified lignin degradation pathway taken by <i>Sphingobium</i> sp. SYK-6 (dashed arrows represent simplified elements). Reproduced from (Bugg T.D.H et al, 2011). ..	22
Figure 1-9 β -keto adipate and genetically modified pathways in <i>Rhodococcus jostii</i> RHA1 for metabolism of lignin degradation products. Reproduced from (Mycroft Z. et al, 2015).	23
Figure 2-1 Gel wells with number above to illustrate in the order that the sets of wells were loaded 8 wells at a time (in this example) by the multichannel pipette in order to have four repeats for each sample across the whole gel. Wells of the same colour represent the same samples.....	35
Figure 2-2 Screenshot showing the rectangular selection tool	35
Figure 2-3 Screenshot of selected bands	36
Figure 2-4 Screenshot of selected bands for HTC	37
Figure 2-5 Screenshot of plotted lanes	37
Figure 2-6 Screenshot of selected wand tool.....	38
Figure 2-7 Screenshot of analyse line graph.....	38
Figure 2-8 Screenshot of plotted lane showing small gap between the peak and the end of the x axis	39
Figure 2-9 Screenshot showing how the peak is 'connected' to the end of the x axis	39
Figure 2-10 Screenshot showing the numerical values produced after ImageJ analysis	40

Figure 2-11 Example chart produced by ImageJ analysis with error bars displayed calculated using standard deviation.	40
Figure 2-12 Example of using the set scale tool to calculate the pixels to millimetre ratio.....	41
Figure 2-13 A = original graph with pixels representing distance migrated. B = graph displaying distance migrated converted into millimetres.....	42
Figure 2-14 Screenshot showing the measurement of the original band selection (A) and the distance between the gel well and the end of the original band selection	42
Figure 3-1 Initial TAE agarose gel with a lignin concentration gradient from 1.75 g/L to 0.25 g/L of L6 lignin	47
Figure 3-2 The effect of varying agarose gel concentration on lignin migration with gels run for 40 minutes: A: 1% (w/v), 120 V. B: 2% (w/v) 120 V. C: 0.5% (w/v) 120 V. D: 1% (w/v) 50V. E: 0.5% (w/v) 50 V.....	49
Figure 3-3 Comparison of Lignin L5 and L6 electrophoresis on a 1% agarose gel in: Left TAE buffer at 100 V for 10 minutes; Right, SB gel for 120 V for 10 minutes.	52
Figure 3-4 Effect of pH on TAE and SB buffer gels with lignin L5 and L6 after electrophoresis at 120 V for 10 minutes. The two samples on the left side of each gel using TAE and SB gels ran at different pHs.	53
Figure 3-5 The effect of adding hydroxide to L6 lignin (5 g/L) samples before electrophoresis.	54
Figure 3-6 Comparing the effect of buffer strength on electrophoresis. A: sodium borate buffer B: higher concentration of sodium borate buffer.....	56
Figure 3-7 Results after extraction and electrophoresis of the top half and bottom half of the gels bands. A: photograph of 100 g/L L6 lignin on a SB 0.75% agarose gel that was ran at 50 V for 40 minutes, with the top band and bottom band marked prior to extraction. B: lignin separation after extraction of the lignin from each of the gel fractions and repeating electrophoresis at 50 V for 40 minutes. C: Imaging of the gel showing emission intensity.	58
Figure 3-8 Image of an agarose gel after electrophoresis at 50 V for 40 minutes using 300 g/L Alkali lignin. With the different gel fraction that were used for purification (top section of the band, bottom section of the band and the whole band).....	60
Figure 3-9 Image of an agarose gel after electrophoresis at 50 V for 40 minutes with 200 g/L L6 lignin. The dimensions of the ‘whole band’ of L6 that was used for extraction and purification are marked.	60

Figure 3-10 Normalised GPC plot of standard Alkali lignin compared to lignin purified from gels (the entirety of the band, the top half and the bottom half of the band). Not all of the AL sample dissolved in the THF, so the plot is not representative of the entire sample. ...	62
Figure 3-11 Normalised GPC plot of the L6 lignin standard compared to the L6 extracted from the whole band on the gel.....	64
Figure 3-12 ¹ H NMR spectra of gel extracted Alkali lignin, with spectra labelled with the corresponding lignin related peaks.....	66
Figure 3-13 ¹ H NMR spectra of extracted L6 lignin, with spectra labelled with the corresponding lignin related peaks	67
Figure 3-14 2D ¹ H and ¹³ C NMR of Alkali lignin (A) and L6 (B). The signal of interest is circled for clarity. The spectra on the top of the figure corresponds to Figure 3-14 and Figure 3-15 respectively. .	68
Figure 3-15 Chromatogram of the peaks produced from pyrolysis GC/MS of agarose standard	69
Figure 3-16 Chromatogram of the peaks produced from pyrolysis GC/MS of Alkali lignin standard.....	71
Figure 3-17 Chromatogram of the peaks produced from pyrolysis GC/MS of Alkali lignin extracted post-electrophoresis (whole band).....	72
Figure 3-18 Chromatogram of the peaks produced from pyrolysis GC/MS of L6 lignin standard	74
Figure 3-19 Chromatogram of the peaks produced from pyrolysis GC/MS of acid precipitated L6 standard.....	75
Figure 3-20 Chromatogram of the peaks produced from pyrolysis GC/MS of L6 extracted post-electrophoresis (whole band).....	77
Figure 4-1 L6 Kraft lignin with either SDS, DTAB or Triton X-100 loaded onto an SB 1% agarose gel before electrophoresis at 120 V for 10 minutes.....	83
Figure 4-2 Diagram illustrating hypothesised lignin-SDS bundle. Adapted from (Rakhmatullin et al., 2016)	84
Figure 4-3 Image of a 1% agarose pH 4 TAE buffer gel after electrophoresis at 100 V for 10 minutes, with lignins L5, L6 and no-lignin, loaded with and without SDS.	86
Figure 4-4 1% agarose gel made with TAE and 0.1% SDS, without lignin, run at 100 V over 40 minutes and imaging every 10 minutes.....	88
Figure 4-5 Gel electrophoresis of DNA dyes ethidium bromide and SYBR Safe for 10 minutes at 100 V on a TAE buffer gel with and without the addition of SDS.	89
Figure 4-6 1% agarose gel made with SDS running buffer and ethidium bromide after electrophoresis at 50 V for 15 minutes (left) and 30 minutes (right).....	90

Figure 4-7 SB buffer gel with just SDS loaded 1% agarose gel with SB buffer, with SDS loaded into each of the gel lanes using an uncontaminated gel tank.	91
Figure 4-8 Gels with decreasing L5 lignin concentration gradients mixed with SDS on TAE and SDS running buffer gels.....	92
Figure 4-9 Comparison of electrophoresis with and without SDS in SB buffer, with lignin L5 and L6 at 120V for 10 minutes	94
Figure 4-10 Effect of pH on TAE and SB buffer gels.....	95
Figure 5-1 Diagram of the flexicaster used in the experiments.....	99
Figure 5-2 Electrophoresis of lignin on a large agarose gel. A: Image of gel run at 50 V for 40 minutes after loading 5 g/L L6 lignin into each lane. B: Results after ImageJ quantification of the gel bands produced in each lane, showing total intensity of the band.	100
Figure 5-3 Lignin concentration gradient on a large agarose gel.....	102
Figure 5-4 Lignin mixed with KCL buffer on a large agarose SB buffer gel.....	103
Figure 5-5 Lignin loaded from right to left (opposite to routine loading) on a large agarose gel.	104
Figure 5-6 Gel poured in a cast the opposite way round to routine.A: Image of gel that was run at 50 V for 60 minutes after loading 5 g/L L6 into each lane. B: ImageJ quantification of the gel bands produced in each lane.	105
Figure 5-7 Electrophoresis on a large agarose gel, levelled using a flexi caster.	106
Figure 5-8 Electrophoresis on a large agarose gel, levelled using a flexi caster with the lignin 'incubated' in the gel for one hour before electrophoresis.....	107
Figure 5-9 Lignin loaded and then incubated onto a large agarose gel at different time points.....	109
Figure 5-10 Electrophoresis of lignin loaded onto a large agarose gel with a multi-channel pipette.....	110
Figure 5-11 Electrophoresis of a concentration gradient of lignin loaded onto a large agarose gel with a multi-channel pipette.	111
Figure 5-12 Diagram to illustrate the possible effect of sample incubation in the agarose gel.	114
Figure 6-1 Absorption spectra of 1 g/L L6 lignin.....	119
Figure 6-2 Fluorescence intensity (counts per second) measured from 690-900 nm after exposure to 680 nm light.....	120
Figure 6-3 GPC plot of two acetylated L5 samples and a non-acetylated sample dissolved in THF.....	122

Figure 6-4 Normalised GPC plot of a lignin 5 sample precipitated prior to acetylation and two acetylated lignin 5 samples.	123
Figure 6-5 GPC plot of a L5 lignin sample precipitated prior to acetylation, two acetylated L5 lignin samples, and a non-acetylated sample dissolved in THF	124
Figure 6-6 GPC plot of two acetylated L6 lignin samples and a non-acetylated sample dissolved in THF	125
Figure 6-7 Normalised GPC plot of a L6 lignin sample precipitated prior to acetylation (with either 500 µl of concentrated HCL or 1 drop of concentrated HCL) and acetylated L6 lignin dissolved in THF ...	126
Figure 6-8 Normalised GPC plots of acid precipitated L5 and L6 lignins prior to acetylation	127
Figure 6-9 GPC of the SB buffer soluble fraction of Z4, Z5 and Z6 protobind lignins post precipitation and acetylation.....	128
Figure 6-10 GPC of the SB buffer soluble fraction of ECN A, ECN B and ECN C organosolv lignins post precipitation and acetylation. ...	129
Figure 6-11 Compiled GPC plots of the Kraft, organosolv and protobind samples.....	130
Figure 6-12 Gel with all protobind, Kraft and organosolv samples.....	132
Figure 6-13 Electrophoretic separation of protobind Z4, Z5 and Z6 lignins produced using Figure 6-12	133
Figure 6-14 Electrophoretic separation of L5, L6 and AL Kraft lignins produced using Figure 6-12	134
Figure 6-15 Electrophoretic separation of organosolv ECN A, ECN B and ECN C lignins produced using Figure 6-12	135
Figure 6-16 Agarose gel post-electrophoresis (top) and corresponding traces D-F, also a comparison with GPC traces. GPC plots for protobind lignins (A), Kraft lignins (B) and organosolv lignins (C) and the electrophoretic separation of protobind lignins (D), kraft lignins (E) and organosolv lignins (F).....	136
Figure 7-1 Fluorescent intensity of 5 g/L Alkali lignin (A and B) and 5 g/L L6 lignin (C and D) incubated at 37 °C for 72 hours in total.....	145
Figure 7-2 Electrophoretic separation of <i>Pseudomonas</i> treated 1.5 g/L L6 lignin sample. A: raw data B: normalised data.....	146
Figure 7-3 Electrophoretic separation of <i>Pseudomonas</i> treated 5 g/L L6 (A and B) and 5 g/L Alkali lignin (C and D). A and C = raw data B and D = normalised data. Samples taken at 0, 7 and 11 days.	147
Figure 7-4 Electrophoretic separation of <i>Pseudomonas</i> treated 1.5 g/L L6 lignin sample that was treated to remove protein. A: raw data B: normalised data.	148

Figure 7-5 Electrophoretic separation of <i>Pseudomonas</i> treated 1.5 g/L L6 lignin sample after microwaving at 95 °C for 30 minutes. A: raw data B: normalised data.	149
Figure 7-6 Electrophoretic separation of <i>Rhodococcus jostii</i> treated 1.5 g/L L6 without 0.1 g/L vanillic acid (A and B) and 1.5 g/L L6 with 0.1 g/L vanillic acid (C and D). A and C = raw data B and D = normalised data. Samples taken at 0, 7 and 11 days.	150
Figure 7-7 Electrophoretic separation of <i>Rhodococcus jostii</i> treated and microwaved 1.5 g/L L6 without 0.1 g/L vanillic acid (A and B) and 1.5 g/L L6 with 0.1 g/L vanillic acid (C and D). A and C = raw data B and D = normalised data.	152
Figure 7-8 Agarose gel containing a lignin concentration gradient, controls and 1.5 g/L <i>R. jostii</i> degraded L6 Kraft lignin.....	153
Figure 7-9 Lignin concentration gradient produced using Figure 7-8	154
Figure 7-10 Estimated concentration of <i>R. jostii</i> degraded lignin and controls samples produced using Figure 7-9	155
Figure 7-11 Electrophoretic separation of control and <i>R. jostii</i> treated samples produced using Figure 7-8	156
Figure 7-12 Agarose gel containing a lignin concentration gradient, controls and 100 g/L (diluted 20x) Alkali lignin.....	157
Figure 7-13 Intensity of the solid fraction of lignin in the gel well, the soluble fraction that migrated down the gel and the combined solid and soluble to represent the full sample.	158
Figure 7-14 Estimated concentration of HTC treated lignin produced using Figure 7-12.....	159
Figure 7-15 Electrophoretic separation of control and HTC treated lignin samples produced using Figure 7-12.	160
Figure 7-16 Decrease in band intensity (A and C) and electrophoretic separation (B and D) after enzymatic lignin degradation of 5 g/L Alkali lignin (A and B) and 5 g/L L6 Kraft lignin (C and D) over a period of 72 hours. C= control and T= laccase degraded sample. Samples were taken after 0, 24, 48 and 72 hours.	162
Figure 7-17 Agarose gel containing a lignin concentration gradient, controls and 5 g/L enzymatically degraded L6 Kraft lignin.....	165
Figure 7-18 Estimated concentration of enzymatically degraded lignin samples produced using Figure 7-17.	166
Figure 7-19 Electrophoretic separation enzymatically degraded lignin samples produced using Figure 7-17.	167
Figure 7-20 Decrease in band intensity (A and C) and electrophoretic separation (B and D) after hydrogen peroxide lignin degradation of 5 g/L Alkali lignin (A and B) and 5 g/L L6 Kraft lignin (C and D) over a period of 72 hours.	168

Figure 7-21 Agarose gel containing a lignin concentration gradient, controls and 5 g/L hydrogen peroxide degraded L6 Kraft lignin.	170
Figure 7-22 Estimated concentration of hydrogen peroxide degraded lignin and controls produced using Figure 7-21.	171
Figure 7-23 Electrophoretic separation of control and hydrogen peroxide degraded lignin samples produced using Figure 7-21.	172
Figure 8-1 Annotated image of gel tank (left) along with diagram of gel electrophoresis equipment (right) (gel shown in figure is only an example and was not used to generate any results)	177
Figure 8-2 UV absorbance of gel buffer taken every 15 minutes for 1 hour after running lignin standards, treated lignin and low molecular weight compounds.	180
Figure 8-3 Full ¹ H NMR spectra of extracted compounds from the gel electrophoresis buffer eluent.	182
Figure 8-4 Aromatic region on the ¹ H NMR spectra of the extracted compounds from the gel buffer eluent	183
Figure 8-5 Diagram of proposed capillary electrophoresis method for the assessment of low molecular weight products	185
Figure 9-1 Proposed experiment to create molecular weight standards	195

List of abbreviations

C	Control (without bacteria, H ₂ O ₂ , HTC treatment or enzymes)
DNA	Deoxyribonucleic acid
DN _o	Number of days of incubation
EDTA	Ethylenediaminetetraacetic acid
GPC	Gel permeation chromatography
HN _o	Number of hours of incubation
HPLC	High pressure liquid chromatography
LB	Lysogeny broth
MALDI-TOF	Matrix-assisted laser desorption/ionisation time-of-flight
mm	Millimetres
M _n	Number average molecular weight
M _w	Weight average molecular weight
MW	Microwaved
NPK	No proteinase K
NMR	Nuclear magnetic resonance
Py-GC/MS	Pyrolysis gas chromatography mass spectrometry
PAGE	Polyacrylamide gel electrophoresis
PK	Proteinase K
SB	Sodium borate buffer

SDS	Sodium dodecyl sulphate
SEC	Size exclusion chromatography
T	Treated sample (by bacteria, H ₂ O ₂ , HTC or enzymes)
TAE	Tris acetate EDTA buffer
THF	Tetrahydrofuran
UV-VIS	Ultraviolet-visible spectroscopy

Chapter 1

Literature review and research objectives

1.1 Introduction

1.1.1 Climate change and sustainability

The world population is predicted to rise to 9.1 billion in 2050 (Gilland, 2002). Currently the total CO₂ emissions are around 10 gigatonnes, so if these were to rise proportionately, it represents a significant pressure on increased global temperatures (Quere C. Le et al, 2015). The demand for electricity is likely to increase faster than population growth due to developing countries becoming wealthier and therefore having access to electrical appliances. Less expensive appliances are less energy efficient so this is likely to make the situation even worse. Fossil fuels are often sourced from unstable regions such as the Middle East, and energy is often used as leverage in international conflicts such as Russia and Ukraine; so this is clearly very detrimental for energy security. As a result there have been large investments in technologies to increase energy security, irrespective of CO₂ emission considerations. An example of this is the US investment in bioethanol, and more recently fracking (Mathews J. A. et al, 2014). Renewable technologies often have the combined benefits of reducing emissions and at the same time providing increased energy security and as a result investment is increasing in these technologies.

1.1.2 Need for renewable aromatics

Currently the only bulk source of aromatic compounds is oil, and, as mentioned above, the use of fossil fuels is unsustainable, so there is a need to switch to sustainable sources. The only sustainable bulk source of aromatics is from

lignocellulose, via the utilisation of lignin, which, in theory, can be broken down to produce aromatic platform chemicals. However, lignin is very difficult to degrade and this has slowed down utilisation of this feedstock. There are many methods to degrade lignin but all have distinct advantages and disadvantages. Thermochemical methods have the disadvantage of requiring lots of heat and producing a complex mixture, with high purification costs. One avenue of research is to use microorganisms which require far less severe conditions, and produce less complex mixtures so should reduce the cost of the process. Conversely, the natural rate of biological lignin degradation is far too slow to be a viable industrial process, so research is looking at modified microorganisms and enzymes to increase this (Beckham et al., 2016). Crucially, in order to increase the rate of a process and optimise it, it is crucial to know how much lignin is present before and after degradation. There are few techniques to analyse lignin, and none are truly high throughput and/or low cost. Furthermore, the vast majority of these, discussed later, do not measure polymeric lignin and are therefore prone to giving false results, through contaminating compounds and lignin degradation products.

1.2 Introduction to lignocellulose

Lignocellulose is the dominating component of woody biomass and consists of three parts: lignin, cellulose and hemicellulose. Lignocellulose is located in the plant cell wall and is used to provide strength and resistance to microbial attack. The exact composition varies with feedstock, and the chemical composition is different in both sugars in the hemicellulose and lignin with different ratios of guaiacol to syringol.

1.2.1 Cellulose structure and characteristics

Cellulose is the most common polymer on earth and consists of D-glucose monomers linked by β -1-4 glycosidic bonds and is a non-branching polymer. The long cellulose chains interact via hydrogen bonds to form cellulose fibrils, which provide strength and resistance to degradation (Florin Ciolacu D C et al, 2011). Cellulose can be found in two major forms: amorphous and crystalline, the higher the amount of crystalline cellulose present then the higher the resistance to degradation.

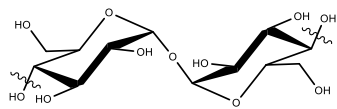


Figure 1-1 Repeating cellobiose disaccharide unit of cellulose polymer

1.2.2 Hemicellulose structure and characteristics

Hemicellulose is the third most common polymer, and like cellulose consists of sugar monomers, but consists of several different sugars, and is branching rather than linear. The most common sugars present includes: glucose, arabinose, xylose and galactose (Mod R R et al, 1978).

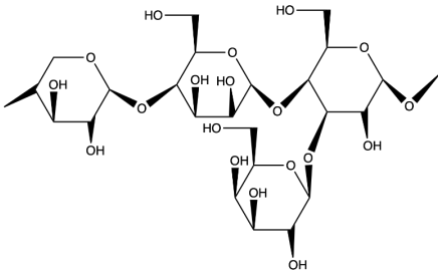


Figure 1-2 Example structure of hemicellulose polymer.

Hemicellulose does not provide the same resistance to degradation as other components in lignocellulose but can lead to issues downstream as yeast strains often cannot metabolise many of the sugars present (unlike in cellulose which consists of glucose).

1.2.3 Lignin structure and characteristics

Lignin is the second most abundant organic biopolymer and is highly variable throughout different plant species (Zhong and Ye, 2009). Lignin aromatic substrates originate from phenylalanine which is converted to three main monomers: *p*-coumaryl alcohols, coniferyl alcohol and sinapyl alcohol (Vanholme R et al, 2010) (Whetten and Sederoff, 1995). The monomers are connected with a variety of different linkages which include β -aryl ether, coumaryl, resorcinyl and dibenzodioxinyl bonds (Dutta et al., 2018). The variety of different linkages is linked to the difficulty to degrade lignin, as there are no repeating units that enzymes can 'recognise' and bind to.

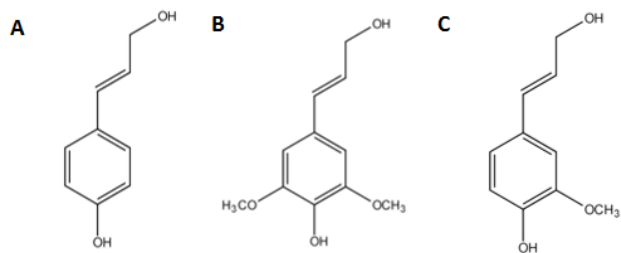


Figure 1-3 The main monolignols used to synthesise lignin A= *p*-coumaryl alcohol, B= sinapyl alcohol and C= coniferyl alcohol.

The precursors shown in Figure 1-3 are present in lignin as the monomers *p*-hydroxyphenyl, syringyl and guaiacyl (Goujon et al., 2003). The monomers present can vary greatly between different plant species, for example lignin in grass species contains guaiacyl, syringyl and a small amount of *p*-hydroxyphenyl units. Whereas gymnosperm lignins from softwoods do not have syringyl units and hardwood lignins largely consist of guaiacyl and syringyl units (Santos et al., 2012).

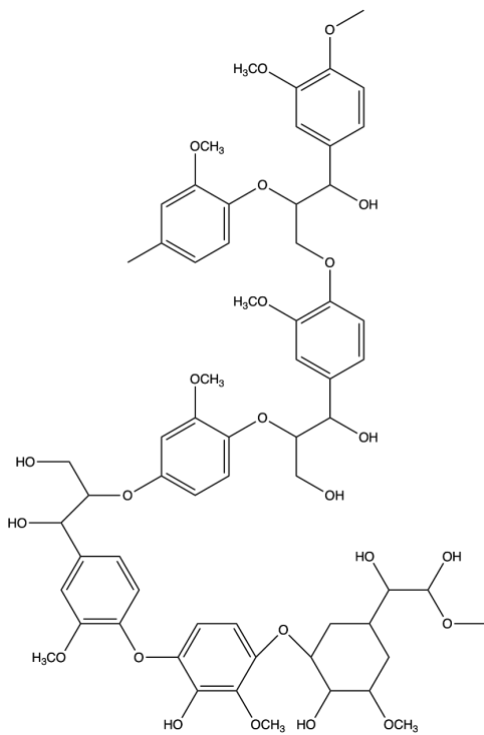


Figure 1-4 Example structure of part of a lignin polymer

The diverse nature of lignin is illustrated by Figure 1-4 where the variation in chemical bonds and overall structure is apparent. The large differences in lignin such as this can have large effects on chemistry. Although lignin is insoluble, chemical treatment can change this, for example with Kraft lignin production (Brandt A et al, 2013). The large varied structure provides many opportunities as many different compounds can be generated from lignin.

1.2.4 Overall lignocellulose structure

The components of lignocellulose do not exist in isolation and instead form specific interactions in order to dictate the overall structure and physical properties of lignocellulose.

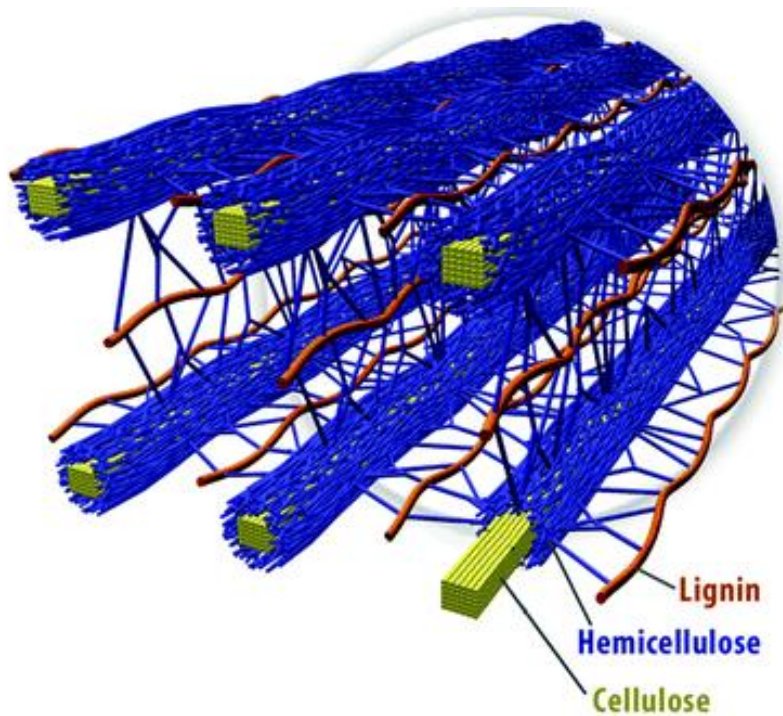


Figure 1-5: Example structure of lignocellulose. Sourced from (Brandt A et al, 2013)

Cellulose forms clear fibrils and it is proposed that hemicellulose binds covalently to the fibrils. This allows distinct fibrils to form and importantly leads to these fibrils being held in place. Lignin then interacts with hemicellulose to form a lignin-carbohydrate complex. In some lignins, ferulic acid bonds to hemicellulose with covalent ester bonds. The lignin therefore provides additional strength and resistance to microbial attack and is important to define the structure of lignocellulose (Brandt A et al, 2013).

1.3 Sources of lignin

There are a plethora of lignin sources available which can differ greatly chemically and physically; for example Kraft lignin is lower in molecular weight and contains large amounts of sulphur compared to raw biomass. Most of these feedstocks can be considered as waste which provides an opportunity to build a circular bio economy if these sources are utilised as a chemical feedstock.

1.3.1 Crude biomass

Crude biomass represents the most obvious source of lignin. Unlike other sources of lignin, this source contains cellulose and hemicellulose which can complicate the fermentation process but could provide a cheap carbon source for microorganisms to utilise to increase growth. Examples of crude biomass include: wheat straw, willow and *miscanthus*. A clear disadvantage of crude biomass is that lignocellulose is insoluble unless pre-treated, which can cause several issues when developing a process. Biomass also has undesirable physical properties, for example straw has a waxy layer which can cause it to float and makes it harder to degrade. Biomass can be pre-treated mechanically but due to the fibrous nature and shape when milled it can have undesirable flow properties. Biomass additionally presents a health and safety risk when utilised on a large scale due to its potential for auto-ignition and the high occurrence of fines which can lead to fires. Biomass can be pre-treated to reduce the severity of these issues, for example by torrefaction or by pelleting. However for microbial lignin degradation, chemical pre-treatment is more applicable (Rentizelas A. A. et al, 2009).

1.3.2 Lignocellulosic biorefineries

As lignocellulose is further utilised as a feedstock to generate 2nd generation bioethanol, waste lignin from this process will become a more prevalent feedstock for valorisation. Currently the waste lignin is combusted in order to provide the power to process the lignocellulose, however this is not taking full advantage of lignin as a source of valuable aromatic chemicals (Daylan and Ciliz, 2016) (Daylan and Ciliz, 2016). It is estimated that the amount of lignin produced from a cellulosic bioethanol plant will be between 100,000 to 200,000 tonnes per year; this therefore represents a significant amount of material that could be utilised in the future (Ragauskas et al., 2014). This lignin will represent a underutilised resource and valorisation of lignin would lead to another revenue stream which could make cellulosic bioethanol more economically viable.

1.3.3 Paper and pulp industries

Output from the paper and pulp industry represents a shrinking, yet extremely large source of lignin. The most common source is through the Kraft process. This starts by adding sodium sulphide and sodium hydroxide to lignocellulose before heating to around 170 °C for around two hours. This is done in order to separate the lignin from the biomass by solubilisation; chemically this is due to breaking the ether bonds between the subunits of lignin (carbon-carbon bonds are relatively intact). The remaining lignin is then dissociated using bleaching methods, leaving cellulose fibres used to manufacture paper. The lignin waste produced as a result of the Kraft process is referred to black liquor. Black liquor liquid can be used in fermentation processes (Da Re and Papinutti, 2011), but the lignin is modified and contains sulphur groups which increase its toxicity,

which makes microbial degradation more challenging (Košíková et al., 2002). Due to the toxicity and colour, microbial degradation of Kraft lignin would also have the added benefit of being a form of bioremediation (Chakar F S et al, 2004). Organosolv is another process that can be used to separate lignin as part of the paper and pulp industry. Unlike the Kraft process organosolv pulping uses an organic solvent such as ethanol to extract lignin and has been reported to have higher yields (Sannigrahi P. et al, 2013). Protobind lignin is produced by GreenValue and involves aqueous sodium hydroxide extraction of lignin from grass, so also lacks contamination with sulphur (Fackler K. et al, 2011).

1.4 Products from lignin

The variability of lignin means that the polymer can be valorised to produce a multitude of products. Several applications take advantage of the physical property of lignin, for example carbon fibre (Kadla et al., 2002). Platform chemicals represent perhaps the most promising product stream from lignin. Examples include: aromatic aldehydes such as p-hydroxybenzaldehyde, syringaldehyde and vanillin that are potential feedstocks for industries including the pharmaceutical, food and the cosmetic industry (Kang S et al, 2013). Vanillin for example can be used for vanilla flavouring, a platform chemical to produce L-DOPA (used to treat Parkinson's disease) and in the cosmetic and perfume industries (Valdes R H et al, 2004) (Esposito L J et al, 2000). When it is degraded, the complex mixture of products leads to high separation and purification costs. Problems such as this has prompted the phrase "you can make anything you want out of lignin - except money" (Graichen et al., 2017).

1.5 Degradation of lignin

Lignin can be degraded in a number of ways, many of which are energy intensive and time consuming, due to its recalcitrance. Oxidative, reductive and hydrolytic chemical methods have been assessed to break lignin. Thermochemical methods use heat to 'crack' the lignin polymer, whilst biological methods utilise the ability of organisms or enzymes to oxidise or hydrolyse the lignin structure.

1.5.1 Chemical degradation

There are several methods of chemical degradation of lignin. Hydrolytic methods utilise an acid or base (Abdelaziz et al., 2016), whilst oxidative methods involve metal catalysts and oxidants such as air, oxygen or peroxide (Lange et al., 2013). Reductive methods employ hydrogen or hydric reductants and metal catalysts (Key and Bozell, 2016). To increase breakdown rates, ionic liquid or supercritical fluids solvents have been used to dissolve the polymer (Akiba et al., 2017) (Gosselink et al., 2012). For acid catalysed degradation, formic acid is often used in combination with alcohols such as ethanol at elevated temperatures such as 400 °C for several hours. Acid degradation involves cleaving the β -O-4 linkage utilising the acid as a proton donor (Wang H. et al, 2013). This method can be used to produce chemicals such as: catechols, phenols and anisoles in yields ranging from 0.5 to 2.9 wt% (J. R. Gasson et al, 2012) (Forchheim D. et al, 2012). Lignin degradation involving bases commonly involves sodium hydroxide, increased temperature (~300 °C) and high pressures of around 10 MPa. Like acid, degradation the β -O-4 is commonly cleaved as part of this process (Wang H. et al, 2013). Several different chemical products are produced including: vanillin, guaiacol, and catechol, in yields ranging from 0.5 to 3 wt% (Lavoie J. M.

et al, 2011). Hydrogen peroxide is commonly used in paper pulping as a bleaching agent but can also be utilised to degrade lignin to produce platform chemicals such as vanillin (Sun et al., 2000). Hydrogen peroxide converts to oxidative compounds such as the hydroperoxide anion which can then diffuse and degrade lignin (Das et al., 2016). However, one of the disadvantages is that it can further oxidise the low molecular weight products, making their use more difficult (Seesuriyachan et al., 2015).

1.5.2 Thermochemical degradation

Thermochemical degradation of lignin involves heating biomass to temperatures commonly ranging from ~300-700 °C sometimes under elevated pressure which can be as high as 20 MPa; this is often carried out using organic solvents or water (Cheng et al., 2012) (Sangchoom and Mokaya, 2015). Each of these processes can be optimised to produce different products and can enter into several product streams such as fuel and value added chemical production.

A common method for valorisation of lignin is pyrolysis which involves heating to between 200 and 750 °C with the absence or limitation of oxygen, the α -O-4 bond is most commonly cleaved bond. This process can be optimised to produce solid, liquid or gaseous products, an example of this is that heating above 400 °C is used to produce higher volumes of liquid products. Catalysts can also be used to influence the rate or yield or products as part of the process, examples use zeolite HZSM-5, or more commonly NiMo, to increase the yield of non-oxygenated aromatics (Joffres B. et al, 2013). Pyrolysis can be used to produce several value added chemicals such as vanillin (Pandey M. P. et al, 2010). Other thermochemical processes for degradation of lignin are used to treat high

molecular weight products as part of petroleum refining such as catalytic cracking, hydroprocessing and hydrotreatment. Conversely, distinct processes can be used such as solvolysis which utilises organic solvents but this process does not lead to favourable yields (Joffres B. et al, 2013). A major disadvantage of these processes is that high temperatures are required which consume large amounts of energy, a process that can be carried out at ambient temperatures would be much more favourable. A major problem with any non-selective process like thermochemical conversion is that the valuable products are formed in a complex mixture with impurities such as olefins. Additionally many of these impurities can have similar chemical and physical properties to the product of interest making it very expensive and difficult to attempt to separate them (Dalton R. et al, 1974).

1.5.3 Biological degradation

Biological degradation of lignin is an integral part of nutrient recycling within the ecosystem and a plethora of different organisms occupy this niche, mainly consisting of fungi and bacteria. A major advantage of biological degradation is that organisms are selective and as lignin is degraded it is consumed, therefore the downstream purification is much less complicated and cheaper. The process can be carried out at ambient temperatures which decreases the costs further. However, there are still several challenges, as unlike thermochemical degradation of lignin, there are no commercial processes for biological lignin degradation (Borregaard ASA, 2014).

Degradation of lignin by fungi is by the far most explored area, and research began in the 1980s with very little progress in developing industrial level

processes. The two major types are white rot and brown rot fungi, which are both filamentous but carry out lignocellulose degradation by different methods. For example, brown rot such as *Serpula lacrymans* carries out indirect degradation of cellulose and hemicellulose utilising the Fenton reaction by reducing Fe_{3+} to Fe_{2+} . Ferric iron then reduces oxygen to generate highly reactive superoxide radicals that cleave the bonds in cellulose and hemicellulose allowing the fungi to utilise the constituent sugars. Once this process is complete the remaining lignin is demethylated (Arantes et al., 2012).

In white rot fungi, several enzymes once again utilise low molecular weight radicals to cleave bonds within the lignin polymer and metabolise the degradation products. The difference between them is that brown rot fungi converged from white rot fungi in evolution, due to temperate forests having a shorter period of time where the climate is favourable for lignocellulose degradation. Brown rot fungi release energetically expensive, extracellular, lignin degrading enzymes in order to improve metabolic efficiency, mainly growing on soft woods, consuming cellulose and hemicellulose (Eastwood D. C. et al, 2011). Due to this white rots and mainly investigated for lignin degradation and has potential applications in lignocellulose pre-treatment for production of cellulosic bioethanol (Dashtban M. et al, 2010).

The two main groups of enzymes involved in lignin degradation in filamentous fungi are laccases and peroxidases. Different species of fungi can vary significantly with the suite of enzymes used and may favour use of laccases over peroxidases or vice versa. Peroxidases also consist of two classes of enzymes which are lignin peroxidases or manganese peroxidase. Although these enzymes function in a similar fashion, they differ in the redox mediators they use.

Additionally both enzymes can target different lignin substrates, for example lignin peroxidases can target non-phenolic part of the lignin structure (Dashtban M. et al, 2010).

Lignin peroxidases are glycoproteins that contain a heme group and utilise hydrogen peroxide. As lignin peroxidases can be as large as 43KDa these enzymes are too large to carry out lignin degradation intracellularly, so target the outside of plant cells in an indirect fashion. This highlights one of the limitations of lignin degradation, as it can only be degraded if structurally accessible. Lignin peroxidases utilise electron transfer to oxidise phenolics to phenoxyl radicals which can then diffuse and oxidise the lignin structure. Unlike other mechanisms of lignin degradation, lignin peroxidases do not utilise mediators as part of this process. Like lignin peroxidases, manganese peroxidases are glycosylated proteins but function with a slightly different, manganese oxidation mechanism. Mn(II) is oxidised to Mn(III) by the enzyme which is then chelated by organic acids, these compounds act as mediators to stabilise the Mn(III). The stabilised Mn(III) then diffuses outwards to the lignin polymer in order to oxidise the phenolic component of the lignin polymer (Perez J et al, 2002) (Dashtban M. et al, 2010).

Like peroxidases, laccases are glycoproteins and utilise an electron transfer mechanism to reduce dioxygen to water. Laccases are part of the multicopper protein family and contain copper centres, which have a role in the electron transfer (Gomaa and Momtaz, 2015). Each of these copper locations are 'labelled' as either type 1, type 2 and binuclear type 3. Type 1 is the site where substrate oxygen occurs before transferring to either the type 2 or 3 sites via the Cys-His pathway, where the reduction of molecular oxygen takes place (Jones SM et al, 2015). Laccases are often used to degrade lignin in conjunction with a

mediator which is first oxidised by the laccase, before diffusion and subsequent oxidation of lignin (Agrawal et al., 2018). Laccases are not just specific to fungi that degrade lignin but can be found in other organisms such as yeast, mammals and plants. Due to the wide range of species in which laccases are found, laccases can have several different functions in each organism. An example of this are laccases in plants that actually have a role in polymerisation of lignin. Laccases function by removal of an electron from a hydroxyl group in the lignin structure, this oxidation generates a phenoxy free radical which can therefore lead to lignin depolymerisation (Gianfreda L et al, 1999).

A plethora of bacteria degrade lignin, although degradation of lignin using bacteria has been studied far less than degradation using fungi. Similarly the enzymes linked to degradation are less studied and there are fewer identified, however these enzymes tend to operate in a similar fashion to fungal enzymes. Bacteria have several distinct advantages over fungi as they grow much faster, far easier to genetically manipulate and tend to still be very resilient to environmental conditions. Bacteria that are capable of degrading lignin can be Gram-positive or Gram-negative and tend to be members of the following phyla: γ -proteobacteria, α -proteobacteria and actinomycetes (Bugg T.D.H et al, 2016). An example of a bacterial lignin degrader is *Rhodococcus jostii* RHA1, which is a Gram-positive soil bacterium. *Rhodococcus jostii* RHA1 contains several different enzymes to degrade lignin such as DypB which is a lignin peroxidase and thought to perhaps be a manganese peroxidase (Ahmad M et al, 2011).

DypB converts Mn(II) to Mn(III) very much like a manganese peroxidase, furthermore H₂O₂ and iron are shown to have a role in the process which is common in fungi. This illustrates the similarity to fungi degradation, so bacteria

could potentially degrade lignin utilising the same methods, but carry it out significantly faster. To add to this, for enzyme production and purification, bacteria have an advantage over fungi as bacterial enzymes are cheaper and simpler to produce (Ahmad M et al, 2011). Bacterial lignin degradation can operate at much lower temperatures and do not require complex engineering to protect from acid corrosion for example, therefore bacteria have distinct advantages over chemical, thermochemical and fungal degradation of lignin. Conversely it is not clear whether these advantages compensate for the extremely slow rate of degradation.

Vanillin and guaiacol are low molecular weight degradation products of lignin which are obtained as part of DypB-linked lignin degradation and are utilised by the microbe as metabolites. Products such as vanillin are high value products and used as platform chemicals in the pharmaceutical industry; this indicates the potential economic gains that can be achieved utilising lignin degraders to produce valuable products (Walton et al., 2003). Clearly, the understanding of bacterial lignin degradation is far less extensive than with fungi but work in this area is rapidly expanding and it is hoped that a process to degrade lignin could be developed using bacteria.

The are two main types of fermentation for lignin degradation are: solid state fermentation and submerged fermentation. Both technologies have different characteristics and present unique engineering challenges. Solid state fermentation is directly on a substrate without water. An example of this is production of soy sauce, and this type of fermentation has been used by certain cultures for thousands of years. There are several reasons for this and is likely

due to the low cost nature of this type of fermentation along with high productivities (Holker U. et al, 2005).

During solid state fermentation the fungus extends into the substrate using penetrative hyphae which allows increased access and higher surface of contact which accelerates degradation. This highlights one of the major problems of this fermentation as any disturbance to the substrate can damage the hyphae and therefore slow or inhibit growth of the fungi. Mixing is often integral to many industrial processes and as this process can produce heat, inadequate mixing can lead to large scale 'spontaneous' fires. This is a common problem which has occurred at biomass power stations and large scale biomass storage sites, where the aim is to store the biomass without it degrading (BBC News, 2011). The engineering challenges for solid state fermentation are therefore immense. Surprisingly, it is claimed that solid state fermentation has a higher volumetric output, but this is less impressive considering that the process is severely scale limited (Subramaniam R. et al, 2012). Interestingly this type of fermentation can lead to markedly different degradation compared to other methods and can produce different metabolites. For example, this process is not limited as much by substrate inhibition. An advantage that solid state fermentation has, is that it is much easier to form synergistic microbial communities which can lead to increased degradation and growth (Holker U. et al, 2005). Conversely, in this type of fermentation, key process variables are very difficult to control compared to submerged fermentation where variables such as dissolved oxygen, pH, mixing and temperature can be controlled and kept constant throughout the whole culture. The economic viability of this process is further damaged when applied

to lignocellulose, as it can take months for filamentous fungi to grow and degrade lignin.

Submerged fermentation takes place in an aqueous environment and can be both aerobic and anaerobic. This process tends to be more applicable to bacteria rather than fungi, as bacteria grow well in high moisture environments. This process is often carried out in a bioreactor due to the process flexibility; in aqueous media there are many different configurations and designs. Bioreactors are designed so that the process can be operated in batch, fed-batch or continuous modes. Due to the design as mentioned above many variables can be controlled, including mixing, that can ensure that the conditions are constant throughout. Using sensors for pH, temperature, dissolved oxygen, substrate and CO₂, the process can be controlled using a computer which significantly reduces maintenance costs. This also makes the process easier to model. The process tends to be much faster than solid state fermentation as the microbes and the substrate are constantly mixing. Unlike solid state fermentation, submerged fermentation is more removed from a 'natural' process, so it is sometimes harder to degrade a complex substrate. This is because the organisms are further from their 'natural' conditions, as no organism acts in isolation in the natural environment, but is often expected to do so in a bioreactor. Submerged fermentation is the dominating process in industry, which is unsurprising given its increased reliability, flexibility and speed (Holker U. et al, 2005).

1.5.4 Bacterial production of metabolites via lignin depolymerisation

As work on fungal lignin depolymerisation has been carried out since the 1980s, and there is no industrial process using this, attention has shifted to bacterial methods.

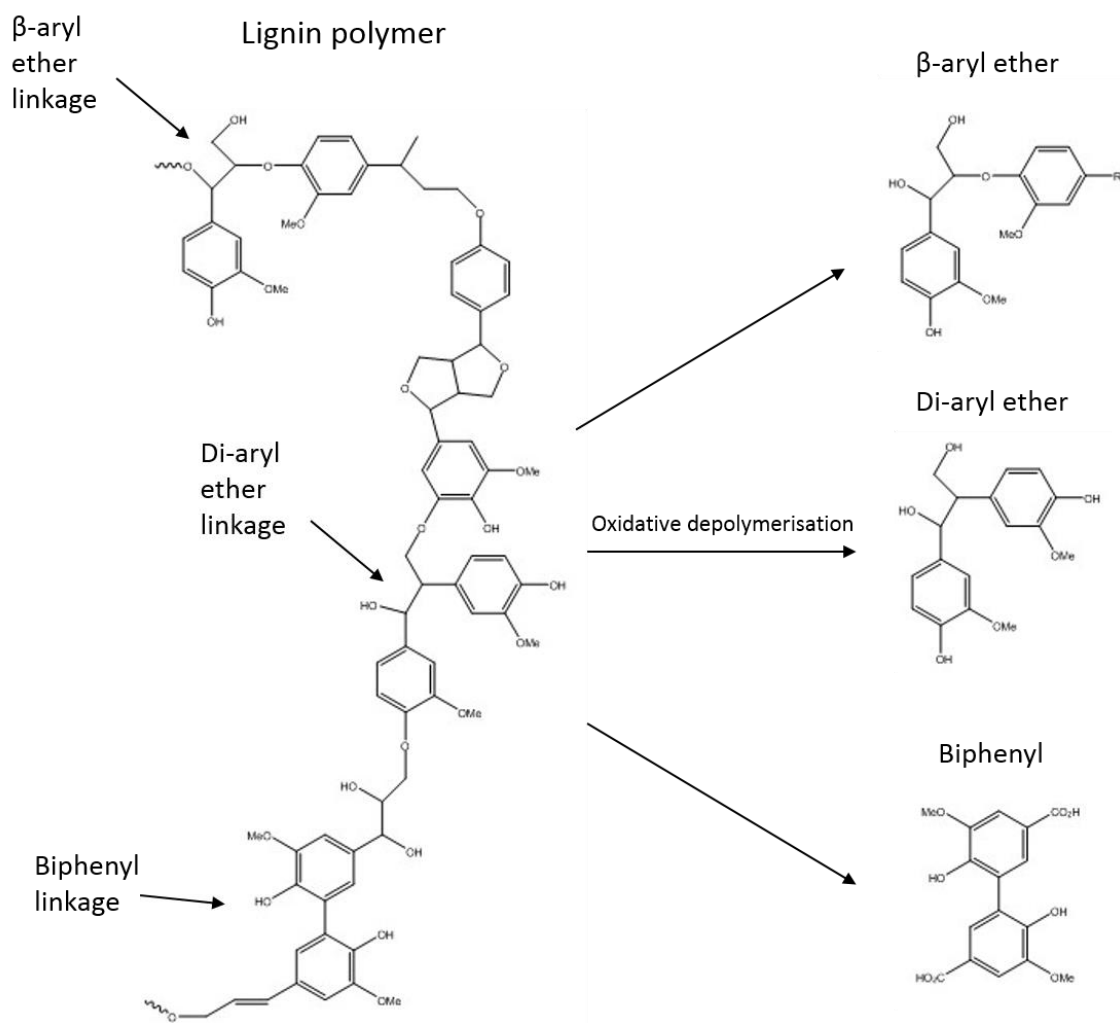


Figure 1-6 Diagram displaying the proposed lignin degradation paths taken by bacteria. Reproduced from (Bugg T.D.H et al, 2011).

Figure 1-6 shows the first part of the lignin degradation pathway found in bacteria and the proposed enzymes involved in this cycle. β -aryl ether, di-aryl ether and

biphenyl can then enter metabolism and produce high value chemicals such as ferulic acid, vanillic acid and vanillin for example (Bugg T.D.H et al, 2011).

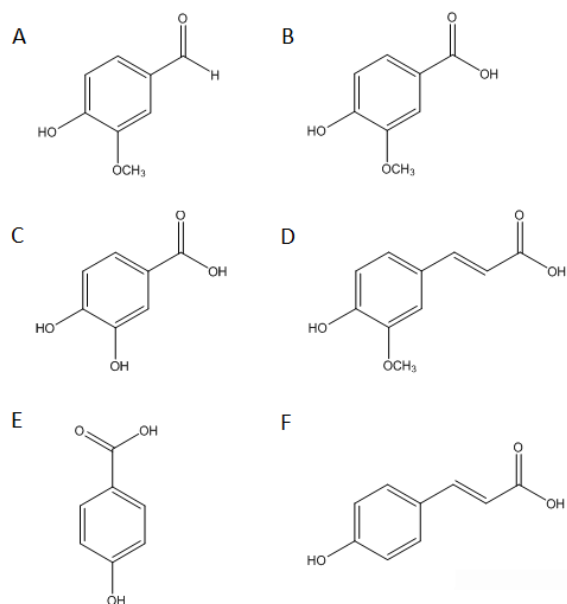


Figure 1-7 Chemical structure of common metabolites produced from lignin degradation by microorganisms. A= vanillin, B= vanillic acid, C= protocatechuic acid, D= ferulic acid, E= p-hydroxybenzoic acid and F= p-coumaric acid (Sainsbury P. D. et al, 2013).

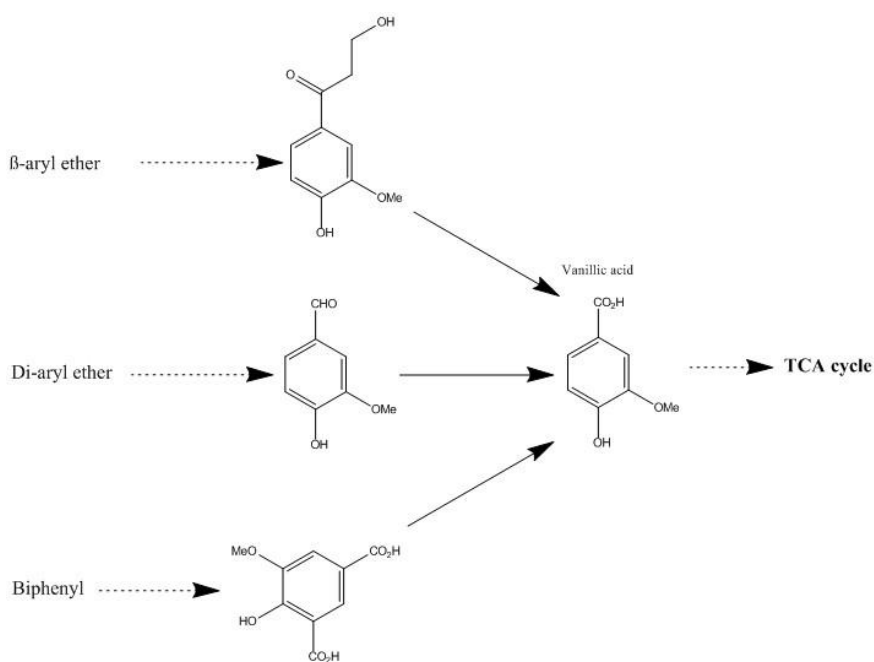


Figure 1-8 Diagram displaying the simplified lignin degradation pathway taken by *Sphingobium* sp. SYK-6 (dashed arrows represent simplified elements). Reproduced from (Bugg T.D.H et al, 2011).

Figure 1-8 illustrates how the lignin degradation products from Figure 1-6 and the metabolites from Figure 1-7 are funnelled into bacterial metabolism, and highlights the complexity of bacterial aromatic degradation, but also the flexibility of these pathways. For example vanillic acid can be produced using β -aryl ether, di-aryl ether and biphenyl, therefore even if there is variation in substrate composition, *Sphingobium* sp SYK-6 is still capable of producing high value metabolites. However, as this is an extremely complex multi-enzyme system then attempting to optimise the process to produce a specific metabolite can be very challenging (Bugg T.D.H et al, 2011).

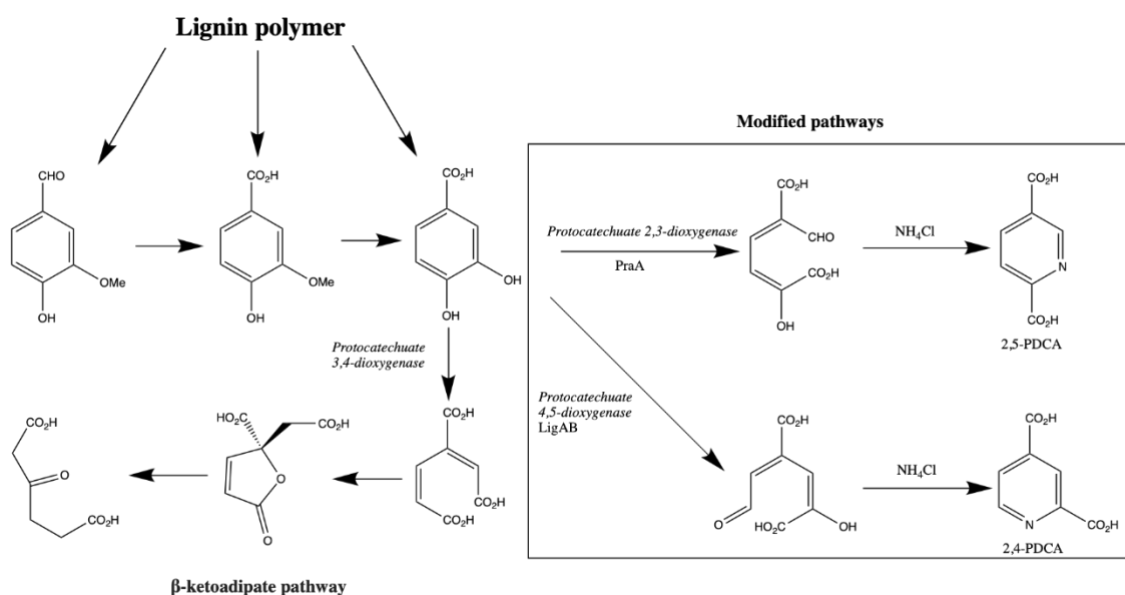


Figure 1-9 β -ketoadipate and genetically modified pathways in *Rhodococcus jostii* RHA1 for metabolism of lignin degradation products. Reproduced from (Mycroft Z. et al, 2015).

Figure 1-9 provides an example of how metabolic pathways can be modified to produce valuable by-products such as 2,4- and 2,5- pyridine dicarboxylic acids (PDCA) that are being researched as monomers in biodegradable plastics. LigAB and PraA are genes non-native to *R. jostii* and were cloned into the organism to re-route protocatechuate acid from the β -ketoadipate pathway. The enzymes act to open the aromatic ring before chemical cyclisation which then 'locks up' the compound as PDCA which *R. jostii* cannot degrade. This would be very difficult if fungi were used, due to the difficulties in their genetic modification. Despite re-routing pathways, eliminating alternative routes makes it challenging to produce large amounts of a specific metabolite, with the only option deletion of competing pathways (Mycroft Z. et al, 2015). There are examples in the literature where organisms have been genetically modified to produce metabolites which can be degraded by the wildtype (whereas PDCA cannot). This is shown by deletion of the vanillin dehydrogenase gene in *Rhodococcus jostii* RHA1 produced a yield of

96mg/L of vanillin; once again competing pathways appear to be activated and the concentration of vanillin peaks and then decreases over time (Sainsbury P. D. et al, 2013).

1.5.5 Routes for process development in lignin valorisation

To overcome the significant issues intrinsic to the lignin feedstock and the organism used to degrade it, a process must be developed and refined to overcome these respective issues. Lignin is generally toxic to bacteria, although lignin-degrading bacteria will tolerate it at higher concentrations. Accordingly, batch fermentation is not the optimum process for degradation, rather batch fed or continuous flow. This also enables processing of higher quantities that improve productivity. The majority of research has focused on batch methods because the breakdown rate is insufficient to develop a continuous flow process. However, continuous flow cultures have been developed using fungi (Bajpai P. et al, 1993). Variables such as extracellular enzyme expression and oxygen concentration might also be optimised to increase lignin degradation. In many bioreactors it is possible to increase oxygen mass transfer by increasing mixing and air flow, however at increased risk of foaming (often made worse by lignin which is prone to foaming). As mentioned above dioxygen is integral to many ligninases such as laccases, so increasing mass flow of oxygen into the process is likely to have a positive effect on rate; therefore there is demand for new bioreactor types to be designed (Gonzalo G. et al, 2016).

The growth rate of bacteria is another issue as they grow slowly (days/weeks) on lignin. As a result, it takes a significant time to create sufficient biomass to degrade lignin at a large enough scale. Therefore, it is important to consider the

use of substrates, such as glucose, to increase the amount of biomass, against factors such as catabolic repression (Magasanik B., 1961). A process that produces the largest amount of biomass in the shortest space of time without any major bacterial preference to substrates other than lignin is crucial. A potential solution would be immobilising cells and operating in continuous flow. As bacterial degradation is a relatively new developing field then the 'library' of bacterial strains that can degrade lignin is quite limited. Lignin degradation might be carried out using a population of bacteria which could increase the rate, compared to using a single organism. Although results are promising for generic lignin degradation/remediation, the ability to produce specific metabolites is limited, as a complex community is likely to degrade any metabolites produced (Wang Y. et al, 2013). Pre-treatment of lignin could be used in order to increase throughput. For example, thermochemical degradation could be used to partially degrade lignin, bacteria could then metabolise and break it down further to produce specific valuable products. This could also reduce the costs of purification, as the bacteria could metabolise unwanted lignin degradation products and therefore 'clean up' the complex mixture present. Although there are many promising routes, there are a lack of methods to assess and understand lignin breakdown. Those used currently are cumbersome, inaccurate and low in throughput (Hatfield and Fukushima, 2005). There is a need to develop a high throughput method to measure lignin digestion, which if achieved would be an important step in developing a process to valorise it.

1.6 Methods to determine lignin content

In order to valorise lignin, a process needs to be developed to effectively degrade the polymer. To do this, it is important to know how much lignin is present before and after degradation has taken place so that different methods can be compared and developed. In chemical degradation, a complex mixture is produced making it difficult to quantify how much has been degraded and how much and what low molecular weight products are produced. In other words, a process mass balance is required, that would enable a measure of conversion.

Methods to measure lignin content can be split into two categories: non-invasive, indirect methods involving solubilisation and direct methods that work on any lignins. Non-invasive methods include spectroscopic techniques such as UV-Vis, FT-IR and NMR. They tend to be simpler and higher in throughput. The disadvantage is the whole sample is analysed which can lead to inaccurate results, which is not a problem, if the aim is to measure native lignin in intact wood, but is if the aim is to assess lignin degradation. An example of this is the UV method that measures strongly absorbing aromatic compounds, however, the absorption of the lignin itself cannot be distinguished from the degradation products. The change in lignin absorption is small, making it impossible to measure its concentration with certainty, and quenching effects make responses non-linear. Methods such as UV are sometimes combined with an extraction method to increase the accuracy. An example is the UV measurement of acid soluble lignin, which is more specific and less susceptible to inaccurate readings due to contaminating compounds (Kaar and Brink, 1991). However, the extraction step decreases the throughput of the method and is incompletely

effective, since proteins can contaminate the sample and low molecular weight species lead to an over-estimation of the lignin present (Hatfield and Fukushima, 2005). An indirect method, that is commonly used by the paper and pulping companies, is permanganate, where the amount of chlorine consumed by the lignin is used to estimate the amount present. This method measures the amount of bleaching required to produce paper rather than directly measuring the lignin present, therefore it is not used in lignin degradation studies. Most common is the Klason method which is a direct technique to measure lignin. It uses sulfuric acid to dissolve polysaccharides present, leaving lignin as an insoluble residue that can then be measured gravimetrically. However, the method is ineffective at the removal of proteins though these can be reduced by prior extraction or proteolytic enzyme treatment. The result of this is even less efficiency, in an already low throughput method (Youn et al., 1995) (Sluiter et al., 2010) (Hatfield and Fukushima, 2005). Furthermore, these methods often produce conflicting values for the amount of lignin present so the overall accuracy of these methods is questionable. An example of this is the study carried out by (Salvachúa et al., 2015) where the amount of lignin present determined by the Klason method and UV analysis produced vastly different results overall. Consequently, there is no reliable high throughput method that can estimate the concentration of polymeric lignin in a degraded sample.

1.7 Molecular weight determination of lignin

Unlike other polymers, lignin does not have a standard molecular weight and this can vary significantly between samples. This is especially true for degraded or partially degraded samples such as Kraft lignin which can contain high molecular

weight insoluble lignin, low molecular weight soluble lignin and monomeric degraded lignin (Jokela and Salkinoja-Salonen, 1992). As a result, when developing a process to degrade lignin, it is important to observe changes in polymeric lignin concentration as well as changes in molecular weight. This is especially important, as certain degradation methods can lead to lignin polymerisation under certain conditions. An example of this is a laccase from *C. versicolor* which simultaneously polymerises and depolymerises lignosulfonate lignin (Youn et al., 1995). The most common method for lignin molecular weight determination is Gel Permeation Chromatography (GPC). This involves a porous gel that separates materials based on size and shape. Larger molecules elute through the column faster as their size means the molecules interact less with the gel pores, whereas, smaller molecules enter the pores and elute more slowly. Polystyrene standards of known molecular weight are often used to calibrate the system. However, polystyrene is a completely different molecule to lignin, so the molecular weight cannot be determined with certainty; therefore only the apparent molecular weight of lignin can be determined using GPC (Kostanski et al., 2004). Alternative methods such as light scattering photometry are also used to estimate molecular weight changes of lignin. The disadvantage of this method is that lignin can aggregate and lead to an overestimation of particles size. This is such a large problem that light scattering has been used to assess the level of lignin aggregation in a sample (Contreras et al., 2008). Ultrafiltration can also be used to assess possible changes in molecular weight by separating based on the ability to pass through a membrane. The disadvantage of this method is that it is not possible to determine the molecular weight of a fraction, just that it is between a range (Toledano et al., 2010).

1.8 Research rationale, aims and objectives

1.8.1 Research rationale and purpose

As discussed above, lignin holds great potential as a source of valuable aromatic platform chemicals that are otherwise produced by the petrochemical industry. One of the main obstacles, is the lack of a high throughput analytical technique to measure polymeric lignin. Furthermore, there is no high throughput method to analyse and assess the quantity of low molecular weight aromatic products in a degraded lignin sample. Such a technique would speed research and innovation within the field and facilitate the development of a process to degrade lignin and produce valuable aromatic platform chemicals.

1.8.2 Project aims

The aim of this project is to develop a versatile technique to analyse different lignins, and to compare different digestion methods enabling monitoring of processes to produce low molecular weight platform chemicals.

1.8.3 Project objectives

The main objective was to evaluate agarose gel electrophoresis as a method to separate polymeric lignin from its respective degradation products:

- Investigate whether electrophoresis of polymeric lignin is possible
- Confirm the identity of the migrating bands as lignin
- Evaluate electrophoresis variables
- Develop the use of imaging software to enable quantification
- Compare the resolution of the technique to standard techniques for lignin analysis such as GPC

- Separate lignin from the gel to produce pure samples, and scale-up to make it preparatively.
- Scale-out the electrophoresis method so that it can be classified as a high throughput method
- Assess the ability of gel electrophoresis to analyse lignin that has been degraded using a variety of different methods. Importantly confirm whether this method can be used to assess the bacterial degradation of lignin.
- Determine whether it can be used to analyse low molecular weight products produced as part of degradation, hence provide information on the mass balance.

Chapter 2

Materials and methods

2.1 Materials

The following is a list of materials commonly used in this work and were purchased from Sigma-Aldrich unless otherwise stated:

Acetic acid (64-19-7, Thermofisher Scientific), acetic anhydride (108-24-7), agarose (9012-36-6, Thermofisher Scientific), agarose, low gelling temperature (39346-81-1), Alkali lignin low sulfonate content (8068-05-1), boric acid (10043-35-3), calcium chloride (10043-52-4), chloramphenicol (56-75-7), dodecyltrimethylammonium bromide (1119-94-4), ethidium bromide (1239-45-8, VWR chemicals), ethylenediaminetetraacetic acid (6381-92-6), glycerol (56-81-5, Thermofisher Scientific), guaiacol (90-05-1), hydrochloric acid (7647-01-0, Thermofisher Scientific), iron (II) sulphate (13463-43-9), LB broth, miller (73049-73-7, Thermofisher Scientific), M9, minimal salts 5x (M6030), manganese II chloride (20603-88-7), magnesium sulphate (7487-88-9), methanol (67-56-1), potassium chloride (7447-40-7, Thermofisher Scientific), potassium phosphate dibasic (7758-11-4), potassium phosphate monobasic (7778-77-0), proteinase K (39450-01-6, Thermofisher Scientific), pyridine (110-86-1), sodium dodecyl sulfate (151-21-3), sodium hydroxide (1310-73-2), SYBR safe (1030826-36-8), syringaldehyde (134-96-3), tetrahydrofuran (109-99-9), toluene (108-88-3), triton X-100 (9002-93-1), tris base (77-86-1), vanillic acid (121-34-6), zinc chloride (7646-85-7)

Membrane separated L5 and L6 Kraft lignins were purchased from Canada Ltd. Protobind Z4, Z5 and Z6 lignins were provided by Prof Stéphanie Baumberger

(INRA Versailles) who purchased the lignins from GreenValue. Organosolv ECN A, ECN B and ECN C lignins were provided by Prof Stéphanie Baumberger (INRA Versailles) who purchased them from the Energy research Centre of the Netherlands (ECN). EasiCal polystyrene standards used for GPC molecular weight calibration were purchased from Agilent Technologies.

Rhodococcus. jostii pTipQ2-ligAB was kindly provided by Prof. Tim Bugg, the *Pseudomonas putida* KT2440 strain (DSM number 6125) was purchased from the DSMZ. The laccase enzymes used in this work were purchased from MetGen (MetGen, 2019)

2.2 General method for precipitation, acetylation and GPC

10 mg of lignin was dissolved in 2 ml of H₂O then 500 µl of 6 N HCL before mixing and was kept at 4 °C overnight. The next day the solution was centrifuged at 4500 rpm for 15 minutes at 4 °C, the supernatant was then discarded and the pellet was freeze dried. This sample was then used for acetylation.

For acetylation 10 mg of freeze dried lignin samples were added to a glass tube (the entire reaction was carried out in the same tube for each sample). 200 µl of pyridine (for analysis) was added before vortexing and then addition of 400 µl of acetic anhydride before vortexing again. The mixture was then left for 24 hrs and then 200 µl of methanol was added on ice. The methanol was evaporated and 200 µl of toluene was added before evaporation and this was carried out twice before adding 200 µl of methanol and evaporating again. The remaining acetylated lignin sample was then freeze dried. 1 ml of THF was then added to vials ready for GPC by filtering in a 0.45 µm PTFE filter.

GPC was carried out using THF eluent at 1 mL/min using an Agilent PLgel MIXED-C column, an UltiMate 3000 Autosampler Column Compartment for sample handling, and an UltiMate 3000 Photodiode Array Detector. Chromeleon for used for sample analysis. The GPC plots were normalised by expressing the mAU values as a percentage of the highest mAU value for each respective sample. Molecular weight was expressed in terms of Mn (number averaged molecular weight) and Mw (weight averaged molecular weight). Mn is calculated by dividing the total weight of polymer by the total number of molecules. Mw differs as it takes into the account the mass of individual polymers as molecules that are larger in size contain increased mass compared to smaller molecules. Therefore molecules that are larger in size have higher input into the weight average molecular weight value.

2.3 General method for gel electrophoresis

2.3.1 Gel recipe

Gels were made with either Sodium borate buffer (36.4 mM boric acid and 10 mM sodium hydroxide) or TAE buffer (40 mM tris base, 20 mM acetic acid and 1 mM EDTA).

2.3.2 Gel production method and electrophoresis sample preparation

The electrophoresis equipment used was a Clarit-E Mini gel tank (using a comb with 10 2 mm thick wells to enable high sample loading) or a Clarit-E Maxi gel tank (using a multichannel pipette compatible comb with 40x 1 mm thick wells), using a BioRad PowerPac 300 to apply a fixed voltage across the gel. The

imaging was carried out with a ChemiDoc™ MP Imaging System by exposing to light from 650-675 nm and measuring emission at 700-730 nm unless otherwise stated.

The agarose gels were made using 1% (w/v) agarose in sodium borate (SB) buffer, heating the slurry to ~100 °C until the solution became clear, allowing it to cool to 60 °C before pouring into a gel mould using a comb to define the loading wells. When using a the Clarit-E Maxi gel tank, the gels were poured on a levelled Flexicaster in order to ensure uniform gel thickness (as discussed in Chapter 5) The gel was formed after around 30 minutes and SB buffer was poured into the gel tank until the agarose gel was submerged. Dust causes problems with the gel and image analysis, and was minimised by ensuring all equipment and solutions were clean, using lens cleaning tissues to remove any residual dust. Lignin samples were prepared in Eppendorf tubes by mixing 20 µL of 50% glycerol, 20 µL 0.375 M NaOH with 50 µL of typically 5 g/L lignin sample before mixing using a vortex mixer. Electrophoresis was typically carried out at a fixed voltage of 50 V for 60 minutes, after allowing the loaded samples to equilibrate in the gel for 1 hour before running.

2.3.3 Loading of gel lanes with multichannel pipette

As the multichannel pipette channels do not directly line up with every gel well due to the tight spacing of the gel wells every other lane was loaded at a time.

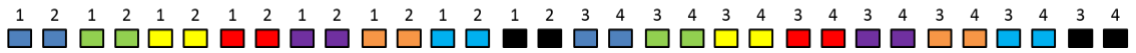


Figure 2-1 Gel wells with number above to illustrate in the order that the sets of wells were loaded 8 wells at a time (in this example) by the multichannel pipette in order to have four repeats for each sample across the whole gel. Wells of the same colour represent the same samples.

Distributing the samples across the whole length of the gel helps to reduce error when comparing samples. Rather than comparing samples from one side of the gel to samples on the other side, which can be inaccurate due to differences in gel thickness across the gel.

2.4 ImageJ analysis method

Gel analysis was carried out using ImageJ (a program developed by the National Institutes of Health and accessible online at no cost <https://imagej.nih.gov/ij/>). Using the software, gel bands were selected (with fixed selection dimensions and fixed vertical alignment) and processed using the in-built gel functions. ImageJ analysis was carried out by first inverting the image by selecting invert via the Edit tab. The rectangular selection tool was utilised to select the lignin band for analysis as shown in Figure 2-2 and Figure 2-3.

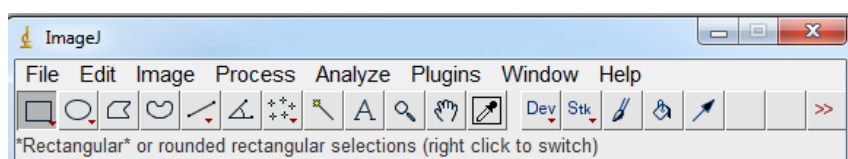


Figure 2-2 Screenshot showing the rectangular selection tool
Analyze > Gels > Select first lane

This marks the selection, an outline of the selection with the same dimensions can be selected and moved over to the next band

Analyse > Gels > Select next lane

This will then assign the second selection as the next gel band, selection will be vertically aligned with the first selection. Therefore it is important that the gel is imaged perfectly straight. If this is not possible, it is more accurate to compare several lignin samples across the gel with repeats rather than comparing lignin samples at opposite ends of the gel for example; sample repeats on the same gel are important for this reason. It can be identified if a gel is not completely straight by including several control samples on the same gel, the migration of these samples can then be compared to see if there are any major differences.

Use this function until all the gel bands are selected an example of the selections of the lignin gels is shown in Figure 2-3. The same method was used for all the gels except for the HTC samples where the gel well was included in the analysis, which is shown in Figure 2-4.

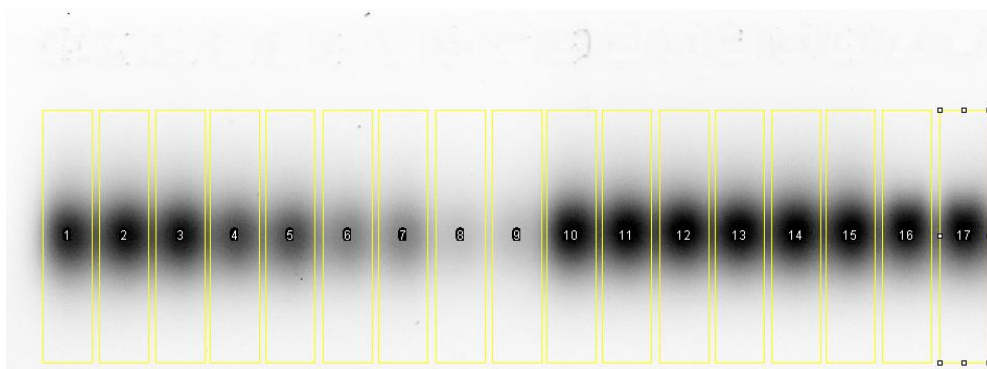


Figure 2-3 Screenshot of selected bands

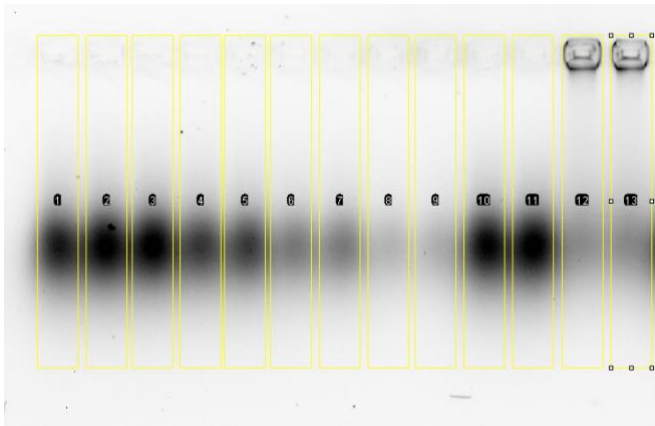


Figure 2-4 Screenshot of selected bands for HTC

Once all the lignin samples are selected the next step is to convert the gel bands into a plot.

Analyse > Gels > Plot lanes

This will produce a graphical representation of each of the gel bands as shown in Figure 2-5.

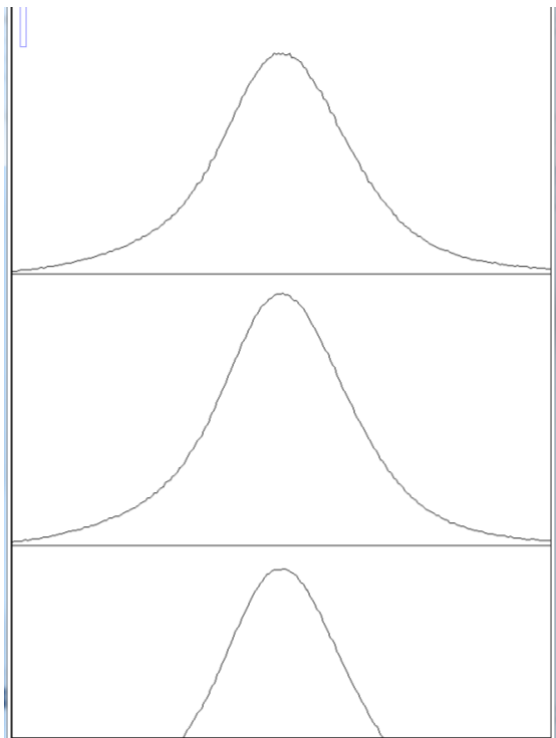


Figure 2-5 Screenshot of plotted lanes

The next steps differ depending whether the aim is to export the separation distribution of the lignin or quantify the total lignin in the sample.

To quantify the band intensity:

Select the wand tool and click on the peak

Using ImageJ it is not possible to analyse the first selection (selected as the first lane) therefore make a selection before the bands that are to be selected for analysis.

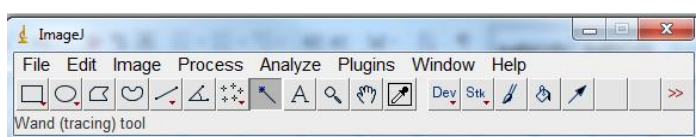


Figure 2-6 Screenshot of selected wand tool

Then select Analyze > Tools > Analyse Line Graph

This will then produce a plot which can be exported to excel by selecting Save and then saving the file in a selected location. The plots can then be compiled using excel.

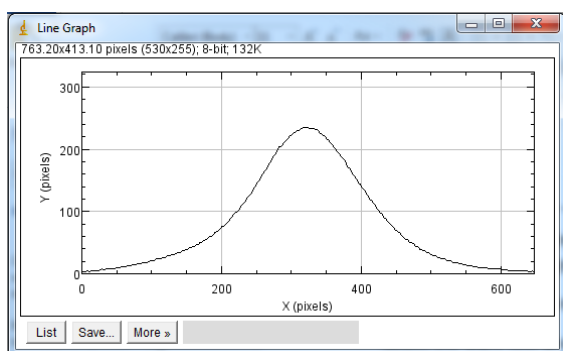


Figure 2-7 Screenshot of analyse line graph

To export the separation distribution of the lignin:

There is a small gap on the right-hand side of the plots shown in Figure 2-5, with a zoomed in version shown in Figure 2-8. This prevents the selection of the peak as the tool used will select the entire plot instead. In order to integrate under the curve it must meet the baseline. Therefore the line tool is used to connect the end of the peak to the side (as shown in Figure 2-9)

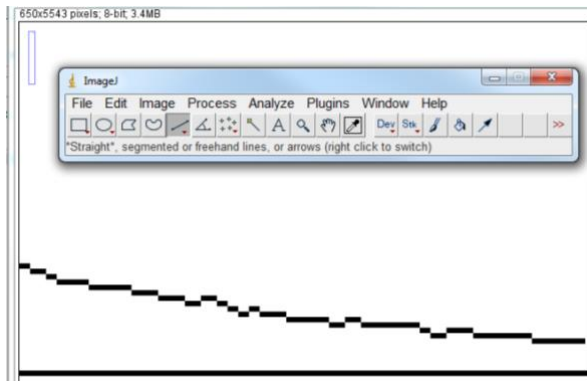


Figure 2-8 Screenshot of plotted lane showing small gap between the peak and the end of the x axis

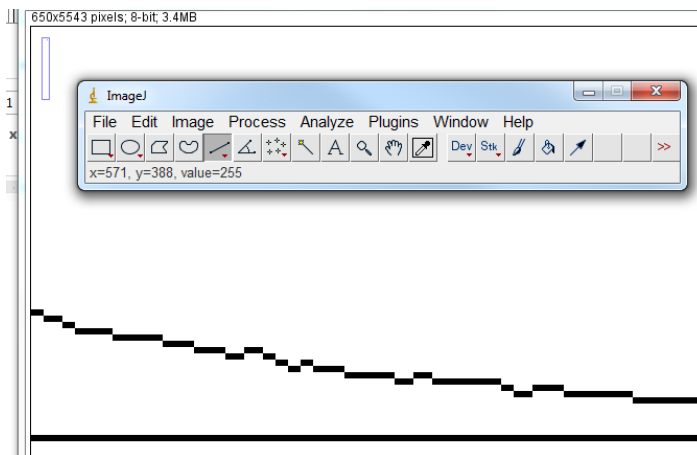


Figure 2-9 Screenshot showing how the peak is 'connected' to the end of the x axis

The peak area can then be converted into a single numerical value using the wand tool show in Figure 2-6. This then opens a results tab with the values for peak area which can then be analysed.

Results			
File	Edit	Font	Results
Area			
1	55542.600		
2	63581.914		
3	62307.136		
4	50160.579		
5	47668.215		
6	34675.446		
7	32140.839		
8	17910.401		
9	21542.836		
10	63942.550		
11	67780.621		
12	67581.136		
13	67576.550		
14	68267.792		
15	66609.307		
16	59280.529		
17	58900.458		

Figure 2-10 Screenshot showing the numerical values produced after ImageJ analysis

The values in Figure 2-10 were then used as values for the band intensities for each of the gel lanes, Figure 2-11. The standard deviation of these values was then used to produce error bars.

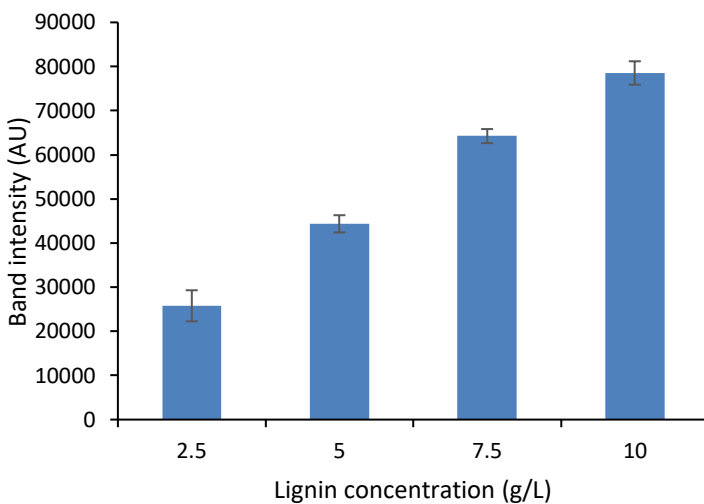


Figure 2-11 Example chart produced by ImageJ analysis with error bars displayed calculated using standard deviation.

2.4.1 Calculation of distance migrated

In order to calculate the distance migrated, the known width of gel wells was used to convert pixels on the image to distance in millimetres. The gel well width was 2.5 mm and the space between each well was 2 mm.

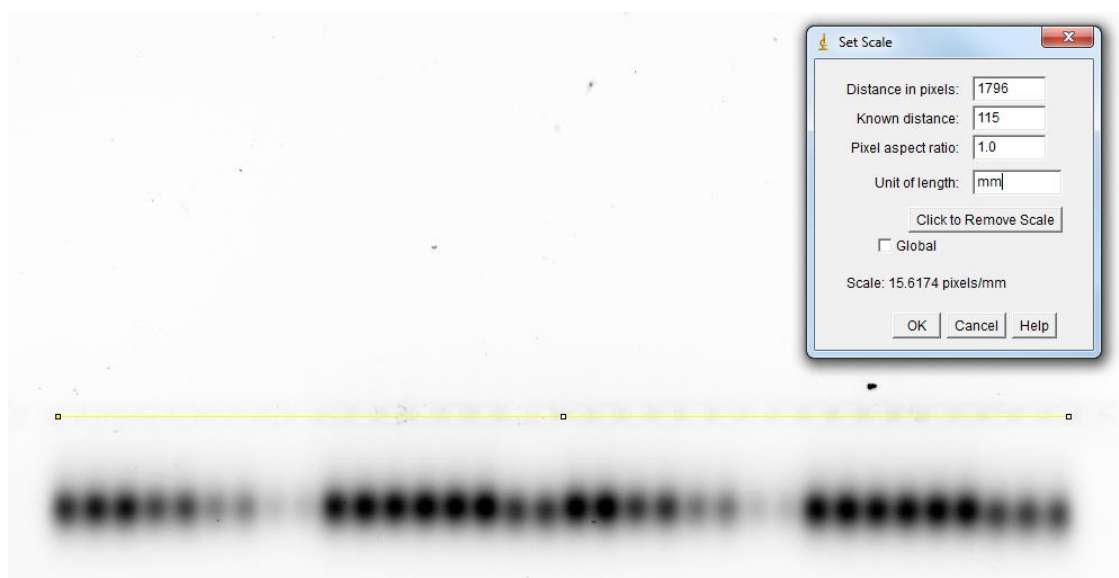


Figure 2-12 Example of using the set scale tool to calculate the pixels to millimetre ratio

Figure 2-12 shows how the set scale tool was used to provide a value for the ratio of pixels to distance (millimetres) which could then be used to work out the distance migrated.

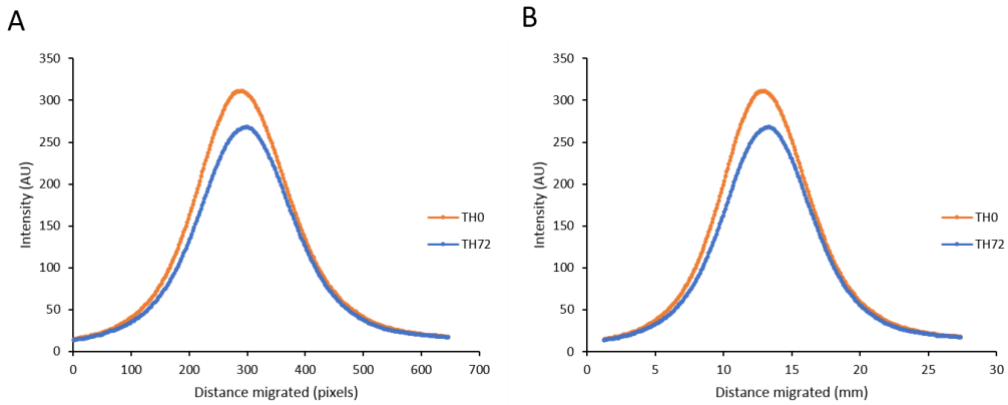


Figure 2-13 A = original graph with pixels representing distance migrated. B = graph displaying distance migrated converted into millimetres.

Figure 2-13 shows the final graph once the distance migrated in pixels is converted into millimetres migrated. For gels that were already analysed the distance

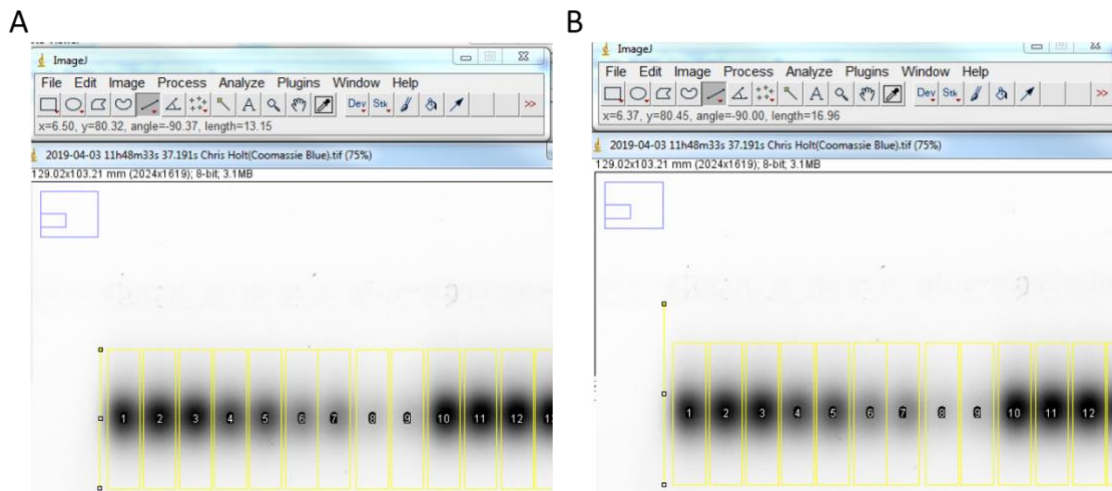


Figure 2-14 Screenshot showing the measurement of the original band selection (A) and the distance between the gel well and the end of the original band selection

For gels that were already analysed without using the method to convert pixels to millimetres, distance was measured as in Figure 2-14 to calculate the difference between the original band selection and the gel wells. Once this was

known the migration distance could then be calculated using the pixels to millimetres ratio.

Chapter 3

Characterisation of lignin agarose gel electrophoresis

3.1 Introduction

Gel electrophoresis is a versatile, high throughput method that is commonly used to provide qualitative and sometimes quantitative information about DNA and protein samples. The two major types of gels used for electrophoresis are agarose and polyacrylamide gels. Typically electrophoresis of agarose gels is carried out horizontally, whereas for polyacrylamide gels it is usually carried out vertically. Polyacrylamide gels are commonly used for proteins whereas agarose gels are almost exclusively used for DNA, except for circumstances when extremely large proteins need to be analysed. An example of this is (Warren C. M. et al, 2003), where SDS-agarose gels were utilised to separate titin which is a protein with the largest known SDS subunit size.

Polyacrylamide gels are produced by cross-linking acrylamide in order to form a complex polymerised porous structure. Usually *N, N'*-methylenebisacrylamide (*bis*) is used to react with the acrylamide and form the cross links. However polyacrylamide gels have high heterogeneity as *bis* can itself polymerise to form nodules (Heuer D. M. et al, 2003). Unlike polyacrylamide gels, agarose gels are made by heating agarose (in the respective buffer) until the agarose become molten, the molten agarose can then be poured and after cooling the gel then becomes solid. Agarose is a polysaccharide that consists of β -D-galactopyranose subunits and is extracted from seaweed. When the agarose cools the structure changes from random coils to a double helix structure and this structure then aggregates to form crosslinks and the porous gel matrix (Armisen R., 1991).

Lignin has been added to polyacrylamide gels in limited previous studies such as (Cherr G. N. et al, 1993) and (Saiz-Jimenez C. et al, 1999). In (Cherr G. N. et al, 1993) lignin from commercial pulp processing was run on PAGE (polyacrylamide gel electrophoresis) and SDS-PAGE. The lignin molecular weight was estimated using protein molecular weight markers, which is extremely unreliable as it is unclear whether lignin migrates like proteins on PAGE gels. The band that was assumed to be lignin was electroeluted and extracted. However, only limited evidence was provided that the extracted compound was lignin. Such as: The interaction with dyes, presence of aldehyde and hemiacetal groups in ^1H NMR and the effect of the extract on the development of sea urchins. In the study carried out by (Saiz-Jimenez C. et al, 1999) lignin, along with other biopolymers such as humic acids, were run on PAGE gels. Crucially, lignin and biologically degraded lignin was run on the gel, but little information was gained from this. Firstly an extremely sharp singular band was produced, therefore it was not possible to analyse the molecular weight distribution of lignin. Secondly the band was not quantified, so it was not possible to determine the level of degradation that had occurred.

The only instance of using agarose gel electrophoresis to provide information about lignin was carried out by (Jankowska D. et al, 2018). The gel was extremely rudimentary, with very poor band migration as several bands 'encroached' on each other. Additionally the gels were visualized with visible light, brown colour was used to indicate lignin. No conclusions were drawn, other than a general comment about how what appeared to be lignin migrated differently when treated enzymatically. With this work there was no direct evidence that lignin, or any fraction of lignin, was responsible for the band produced on the gel. This is

important, as brown colour is insufficient to confirm the band as lignin. To draw conclusions from the electrophoresis of lignin samples, it is crucial to confirm the identity of the migrating bands. It needs to be determined whether all of the lignin sample migrates, or just a fraction, and whether any other components contribute to the band. Furthermore, the electrophoresis conditions must be optimised to ensure the sample migrates in a uniform and reproducible manner to obtain accurate information (Jankowska D. et al, 2018).

3.2 Methods and Results

3.2.1 Preparation of the initial TAE gel

The gel was prepared with 1% (w/v) agarose and 40 ml TAE buffer (40 mM tris base, 20 mM acetic acid and 1 mM EDTA). Samples of L6 lignin were loaded onto the gels made with 8 μ l of each lignin sample and 2 μ l of 50% glycerol. Each sample was serially diluted in water to produce a concentration gradient, to produce a calibration curve. Electrophoresis was carried out at 100 volts for 10 minutes. The gel was imaged using a Gel DocTM XR+ Gel Documentation System using UV light (302 nm) as excitation light and measuring emission at 602/50 nm.

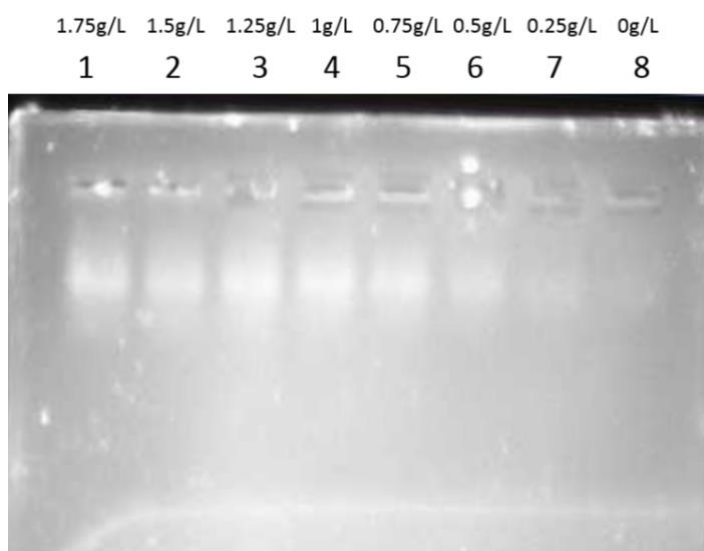


Figure 3-1 Initial TAE agarose gel with a lignin concentration gradient from 1.75 g/L to 0.25 g/L of L6 lignin

Figure 3-1 shows the first lignin concentration gradient that was attempted using agarose gels. Clearly the lignin band decreases in intensity as the lignin concentration decreases, which implied the first initial suggestion that gels could be used to quantify lignin. There is an apparent ‘spread’ of band intensity rather than a single sharp band, this also implied that potentially this could be due to

different lignin polymers having different mass to charge and shape. This would therefore lead to different lignin polymers moving through the gel pores at different rates leading to separation of polymers based on these characteristics. Polymers with a higher mass/charge ratio (as long as shape isn't taken into account) will move through the gel at a lower rate. As lignin polymers with a high molecular weight in theory have a higher mass to charge ratio compared to a lower molecular weight lignin, this method could be used to separate lignin based on molecular weight. Importantly the bands appear to be reproducible with separation appearing at the same point regardless of lignin concentration. It is clear that the imaging of this gel is below the quality needed in order to accurately measure the bands and quantify the lignin. There was a problem with dust particles on the gel overlaying the bands and that the light used to capture the gel provided little contrast between the bands and the agarose gel itself.

Additionally, in order to confirm that agarose gel electrophoresis can be used to provide molecular weight distribution, or to quantify lignin, it needed to be confirmed that lignin is responsible for the band and not a contaminant. Subsequent work was focused on running high mass of lignin samples on gels in order to purify polymeric lignin for analysis. This presented a challenge, as methods such as size exclusion chromatography require samples within the range of 10 mg.

3.2.2 Optimisation of the electrophoretic conditions

Further gels were then prepared, with the electrophoresis carried at either 120 V or 50 V for 40 minutes with varying concentrations of agarose (0.5%, 1% or 2%)

using sodium borate buffer. 16 μ l of 102 g/L L6 Kraft lignin was loaded into each lane along with 4 μ l of 50% glycerol. The gels were imaged using a digital camera.

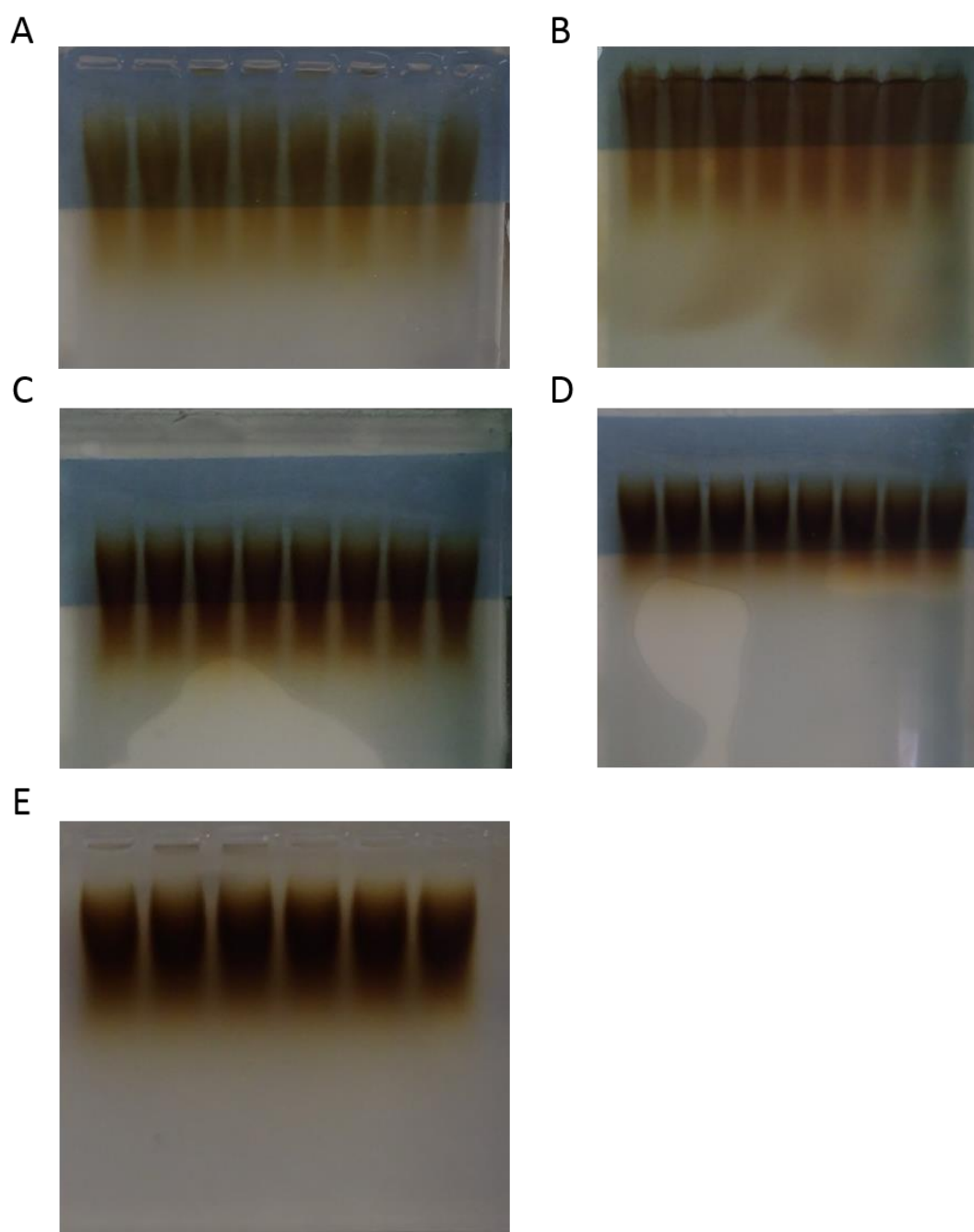


Figure 3-2 The effect of varying agarose gel concentration on lignin migration with gels run for 40 minutes: A: 1% (w/v), 120 V. B: 2% (w/v) 120 V. C: 0.5% (w/v) 120 V. D: 1% (w/v) 50V. E: 0.5% (w/v) 50 V.

Figure 3-2 shows a variety of different gel conditions and how the resolution of electrophoresis is altered, at this point it was assumed that the brown smear was the lignin in the sample; therefore this was used as an indicator of the gel electrophoresis resolution. The unoptimised gel (A) shows a promising band but the reproducibility is very poor, with different bands migrating to different points down the gel. Additionally, at the top of some bands there was some brown colouration between the main band and the well, indicating that some of the sample had remained in the well rather than migrating. This was most likely due to the large volume of sample. For DNA gels, it is standard to load 5 ng to 1 μ g, whereas 2.5 mg of lignin was loaded in each well (Tweedie J. W. et al, 2005).

It was thought that a higher concentration of agarose would lead to higher resolution and improved separation of the lignin. Gel (B) shows how a 2% (w/v) agarose gel slows the migration; a large amount of the sample fails to leave the well. This is explained by the higher concentration increasing the number, and decreasing the size, of the pores in the agarose gel (Maaloum M. et al, 1998). Gel C was run at 0.5% (w/v) agarose, and shows both improved separation and resolution with a faster migration rate. The figure also shows that some bands migrate slightly further than others, especially those in the middle compared to those in the outside lanes. Gel D showed good resolution and reproducibility, with bands migrating almost identically. A combination of the conditions in gels C and D were used to produce gel E (50 V with 0.5% agarose), which has better separation and reproducibility compared to the other gels.

3.2.3 Effect of pH

Lignins are often poorly soluble in water, and their solubility is dependent upon the pH of the solution. This is because phenoxide functional groups in the lignin have a $pK_a \sim 9$ (Ragnar M. et al, 2000), however the wide variety of structural types, and their hydrophobic environment give a wide pH titration curve. Kraft lignins are more soluble as they have structural modification, however as the acidity approaches pH 4 they become insoluble and precipitate, indeed this is a method for their recovery. Therefore the effect of pH (and different buffers) was investigated. Electrophoresis was carried out at 100-120 V for 10 minutes using a Clarit-E Mini gel tank and with either SB buffer (36.4 mM boric acid and 10 mM sodium hydroxide) or TAE buffer (40 mM tris base, 20 mM acetic acid and 1 mM EDTA), pH was adjusted using either 5 M hydrochloric acid or 5 M sodium hydroxide. 5 μ l of 1.5 g/L L5 or L6 Kraft lignin was mixed with 2 μ l of 50% glycerol and loaded onto the gel sequentially before electrophoresis. The gels were imaged using a Gel Doc™ XR+ Gel Documentation System using UV light (302 nm) as excitation light and measuring emission at 602/50 nm.

TAE gel		SB gel	
L5	L6	L5	L6
1	2	1	2

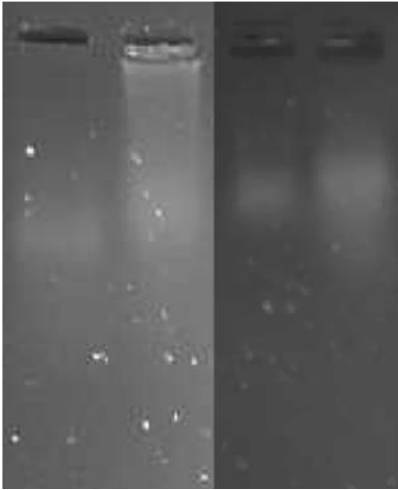


Figure 3-3 Comparison of Lignin L5 and L6 electrophoresis on a 1% agarose gel in: Left TAE buffer at 100 V for 10 minutes; Right, SB gel for 120 V for 10 minutes.

Figure 3-3 shows an image from an experiment to compare separation of lignin on TAE gels compared to SB buffer gels. The L5 lignin moves through the gel matrix as a broad band, and is distinctly different to the migration of L6, where a smear is produced starting from the loading well. This implies that L6 does not move efficiently through the gel. These results differ from those with SB buffer, where L6 effectively migrates through the gel. This is supported by the literature that shows that use of SB buffer can lead to higher resolution in the electrophoretic separation of DNA (Brody J. R. et al, 2004).

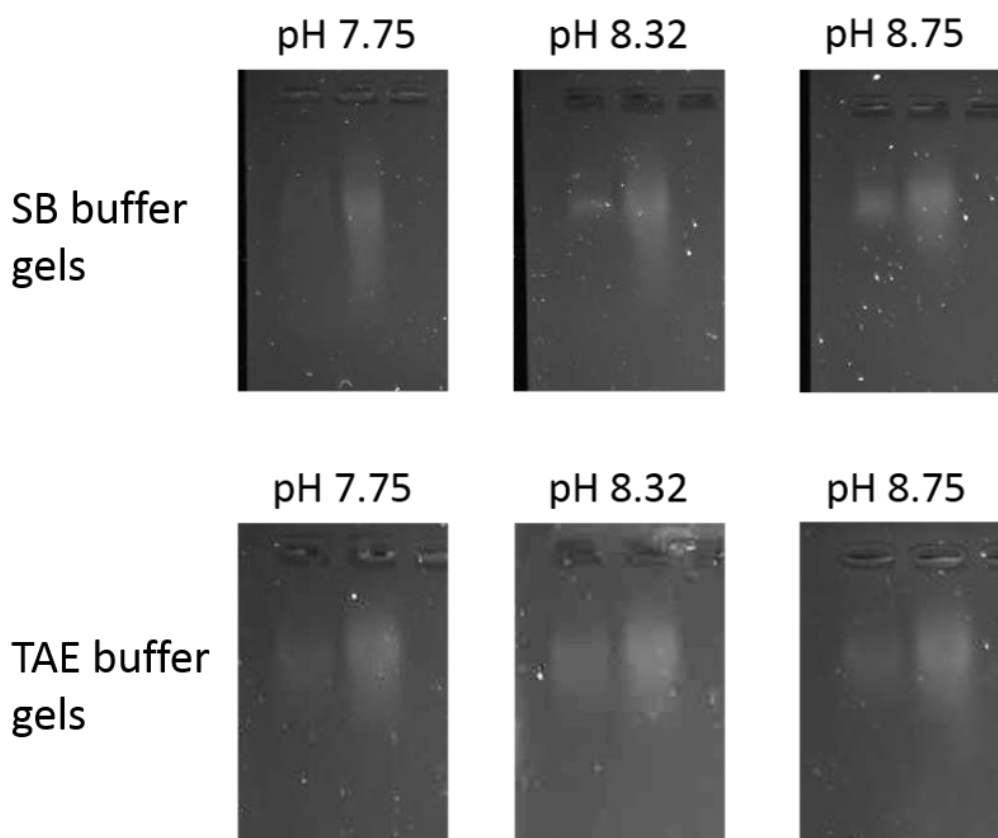


Figure 3-4 Effect of pH on TAE and SB buffer gels with lignin L5 and L6 after electrophoresis at 120 V for 10 minutes. The two samples on the left side of each gel using TAE and SB gels ran at different pHs.

The experiment shown in Figure 3-4 was carried out to test the effect of pH on electrophoresis. SB buffer was used at pH 7.75, 8.32 and 8.75 whilst TAE buffer was also tested at the same pH. 1% agarose gels were used and electrophoresis was carried out at 100 V for 10 minutes with 1.5 g/L L5 and L6 loaded sequentially. For the SB gels, at a lower pH the resolution was poorer because the lignin is less ionised, and also because the buffering capacity at pH 7.75 and 8.32 is outside the SB buffer range. The TAE gels were consistent at each of the pHs used, and this is supported by the literature which states that tris buffers are effective above pH 7.5 (Stoll V. S. et al, 1990). As a result, SB buffer has the most promise for electrophoresis of lignin but not below pH 8.75. This shows that pH

has an important role in separation and that this should be taken into account when selecting electrophoresis buffers.

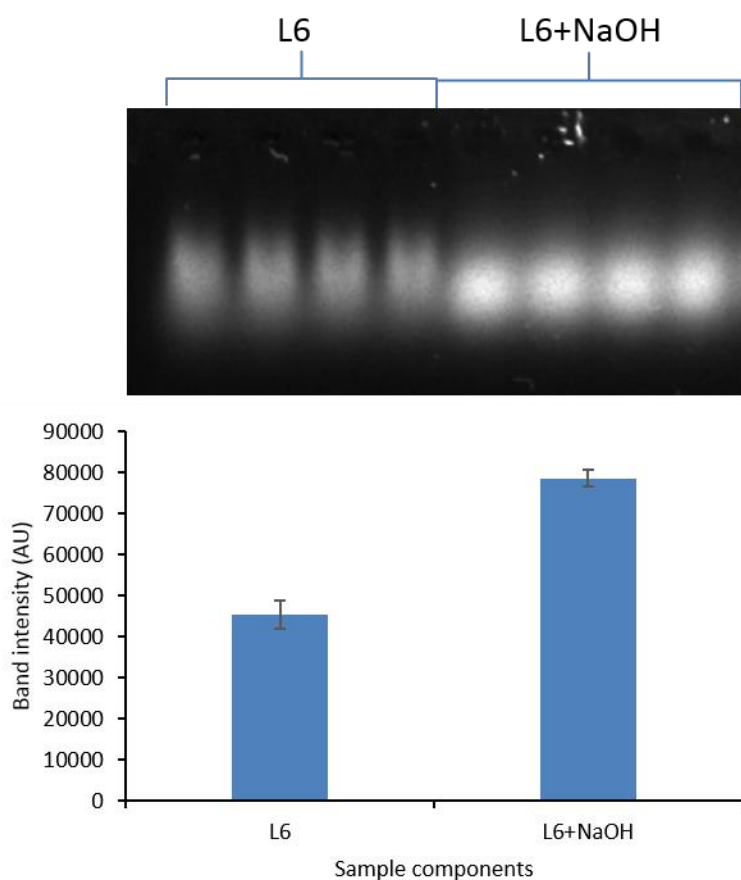


Figure 3-5 The effect of adding hydroxide to L6 lignin (5 g/L) samples before electrophoresis. Control lane L6 in SB buffer and L6 lignin with 0.375 M NaOH.

pH effects on lignin separation were tested with sodium hydroxide added to the samples before electrophoresis. Lignin samples were prepared by adding 50 μ l of 5 g/L L6 kraft lignin to 20 μ l of 50% glycerol and 20 μ l of water for the L6 sample or 20 μ l of 0.375 M NaOH for the L6+NaOH sample. Electrophoresis was carried out using a Clarit-E Maxi gel tank, with 10 μ l of sample added to each lane before carrying out electrophoresis at 50 V for 1 hour using a 1% agarose gel and 73 mM boric acid and 20 mM sodium hydroxide at pH 8.75.

Figure 3-5 shows the change in lignin migration when sodium hydroxide is added to samples prior to electrophoresis. The native L6 Kraft lignin migrates more slowly than the sample with sodium hydroxide. This may be because the lignin is more soluble as a result of ionisation of the phenol residues, but could also be reducing aggregates. The bands with NaOH are more intense than without, and this may be that the absorption or emission extinction coefficients of anionic phenoxide residues are higher, or that with less aggregation there is less quenching. The increase in band intensity means that lower concentrations can be measured more accurately. Electrophoresis without NaOH was found to be ineffective with the organosolv samples as the sample didn't fully migrate and remained within the gel well (data not shown). The method was used mainly in experiments in Chapter 6 onwards.

3.2.4 Effect of buffer strength

Electrophoresis was carried out at 50 V for 60 minutes using a Clarit-E Mini gel tank. A lower buffer concentration of 18.2 mM boric acid and 5 mM sodium hydroxide (half the concentration of the boric acid buffer used in the other experiments) was used for one gel and the other standard boric acid buffer concentration were used (36.4 mM boric acid and 10 mM sodium hydroxide). 25 μ l of 300 g/L Alkali lignin was mixed with 10 μ l of 50% glycerol before adding to each lane. The gels were imaged with a digital camera.

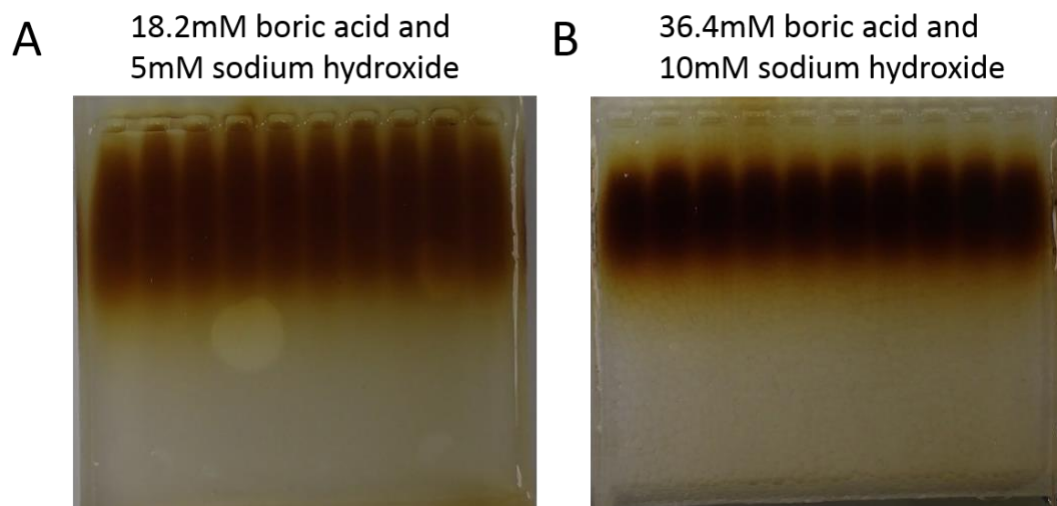


Figure 3-6 Comparing the effect of buffer strength on electrophoresis. A: sodium borate buffer B: higher concentration of sodium borate buffer

Figure 3-6 demonstrates the importance of buffer strength, with the gel using 36.4 mM sodium borate showing better migration than that at 18.2 mM. One of the roles of the buffer is to conduct current, without itself decomposing, another is to control the sample pH, i.e. ionisation of the phenolic residues. Electrophoresis with the lower concentration buffer shows much of the sample remained in the well, and a large smear produced, rather than a defined band. Furthermore the separation was not repeatable between lanes using 18.2 mM but was when using 36.4 mM boric acid. The large sample size perhaps required a higher ionic strength to induce migration. Sodium borate (SB) buffer was preferred, as it gives a higher resolution at lower ionic strengths compared to standard agarose buffers, such as TAE (tris-acetate-EDTA) and TBE (Tris-borate-EDTA) (Brody J. R. et al, 2004). A higher ionic strength can lead to excessive heating with melting of the agarose gel. Furthermore above pH 8.5 lignin is polyanionic due to the phenolate groups and the pH of the SB buffer was 8.75, allowing for effective ionisation and electrophoretic migration.

The preparative possibilities are illustrated by comparing Figure 3-1, with ~2 µg of lignin per lane, with Figure 3-6 gel B ~7.5 mg of lignin per lane, that still produces a defined band.

3.2.5 Initial extraction, electrophoresis and imaging of lignin experiment

In order to check the reproducibility of electrophoretic separation a 0.75% agarose gel was prepared with SB buffer. 16 µl of 100 g/L L6 was mixed with 4 µl of 50% glycerol before loading into each gel lane. Electrophoresis was carried out at 50 V for 40 minutes. After electrophoresis the gel band was cut into two fractions measured using a ruler to measure distance travelled: 0.1-1 cm of distance travelled from well and another fraction between 1-2 cm travelled. Once the bands were cut, the gel fractions were freeze dried until dry. The fractions were then ground into a powder before addition of 3 ml of water to extract the lignin from the agarose. The extracted lignin was then loaded onto a 1% agarose SB gel (5 µl of sample and 2 µl of 50% glycerol) before carrying out electrophoresis at 120 V for 10 minutes. Before imaging using a Gel Doc™ XR+ Gel Documentation System using UV light (302 nm) as excitation light and measuring emission at 602/50 nm.

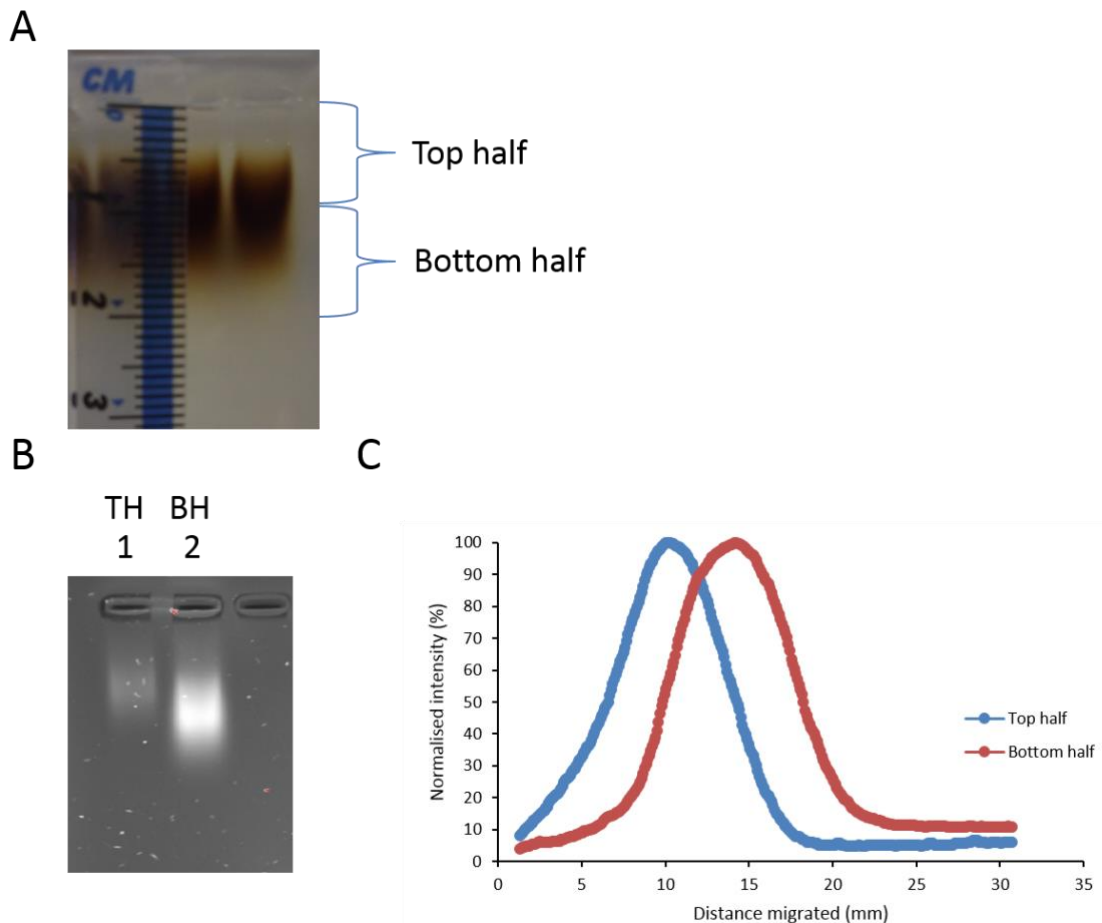


Figure 3-7 Results after extraction and electrophoresis of the top half and bottom half of the gel bands. A: photograph of 100 g/L L6 lignin on a SB 0.75% agarose gel that was ran at 50 V for 40 minutes, with the top band and bottom band marked prior to extraction. B: lignin separation after extraction of the lignin from each of the gel fractions and repeating electrophoresis at 50 V for 40 minutes. C: Imaging of the gel showing emission intensity.

The experiment shown in Figure 3-7 was carried out to determine whether the electrophoretic separation of lignin is repeatable. Figure 3-7 C shows image analysis of the gel in Figure 3-7 B in which there is a clear difference between the extracted lignin, from the top half of the band cut from the gel in Figure 3-7 A compared to the bottom. This demonstrates that different fractions of the lignin sample have different electrophoretic properties. On the other hand despite cutting discrete bands, some overlap occurs when the second gel is run. This

might suggest that agarose gel electrophoresis of lignin does not have a high resolution. However it should be taken into account that it was difficult to cut the band out of gel in a completely repeatable manner; therefore there may be sections of the top half of the band cut out with the bottom half and vice versa. Additionally, as gel electrophoresis was carried out twice, any uniformity errors in the gel will have been increased.

The problem with this experiment is that highly concentrate, overloaded lignin samples are used for the initial gel Figure 3-7 A, and show a lower resolution because large amount of material can lead to 'clogging' of the agarose pores meaning that the material moves through the pores at a changed rate. This will lead to an apparent lower resolution of separation in section C of Figure 3-7.

3.2.6 Purification of lignin from gel

Electrophoresis was carried out at 50 V for 40 minutes in a Clarit-E Mini gel tank with sodium borate buffer and a 0.75% agarose gel. The Clarit-E Mini gel tank was selected to use for the lignin purification experiments because 2 mm thickness gel combs could be used and therefore more lignin sample could be loaded onto the gel (and therefore be able to extract more lignin). 0.75% was used rather than 0.5% agarose due to difficulty removing the gel from the cast without the gel breaking. Alkali lignin was dissolved in water to a concentration of 300 g/L and L6 was freeze dried before re-dissolving in water to a concentration of 200 g/L. 25 μ l of the lignin sample was then mixed with 10 μ l of 50% glycerol before loading onto the gel.

Once electrophoresis was complete the 'whole' of the L6 band was cut out using a scalpel and for the Alkali lignin the same was done except for some gel samples

the band was cut in half to produce a sample of the top half and lower half of the band.

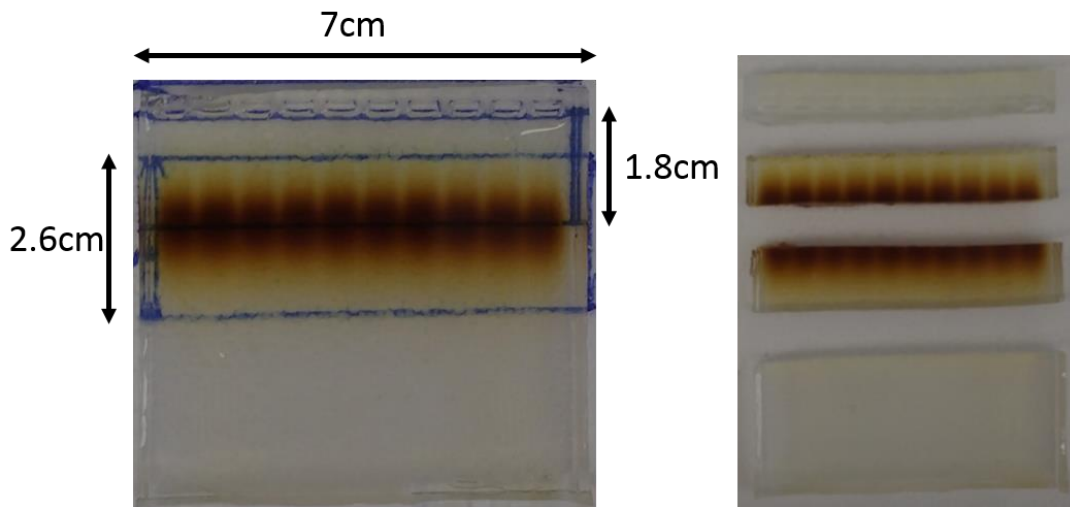


Figure 3-8 Image of an agarose gel after electrophoresis at 50 V for 40 minutes using 300 g/L Alkali lignin. With the different gel fraction that were used for purification (top section of the band, bottom section of the band and the whole band).

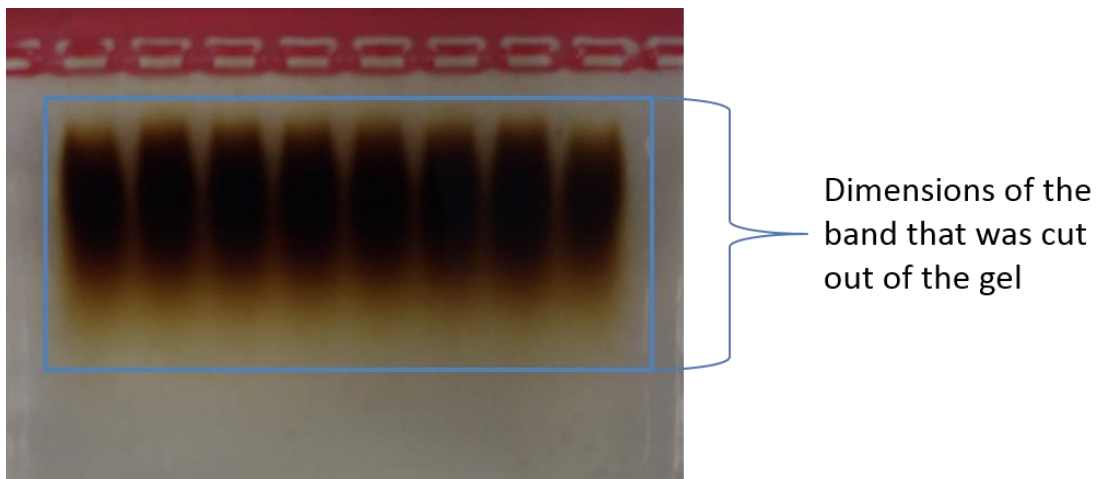


Figure 3-9 Image of an agarose gel after electrophoresis at 50 V for 40 minutes with 200 g/L L6 lignin. The dimensions of the 'whole band' of L6 that was used for extraction and purification are marked.

The gel bands were then freeze dried, once the gels were fully dry, a pestle and mortar was used to grind the gel into a fine powder. The powder was then added to a round bottom flask with around 100 ml of distilled water and stirred overnight. The mixture was then filtered through a glass filter tube. Concentrated hydrochloric acid was then added to the lignin solution, until the solution turned opaque and then the mixture was kept at 4°C overnight. The solution was then centrifuged at 4500 rpm for 15 minutes, the supernatant was then discarded and the pellet was freeze dried- the freeze dried sample was then ready for analysis.

3.2.7 GPC Analysis

10 mg of freeze dried lignin samples were added to a glass tube (the entire reaction was carried out in the same tube for each sample). 200 µl of pyridine (for analysis) was added before vortexing and then addition of 400 µl of acetic anhydride before vortexing again. The mixture was then left for 24 hrs and then 200 µl of methanol was added on ice. The methanol was evaporated and 200 µl of toluene was added before evaporation and this was carried out twice before adding 200 µl of methanol and evaporating again. The remaining acetylated lignin sample was then freeze dried. 1 ml of THF was then added to vials ready for GPC by filtering in a 0.45 µm PTFE filter.

SEC was carried out with THF as eluent at 1 ml/min using an Agilent PLgel MIXED-C column, an UltiMate 3000 Autosampler Column Compartment for sample handling, and an UltiMate 3000 Photodiode Array Detector. A Chromeleon was used for initial sample analysis and export before using Agilent Cirrus GPC software for molecular weight analysis.

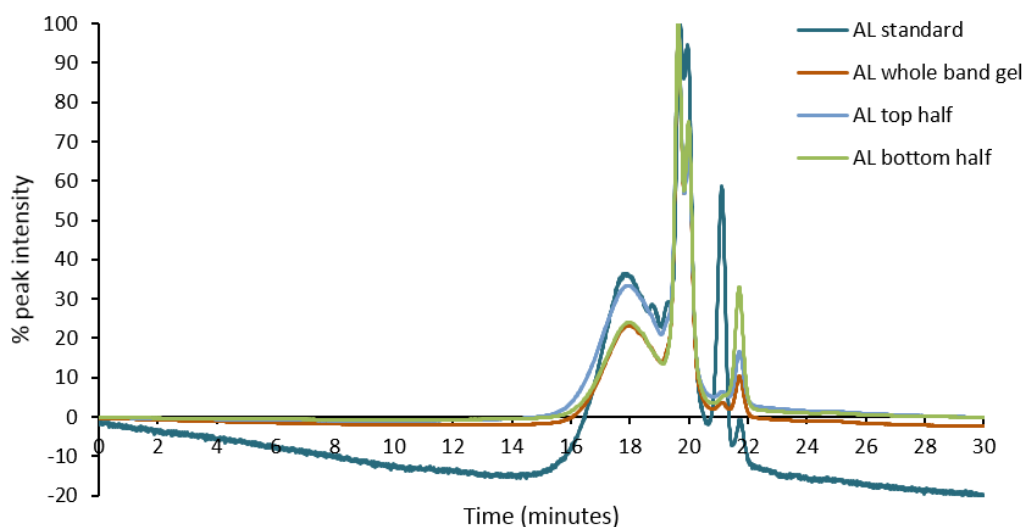


Figure 3-10 Normalised GPC plot of standard Alkali lignin compared to lignin purified from gels (the entirety of the band, the top half and the bottom half of the band). Not all of the AL sample dissolved in the THF, so the plot is not representative of the entire sample.

The GPC chromatogram in Figure 3-10 shows all of the AL samples had similar elution profiles, with a broad peak at 18 minutes, sharp large peak at around 20 minutes and small peaks at 22 minutes. A difference in the samples is a sharp peak at around 21 minutes for the AL standard which could be due to a low molecular weight compound that passes through the agarose gel which could be residual toluene from incomplete evaporation prior to SEC. Since not all the acetylated AL dissolved in the THF, it is not possible to confirm the chromatogram is representative of the entire lignin sample. Furthermore, absorbance at 280 nm was used to measure the samples and since aromatic absorption occurs at this wavelength, this indicates the presence of lignin (Tanaka K. et al, 1999).

Table 3-1 List of the Mn and Mw values for molecular weight for standard Alkali lignin, Alkali lignin purified from the entirety, the top half and the bottom half lignin band on the gel.

Sample Name	Mn	Mw
AL standard	291	1132
AL whole band	250	790
AL top half	281	1123
AL bottom half	245	793

In Table 3-1, the AL standard and the lignin extracted from the top half of the band, have similar values for Mn and Mw. The molecular weight values of lignin extracted from the whole band and the bottom half are different, but this is probably due to the poor chromatography of these samples. It is unexpected that the lignin from the top half of the band would have such similar values to the lignin standard, but this is likely because only a fraction of the lignin sample was able to dissolve in THF, so the chromatogram is not representative of the whole lignin sample. Therefore no conclusions can be drawn from these values.

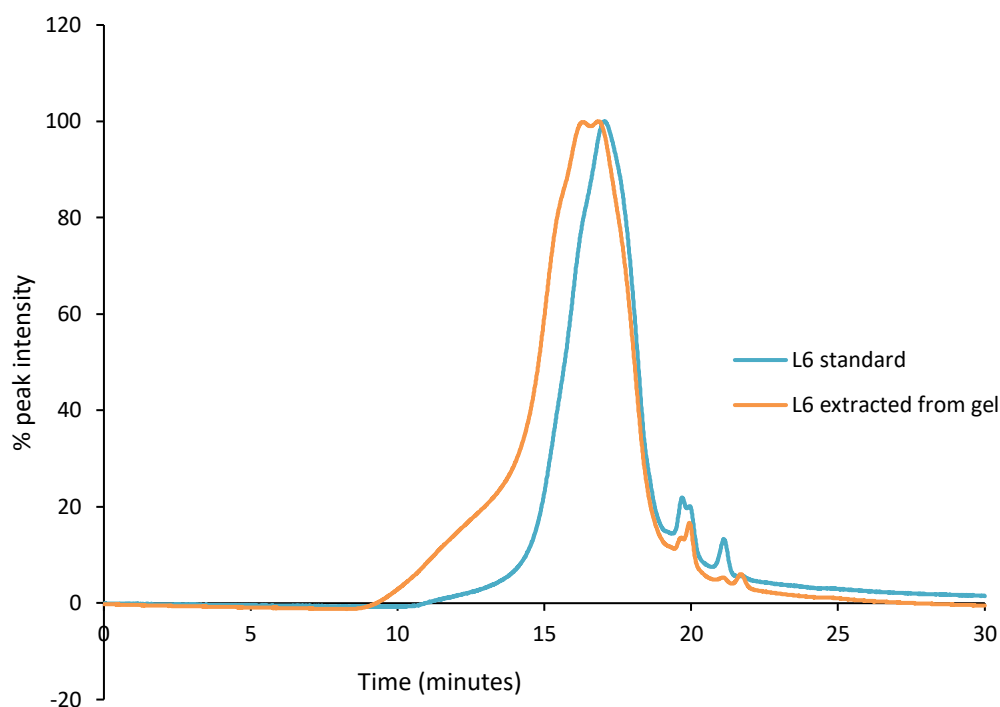


Figure 3-11 Normalised GPC plot of the L6 lignin standard compared to the L6 extracted from the whole band on the gel

Figure 3-1 shows the similarity of the L6 standard and the material extracted from the gel band. The L6 standard has a major peak between 15 and 19 minutes with a shoulder starting at 11 minutes, whilst the L6 gel lignin shows the same peak centred at 16.5 minutes, but the shoulder starts at around 10 minutes. This may be due to sample aggregation caused by twice freeze drying the sample as part of the extraction procedure. The slope of the major peak is very similar in both samples. This is significant as it shows that the band on the gel not only includes the high molecular weight fraction but the entirety of the lignin molecular weight distribution. This, combined with the aromatic detection wavelength, is convincing evidence that lignin is responsible for the band on the gel. The results indicate that gel electrophoresis can be used to assess molecular weight and the quantity

of lignin in a sample. The same minor peaks at around 20 and 21 minutes are observed in each of the sample but this is perhaps due to residual toluene or pyridine in the sample.

Table 3-2 Values for Mn and Mw for molecular weight of L6 standard and L6 extracted from the whole band on a gel.

Sample Name	Mn	Mw
L6 standard	1076	12243
L6 whole band gel	1698	95929

Table 3-2 includes the values for Mn and Mw, for which the lignin extracted from the gel is higher for both of the values. This is due to the aggregation leading to an artificially high value for molecular weight.

3.2.8 MALDI-TOF Analysis of Lignin standards

MALDI-TOF mass spectrometry was tested as a way of providing a molecular weight distribution of lignin standards, which could then be used as a gel marker. Samples of L6 were sent to the Proteomic Laboratory at the University of York. Samples were analysed at 1 mg/ml and 10 mg/ml with 10 mg/ml of the following matrices made up in 50% acetonitrile and 0.1% TFA: α -Cyano-4-hydroxycinnamic acid (CHCA), 2',4',6'-Trihydroxyacetophenone monohydrate (THAP), Sinapic acid (SA) and 2,5-Dihydroxybenzoic acid 2-(4-Hydroxyphenylazo)benzoic acid. The samples were analysed using reflection mode from 100 Da to 4000 Da.

The results showed no major differences and just noise outside of the peaks for the matrices. This indicates that the lignin was not ionised. This could have been due to contaminants in the lignin sample. This highlights the challenges in obtaining the molecular weight distribution of lignin.

3.2.9 ^1H NMR of gel extracted lignin

Lignin extracted from the agarose gels were dissolved in DMSO and analysed using a Bruker Biospin Avance III 400MHz spectrometer. The ^1H NMR, was carried out by Dr Betty Cottyn at INRA Versailles.

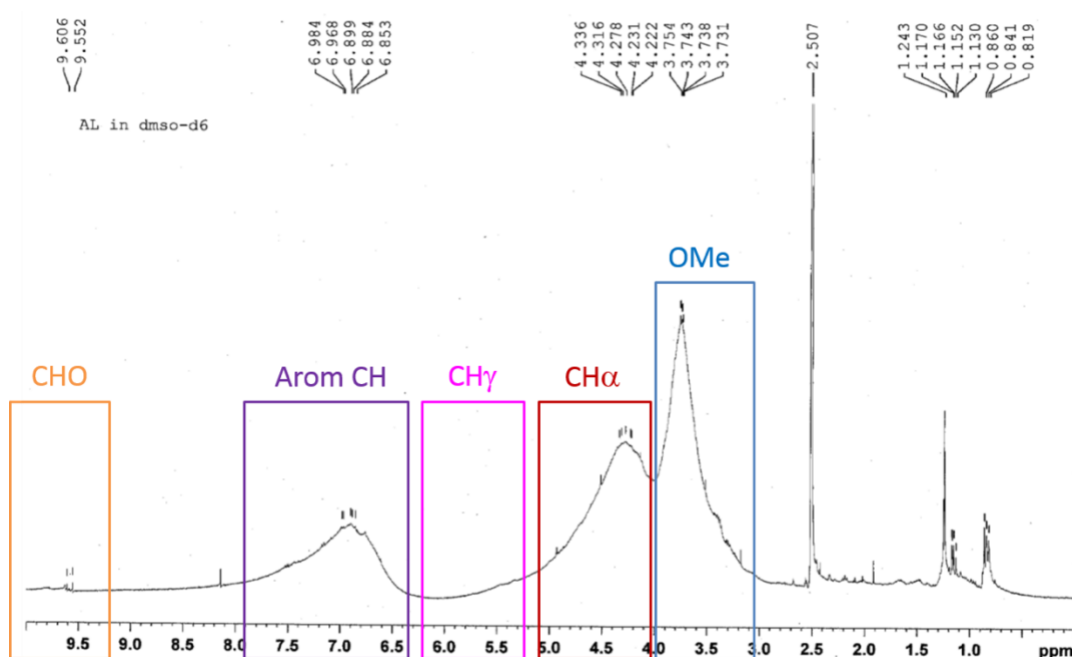


Figure 3-12 ^1H NMR spectra of gel extracted Alkali lignin, with spectra labelled with the corresponding lignin related peaks

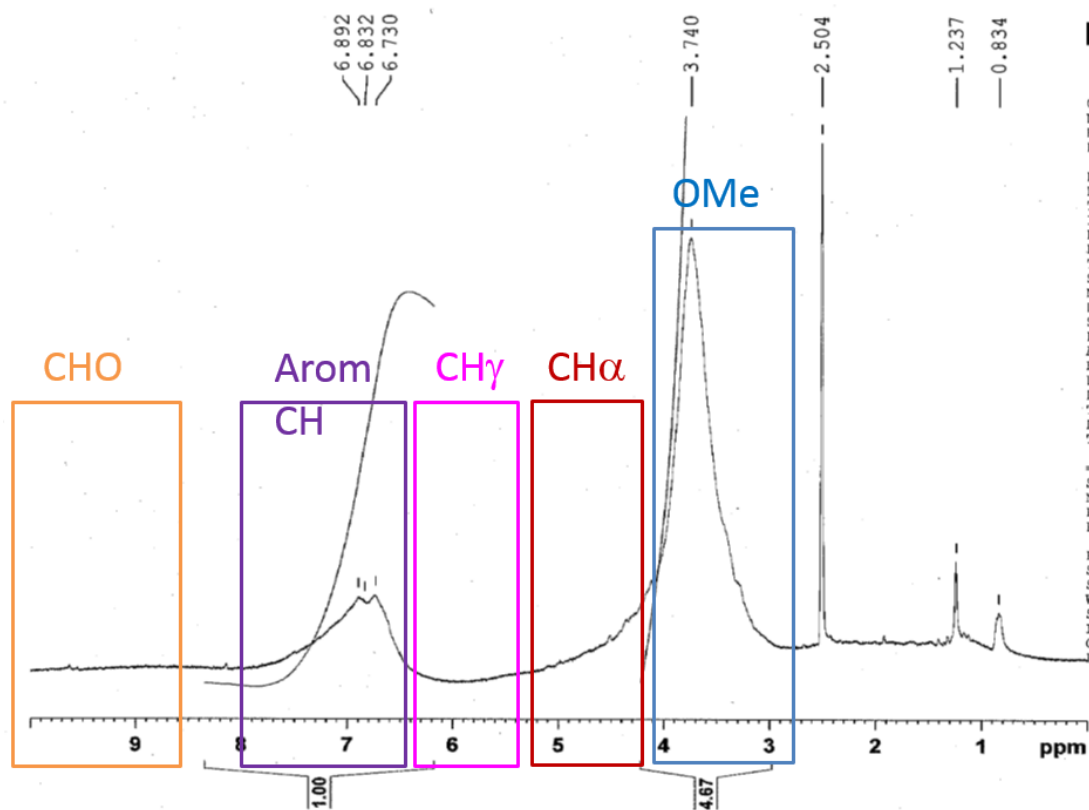


Figure 3-13 ^1H NMR spectra of extracted L6 lignin, with spectra labelled with the corresponding lignin related peaks

Figure 3-12 and Figure 3-13 show samples of the AL and L6 bands extracted from the gel, respectively. Multiple peaks are observed that are characteristic of lignin, such as peaks for: CHO (just after 9.5 ppm), aromatic CH (at around 7 ppm), CH_γ (at around 5.5 ppm), CH_α (just before 4.5 ppm) and OMe peak (at around 3.75 ppm). The similarity of the spectra indicate that the material extracted from the gel is lignin. This is highly indicative for the presence of lignin. However these results alone do not indicate whether the methoxy peak (characteristic of lignin) is due to sugars present or lignin.

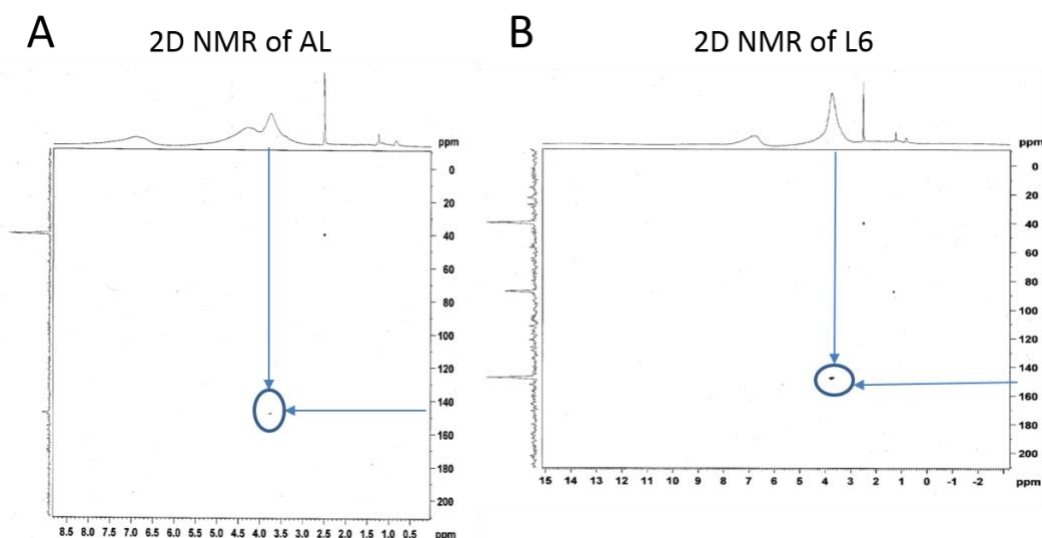


Figure 3-14 2D ^1H and ^{13}C NMR of Alkali lignin (A) and L6 (B). The signal of interest is circled for clarity. The spectra on the top of the figure corresponds to Figure 3-12 and Figure 3-13 respectively.

The spectra in Figure 3-14 confirm that the methoxy peak is due to lignin and not due to the presence of sugars. This additionally confirms that the aggregation shown in Figure 3-11 was not due to agarose binding to lignin polymers but due to aggregation of lignin polymers. Additionally, these results match with NMR spectrum produced using Kraft lignin in the literature (Nagy et al., 2010).

3.2.10 Pyrolysis GC/MS

Pyrolysis was carried out according to (Biller P. et al, 2014). Samples of L6 standard, L6 that had been acid precipitated, L6 extracted from an agarose gel, AL standard and AL extracted from an agarose gel were used for pyrolysis GC/MS. Around 0.1-5 mg of each sample was pyrolysed in a quartz tube (with quartz wool at either end of the sample to fix the sample in place) using a CDS 5200 pyrolyser (CDS Analytical LLC, Oxford, PA 19363, USA) to heat the samples to 550 °C at a heating rate of 20 °C per millisecond, with a probe hold

time of 60 seconds. Helium was used as the carrier gas to ensure that oxygen did not contact the sample and was flowed at a pressure of 49.2 kPa with a total flow rate of 17.7 ml per minute. A TENAX absorbent trap was used to contain the pyrolysed compounds before desorbing and injecting into a GC-MS-QP2010 mass spectrometer (Shimadzu Corporation, Kyoto, Japan) at an injection temperature of 280 °C using split injection onto a Rtx 1701 60m column, with a column thickness was 0.25 µm. Compounds were analysed that had a mass to charge ratio between 50 and 600 and peaks were identified using the NIST mass spectral database (database versions used were 27 and 147).

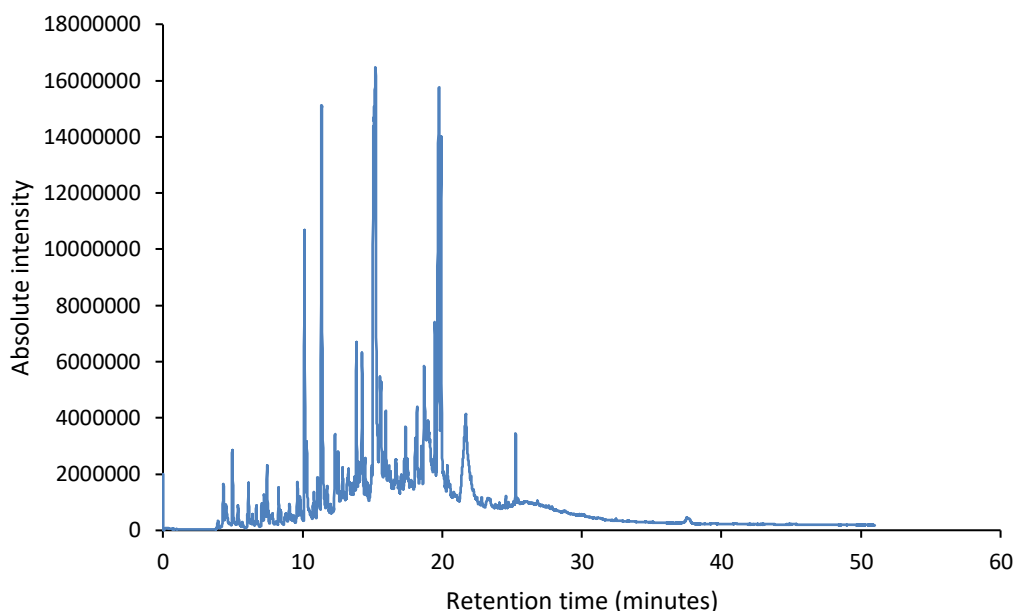


Figure 3-15 Chromatogram of the peaks produced from pyrolysis GC/MS of agarose standard

In the control, the majority of the peaks resulting from agarose pyrolysis appear between 5 and 20 minutes. From 20 to 30 minutes there are two peaks, but a significant shoulder is present that indicates incomplete depolymerisation of the agarose prior to gas chromatography.

Table 3-3 List of the top 10 identified peaks from the agarose sample at the end of the pyrolysis GC/MS

Ret. Time	Compound name
10.144	Furfural
10.295	2-propyl-Furan,
11.357	1-(2-furanyl)-Ethanone,
13.854	3-methyl-1,2-Cyclopentanedione,
14.259	3-Hydroxypyridine monoacetate
15.223	Methyl 2-furoate
15.621	2-methoxy-1,4-Benzenediol,
19.477	1-(2-furanyl)-1-Propanone,
19.768	Allyl isovalerate
19.928	1,4-dihydro-2,3-Quinoxalinedione,

Table 3-3 shows that the majority of the peaks identified were due to furan related compounds produced by the pyrolysis of the agarose polymer. It has been shown in the literature that furan related compounds have been identified after Py-GC/MS of an agarose sample (Helleur R. J. et al, 1985). Large amounts of these compounds in any of the gel extracted lignins would indicate agarose contamination.

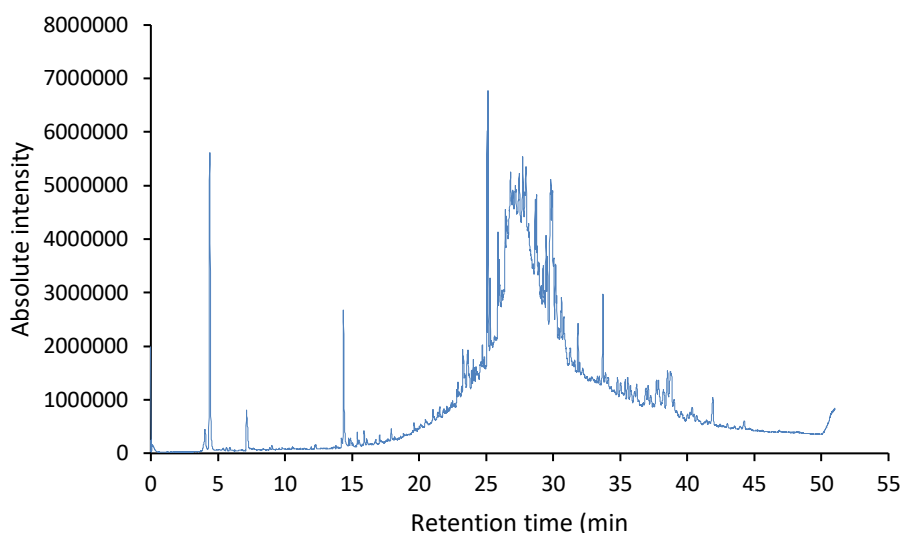


Figure 3-16 Chromatogram of the peaks produced from pyrolysis GC/MS of Alkali lignin standard

Pyrolysis GC of the AL standard showed several singular, sharp peaks that occur around 5, 15 and 25 minutes. A large rounded peak appears at 15 and continues to 50 minutes, which is likely to be the AL failing to undergo full pyrolysis resulting in a large number of high molecular weight compounds. Sulphur containing inhibitor compounds can reduce pyrolysis efficiency; lignin consists of 4% of sulphur by mass.

Table 3-4 List of the top 10 identified peaks from the Alkali lignin standard at the end of the pyrolysis GC/MS

Ret. Time	Compound name
4.391	Ethanethiol
14.361	2-methoxy-Phenol,
25.072	9-Octadecenoic acid (Z)-, methyl ester
25.14	9,12-Octadecadienoic acid, methyl ester, (E,E)-
28.753	Benzedrex
29.474	N,N-dimethyl-Octanamide,
29.585	9,12-Octadecadienoic acid (Z,Z)-
29.835	9-Octadecenamide, (Z)-
30.186	9,12-Octadecadienoyl chloride, (Z,Z)-
33.721	bis(2-ethylhexyl) ester1,3-Benzenedicarboxylic acid,

Table 3-4 shows that several phenolic compounds were detected. Other compounds identified are high molecular weight triglycerides not found in lignin, so this identification may be false.

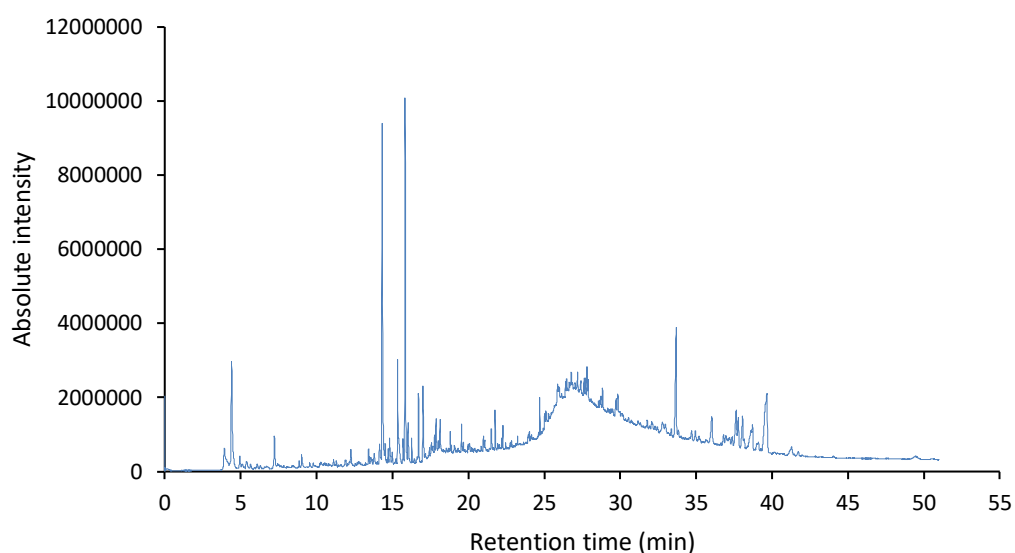


Figure 3-17 Chromatogram of the peaks produced from pyrolysis GC/MS of Alkali lignin extracted post-electrophoresis (whole band).

Figure 3-17 shows AL extracted from the electrophoresis gel, and is considerably cleaner than the standard AL in Figure 3-16. The gel electrophoresis appears to have improved the purity based on the pyrolysis trace. Large sharp peaks occur around 15 minutes, that in Figure 3-16 were identified as guaiacol, cresol, dimethoxytoluene and related phenols which is what would be expected by pyrolysis of lignin.

Table 3-5 List of the top 10 identified peaks from the gel extracted Alkali lignin sample at the end of the pyrolysis GC/MS

Ret.Time	Compound name
4.405	dimethyl Peroxide,
14.32	2-methoxy-Phenol,
15.339	Cresol
15.829	Cresol
16.714	2,3-Dimethoxytoluene
17.007	4-ethyl-2-methoxy-Phenol,
18.135	2-methoxy-4-propyl-Phenol,
21.758	tetradecyl-Oxirane,
24.698	2-propenyl esterDecanoic acid,
33.681	bis(2-ethylhexyl) ester1,3-Benzenedicarboxylic acid,

Additionally, there are no furan containing compounds indicating that lignin can be purified from the gel without entraining agarose. The method could be used to produce technical lignins by cutting-out bands and fractions and isolated. For example, different molecular weight fractions could be purified and used in degradation studies to identify the most degradable/toxic part of the lignin sample.

Alternatively electrophoresis could be used to purify polymeric lignin from low molecular weight compounds and used for multiple different applications.

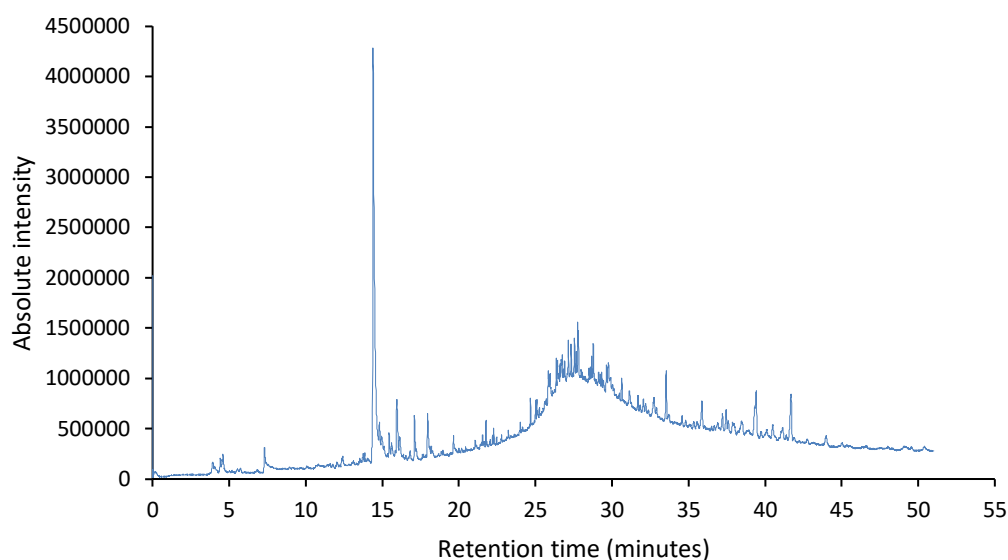


Figure 3-18 Chromatogram of the peaks produced from pyrolysis GC/MS of L6 lignin standard

Figure 3-18 shows similar results to Figure 3-16 in terms of the poor depolymerisation indicated by the large peak between 20 and 50 minutes. A large sharp peak is observed at around 15 minutes, similar to the gel extracted lignin in Figure 3-17. Table 3-6 shows several peaks produced by phenolic compounds, and notably guaiacol and cresol. Like the AL standard, high molecular weight compounds at >26 minutes are likely false library matches confirming the hypothesis of incomplete pyrolysis.

Table 3-6 List of the top 10 identified peaks from the L6 standard sample at the end of the pyrolysis GC/MS

Ret.Time	Compound name
14.396	2-methoxy-Phenol,
15.946	Creosol
17.097	4-ethyl-2-methoxy-Phenol,
26.741	Octacosane
27.328	N,N-Dimethylvaleramide
27.547	(Z)-9-Octadecenamide,
27.762	1-Docosene
27.808	octyl-Cyclohexane,
28.775	1-Docosene
33.536	bis(2-ethylhexyl) ester1,3-Benzenedicarboxylic acid,

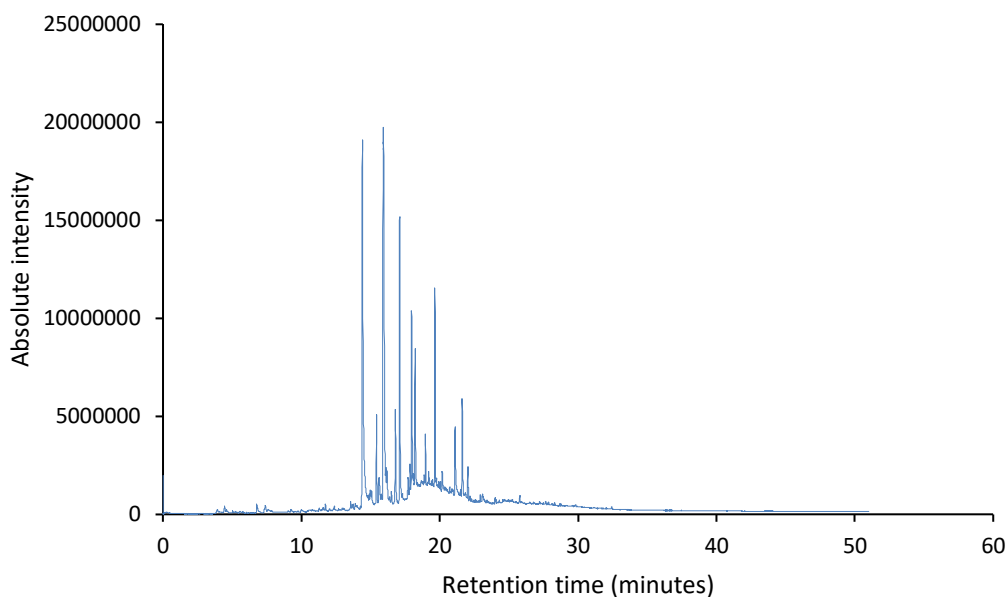


Figure 3-19 Chromatogram of the peaks produced from pyrolysis GC/MS of acid precipitated L6 standard.

Figure 3-19 shows a pyrolysis GC trace of L6 after acid precipitation, that is considerably cleaner than the L6 standard, Figure 3-16 with only sharp peaks observed. Precipitation could be used as an effective method of sample preparation for pyrolysis GC/MS. The majority of the peaks were present between 15 and 22 minutes, and Table 3-7 shows low molecular weight aromatic compounds expected by pyrolysis of lignin.

Table 3-7 List of the top 10 identified peaks from the L6 precipitated sample at the end of the pyrolysis GC/MS

Ret.Time	Compound name
14.412	2-methoxy-Phenol,
15.428	2-Methoxy-5-methylphenol
15.927	2-Methoxy-5-methylphenol
16.794	3,4-Dimethoxytoluene
17.104	4-ethyl-2-methoxy-Phenol,
17.964	4-Hydroxy-2-methylacetophenone
18.222	2-methoxy-4-propyl-Phenol,
19.651	trans-Isoeugenol

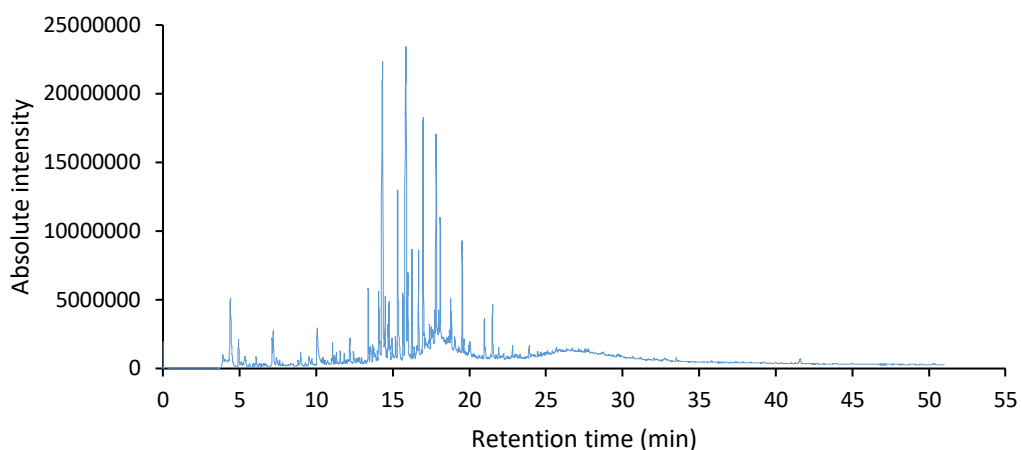


Figure 3-20 Chromatogram of the peaks produced from pyrolysis GC/MS of L6 extracted post-electrophoresis (whole band).

Figure 3-20 shows a trace of L6 after gel extraction with a large number of peaks between 5 and 25 minutes that in Table 8 are similar to the acid precipitated L6 in Figure 3-17. Several compounds such as mequinol and 2-methoxy-5-methylphenol are present in both the results for the precipitated lignin and the lignin extracted from the gel band. This is further supported by the literature, where pyrolysis of kraft lignin produced similar products (Lazaridis P. A. et al, 2018) (Zhang et al., 2012). and provides further evidence that band extracted from L6 is lignin. The lack of sugar derived compounds indicates that contamination of cellulose or hemicellulose is not responsible for the band. Agarose related peaks are also not detected, indicating that that the aggregation shown in the GPC of gel extracted L6 is due to aggregation of lignin polymers, and not the aggregation of lignin and agarose.

Table 3-8 List of the top 10 identified peaks from the gel extracted L6 sample at the end of the pyrolysis GC/MS

Ret. Time	Compound name
14.339	Mequinol
15.317	Cresol
15.65	2-Methoxy-5-methylphenol
15.868	2-Methoxy-5-methylphenol
15.995	2,3-Dimethoxytoluene
16.684	3,4-Dimethoxytoluene
16.986	4-ethyl-2-methoxy-Phenol,
17.827	1-(2-hydroxy-5-methylphenyl)-Ethanone,
18.097	Eugenol
19.528	trans-Isoeugenol

3.3 Conclusions

The purpose of this work was to isolate quantities of lignin from the gel, to confirm its identity. To do this, the electrophoretic conditions have been optimised so that high loadings can be run in a repeatable manner which has enabled extraction and characterisation of the lignin by various methods. Loading multiple samples enables preparative isolation and possibly purification of lignins. Isolating it, allows comparison of intact and degraded lignin, quantification of the bands and detection of changes in migration and m/z. With previous work such as (Jankowska D. et al, 2018) this was not possible due to the poor band migration. Reliable migration is critical, otherwise it is impossible to attribute changes in migration to lignin degradation. Previous studies such as (Saiz-Jimenez et al, 1999) have failed to confirm the identity of the migrating species, with a single sharp band, providing little information. Whereas in this work, a 'smear' was produced, with the possibility of correlating molecular weight to charge and changes in the lignin structure. This would be a significant advance in the field.

Several hundred milligrams of lignin were purified from agarose gels and used for subsequent analysis. This can be compared to GPC, for example, where a tiny quantity of lignin is loaded onto the column, making it difficult to produce preparative quantities. This is highlighted by (Baumberger S. et al, 2007) where in alkaline GPC experiments only 50 µg of lignin was loaded, and for organic GPC between 50 and 400 µg, from a stock of 10 mg/ml lignin. In comparison, using agarose gel electrophoresis it was possible to detect 2 µg lignin in each lane using a stock of 0.25 mg/ml. Additionally, for purification, 5 mg lignin was loaded per lane using a stock concentration of 250 mg/ml.

Lignin extracted from the gel were analysed by GPC, NMR and pyrolysis GC/MS. The electrophoresis generated material was similar in all respects to the authentic standards, and to reported analytical data for lignin, demonstrating the potential of electrophoresis as a novel method for lignin purification (Nagy et al., 2010) (Zhang et al., 2012). There was difficulty analysing Alkali lignin using GPC, but as Alkali lignin was successfully run on agarose gels this demonstrates the benefit of electrophoresis over GPC. L6 lignin was successfully analysed via GPC, and it was shown that the gel band was similar to the L6 standard. There was however a problem with lignin aggregation, most likely due to the freeze drying as part of extraction, which lead to an overestimation of the molecular weight of the extracted sample. It was confirmed using ^1H NMR and py-GC/MS that this aggregation was likely due to lignin-lignin interactions and not those with agarose or hemicellulose. These results show that agarose gel electrophoresis can be used to purify lignin, due to the absence of sugars in the py-GC/MS results. In summary, these results demonstrate that gel electrophoresis can be used for evaluation and quantification of lignin as the migratory band is representative of the entire polymeric lignin sample using GPC, and is partially purified as shown by py-GC/MS.

Chapter 4

Electrophoresis of lignin with detergents

4.1 Introduction

Electrophoresis using detergents is commonplace for analysis of proteins. As proteins can form many different intra- and inter-molecular interactions, such as hydrogen bonds and van der Waals forces, sodium dodecyl sulfate (SDS) is often added to break these interactions. The addition of SDS denatures and unfolds the proteins to form a 'rod-like' structure, which removes shape as a variable in electrophoretic separation. Reducing agents such as beta-mercaptoethanol are added prior to the SDS to reduce or inhibit any disulphide bonds. In order to visualise proteins on a gel, the gel must be first stained and then de-stained, usually using Coomassie Brilliant Blue before imaging; this is because proteins do not absorb visible light. This differs to imaging of DNA, where stains such as ethidium bromide are usually added to molten agarose prior to cooling and gelling and de-staining is not necessary (Drabik A. et al, 2016).

As SDS and other detergents play an important role in the electrophoresis of proteins, this work was carried out to investigate the potential role of detergents with lignin. The idea has been reported by (Saiz-Jimenez et al, 1999) where a single sharp band was produced on a polyacrylamide gel, though it was not characterised as lignin. Although the SDS method might be less informative about molecular weight distribution, a single sharp 'bright' band could be useful for quantification of lignin.

4.2 Methods

The gels were made using either pH 8.32 TAE buffer (40 mM tris base, 20 mM acetic acid and 1 mM EDTA), pH 8.75 sodium borate buffer (36.4 mM boric acid and 10 mM sodium hydroxide) or pH 8.5 SDS running buffer (0.1% SDS, 0.025 M tris base and 0.192 M glycine). In Figure 4-3 the pH of the TAE buffer was adjusted to pH 4 using 5 M hydrochloric acid and in Figure 4-10 the pH of the TAE and SB gels was decreased using 5 M hydrochloric acid or increased using 5 M sodium hydroxide. All gels were made with 1% agarose and ran at 100-120 V for 10 minutes. 5 μ l of 1.5 g/L L5 or L6 lignin were mixed with 2 μ l of 50% glycerol and 2 μ l of either 10% SDS, 10% Triton X-100, 10% DTAB or water.

Gels were imaged using UV trans as excitation light and measuring emission at 602/50 nm. Electrophoresis was carried out using a HU6 Mini horizontal gel unit using a Biorad PowerPac 300 to apply a voltage across the gel, except for the gel in Figure 4-7 where a Clarit-E Mini gel tank was used. A gel containing SDS running buffer and 1% agarose was mixed with 0.5 μ g/ml ethidium bromide (after the gel was molten due to safety reasons). The gel was run at 50 V and images were taken after 15 and 30 minutes of electrophoresis.

Control experiments were run without lignin using TAE buffer and 1% agarose. SDS was added to both the gel (after microwaving but before pouring in order to reduce problems with foaming during boiling) and the gel buffer to a final concentration of 0.1%. No samples were loaded onto this gel. Gel electrophoresis was carried out at 100 V stopped every 10 minutes and the gel was removed from the gel buffer in order to image.

4.3 Results and Discussion

4.3.1 Investigation of surfactant electrophoresis of lignin

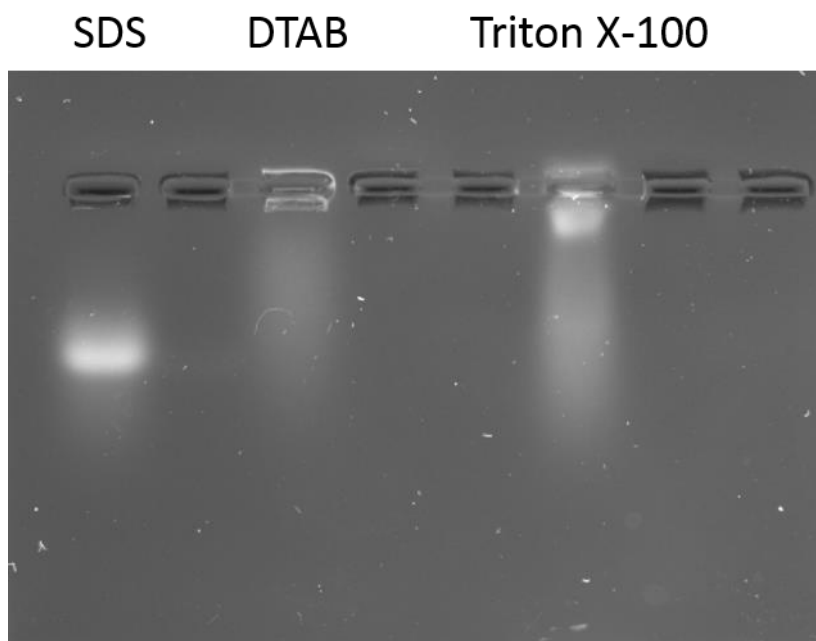


Figure 4-1 L6 Kraft lignin with either SDS, DTAB or Triton X-100 loaded onto an SB 1% agarose gel before electrophoresis at 120 V for 10 minutes.

Figure 4-1 shows the results of adding different detergents to determine which improves lignin separation, and to inform how they interact with lignin. Firstly, addition of SDS produced a single smeared band that migrates down the gel. This could be due to surfactant interactions with the lignin forming an ‘envelope’ around the lignin, as has been reported with electrophoresis of carbon nanotubes with SDS (Duan W. H. et al, 2011). As with proteins, SDS might minimise charge as a factor in separation, due to electrostatic, or hydrophobic, interactions with the lignin. SDS may destabilise inter-molecular interactions within the lignin, such as hydrogen bonding, van der Waals or π -stacking forces, making the separation correlate more directly to molecular weight; similar to how SDS is used in protein electrophoresis (Drabik A. et al, 2016).

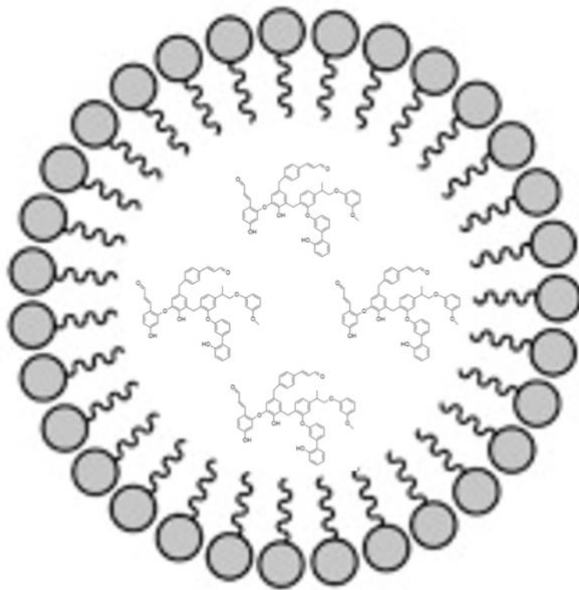


Figure 4-2 Diagram illustrating hypothesized lignin-SDS bundle. Adapted from (Rakhmatullin et al., 2016)

Another hypothesis is that, unlike carbon nanotubes, lignin has a lower average molecular weight, so rather than films it lignin may interact with SDS micelles. Lignin could form hydrophobic interactions with the tail group of the SDS molecules in the interior of the micelle, with the sulfonate head group of the SDS interacting with water on the outside of the micelle as in Figure 4-2. This would also be different to protein interactions with SDS, where monomers form around sections of the protein (Parker W. et al, 1992). This would explain why the lignin migrates in a single dense band rather than separating in a smear type band due to the different molecular weight lignin in the sample.

Dodecyltrimethylammonium bromide (DTAB) is a detergent which has a cationic head-group, so may interact with the lignin by charge neutralisation of the phenoxide groups. Lignin was visible at the back of the well pocket after electrophoresis, implying that the net negative charge of the lignin molecules

compared to the net positive charge of the DTAB molecules was equal, or that precipitation had occurred. Some material was visible in a smear type band below the gel pocket, which implied that these molecules still had a net negative charge. Triton X-100 is a neutral detergent, known to destabilise hydrophobic interactions with, for example, lipid bilayers in cells. The results using Triton-X were similar to those using DTAB, this time with a strong absorption seen at the front of the well. This implies that the neutral detergent is bound strongly to the lignin, and increases its mass to charge to slow its migration through the gel. Similar to DTAB, there is a smear after the well, which might be low mass lignin species that interact little with the detergent. The results indicate that neither DTAB nor Triton X-100 benefit lignin separation, but that SDS might be used to do this, and assist in its quantification.

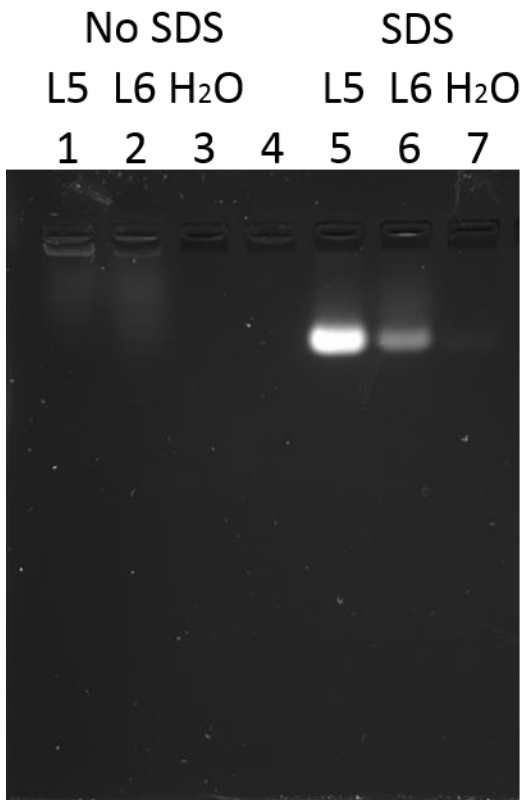


Figure 4-3 Image of a 1% agarose pH 4 TAE buffer gel after electrophoresis at 100 V for 10 minutes, with lignins L5, L6 and no-lignin, loaded with and without SDS.

Figure 4-3 shows the effects of a pH 4 on lignin L5 and L6 migration, and the effect of SDS. When the sample was prepared, the lignin still appeared to be soluble (though centrifugation was not done), but pH 4 is close to where lignin becomes insoluble. Electrophoresis of lignin at pH 4 shows that much of it fails to migrate from the loading well, though a faint smear can be seen in lanes 1,2 showing movement of some species. One of the limitations of handling acidic lignin samples, is that unless the pH of the sample is adjusted, the lignin cannot be run down the gel. Adjusting the pH of samples with sodium hydroxide, prior to loading them, solves this problem. If SDS micelles form around the lignin and contribute to the anionic charge, this will accelerate the migration and make mass less important. Lignin L5 and L6, that are different Kraft lignin fractions from

molecular weight cut-off membranes, migrate with similar velocities, though with quite different band intensities. SDS electrophoresis may not give a band intensity that is representative of the lignin concentration. It was not possible to purify enough lignin for analysis using SDS, as when used at high concentrations, the lignin appeared to be unaffected by the SDS.

Lane 7 is a control in which no SDS was added, however there is a faint band running at the same place as the samples with SDS. This implies that something other than lignin, within the buffer or the SDS, is producing a band. This could be potentially due to DNA stains (such as ethidium bromide) as it was a communal gel tank and other researchers were using such dyes. Alternatively, it may be due to SDS micelles migrating due to their negative charge. If the band is due to SDS micelles, this is not necessarily a problem, as a 0 g/L lignin with SDS control could be included, along with a concentration gradient of lignin samples. If the band is due to contamination, as long as the source is identified, it could be removed as a factor. The addition of SDS appears to negate any separation based on molecular weight, as a sharp band is produced, rather than a smear. The analysis appears to show that SDS could be used to analyse acidic lignin samples.

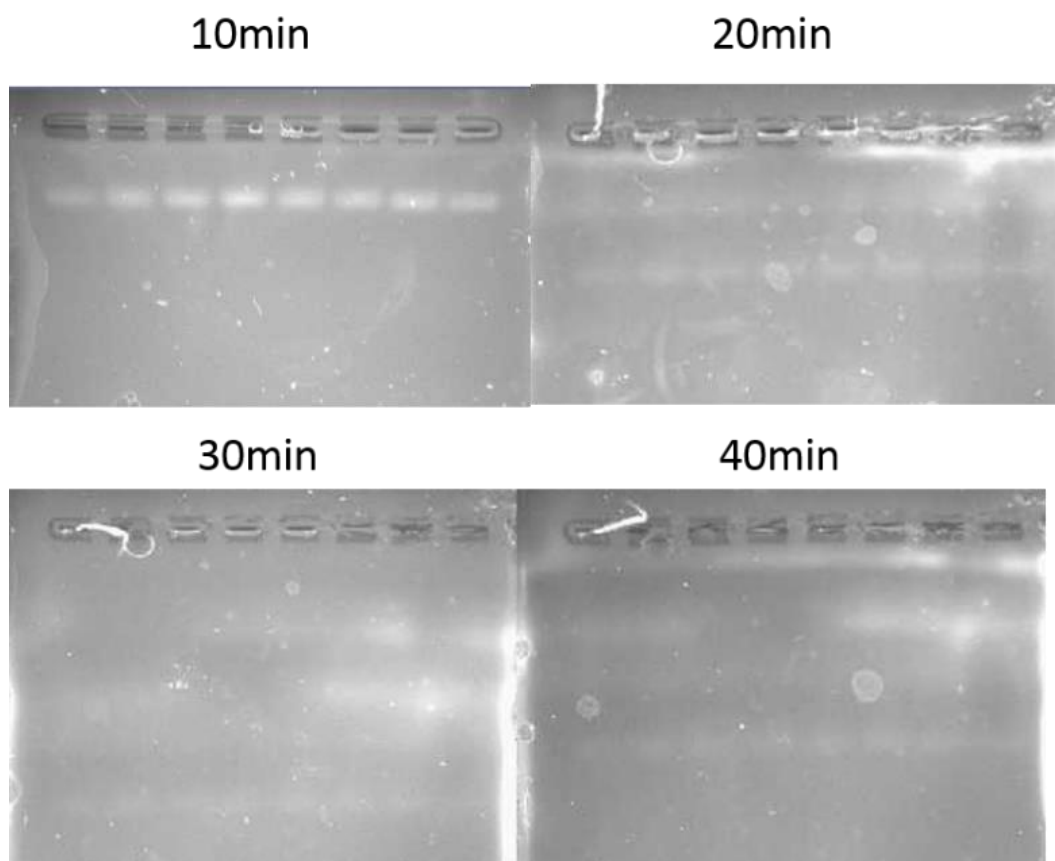


Figure 4-4 1% agarose gel made with TAE and 0.1% SDS, without lignin, run at 100 V over 40 minutes and imaging every 10 minutes.

Figure 4-4 is a gel with TAE and 0.1% SDS alone. The gel was taken out of the tank every 10 minutes and imaged, then re-immersed and re-electrophoresed. Upon, close inspection it can be seen that bands appear at each gel run. This implies that something is present in the buffer, such that when it enters the wells, the compound migrates. Since there is no mixing, the buffer inside the wells is not replaced, however when removed, imaged and then placed back into the tank, 'new' buffer enters the wells and forms a new band. This is evidence that the band seen in Figure 4-3, Lane 7 is produced by something in the buffer.

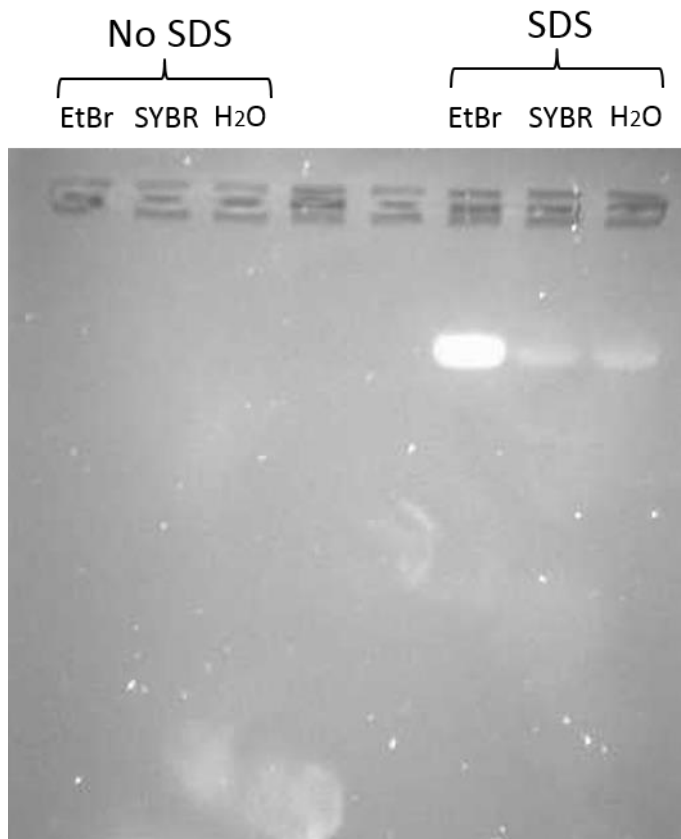


Figure 4-5 Gel electrophoresis of DNA dyes ethidium bromide and SYBR Safe for 10 minutes at 100 V on a TAE buffer gel with and without the addition of SDS.

An experiment was carried out to test the hypothesis that residual dye in the electrophoresis gel tank is interacting with the SDS to form a band on the gel, Figure 4-5. Ethidium bromide and SYBR safe were screened as contaminants by adding 2 μ l of stock solution to 6 μ l of water and 2 μ l of 50% glycerol before loading (with and without 2 μ l of 10% SDS) and running at 100 V for 10 minutes on a TAE gel with 1% agarose. Ethidium bromide and SYBR Safe did not produce a band when SDS was absent, however when SDS is present ethidium bromide interacts strongly with it, which is clear by the intensity of the band. Though not well known, previous work has shown that ethidium bromide forms interactions with SDS (Pal K. S. et al, 1998). This result is interesting as ethidium bromide is cationic,

however the SDS may form micelles with it that have a net negative charge. These experiments have exposed a potential weakness of using SDS to separate lignin, as the SDS may interact with any hydrophobic molecule, reducing the selectivity and making quantification more difficult. If SDS is not used, only molecules which have a net negative charge will migrate. The intensity of the band using SYBR Safe dye is much less than ethidium bromide, but the position is the same. The difference in band intensity is due to the wavelength used to image the gel. The imaging equipment is set-up for DNA analysis, and was based upon the absorption and emission properties of ethidium bromide. On the other hand, SYBR Safe has a different absorbance/emission spectra to Ethidium bromide and does not absorb or emit strongly at these wavelengths. This confirms that SYBR Safe alone is not responsible for the band produced on the gel, but since it is also a cationic dye, it was probably in a SDS complex, similar to the ethidium-SDS complex.

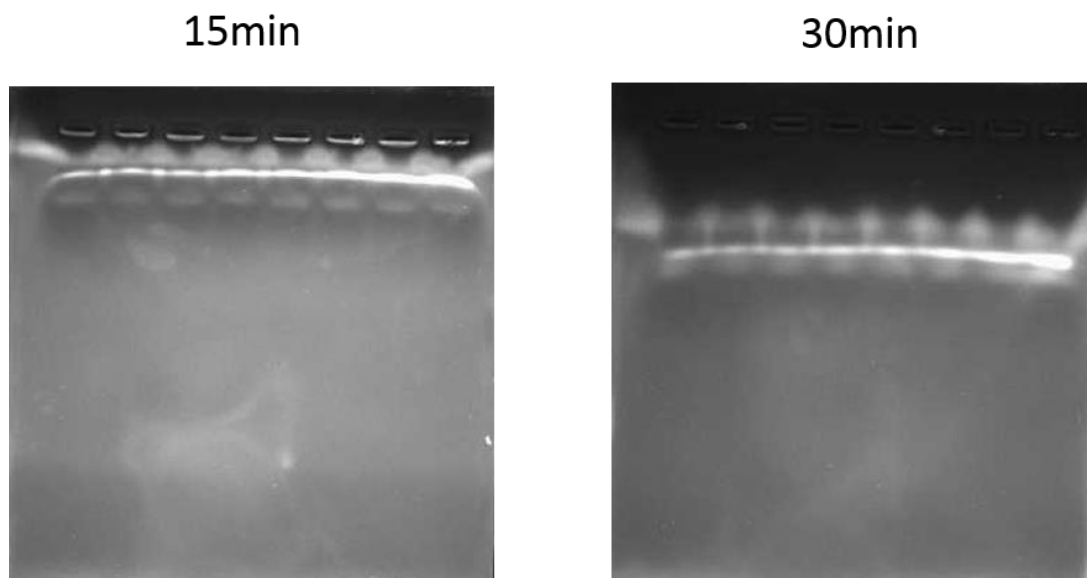


Figure 4-6 1% agarose gel made with SDS running buffer and ethidium bromide after electrophoresis at 50 V for 15 minutes (left) and 30 minutes (right).

Figure 4-6 shows that as electrophoresis occurs, a section of low intensity appears at the top of the gel. This is most likely due to ethidium bromide migrating within the gel and interacting with SDS. The longer the duration of electrophoresis, the further the ethidium bromide-SDS complex moves down the gel. This supports the hypothesis that ethidium bromide could be responsible for the band, though it is surprising that it would be present in such concentrations, and indicates a gel-tank should be used that has not previously been exposed to dye.

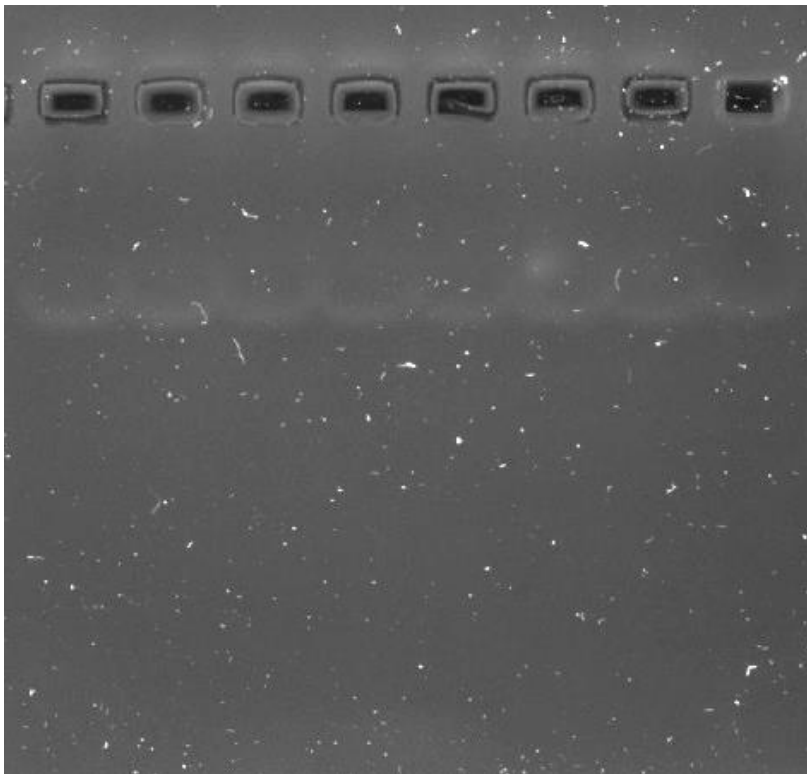


Figure 4-7 SB buffer gel with just SDS loaded 1% agarose gel with SB buffer, with SDS loaded into each of the gel lanes using an un-contaminated gel tank.

Figure 4-7 is a gel image using a new gel-tank, that surprisingly shows a faint visible band when SDS was loaded. The gel tank has never come into contact with ethidium bromide or any DNA stains, therefore is either a plasticizer such as phthalate, or SDS itself. Since SDS has no visible wavelength absorption or fluorescence emission, it is perhaps the SDS micelle that has these properties. If a standard curve is produced for lignin concentration using SDS, a sample of SDS alone, without lignin, could be used to correct for this. This work has shown the necessity to control carefully samples used, and not to assume migrating bands are due to lignin alone.

4.3.2 Electrophoresis and imaging of lignin with different buffers

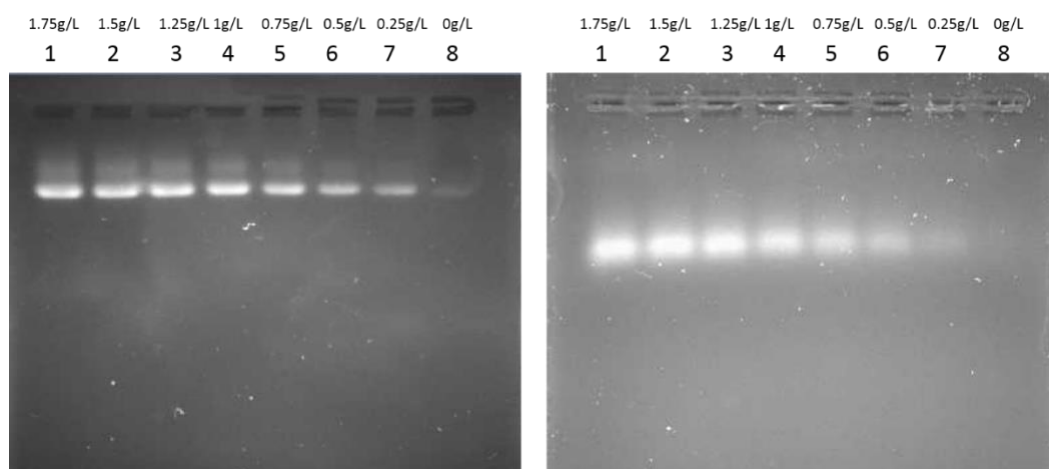


Figure 4-8 Gels with decreasing L5 lignin concentration gradients mixed with SDS on TAE and SDS running buffer gels. Left: Electrophoresis carried out using L5 on a 1% agarose TAE gel for 10 minutes at 100 V. Right: Electrophoresis carried out at 50 V for 30 minutes using a 1% agarose gel made with SDS running buffer.

Figure 4-8 shows that using both TAE and SDS running buffer gels, bands are produced that decrease in intensity as lignin concentration decreases. The TAE

gel produces a single sharp band and a smear directly above this band which is lower in intensity. This suggest that the majority of the lignin sample migrates with the SDS but a fraction of the lignin sample does not migrate along with the SDS micelles. Ideally the entirety of the polymeric lignin would migrate at the same speed in order to produce a single sharp band for simple quantification, otherwise there is no reason to use SDS instead of quantifying the lignin sample without SDS; as more information such as molecular weight distribution could potentially be determined.

The SDS running buffer gel shows more favourable separation with a single band produced post electrophoresis for each lignin concentration. There is an apparent difference in migration, with a 'smile' produced on the gel. This is most likely due to the high ionic strength of the buffer, leading to heating during electrophoresis causing the gel to contort (Brody J. R. et al, 2004). As a result, SDS running buffer is not favourable for use in agarose gel electrophoresis of lignin.

No SDS SDS
┌───┬───┐ ┌───┬───┐
L5 L6 L5 L6 H₂O H₂O

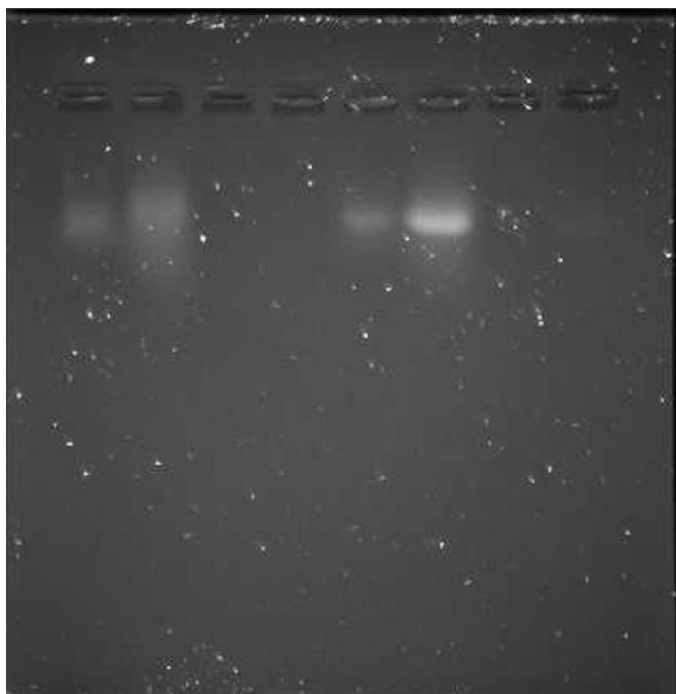


Figure 4-9 Comparison of electrophoresis with and without SDS in SB buffer, with lignin L5 and L6 at 120V for 10 minutes

Figure 4-9 confirms that SB buffer can be used for the electrophoresis of lignin, either with or without SDS. Unlike TAE buffer, electrophoresis with SDS on a SB gel produces a single well defined band. There is less smearing, which infers that the lignin travels in a uniform manner with the SDS micelles. The use of SB buffer with SDS and lignin has promise for quantification of lignin concentration.

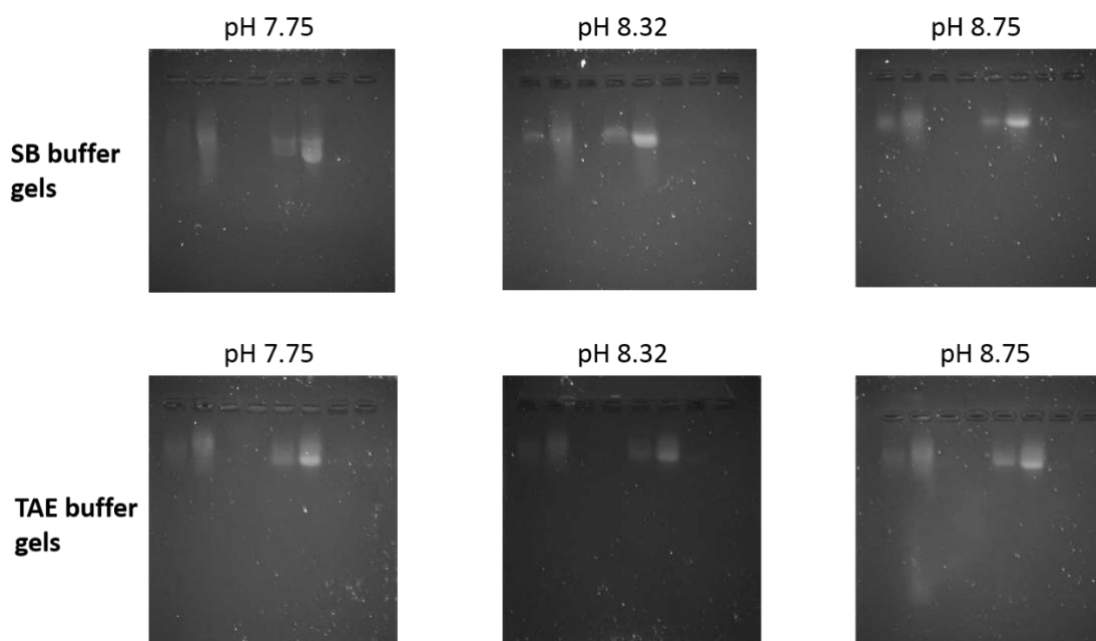


Figure 4-10 Effect of pH on TAE and SB buffer gels L5 and L6 after electrophoresis at 120 V for 10 minutes with (2 samples on the right side of each gel) and without SDS (two samples on the left side of each gel) using TAE and SB gels ran at different pHs.

The experiment shown in Figure 4-10 tests the role of pH and buffer in the electrophoresis of lignin with SDS. The resolution of electrophoresis falls once the pH of the SB buffer drops below 8.75, with the resolution poorest at pH 7.75. This is likely due to pH 7.75 and 8.32 being outside of the effective buffering range of SB buffer. The TAE gels showed a higher level of consistency at all pH values but a smear was still present above all of the bands. Therefore, SB buffer is the most effective buffer for electrophoresis of lignin with SDS but only at pH 8.75.

4.4 Conclusions

Overall these results show that lignin can interact with surfactants, and these can be used as an additive to electrophoresis. The results confirm that negatively charged surfactants in the form of SDS appear to be the best candidate as an additive for electrophoresis. The major disadvantage of using SDS is that lignin elutes at the same position regardless of the molecular weight distribution of the respective lignin. As a result an important piece of information is missed, so in routine electrophoresis of lignin it is advisable to not use detergents. This is confirmed by Figure 4-9, as without SDS a smear is generated, which migrates in a repeatable fashion and the separation could potentially be due to m/z differences. However, the use of surfactants may help when a low pH sample is tested, as shown in Figure 4-3. A positive outcome of this work was further confirmation that boric acid (SB buffer) is the best conductive buffer to carry out electrophoresis. Lignin separated on SB was improved compared to TAE buffer even with SDS. As a result SB buffer was used for all subsequent work.

Chapter 5

Investigation of gel conditions to scale up the electrophoresis of lignin

5.1 Introduction

Not only is there lack of methods to provide information about lignin structure and concentration, the current methods are low in throughput and suffer inaccuracy (Sluiter et al., 2010). Perhaps the most high throughput method to estimate lignin concentration is UV analysis, but the whole sample is analysed rather than the polymeric lignin fraction. This means that degradation products such as lignin monomers or even unrelated degradation products such as furfural and furan compounds interfere (Lee et al., 2013). Methods to measure lignin molecular weight such as GPC are low throughput as previously discussed. Therefore there is a need for a high throughput method to quantify polymeric lignin and to provide information about the molecular weight distribution. Building on previous work showing that GPC molecular weight distributions are comparable to that of the separation via electrophoresis, the work in this chapter aims to confirm that gel electrophoresis is a high throughput method able to provide information about polymeric lignin. Previous work has shown that agarose gel electrophoresis is an effective method to analyse DNA in high-throughput, which provides evidence that it may be possible to analyse polymeric lignin in the same fashion (Marra et al., 1997).

5.2 Methods

All gels were prepared using standard SB buffer concentrations, standard imaging and standard electrophoresis sample preparation. All samples were run using a Clarit-E Maxi gel tank and a BioRad PowerPac 300 as standard. Length and voltage of electrophoresis are detailed in the figures descriptions and lignin concentrations were prepared by dilution of L6 kraft lignin in water.

Table 5-1 Electrophoresis conditions and gel information

	Voltage and time	Additives	Incubation time (min)	Flexicaster used (Y/N)	Additional information
Figure 5-2	50 V 40 min	Standard	0	N	
Figure 5-3	50 V 60 min	Standard	0	N	
Figure 5-4	50 V 60 min	Standard and KCl buffer	0	N	
Figure 5-5	50 V 60 min	Standard	0	N	Loaded from right to left
Figure 5-6	50 V 60 min	Standard	0	N	Gel cast opposite way round to convention
Figure 5-7	50 V 60 min	Standard	0	Y	
Figure 5-8	50 V 60 min	Standard	60	Y	
Figure 5-9	50 V 60 min	Standard	0, 30, 60 and 90	Y	Samples loaded at different time points
Figure 5-10	50 V 60 min	Standard	60	Y	Multichannel pipette used
Figure 5-11	50 V 60 min	Standard	60	Y	Multichannel pipette used

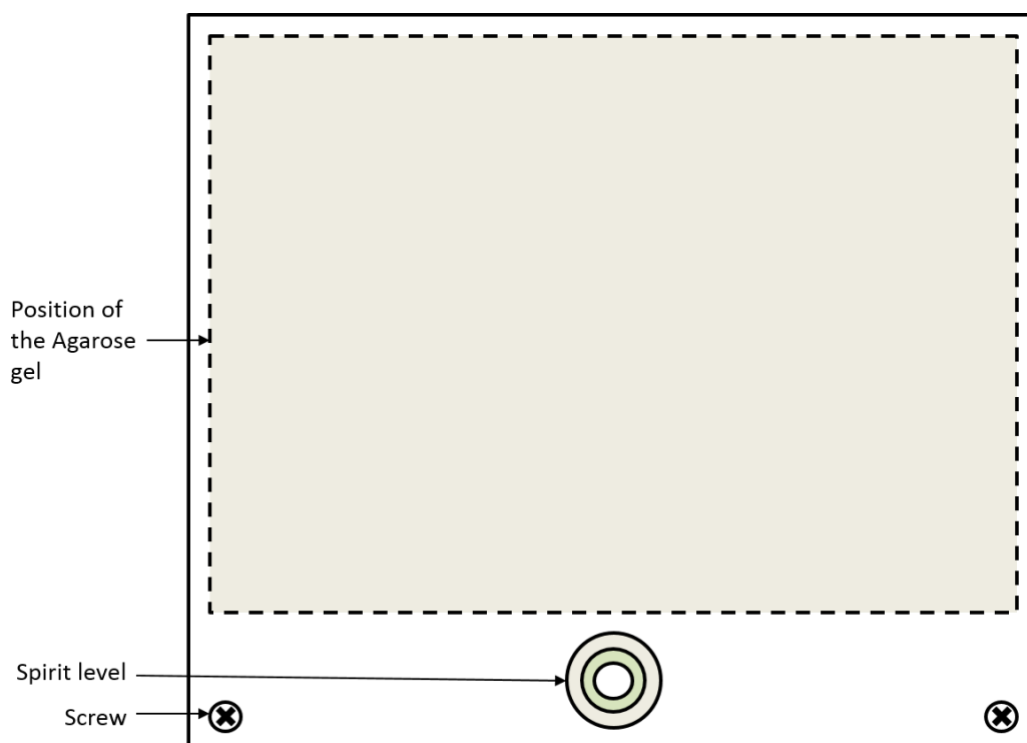


Figure 5-1 Diagram of the flexicaster used in the experiments

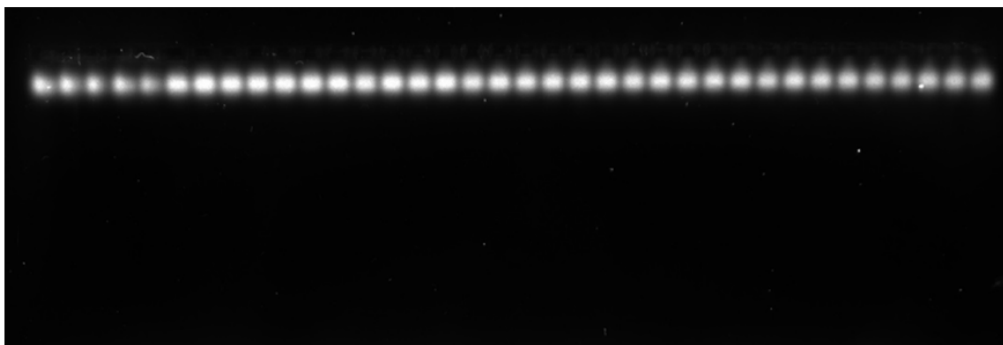
Figure 5-1 shows the flexicaster used to ensure uniform gel thickness in certain gels listed in Table 5-1. The flexicaster works using screws to adjust the level of the casting surface, the spirit level is then used to judge how level the surface is. The agarose gel is then cast as standard on the levelled surface.

The KCl buffer used in Figure 5-3 consisted of 0.2 M potassium chloride and 0.2 M sodium hydroxide; 20 μL was added to 20 μL of 50% glycerol, 20 μL 0.375 M NaOH with 50 μL of the 5 g/L lignin sample, with 10 μL loaded into each gel well as standard.

5.3 Results and discussion

5.3.1 Electrophoresis using unlevelled gels

A



B

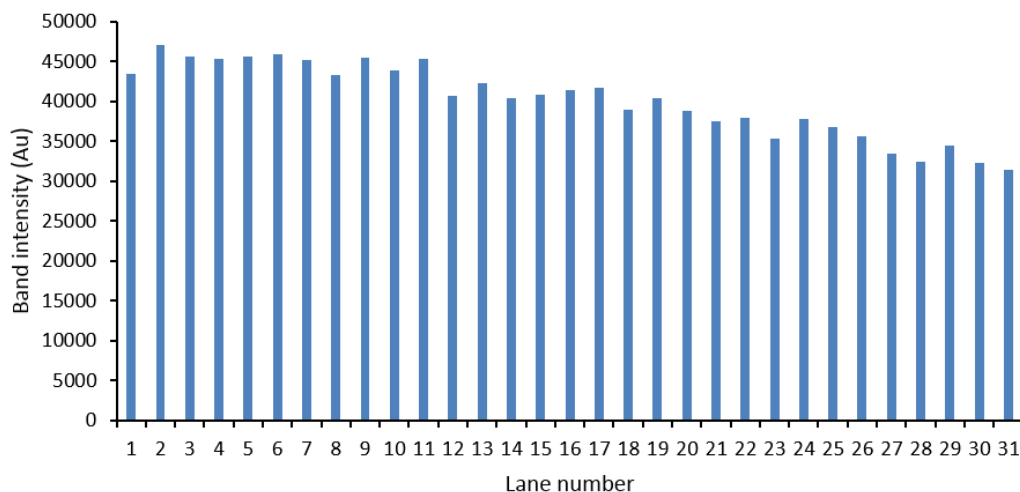


Figure 5-2 Electrophoresis of lignin on a large agarose gel. A: Image of gel run at 50 V for 40 minutes after loading 5 g/L L6 lignin into each lane. B: Results after ImageJ quantification of the gel bands produced in each lane, showing total intensity of the band.

Figure 5-2 shows a gel with the same type and concentration of lignin in each lane. However a decrease in band intensity is observed from left to right. This is unexpected as the band intensity should be around the same values regardless of the order that the samples were loaded (samples were loaded from left to right) or the position of the samples on the gel. This is most likely due to a factor leading

to higher band intensity the longer the lignin is present in the gel (and therefore linked to order of sample loading) or a physical difference across the agarose gel leading to bands on one side of the gel appearing more intense than the other. Gel samples were loaded with glycerol, so lignin should not have diffused out of the pockets, and even if this was to have happened, the band intensity would decrease not increase. Perhaps SB buffer diffused into the pocket and altered the pH of the lignin sample (loaded in combination with sodium hydroxide), decreased the pH and lead to a change in band intensity. The samples loaded first would have been on the gel pockets for a longer period of time so diffusion is more likely, which could explain the trend observed. pH is well known to affect the fluorescence emission of ionisable molecules (Ikeda and Okamoto, 2007). Another explanation would be that either the gel pouring, or the gel electrophoresis tank leads to this decrease in band intensity. There are a multitude of factors involved in gel electrophoresis such as the gel mould, gel pouring, uniformity of current across the gel, thickness of the gel and many more which all could have had an effect. The intensity values range between 35 and 45,000 which is significant and if left uncorrected, will prevent comparison of electrophoresed samples. The reliability could be improved by carrying out repeats across the whole gel rather than in the first lanes.

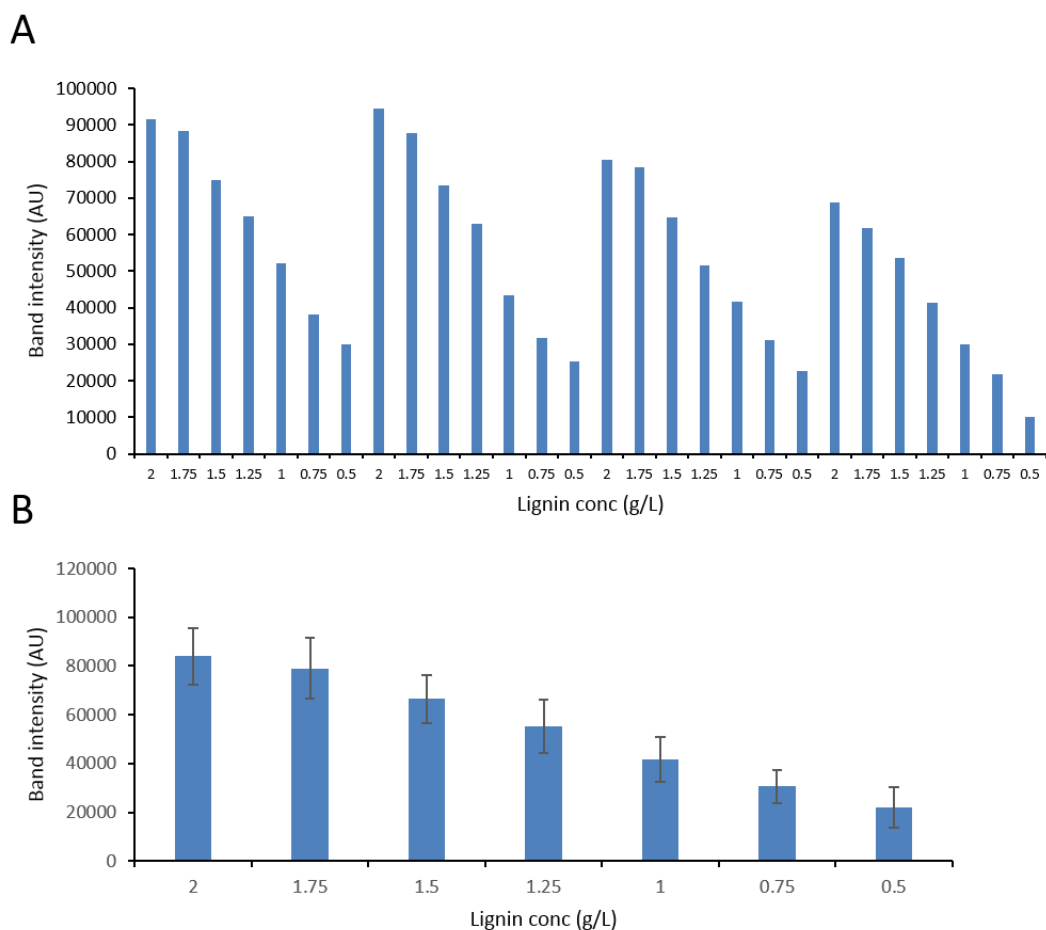
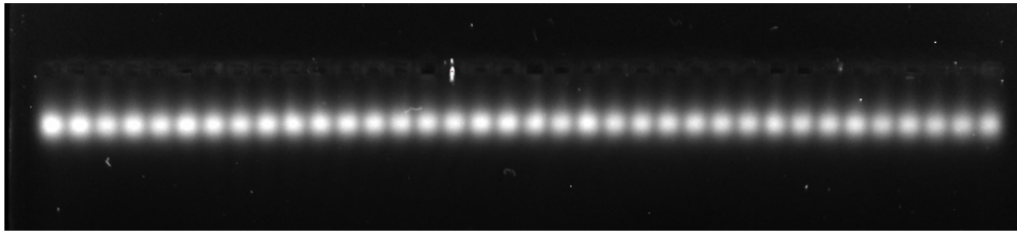


Figure 5-3 Lignin concentration gradient on a large agarose gel A: ImageJ quantification of gel bands after loading 2 g/L, 1.75 g/L, 1.5 g/L, 1.25 g/L, 1 g/L, 0.75 g/L and 0.5 g/L sequentially (with 4 repeats for each sample) onto a gel before running for 1 hr at 50 V. B: average values for each of the lignin concentrations, using standard deviation to produce error bars.

Figure 5-3 shows a lignin concentration gradient run on a large agarose gel and then analysed by ImageJ. The results are interesting as they corroborate those in Figure 5-2, where the band intensity decreases across the gel. This leads to significant error, preventing accurate determination of lignin concentration. However, it is observed that the first half of the gel appears to be relatively similar in band intensity.

A



B

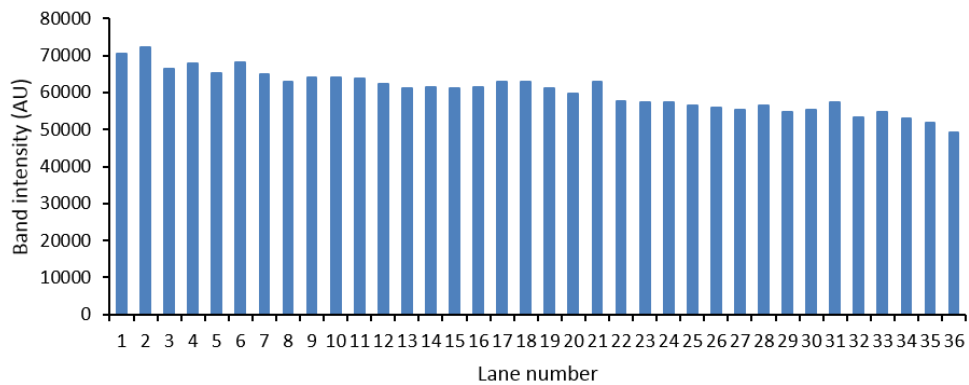
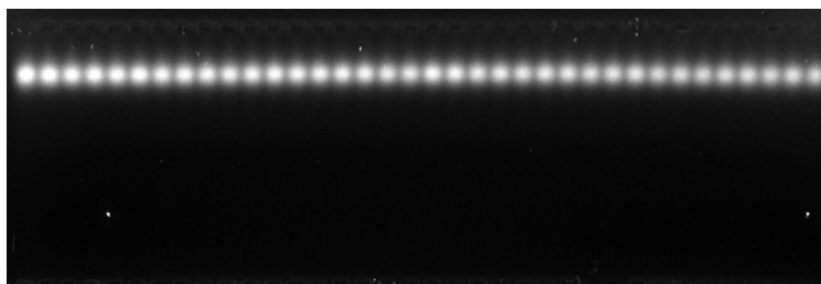


Figure 5-4 Lignin mixed with KCL buffer on a large agarose SB buffer gel. 5 g/L L6 lignin was loaded into each lane after being mixed with KCL buffer before electrophoresis at 50 V for 1 hour. A= image of the gel post electrophoresis B= ImageJ quantification of each gel band.

In Figure 5-4 lignin samples were loaded onto the gel after mixing with pH 12.6 KCl buffer. This was carried out to test whether the change in band intensity is due to SB buffer in the tank diffusing into the pockets and decreasing the pH of the lignin samples (as the samples were loaded mixed with NaOH). The mixture with KCl buffer should prevent SB buffer diffusing into the pocket. However, the same trend was observed as previously. Although the overall trend of less intensity left to right is still observed, it is less significant than before. To further determine the cause of the problem, the gel was loaded in reverse, i.e. from right to left.

A



B

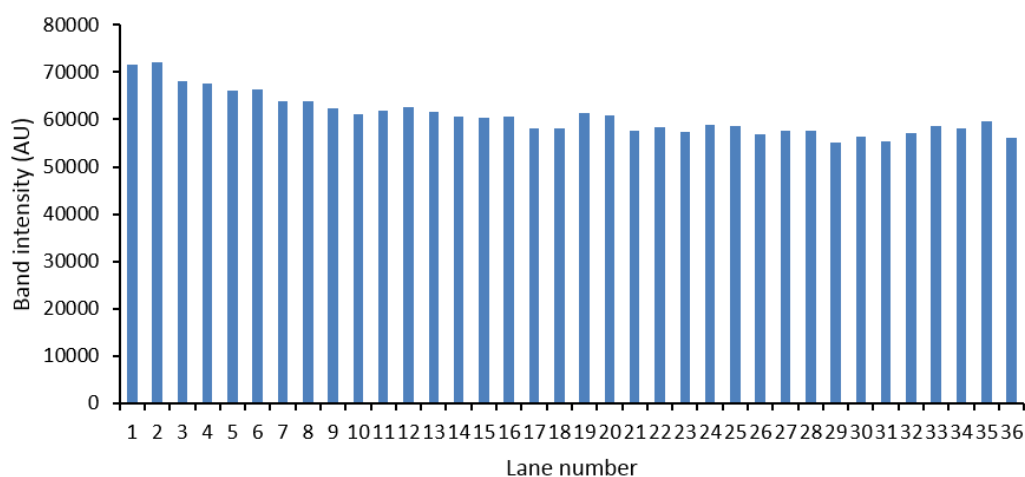
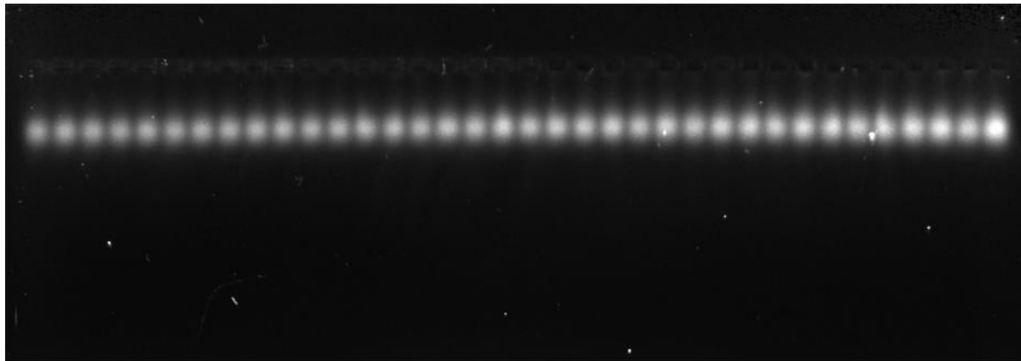


Figure 5-5 Lignin loaded from right to left (opposite to routine loading) on a large agarose gel. A: Image of gel after electrophoresis at 50 V for 60 minutes after loading 5 g/L L6 into each lane, with the gel loaded from right to left rather than left to right (as was carried out for all the other gels). B: ImageJ quantification of the gel bands produced in each lane.

Figure 5-5 demonstrates that the order in which the samples are loaded does not change the band intensity. This confirms that the longer 'incubation' of lignin samples in the gel pockets before electrophoresis does not have any effect and therefore confirms that diffusion of lignin samples or buffer is not responsible for the change in band intensity across the gel. Consequently, the issue must be related to either the gel itself as a result of the gel pouring and casting for example or the electrophoresis and likely to be an equipment issue rather.

A



B

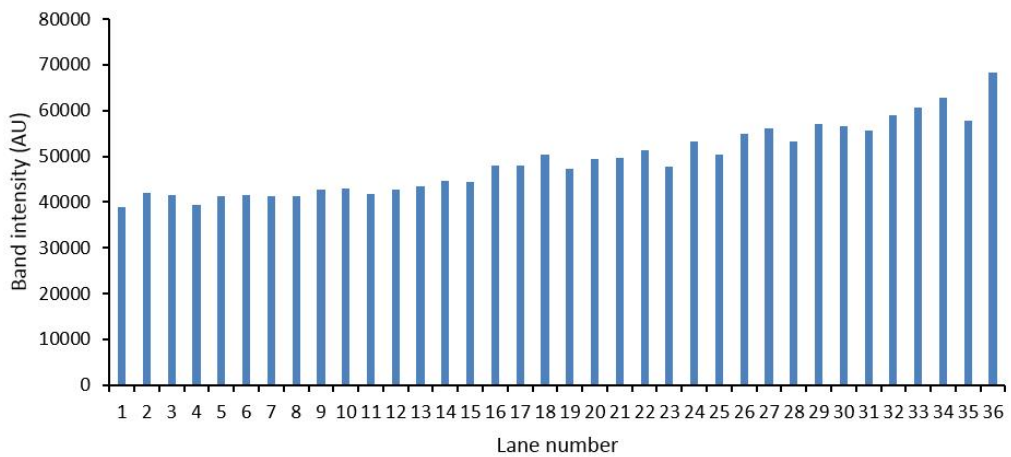


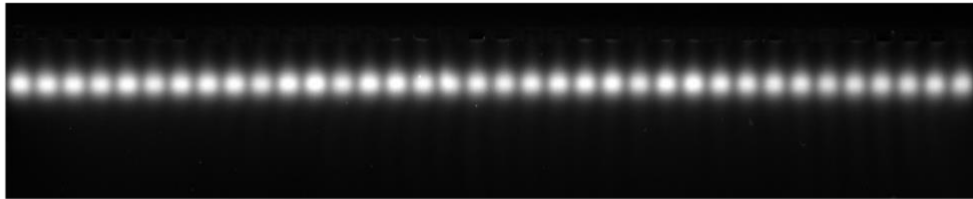
Figure 5-6 Gel poured in a cast the opposite way round to routine. A: Image of gel that was run at 50 V for 60 minutes after loading 5 g/L L6 into each lane. B: ImageJ quantification of the gel bands produced in each lane.

The experiment in Figure 5-6 was carried out to test whether uniformity of gel thickness could have been a factor leading to the changes in intensity. The gel mould was prepared as with the previous experiments but the mould was turned around so it was in the opposite orientation to normal. This would correct for any slight incline or decline of a table on which the gel was poured onto (not visible by eye) and also determine that the observation is not related to the amount of time a sample has been loaded onto the gel prior to electrophoresis. The results

clearly show that the opposite trend was observed compared to before, therefore the gel thickness (due to an unlevelled gel pouring surface) leads to changes in band intensity. Therefore any gel needs to be poured on a level surface to ensure reliability across the gel.

5.3.2 Electrophoresis using levelled gels

A



B

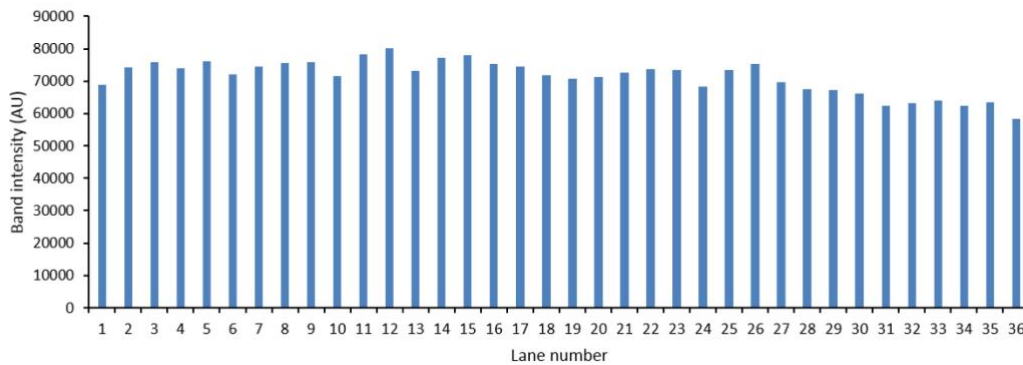


Figure 5-7 Electrophoresis on a large agarose gel, levelled using a flexi caster. A: Image of gel that was poured and set on top of a levelled flexi caster before running for 1 hr at 50 V. B: ImageJ quantification, with the first and last 5 samples removed from analysis.

Figure 5-7 shows the results from a gel which was levelled using a flexicaster, compared to the results in Figure 5-2 for an unlevelled gel the results are much more consistent as no major decrease in band intensity is observed across the gel. This confirms that the change in intensity across the gel is related to the surface that is not completely level and therefore due to changes in the thickness across the gel. There still appears to be slight change across the gel which

highlights how sensitive the imaging of the gel must be to changes in agarose gel thickness. However there still appears to be an issue with reliability, as there is still variability between what should be identical samples.

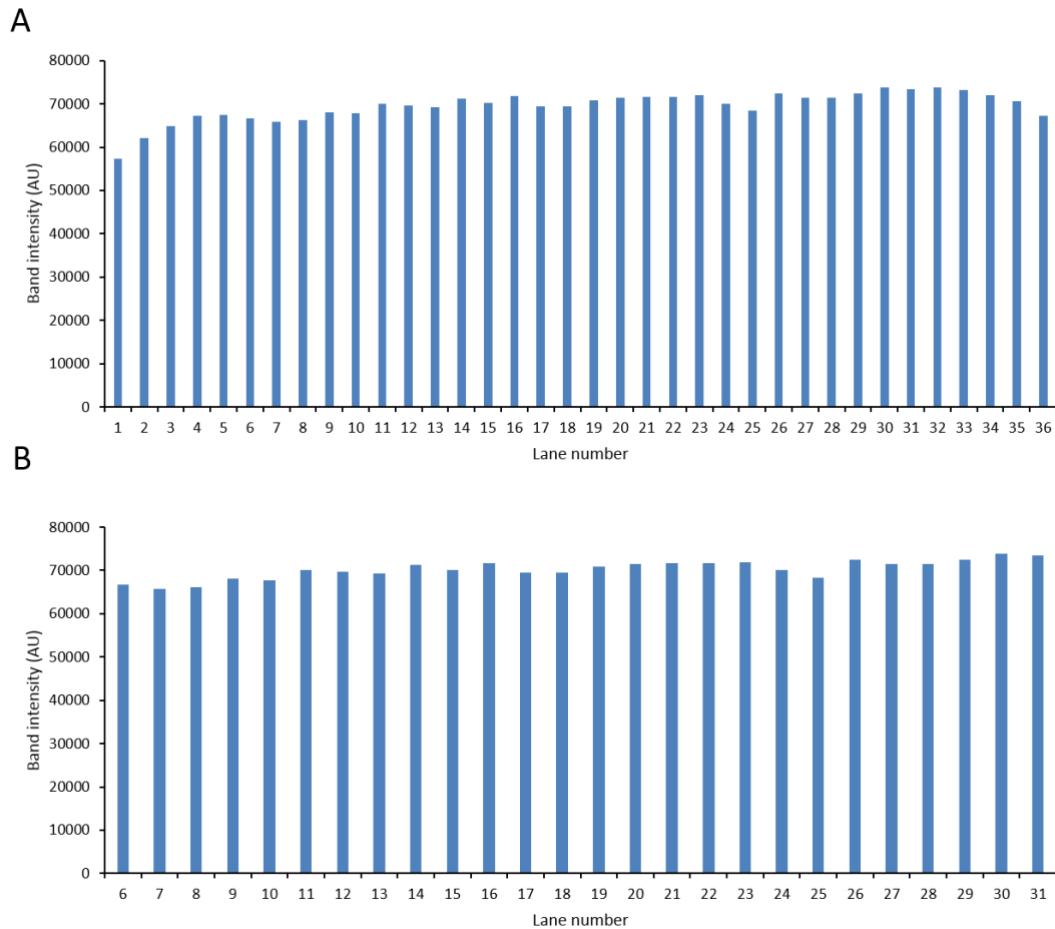


Figure 5-8 Electrophoresis on a large agarose gel, levelled using a flexi caster with the lignin ‘incubated’ in the gel for one hour before electrophoresis. A: ImageJ quantification of gel bands after loading 5 g/L L6 lignin onto a gel that was poured and set on top of a levelled flexi caster before running for 1 hr at 50 V. Samples were allowed to incubate after loading for a period of one hour. B: ImageJ quantification, with the first and last 5 samples removed from analysis.

Figure 5-8 shows the results of equilibrating samples on the gel for an hour, ensuring that all of the samples are in the same condition when the gel is run. This was trialled as it was noticed that samples loaded at first appear darker

before becoming a lighter colour, which could be due to the lignin in glycerol equilibrating into the gel conditions or 'settling' in the wells. There appears to be less variability compared to Figure 5-7 with the samples appearing more uniform in intensity. However, the first and last five samples show a change in intensity compared to the others. Lanes at the edge of the gel might suffer "edge effects". When the gel is poured into the mould, surface tension at the sides of the mould causes the sides of the gel to be slightly thicker, and they are colder which means the gel can set more quickly, which could therefore influence the results. If however, the first and last five samples are removed from the analysis, the variance between samples is greatly decreased. This demonstrates that the first and last sections of the gel should not be used in order to increase reliability. This is an important result as it shows that lignin can be analysed accurately using a large gel.

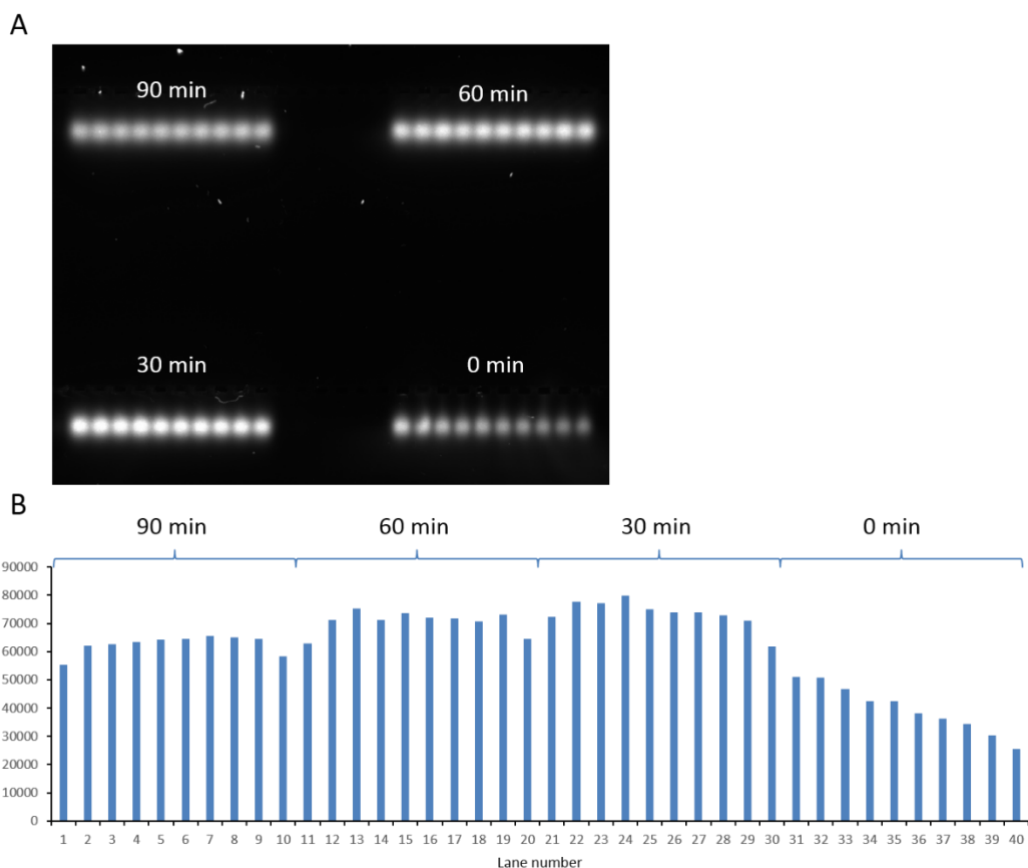


Figure 5-9 Lignin loaded and then incubated onto a large agarose gel at different time points. A: Image of a gel run at 50 V for 60 minutes after loading 5 g/L L6 into each lane. Four sets of 10 samples were loaded every 30 minutes before running the gel. B: ImageJ quantification of the gel bands produced in each lane.

Figure 5-9 was carried out to test the effect of incubating samples for different periods of time. When the samples were not incubated (0 minutes), i.e. run immediately, a clear decrease in intensity was observed, with samples loaded first having the lowest intensity. This could be because a period of equilibration is required with the gel buffer. Samples incubated for between 30-60 minutes show reasonable similarity however there is quite a lot of variation within the lanes. There is also a slight decrease in band intensity between 60 and 90 minutes, perhaps because some of the lignin begins to diffuse out of the gel

pockets when left too long. Nevertheless, the samples loaded and incubated for 90 minutes have low variability. These results show a problem with the method as it takes time to load the gel lanes so if several sets of lanes are required then this could limit the total number of lanes that can be used. To overcome this, a multichannel pipette was used to speed up the loading (assuming these can load several samples at a time accurately).

5.3.3 Electrophoresis using levelled gels loaded using a multichannel pipette

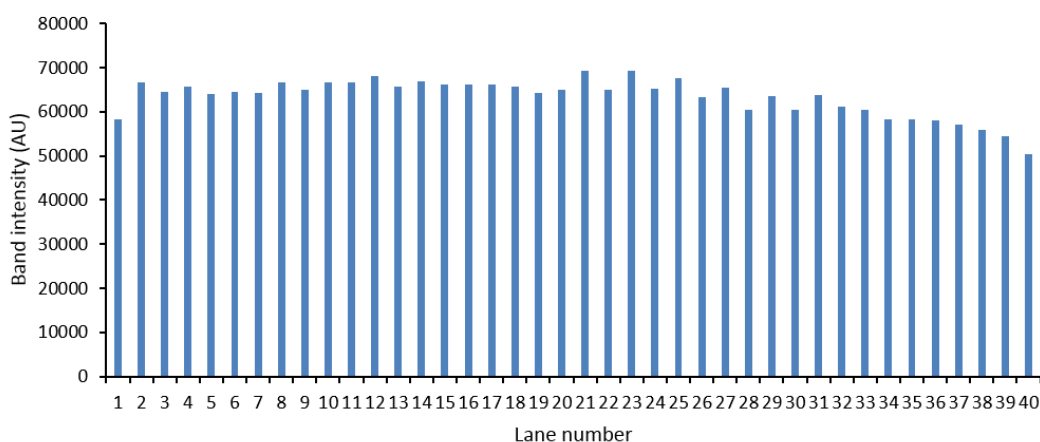


Figure 5-10 Electrophoresis of lignin loaded onto a large agarose gel with a multi-channel pipette. ImageJ quantification of gel bands after loading 5 g/L L6 onto a gel made using a flexicaster and loaded using a multichannel pipette, Samples were allowed to incubate after loading for a period of one hour.

Figure 5-10 shows a gel loaded with a 12-channel pipette, and was able to significantly reduce the loading time. Although loading of samples onto an agarose gel is fast, if 280 samples were loaded onto the gel (the maximum possible using the 20x15 cm gel tray used in this work) then this would lead to diffusion of lignin from the wells; the multichannel pipette overcomes this by speeding up the loading process. A fall in the accuracy of loading is not observed, with consistent band intensities observed. This is a positive result, as the method

is now high throughput which opens up the possibility of analysing large numbers of lignin samples.

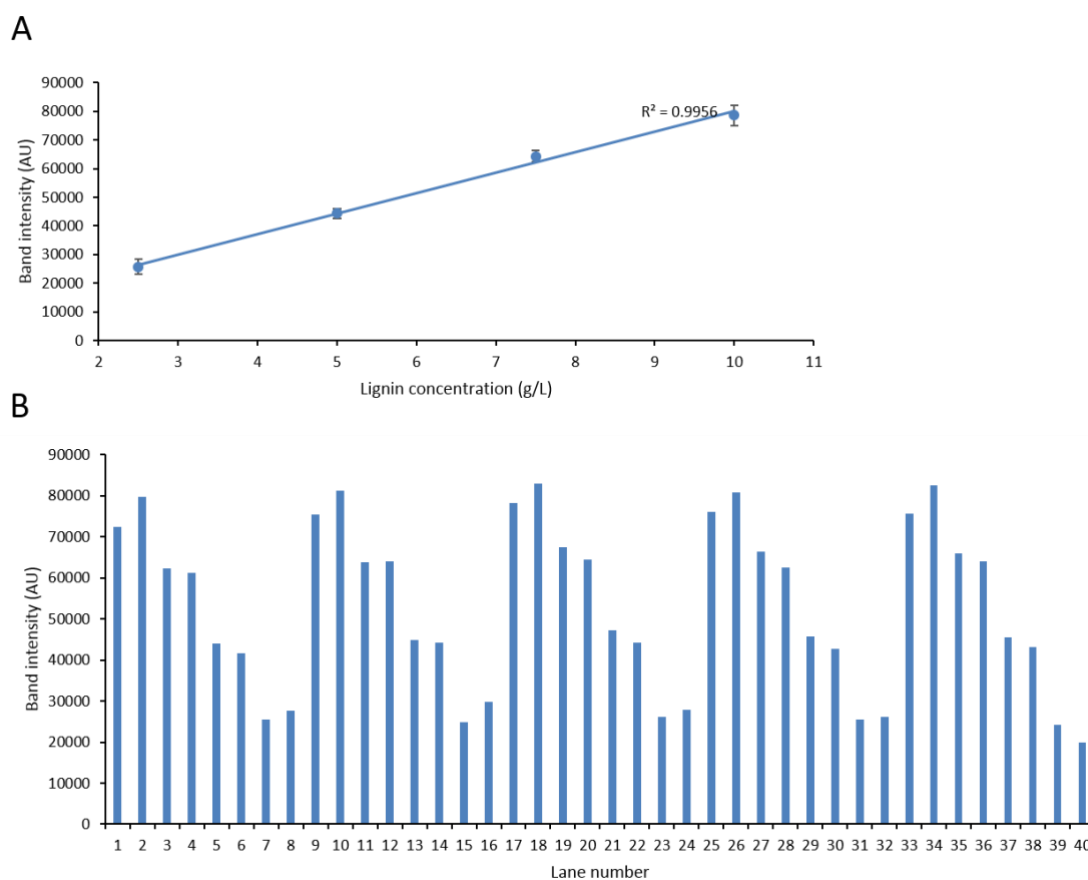


Figure 5-11 Electrophoresis of a concentration gradient of lignin loaded onto a large agarose gel with a multi-channel pipette. A: ImageJ quantification of gel bands after loading 2 g/L, 1.75 g/L, 1.5 g/L, 1.25 g/L, 1 g/L, 0.75 g/L and 0.5 g/L in duplicate sequentially (the sequence was loaded 5 times in order to create 10 repeats for each sample) onto a gel made using a flexicaster and loaded using a multichannel pipette. The gel was ran at 50 V with an incubation period of 1 hour B: standard curve produced using the ImageJ analysis of band intensity for each of the lignin concentrations.

Figure 5-11 show a lignin concentration gradient produced on a level gel with lignin samples that were loaded in high throughput using a multi-channel pipette. The results show improvement compared to Figure 5-3 where the variability of intensity between samples was high. Additionally, samples at the far left of the gel can be compared to the samples on the far right demonstrating the low error.

Furthermore the R_2 number in section A is 0.9956, which shows the high accuracy of this technique. This demonstrates the potential of using a lignin standard curve to estimate the concentration of an unknown sample of lignin. However there are still issues with the analysis of the 2 g/L samples, as the first sample in each duplicate appears to have lower intensity compared to the second loaded (from left to right), the 0.5 g/L lignin sample closest to the 2 g/L sample also appears to have a high intensity compared to the sample loaded first. This might be that the lignin fluorescence in one lane might illuminate lignin in the adjacent lane. In other words, some of the light could be absorbed, then re-emitted making that sample appear to be higher in concentration due to the higher emission. Or it could be due to a slight crossover of sample between wells. Highly concentrated lignin samples adjacent to low concentration ones could lead to overestimated concentrations. This could be controlled leaving an empty well between each lignin sample, but would significantly decrease the throughput.

5.4 Conclusions

Overall, the results show that electrophoresis can be successfully scaled up to analyse around 40 lignin samples per lane, with a maximum of 7 lanes per gel which means a potential of 280 samples can be analysed on a single gel in around 2 hours. Compared to GPC where a lignin sample first has to be acetylated (which takes around 24hrs), then each sample takes around 30 minutes to run, so around 7 days to analyse the same amount of samples via SEC. It is clear that gel electrophoresis is unique in the field in its ability to analyse polymeric lignin in high throughput. The way in which the gel is cast has been shown to be important in giving a consistent band intensity. To be able to compare lignin samples that are far apart on the gel, it needs to be poured and set on a level surface to ensure uniform gel thickness but this is easily solved using commercially available gel pouring equipment. Also, the avoidance of edge effects, and appropriately placed repeats using rapid loading method achieved using a multichannel pipette. There appears to be no negative effect using a multichannel pipette compared to a single channel pipette. The time taken to load samples and the equilibration of samples in the pocket were also shown to influence the band intensity.

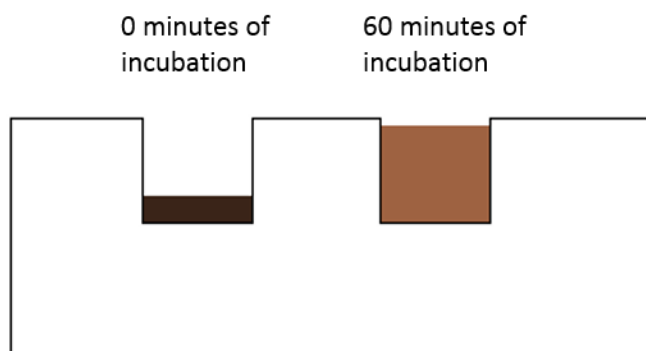


Figure 5-12 Diagram to illustrate the possible effect of sample incubation in the agarose gel.

It appears important to incubate lignin samples before carrying out electrophoresis. This may be the sample equilibrating into the gel illustrated in Figure 5-12. Perhaps when the lignin is first loaded onto the gel it may not be distributed in the well evenly which could lead to inaccuracy in analysis, whereas when the sample is allowed to 'settle' it is distributed evenly in the well. Distribution of the sample in the well is important as the image taken of the gel is a 2D representation of a 3D gel. Overall these results show that gel electrophoresis can analyse polymeric lignin in high-throughput, the next step is to confirm that this method can analyse degraded lignin samples.

Chapter 6

Determining the separation resolution of agarose gel electrophoresis

6.1 Introduction

The molecular weight distribution of lignin is a useful piece of information to compare different lignin substrates, and to assess the level and type of degradation that has occurred. Methods, such as the Klason, are used to assess lignin degradation, but are unable to provide information about the lignin structure, and, therefore, important information can be missed (Li et al., 2007). It is challenging to determine the molecular weight distribution of lignin as it is a heterogeneous and complex structure with many different subunits cross-linked in different ways. Methods have been trialled with limited success, an example is (Pinto et al., 2002) where several different methods (such as electrospray ionisation mass spectrometry and NMR) were utilised in provide information about lignin structure with limited success and reliability. Not only is this complex, it is also time and resource efficient as many of these methods are extremely low throughput and contain many steps. The most established method for molecular weight determination of lignin is GPC, it requires expensive specialist equipment so is relatively inaccessible to the average laboratory. Additionally, GPC is time consuming to carry out with several steps involved in preparing and running samples and controls. Firstly, acetylation is required in order to increase the solubility of lignin in the respective solvent and is also effective in removing the charge and ionisation. Acetic anhydride is used, with pyridine employed as the base (Glasser et al., 1993). Sample preparation is relatively simple but laborious and typically takes around 24 hours. Post-acetylation, toluene is used repeatedly

to wash residual pyridine and acetic acid (Asikkala et al., 2012). This is then evaporated and methanol is added to remove the toluene, which is itself evaporated. Once complete, the lignin is soluble in the solvent, with THF commonly used. The GPC takes around 30 minutes to run one sample (not including analysis). Although GPC can provide high resolution data about the molecular weight distribution of lignin, a method that could provide similar information while being much higher in throughput could be a key tool for lignin research. Having already confirmed that gel electrophoresis can be used to separate lignin, it was identified as a method to monitor different types of lignin and their digestion. However, it is unclear how well it might resolve different lignins and their fragmentation, based on molecular weight and charge distributions.

6.2 Methods

6.2.1 Absorbance of lignin measurements

Absorption readings were taken using a Agilent Carry 100 UV-Vis spectrometer, scanning from 625-800 nm. The spectrometer was firstly blanked using SB buffer with no lignin as a blank, before measuring the absorbance of 1 g/L L6 Kraft lignin in SB buffer.

6.2.2 Fluorescence of lignin measurements

Fluorescence was measured using a Horiba Fluoromax fluorometer. Samples were prepared by adding SB buffer to low temperature melting agarose (in order to stop solidification of the agarose) before boiling in order to solubilise the agarose. The samples were then added to the cuvette and kept at 40 degrees Celsius using an Julabo EH heating immersion circulator during fluorescence measurements. Samples were analysed with and without 1.6 g/L L6 Kraft lignin.

6.2.3 GPC of lignin standards

Precipitation, acetylation, GPC and molecular weight determination were carried out as standard as described in Chapter 2.

6.2.4 Preparation of lignin standards for gel electrophoresis

5 g/L L6 Kraft lignin solution was prepared by dilution in water. 5 g/L L5 Kraft lignin was prepared by addition to water and addition of 5 M NaOH dropwise until complete solubilisation, before adjusting to pH 7 with HCl. Sample dilution was carried out in water and used to produce the standard concentration curve. Protobind lignin samples were prepared by adding 2 mL of SB buffer solution to 10 mg of the lignin solid. Organosolv lignin samples were prepared by suspending

30 mg of the solid in 0.5 mL SB buffer. The solid fraction of the organosolv and protobind samples was removed by centrifuging at 4500 rpm for 15 minutes before pipetting the supernatant that was then used for electrophoresis. For the results shown in Figure 6-2 in order to ensure similar band intensities on the gel, the different lignin samples were diluted in water as follows: 4x dilution for L5, L6, protobind lignin samples, 2x dilution for Alkali lignin and no dilution for the organosolv lignin samples.

6.2.5 Gel electrophoresis of lignin standards

Electrophoresis was carried out using standard procedure for Maxi gels.

6.3 Results and Discussion

6.3.1 Absorbance and fluorescence measurements of lignin

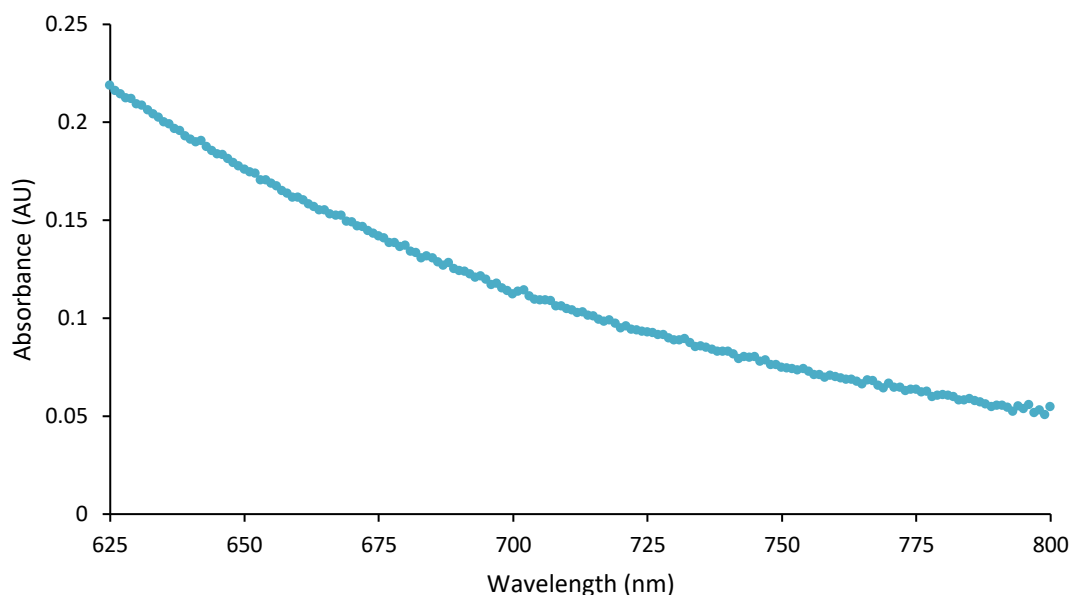


Figure 6-1 Absorption spectra of 1 g/L L6 lignin

An experiment was carried out to investigate whether lignin could absorb light in the far-red excitation region used by the gel imager, Figure 6-1. This corresponds with the Coomassie imaging setting which has been shown as an effective and sensitive method with low background interference using PAGE (Neuhoff et al., 1985). It is important to assess whether lignin can absorb light at this wavelength because if there is no absorption then there can be no fluorescence. Considering a high, 1 g/L of L6 Kraft lignin is used it is evident that lignin does not absorb strongly in this region: the absorbance at 625 nm is around 0.21 AU, which steadily decreases to around 0.05 AU at 800 nm. For gel imaging, it is better to have low intensity light produced on a completely dark background than high

emission on a light emitting background. Therefore lignin has the potential to fluoresce if excited using light within these wavelengths.

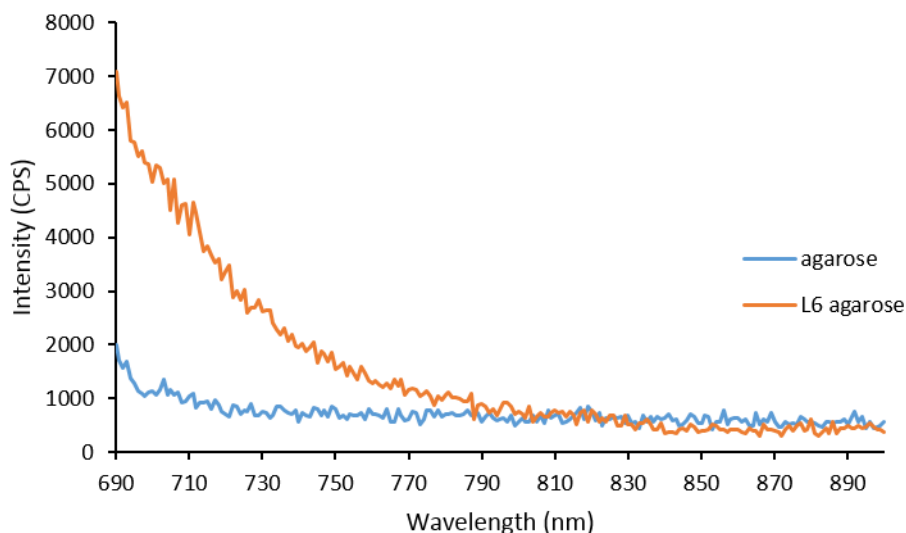


Figure 6-2 Fluorescence intensity (counts per second) measured from 690-900 nm after exposure to 680 nm light. Results are shown for 1% molten agarose and 1% molten agarose with 1.6 g/L L6 lignin

Figure 6-2 shows the fluorescence emission spectra by excitation at 680nm, which corresponds to far red epi using the gel imager. A control with agarose shows, beyond 700 nm, only a background fluorescence of 750 CPS. The noise observed is because the detector is near the limit. When lignin is present in the agarose a fluorescence intensity of around 7000 CPS is observed at 690 nm which then declines until around 790 nm, where the emission levels-out. The excitation wavelength of 680 nm and emission measurement at 715-730 nm corresponds to the Coomassie blue gel imaging setting. When lignin is imaged using this, a strong sharp band is observed in contrast the agarose gel which is in contrast extremely dark on the image (see result in Figure 6-12). This is supported by the graph in Figure 6-2 that shows the lignin fluorescence is

significantly higher than that of agarose. The Coomassie image setting was used in all of the following experiments.

6.3.2 Preparation of lignin standards for GPC and subsequent comparison with gel electrophoresis.

GPC of lignin standards was carried out so that the molecular weight distributions could be compared to that of the gels to see whether the same trends were observed, and to assess the resolution compared to GPC. Authentic lignin standards were prepared for GPC, and a critical point is the solubility of the derivatized lignin in THF. If some of the sample doesn't dissolve, then the GPC plots will fail to give a true picture of the molecular weight distribution, and can only provide information about the soluble fraction. In total, three major types of lignin were analysed (Kraft, protobind and organosolv lignins) and at least two distinct lignin samples were analysed for each type. Therefore, the accuracy and resolution of agarose gel electrophoresis could be accurately assessed.

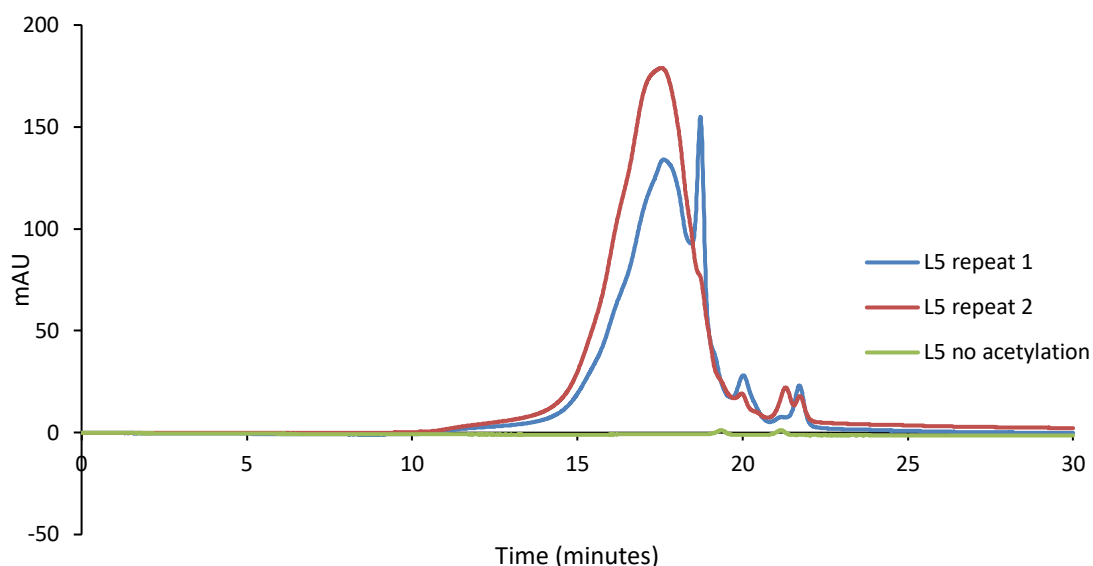


Figure 6-3 GPC plot of two acetylated L5 samples and a non-acetylated sample dissolved in THF.

Figure 6-3 shows that the main peak for L5 lignin repeat 1 and repeat 2 between 15 and 20 minutes, with L5 repeat 2 eluting earlier than L5 repeat 1. There was also a peak in the L5 repeat 1 sample at around 19 minutes that was not detectable in the L5 repeat 2 sample. Both L5 lignin samples that were acetylated, appear to have different molecular weight distributions and different peaks (shown by L5 repeat 1 having a large peak before 20 minutes). This is surprising, given that the materials are identical, and shows there is irreproducibility in the method. It is also confirmed in a control, that if the lignin is not derivatized it shows no elution from the GPC.

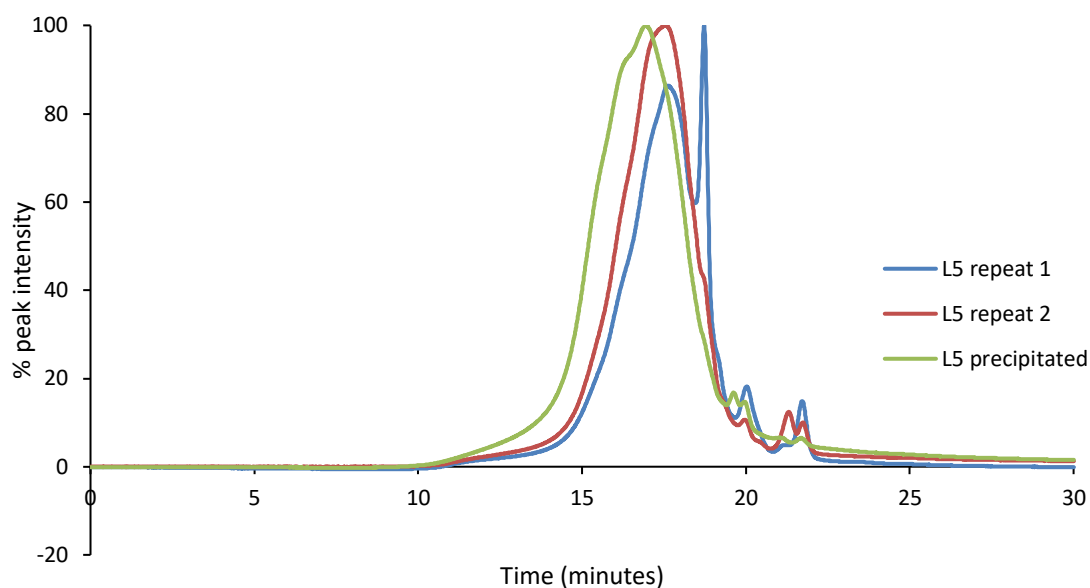


Figure 6-4 Normalised GPC plot of a lignin 5 sample precipitated prior to acetylation and two acetylated lignin 5 samples.

After precipitation, all the L5 lignin sample dissolved in THF, showing that precipitation can be used to increase lignin solubility, presumably as it is more neutral and therefore, less ionised. The peak height in Figure 6-3 clearly shows that more sample is present due to the higher UV absorbance. Figure 6-4 illustrates that after precipitation more higher molecular weight compounds were present, as there are more species with a shorter retention time. This suggests that the compounds that weren't soluble in THF are high in molecular weight, which is unexpected as they should be more hydrophobic and therefore more soluble. Perhaps the shape of the lignin is a factor, or contaminating compounds affect the acetylation. The result indicates that precipitation can be used to ensure better THF solubility to allow analysis of the whole L5 sample.

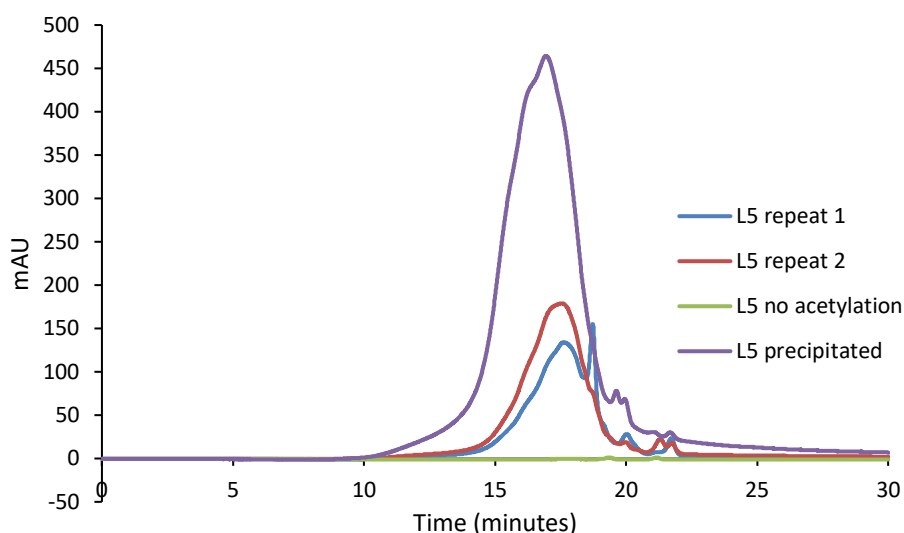


Figure 6-5 GPC plot of a L5 lignin sample precipitated prior to acetylation, two acetylated L5 lignin samples, and a non-acetylated sample dissolved in THF

Figure 6-5 confirms that significant amount of lignin was dissolved as a result of precipitation, leading to a large increase in overall intensity. Precipitation can therefore be used to increase lignin solubilisation in THF.

Table 6-1 Molecular weight data for precipitated and non-precipitated acetylated

Lignin sample	Mn	Mw
L5 repeat 1	782	14693
L5 repeat 2	1120	11889
L5 precipitated	1224	23042

The data in Table 6-1 again highlights the different compositions of the non-precipitated lignin 5 samples. The data also shows that the molecular weight of the lignin soluble in THF after precipitation is significantly higher than the other samples.

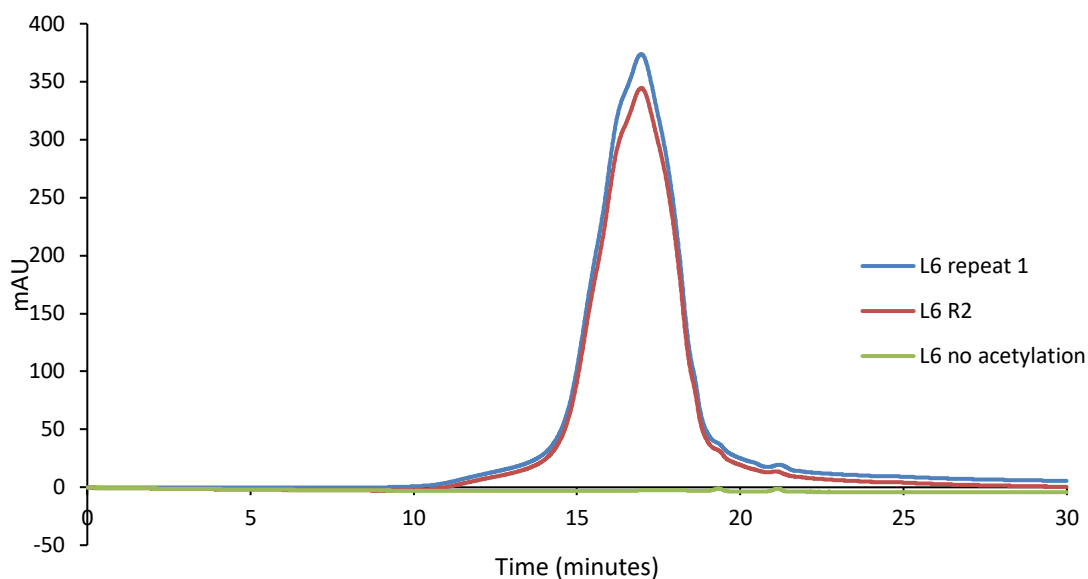


Figure 6-6 GPC plot of two acetylated L6 lignin samples and a non-acetylated sample dissolved in THF

The elution profiles in Figure 6-6, show that without acetylation, L6 lignin is insoluble in THF with no UV absorption detected, and with acetylated lignin repeats, R1 and R2, reproducible results achieved, unlike for L5 lignin. This is because all of the L6 sample dissolved in THF, so it was possible to analyse the whole sample.

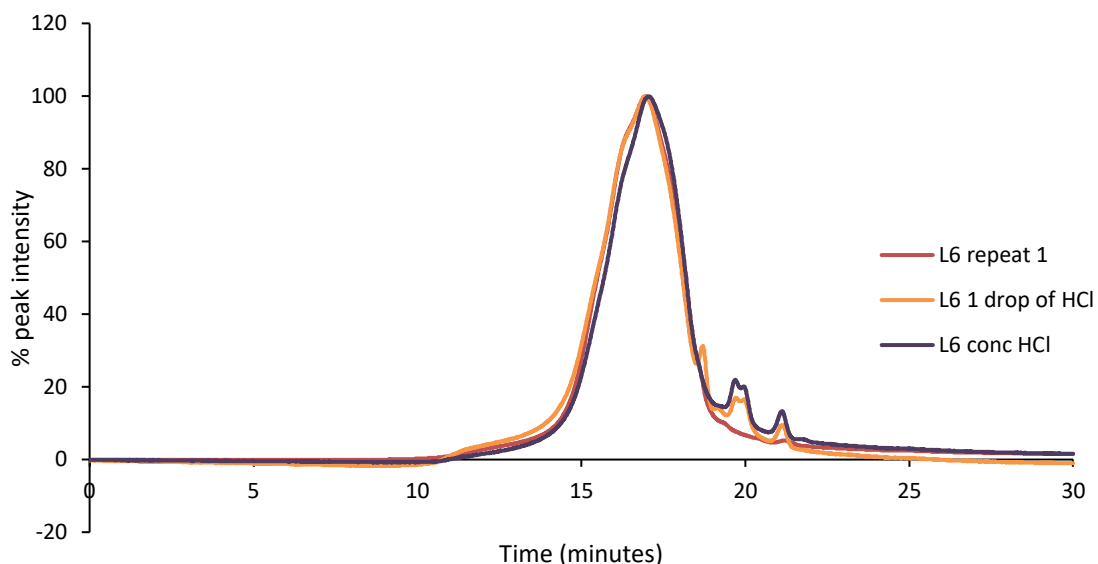


Figure 6-7 Normalised GPC plot of a L6 lignin sample precipitated prior to acetylation (with either 500 μ l of concentrated HCL or 1 drop of concentrated HCL) and acetylated L6 lignin dissolved in THF

In Figure 6-7, acetylated L6 lignin is compared to acid precipitated lignin, and are almost identical. The small differences in amount of acid used may be due to technique: in the centrifuged lignin pellet, low molecular weight products remain the supernatant and are therefore discarded. Precipitation should be carried out with an excess of acid to ensure this does not occur. This also shows that adding HCl does not lead to depolymerisation as the peak shape is unchanged.

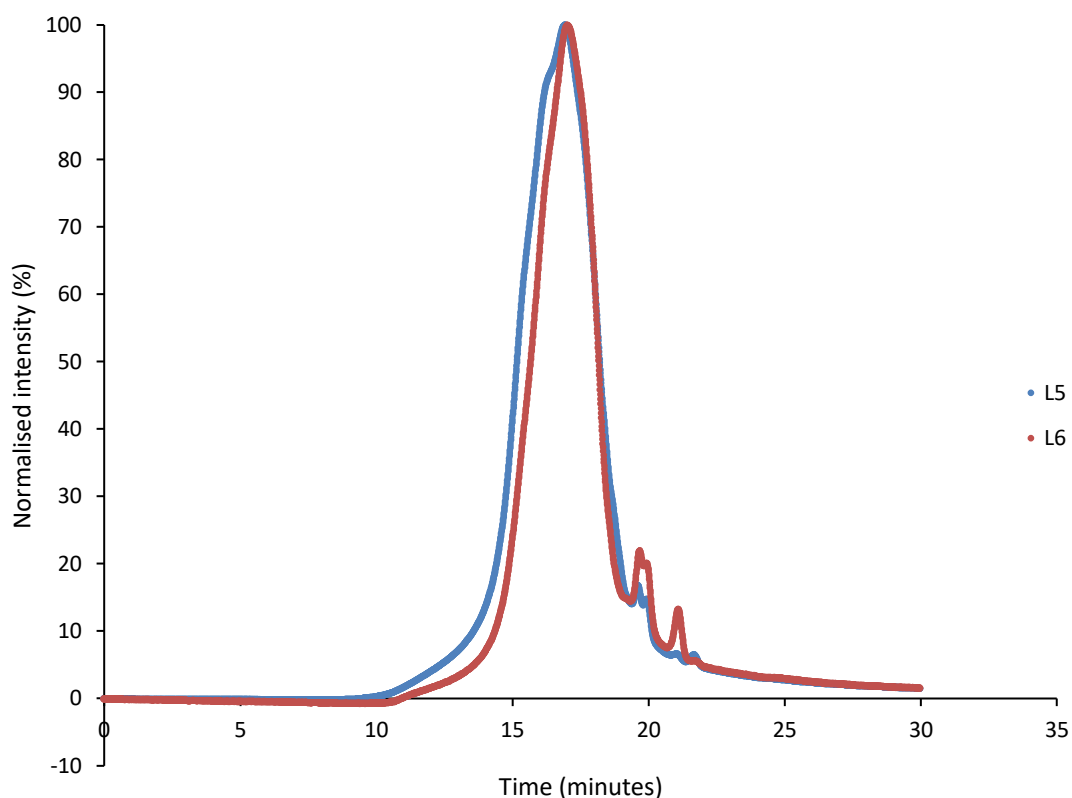


Figure 6-8 Normalised GPC plots of acid precipitated L5 and L6 lignins prior to acetylation

The GPC plots for L5 and L6 in Figure 6-8 are very similar, with the major peak eluting between 10 and around 20 minutes. L5 lignin has a slightly higher molecular weight with the sample eluting slightly before the L6 lignin sample, whilst the low molecular weight fractions, peak shapes between 17 to 19 minutes are almost identical. The two minor peaks around 20 minutes are due to toluene or pyridine. The results show a small difference between L5 and L6 lignin molecular weight distribution, which is expected as these lignins were produced as fractions separated by molecular weight cut-off membranes.

6.3.3 GPC of Protobind and organosolv lignin

To compare the separating power of gel electrophoresis to GPC, reliable lignin standards were prepared. However, this requires comparison of acetylated acid precipitated lignins in THF and samples soluble at pH 8.75 in SB buffer, at which the electrophoresis was carried out. In this work, protobind and organosolv lignin fractions that are soluble in SB buffer were used for both GPC and electrophoresis.

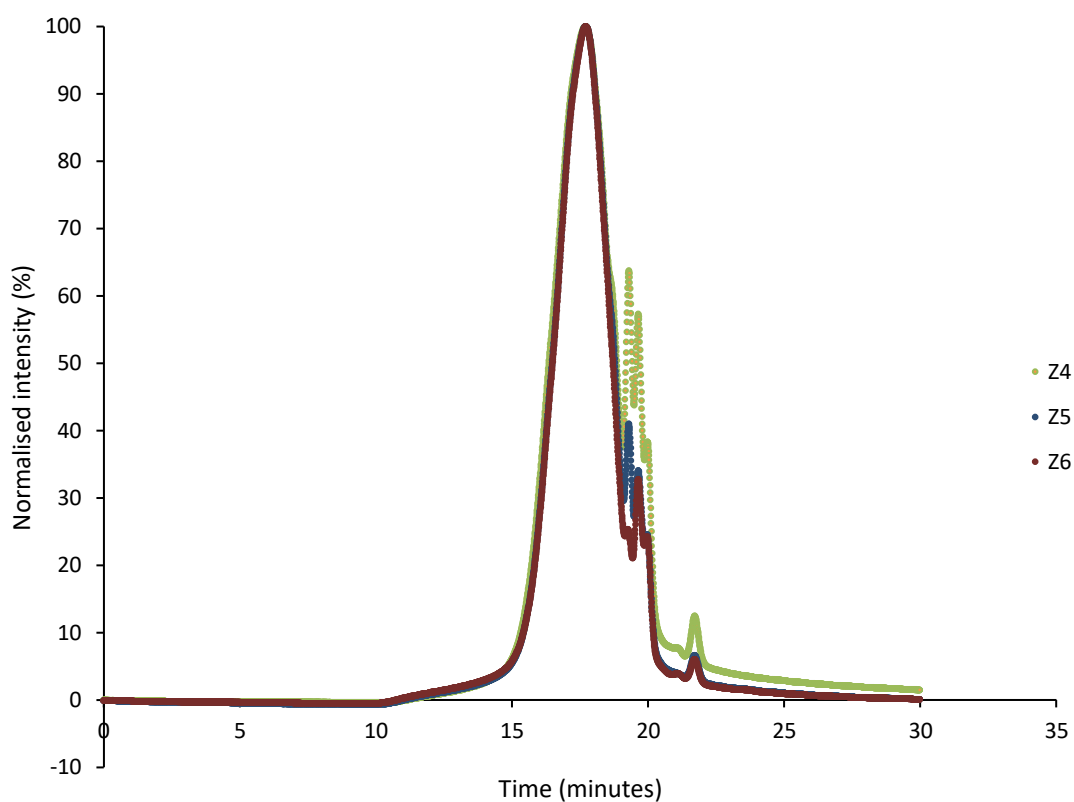


Figure 6-9 GPC of the SB buffer soluble fraction of Z4, Z5 and Z6 protobind lignins post precipitation and acetylation.

The aim of this experiment was to characterise protobind lignin standards by GPC which could then be compared to the migration profiles after gel electrophoresis. The protobind lignin samples Z4, Z5 and Z6, in Figure 6-9 have similar elution

profiles during GPC. There is a major peak between 15 and 20 minutes, with a shoulder at 10 to 15 minutes. The main differences are the minor spiked peaks between around 19 and 20 minutes, which vary in height for each of the samples. A small peak at 22 minutes is due to toluene. Although these protobind samples vary little in molecular weight, the small differences in minor spiked peaks could be useful for characterising gel electrophoresis.

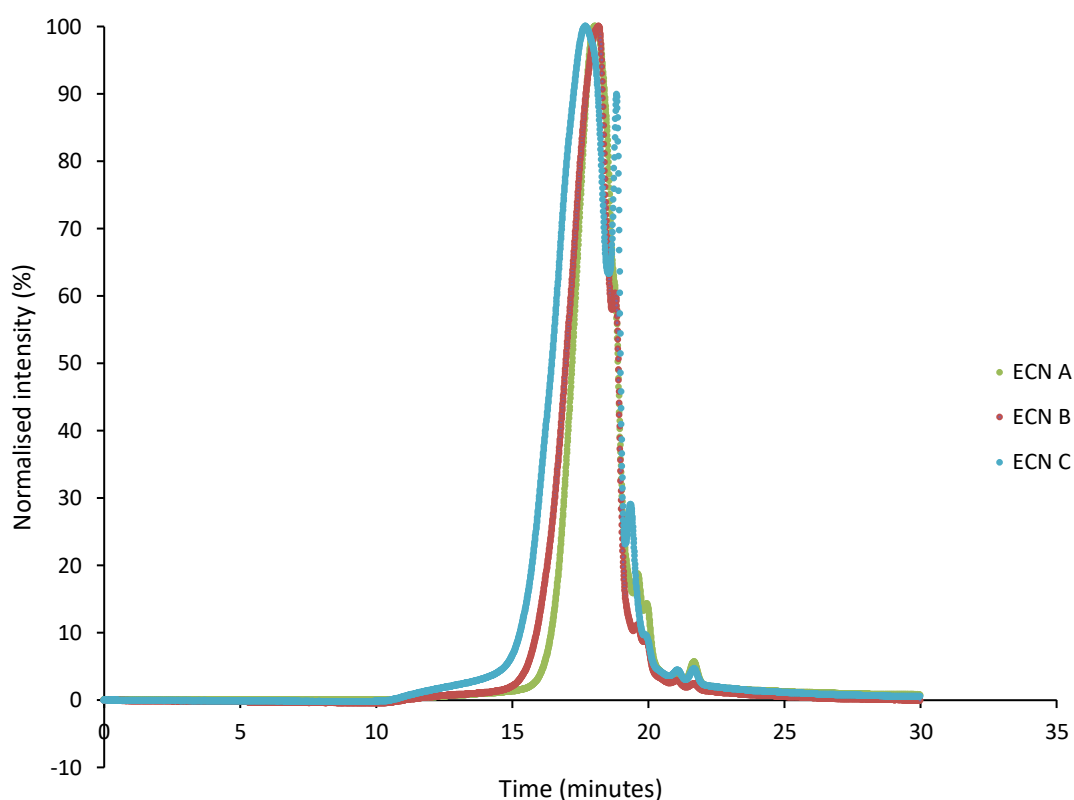


Figure 6-10 GPC of the SB buffer soluble fraction of ECN A, ECN B and ECN C organosolv lignins post precipitation and acetylation.

The organosolv lignins ECN A, B and C in Figure 6-10 have similar peak shapes by GPC, but elute at slightly different times. The major peak in each lignin is between 15 and 20 minutes. The samples elute in the following order ECN C, B then A, with ECN C having a shoulder between 11 and 15 minutes, which is

smaller than in ECN B or A. ECN C lignin has the highest molecular weight. There is a minor peak for ECN C just before 19 minutes but is relatively sharp and has a low peak area.

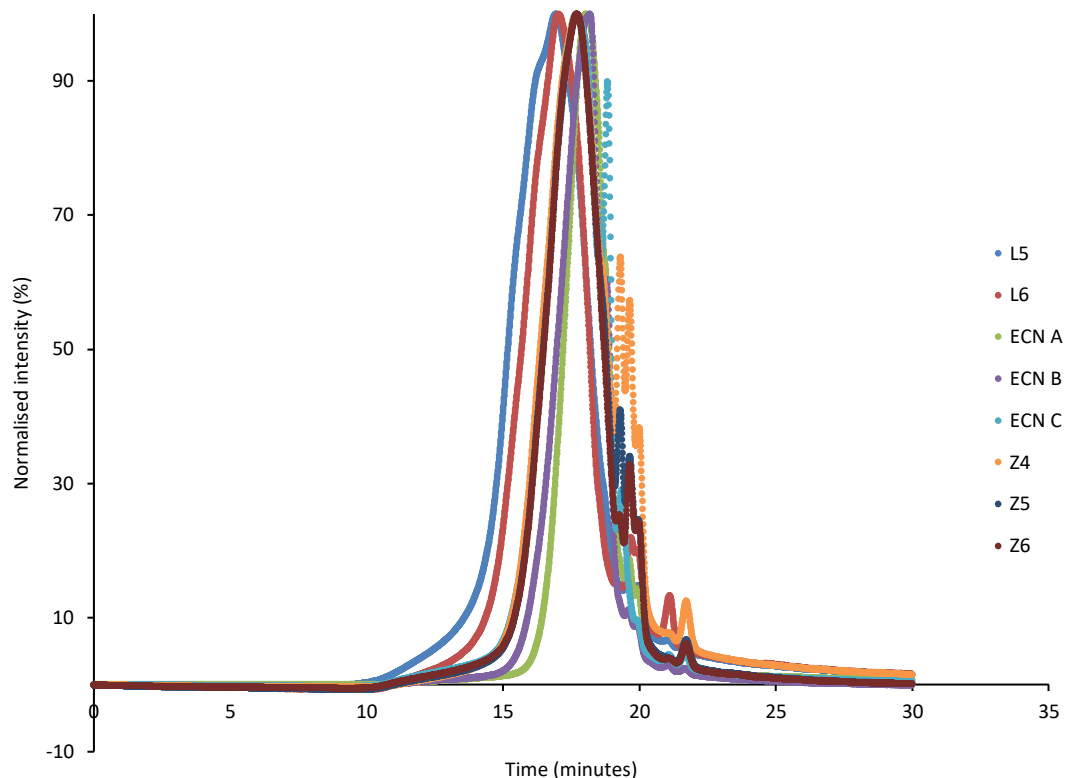


Figure 6-11 Compiled GPC plots of the Kraft, organosolv and protobind samples

All the lignins investigated via GPC are compiled in Figure 6-11, which demonstrates the variation in molecular weight distribution in different lignin samples. L5 and L6 Kraft lignins are higher in molecular weight as they clearly separate from the others. The protobind and ECN C lignins elute next and are similar in molecular weight. The lowest molecular weight lignins are ECN B and

A. Electrophoresis is a mass to charge technique, if the relative masses are known then some estimation of charge can be made (Gordobil et al., 2018).

Table 6-2 Mn and Mw values for Kraft, organosolv and protobind samples. *value provided by manufacturer Sigma-Aldrich

Lignin sample	Mn	Mw
L5	1224	23042
L6	1076	12243
AL	N/A	~10000*
protobind Z4	560	5568
protobind Z5	694	7657
protobind Z6	720	9888
ECN A	634	3198
ECN B	787	5919
ECN C	862	8802

Table 6-2 displays a numerical value for molecular weight, calculated using the lignins in Figure 6-11. Alkali lignin was added to the table using data provided by (Sigma-Aldrich, 2019), it was not possible to analyse this lignin via GPC (see data in Chapter 3); however it is water soluble, and therefore can be analysed via gel electrophoresis. As it is only possible to analyse lignins soluble in specific eluents, (Lange et al., 2016) this would highlight the benefit of gel electrophoresis over GPC. Table 6-2 highlights that the average molecular weight value should not be used in isolation as it does not provide information about the overall molecular weight distribution of a lignin; although it does provide clarity when comparing

many different lignins in terms of average molecular weight. Molecular weight distributions are arguably more useful than a number for molecular weight.

6.3.4 Electrophoresis of lignin standards

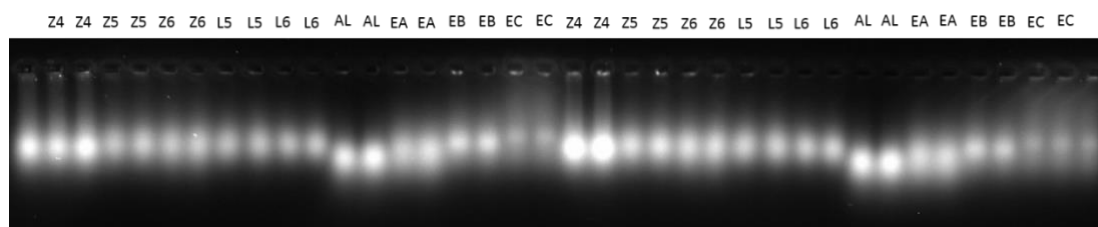


Figure 6-12 Gel with all protobind, Kraft and organosolv samples. Electrophoresis of Z4, Z5 and Z6 protobind samples, L5, L6 and AL Kraft lignin samples and ECN A (EA), ECN B (EB) and ECN C (EC) lignin samples all with 4 repeats each run at 50 V for 1 hour.

Figure 6-12 shows a gel with all of the lignin samples. The high throughput is evident with 9 different samples and 4 repeats each. This took approximately 4 hours to carry out and fully analyse (45 minutes to make the gel and prepare samples, 15 minutes to load them, 60 minutes to incubate the samples, 60 minutes to run the gel and 60 minutes to image and analyse. In comparison, including acetylation, GPC would take at least two days. Looking at the gel, differences are observed between samples. Clearest is the difference in migration between L6 and AL kraft lignin, with the AL lignin moving much further down the gel.

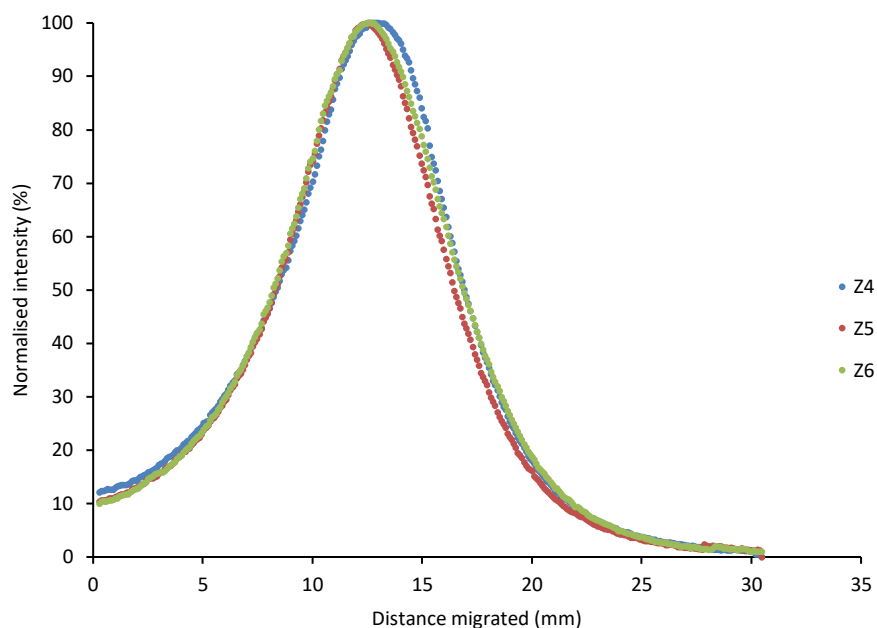


Figure 6-13 Electrophoretic separation of protobind Z4, Z5 and Z6 lignins produced using Figure 6-12

Figure 6-13 shows the similarity in electrophoretic separation between samples of protobind lignins. From 0-5 mm, Z5 and Z6 lignins show related profiles, but Z4 lignin has slightly higher intensity, perhaps due to poorly solubilised aggregates migrating slowly through the gel matrix. Z5 and Z6 lignins continue to follow a similar trend between 5 and 13 mm, with Z4 having slightly lower normalised intensity within this region. Z4 has a peak which extends past the other samples. The experiment shows that minor changes in lignin migration can be detected using gel electrophoresis, even though the samples are similar and therefore likely have a similar mass to charge ratio. The result mirrors the GPC data in Figure 6-9.

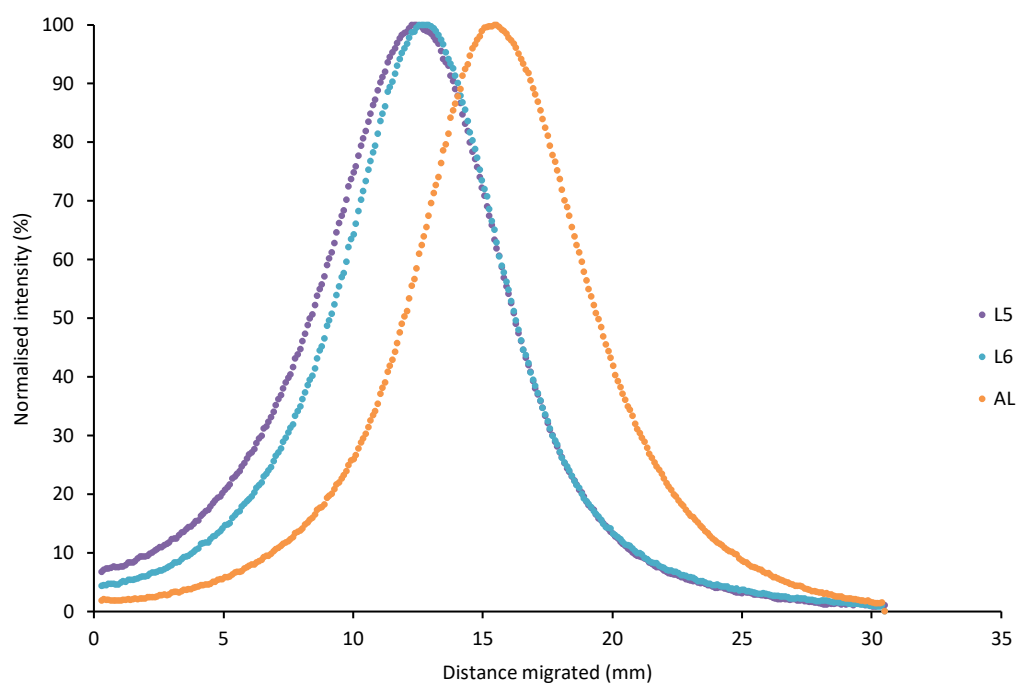


Figure 6-14 Electrophoretic separation of L5, L6 and AL Kraft lignins produced using Figure 6-12

Figure 6-14 shows clear differences between the L5, L6 and AL Kraft lignin samples. L5 is similar in electrophoretic distribution to L6, with both samples peaking at around 12 mm and following a similar trend thereafter. However, L5 has higher normalised intensity, compared to L6, until the sample the samples peak. AL lignin has quite a different migration profile, with a relatively sharp peak at around 13.5 mm. Compared to L6 lignin, L5 lignin is has more slower migrating species, with a higher m/z , but is similar in lower m/z species. AL lignin migrates more quickly, and has therefore a lower average m/z than L5 and L6. This fits with the data provided by Sigma-Aldrich in Table 6-2, where AL has a distinctly lower molecular weight compared to L5 and L6.

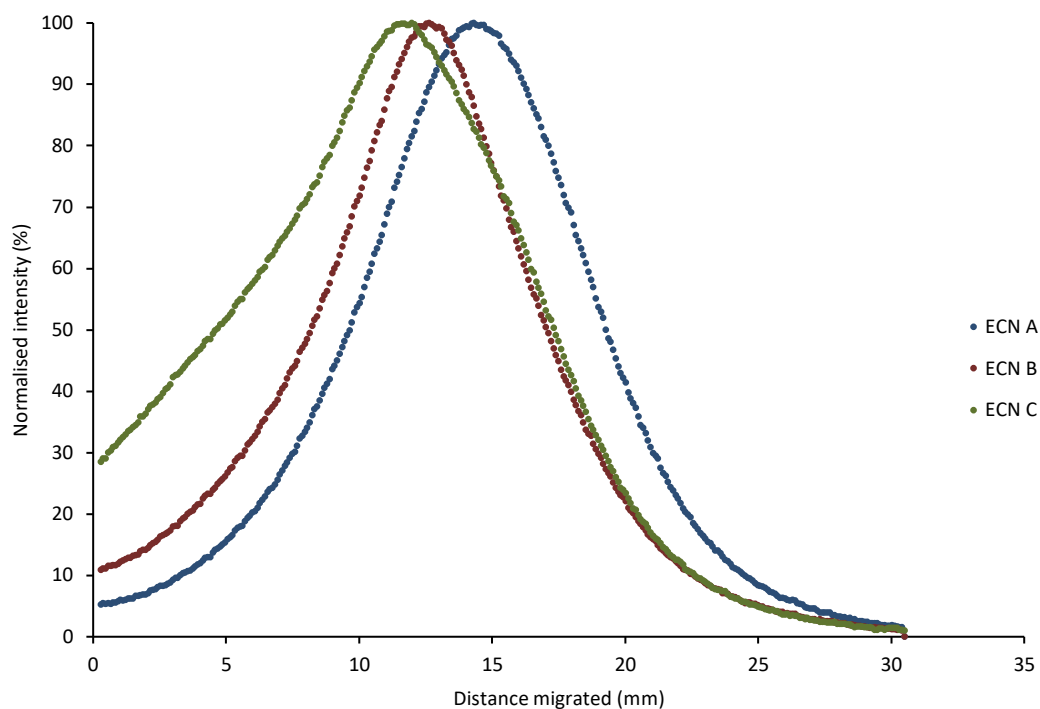


Figure 6-15 Electrophoretic separation of organosolv ECN A, ECN B and ECN C lignins produced using Figure 6-12

The ECN A, B and C organosolv lignins, shown in Figure 6-15, each have distinctive electrophoretic separation. The overall trend is that ECN C migrates less quickly than ECN B which in turn migrates less than ECN A. This matches the order of elution seen in the GPC shown in Figure 6-10 and Table 6-2. ECN C has a much higher normalised intensity between 0 and 10 mm, which could imply that this fraction has a higher m/z compared to the other samples. This may be due to aggregates, or poorly soluble lignin which migrates down the gel at a slower rate. ECN B is significantly less intense in this region but is still higher than ECN A.

6.3.5 Comparison of gel electrophoresis to GPC

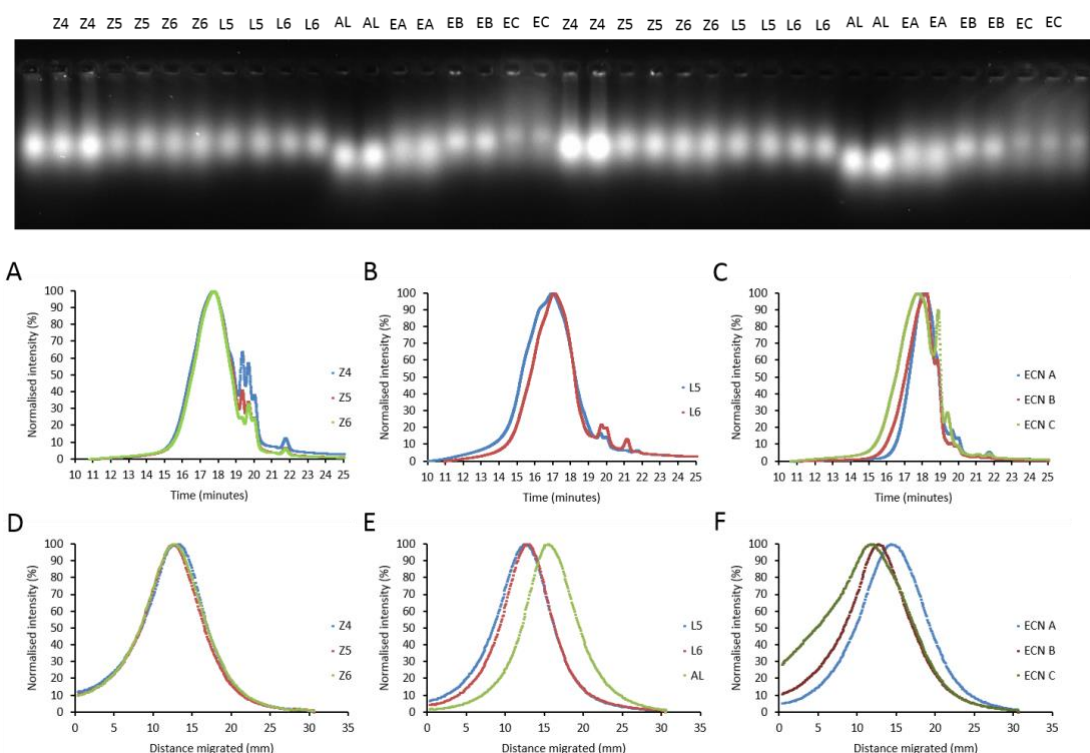


Figure 6-16 Agarose gel post-electrophoresis (top) and corresponding traces D-F, also a comparison with GPC traces. GPC plots for protobind lignins (A), Kraft lignins (B) and organosolv lignins (C) and the electrophoretic separation of protobind lignins (D), kraft lignins (E) and organosolv lignins (F).

Figure 6-16 shows a compilation of the GPC and gel data to enable comparison. The GPC plots for the protobind samples are very similar, however minor differences are detected using electrophoresis. Both GPC and the gel show low m/z fractions in Z4 compared to Z5 and Z6, this shows the m/z electrophoretic separation is comparable to that based on molar mass. Additionally, the low molecular weight fraction is very similar between Z5 and Z6, which is shown on the gels, though Z5 appears to have more low molecular weight fractions

compared to Z6 and the opposite is shown on the gels. For the Kraft lignins, a remarkably similar trend is observed between the GPC and electrophoretic separation. This suggests that mass to charge and molecular weight separations are comparable. This is further supported by the Alkali lignin which separates as expected when the molecular weight provided by Sigma-Aldrich is compared to that of L5 and L6 in Table 6-2. Caution is needed though, as a different molecular weight method was used (Bartzoka et al., 2016). The fact that Alkali lignin can be compared to L5 and L6 using electrophoresis is a nice result, as it was impossible to carry out this using GPC. For the organosolv lignins, the overall separation trend is observed, however there are differences in peak shape. This indicates that with this lignin the results cannot be compared with the same confidence as the Kraft or protobind lignins. This may be due to the lower solubility of the organosolv samples, leading to poor electrophoretic migration. Nevertheless, the result is positive and does infer that it would still be possible to detect molecular weight changes in organosolv samples.

6.4 Conclusions

A suitable lignin light absorption and fluorescence emission wavelength has been identified which is independent of agarose absorption and helpfully corresponds with the Coomassie blue imaging setting. Lignin fluorescence can be detected at 715-730 nm when excited at 680 nm wavelength. Importantly, this means that the lignin can be imaged as a black background, with the lignin showing clearly as a white band. This enables use of ImageJ software to analyse each lane and produce a migration distance vs. fluorescence intensity trace. One of the challenges when characterising lignin standards for GPC was that not all the

sample dissolved in THF. It was found that acid precipitation could be used to increase lignin solubility without affecting the molecular weight of lignin. Using precipitation it was possible to characterise lignin standards (except Alkali lignin) and obtain a molecular weight distribution, which could then be compared to the separation that occurs on a gel.

Gel electrophoresis of various lignin types was successful, and demonstrated the high throughput technique. Electrophoretic separation of lignin was compared to the separation via GPC. For all of the different lignin types tested there was remarkable similarity between the methods. Electrophoresis showed as high a resolution as GPC, and this was especially evident with the protobind lignins where small changes in migration were detectable. Electrophoresis evaluates migration as a function of mass to charge, whilst GPC analyses mass, so the similarity indicates that the charge component is closely correlated to the mass. If the separation were due to charge alone the profile would not match the GPC profile. As a result, gel electrophoresis could also be used to monitor molecular weight or charge change in lignin degradation. If lignin standards of known molecular weight were available, these could be used to correlate the extent of its digestion, in a similar manner to DNA studies that commonly use a molecular weight marker lane (Southern, 1979). The technique may also be useful in determining changes in charge, for example by enzymes that demethylate methoxy aromatic residues (Hämäläinen et al., 2018).

Chapter 7

Gel electrophoresis to analyse and estimate the degradation of lignin

7.1 Introduction

Monitoring lignin degradation and changes in lignin structure is challenging and is a barrier to developing processes to valorise lignin. To optimise its degradation it would be beneficial to observe changes in mass and structure directly, not just infer it by indirect methods. The difficulties are summarised by (Hatfield and Fukushima, 2005) who have reviewed different methods to measure lignin. They end the article by stating that each method gives different values of lignin concentration and there is no best method. It is very hard to assess the level of degradation of lignin by bacteria, especially as a complex mixture of lignin, degraded lignin, proteins and DNA is produced. For example, analysing the production of metabolites gives poor estimates of breakdown, as changes in the starting material are unseen, so there is no mass balance (Tian et al., 2016). In the respective work the decolourisation of dyes was used to infer degradation, but, because there are many mechanisms for this, false estimates are given. The situation is similar with enzyme mediated breakdown, where the nitrated lignin assay has been used (Ahmad et al., 2011). This involves chemical modification post-digestion, and measures changes in the absorbance of soluble species, but fails to identify what they are or how much breakdown has occurred. Analysis of lignin that has undergone hydrothermal carbonisation (HTC) is complex due to the production of solid, liquid and gaseous products. Methods that have been used to assess the level of degradation are NMR, FTIR, TGA and pyrolysis GC/MS (Wikberg et al., 2015). None of these are able to assess accurately lignin

concentration or structure. Particle size distribution of untreated and HTC treated lignin were used to assess the level of polymerisation, but this is unreliable due to its predisposition to aggregate (Sipponen et al., 2018). In this work, gel electrophoresis was identified as a high-throughput technique to detect changes in lignin concentration and structure able to monitor degradation.

7.2 Methods

7.2.1 Control sample - pre-degradation tests

The experiment was carried out with a total volume of 50 ml in a 250 ml conical flask containing: 5 g/L L6 Kraft lignin or 5 g/L Alkali lignin, 70 mM pH 7 potassium phosphate buffer. The flask was incubated in a shaker incubator at 180 rpm set at 37 °C. 1 ml samples were taken before incubation and every 24 hours thereafter, for 72 hours. Each sample was centrifuged for 15 minutes at 4500 rpm and the supernatant used for electrophoresis.

7.2.2 Bacterial lignin degradation

All bacterial growth was carried out with a working volume of 50 ml in 250 ml conical flasks in a shaking incubator at 30 °C and 180 rpm. Degradation conditions were based on (Salvachúa et al., 2015) with pH 7 sterilised M9 media containing 6.78 g/L Na₂HPO₄, 3 g/L KH₂PO₄, 1 g/L NH₄Cl, 0.5 g/L NaCl and 1.5 g/L L6 Kraft lignin (Salvachúa et al., 2015). The following elements were added after sterilisation with a syringe filter with 0.2 µm pore size: 2 mM MgSO₄, 100 µM CaCl₂, 100 µM CuSO₄, 100 µM MnSO₄, 100 µM FeSO₄, 100 µM ZnSO₄, and 0.1 g/L vanillic acid to supplement growth for *Rhodococcus jostii* and 10 g/L glucose for *Pseudomonas putida*. For the *R. jostii* experiments, 50 µg/ml chloramphenicol dissolved in ethanol was added (without thiostreptone inducer). Prior to inoculation into the media *R. jostii* and *P. putida* were grown in LB medium for 24 hours and used to inoculate the above media to a starting OD₆₀₀ of 0.1. No bacteria were added to the control sample. 1 ml samples were taken at specific time points and centrifuged for 15 minutes at 4500 rpm to pellet the bacteria, the supernatant was then used for electrophoresis.

7.2.3 Proteinase K and heat treatment of bacterially degraded lignin

40 µl of 10 mg/ml proteinase K solution was added to 1 ml of 1.5 g/L *P. putida* treated L6 lignin solution. The mixture was then incubated overnight in a shaking incubator at 200 rpm set at 37 °C. The sample was then centrifuged at 4500 rpm for 15 minutes and the supernatant was used for electrophoresis. For the heat treatment test, 1 ml of the *P. putida* sample was heated to 95 °C for 5 minutes using a heat block. The sample was then centrifuged at 4500 rpm for 15 minutes and the supernatant was then used for electrophoresis.

7.2.4 Microwave treatment of bacterially degraded lignin

2 ml of *P. putida* treated lignin samples were added to a 10 ml pressure reaction vial, using a lid to ensure the reaction was sealed and to prevent water evaporation. Microwaving was carried out with a CEM Discover SP automated microwave using a stir bar to ensure proper mixing. Microwaving was carried out at 95 °C for 30 minutes in order to denature any proteins present without boiling the sample.

7.2.5 Hydrothermal Carbonisation (HTC) degradation of lignin

Alkali lignin, low sulfonate content (used due to the high mass of lignin required) was dissolved in water (210 ml total volume) to make a 100 g/L solution which was transferred to a 600 ml non-stirred Parr reactor and heated to 250 °C using a 4836 reactor controller to raise the temperature of the surrounding heating jacket through PID control. The lignin solution was kept at 250 °C for 1 h under self-generated pressure. A 10 ml sample was taken before heating. After cooling to room temperature the reaction

mass the process water was filtered using Whatman Grade 4 filter paper to remove the residual solids, the filtrate was then used for gel electrophoresis. Prior to electrophoresis the samples were diluted 20 times in water, as the highly concentrated lignin samples migrate slower on the gel compared to the diluted samples in the lignin standard curve on the gel.

7.2.6 Laccase degradation of lignin

Enzyme treatment was carried out in a 250 ml conical flask with a total reaction volume of 50 ml containing: 5 g/L L6 Kraft lignin, 70 mM pH 7 potassium phosphate buffer, 0.55 mM syringaldehyde (100 μ L of a 275 mM stock solution dissolved in methanol) and 11.8 units of the MetZyme LIGNO laccase enzyme mixture. The control sample was identical in composition and volume except for the presence of enzyme. 1 ml samples were taken pre-incubation and at the respective time points and centrifuged for 15 minutes at 4500 rpm, the supernatant was then used for electrophoresis. The enzymatic digestion was carried out shaker incubator at 180 rpm set at 37 °C.

7.2.7 Hydrogen peroxide degradation of lignin

Degradation was carried out in a 250 ml conical flask with a total reaction volume of 50 ml containing 5 g/L L6 Kraft lignin, 70 mM pH 7 potassium phosphate buffer and 0.35 M H₂O₂. The control sample was identical in composition and volume except for the presence of hydrogen peroxide. 1 ml samples were taken pre-incubation and at the respective time points and centrifuged for 15 minutes at 4500 rpm, the supernatant was then used for electrophoresis. The hydrogen peroxide degradation was carried out in a shaker incubator at 180 rpm set at 37 °C.

7.2.8 Quantification of lignin degradation

All gels were produced and analysed using standard methods for the Clarit-E Maxi gel tank and analysed via the standard ImageJ analysis method. Samples for the standard curve were prepared by dilution of the lignin in water.

7.3 Results and discussion

7.3.1 Pre-degradation tests

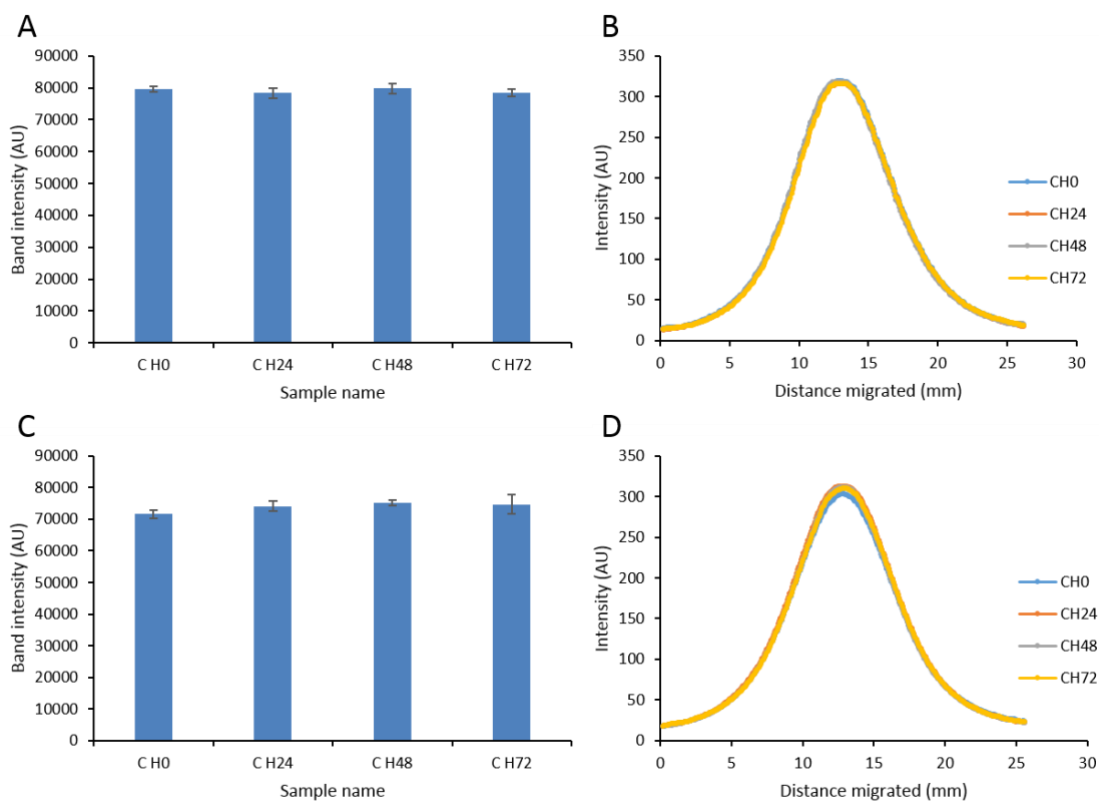


Figure 7-1 Fluorescent intensity of 5 g/L Alkali lignin (A and B) and 5 g/L L6 lignin (C and D) incubated at 37 °C for 72 hours in total.

The band intensities in the control samples for Alkali lignin and L6 lignin (A and C) incubated over 72 hours are shown in Figure 7-1 are very similar. This shows that during incubation the lignin fluorescence intensity does not change. The slight increase in graph C is most likely due to the gel being incompletely uniform. The electrophoretic migration graphs (shown in B and D) are similar, which shows that during incubation there are no structural changes. This is important to test as for example the lignin could aggregate in solution.

7.3.2 *Pseudomonas putida* KT2440 degradation of lignin

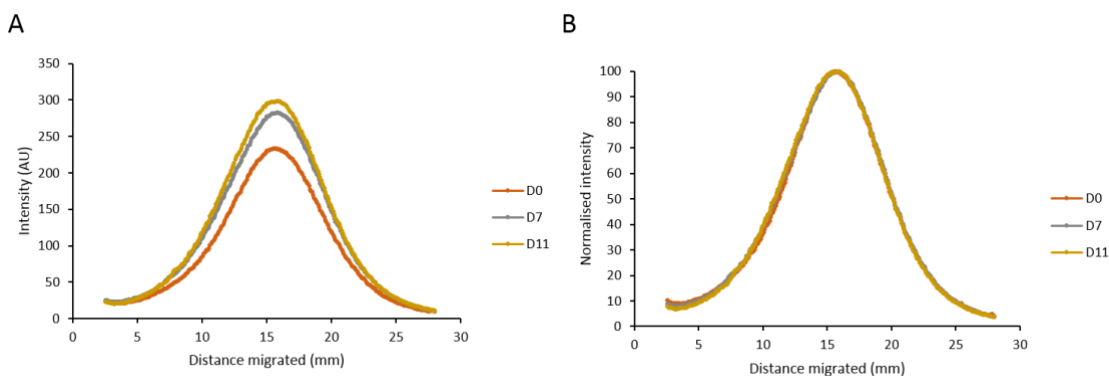


Figure 7-2 Electrophoretic separation of *Pseudomonas* treated 1.5 g/L L6 lignin sample. A: raw data B: normalised data. Samples taken at day 0, 7 and 11.

Figure 7-2 shows the effects of *Pseudomonas putida* KT2440 degradation of lignin. There was large increase in band intensity from 0-7 days and then another smaller increase from 7 to 11 days of incubation. This is surprising as it would be expected for the intensity to decrease and not increase. This could be due to chemical modification of the lignin by the bacteria leading to a more open structure with less fluorescence quenching. However, it may also be due to proteins binding and migrating with the lignin leading to an overestimation of the lignin concentration. Lignin has been shown to bind to proteins to inhibit enzymes to prevent hemicellulose degradation (Kumar et al., 2012). This is supported by graph B in Figure 7-2 which shows a slightly higher intensity between 7.5 and 12.5 mm. An increase in the mass to charge ratio (m/z) was likely responsible for this and could be explained by the binding of proteins to lignin and the subsequent slower migration of this complex during electrophoresis.

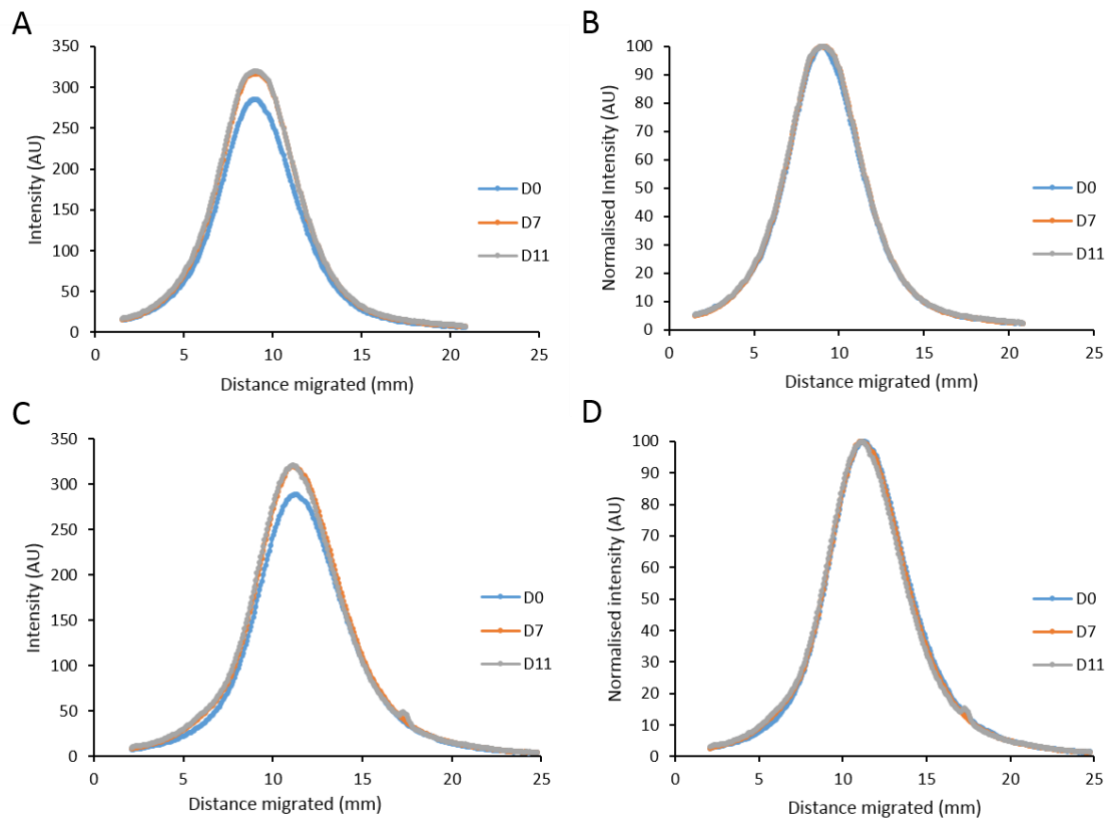


Figure 7-3 Electrophoretic separation of *Pseudomonas* treated 5 g/L L6 (A and B) and 5 g/L Alkali lignin (C and D). A and C = raw data B and D = normalised data. Samples taken at 0, 7 and 11 days.

An experiment was carried out to compare L6 Kraft lignin and Alkali lignin digestion by *Pseudomonas*. Figure 7-3 shows a similar trend to Figure 7-2 with increasing fluorescence, though not as high, and there was no observable increase from day 7 to day 11. If higher concentrations of lignin were used, the protein binding would be less significant. Conversely, high concentrations of lignin are toxic to bacteria so this is likely not viable (Chandra et al., 2008). In Figure 7-2 A and B the peak shape becomes more rounded, perhaps due to the binding of protein leading to changes in electrophoretic migration. *P. putida* is known to produce extracellular enzymes, and is not catabolically repressed when grown on glucose (unlike *R. jostii*) (Salvachúa et al., 2015). The growth of *P.*

putida with 10 g/L glucose likely led to a large export of proteins which perhaps bind to the lignin.

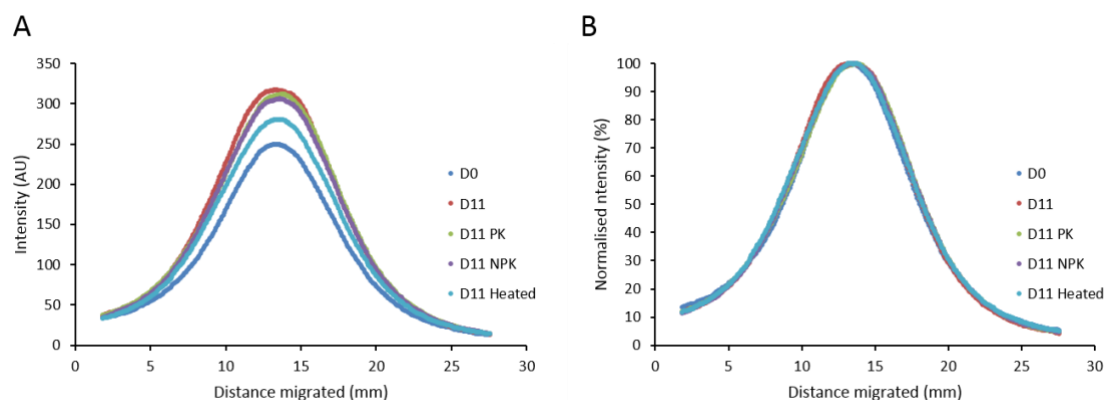


Figure 7-4 Electrophoretic separation of *Pseudomonas* treated 1.5 g/L L6 lignin sample that was treated to remove protein. A: raw data B: normalised data. Samples taken at 0 and 11 days. PK= proteinase K, NPK= no proteinase K, Heated= sampled heat treated prior to electrophoresis.

The hypothesis that protein was responsible for the increase in band intensity was tested using several protein removal methods. Ammonium sulphate and sodium chloride precipitation were tested, however, the lignin precipitated, so were unsuitable. Treatment with proteinase K, Figure 7-4 shows little change in fluorescence to the control, perhaps the lignin bound proteins were inaccessible to the proteinase K, or it was deactivated by binding to lignin. However, heat treating the sample at 95 °C for 5 minutes without mixing, prior to electrophoresis, gave a clear difference to the control. Heat treatment causes proteins denature and form aggregates which can then be removed via centrifugation and this may have led to the decrease in intensity, however lignin may also change upon heat treatment.

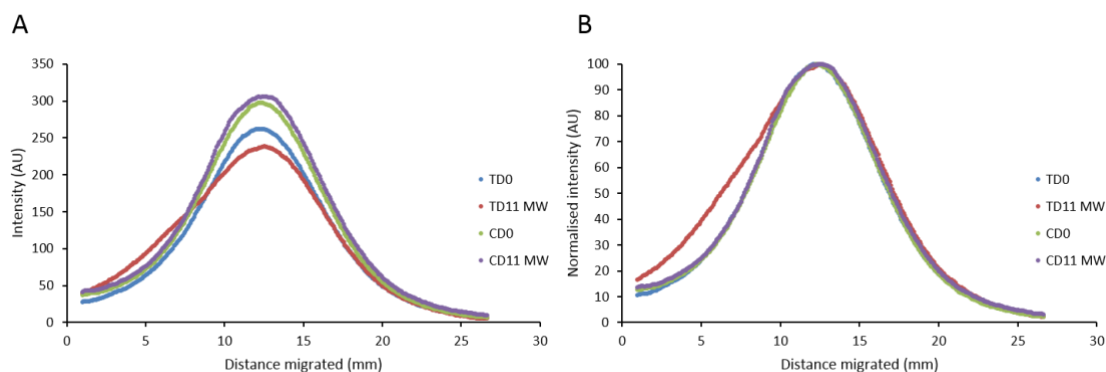


Figure 7-5 Electrophoretic separation of *Pseudomonas* treated 1.5 g/L L6 lignin sample after microwaving at 95 °C for 30 minutes. A: raw data B: normalised data. TD0 and CD0 were lignin samples pre-incubation with bacteria and without bacteria respectively. TD11 MW and CD11 MW were microwaved lignin samples after 11 days of incubation, with and without bacteria respectively.

The heat treatment procedure was further investigated. The results in Figure 7-5 involve microwaving at 95 °C for 30 minutes with stirring. There were few changes in the control samples, showing that heat treatment does not lead to aggregation of lignin. However, there was a decrease in intensity for the microwave treated *Pseudomonas* degraded sample compared to the pre-incubation control sample. Moreover, an increase in intensity was observed between 0 and 12.5 mm for the day 11 *Pseudomonas* microwave treated sample, which was likely due to large aggregates moving slowly through the agarose matrix. This fits with the hypothesis that protein was responsible for the increase in lignin intensity. More analysis of bacterially degraded lignin should be carried out in the future to test whether protein can be effectively separated from polymeric lignin. Perhaps this could be tested by carrying out Py-GC/MS on the pellet produced after microwaving and then centrifugation of the lignin sample; the presence or absence of lignin degradation products would confirm whether lignin is present.

7.3.3 *Rhodococcus jostii* RHA1 degradation of lignin

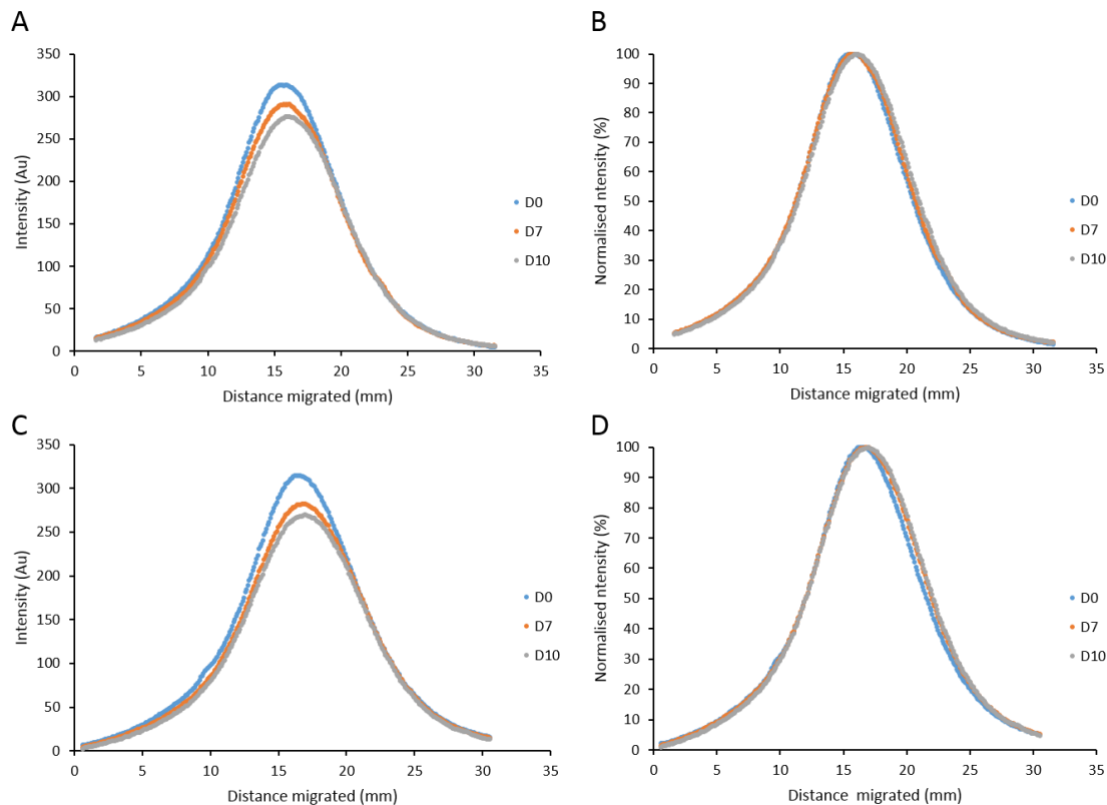


Figure 7-6 Electrophoretic separation of *Rhodococcus jostii* treated 1.5 g/L L6 without 0.1 g/L vanillic acid (A and B) and 1.5 g/L L6 with 0.1 g/L vanillic acid (C and D). A and C = raw data B and D = normalised data. Samples taken at 0, 7 and 11 days.

Unlike *R. jostii*, *P. putida* exhibits limited lignin degradation when grown in nutrient limited conditions (Salvachúa et al., 2015) Using *R. jostii* in nutrient limited conditions should lead to lignin breakdown without excessive extracellular protein production. Vanillic acid is an intermediate produced by the degradation of lignin and induces enzymes in the aromatic degradation pathways, without catabolic repression. Furthermore, vanillic acid is a low molecular weight aromatic compound and is much less energetically expensive to metabolise, so may stimulate the growth of *R. jostii* (Xu et al., 2019). Graph A in Figure 7-6 shows a

decrease in band intensity, hence lignin concentration, between 0 and 7 days of incubation with little change in electrophoretic migration. Between 7 and 10 days there was small decrease in band intensity, and a small shift to the right that indicates a decrease in m/z , inferring that lignin has been degraded by the bacteria. This is supported by the normalised graph B. The addition of vanillic acid between 0 and 7 days gives a larger electrophoretic difference in lignin migration than without, and is seen clearly when the traces are normalised in graph D. This implies that vanillic acid stimulated growth and/or the aromatic degradation pathways leading to faster lignin degradation. After 10 days there was only a small decrease in intensity, which suggests the 'accessible' lignin has been degraded by this point. These experiments show bacterial lignin degradation can be monitored using gel electrophoresis. However, the presence of proteins could still be leading to an underestimate of its degradation.

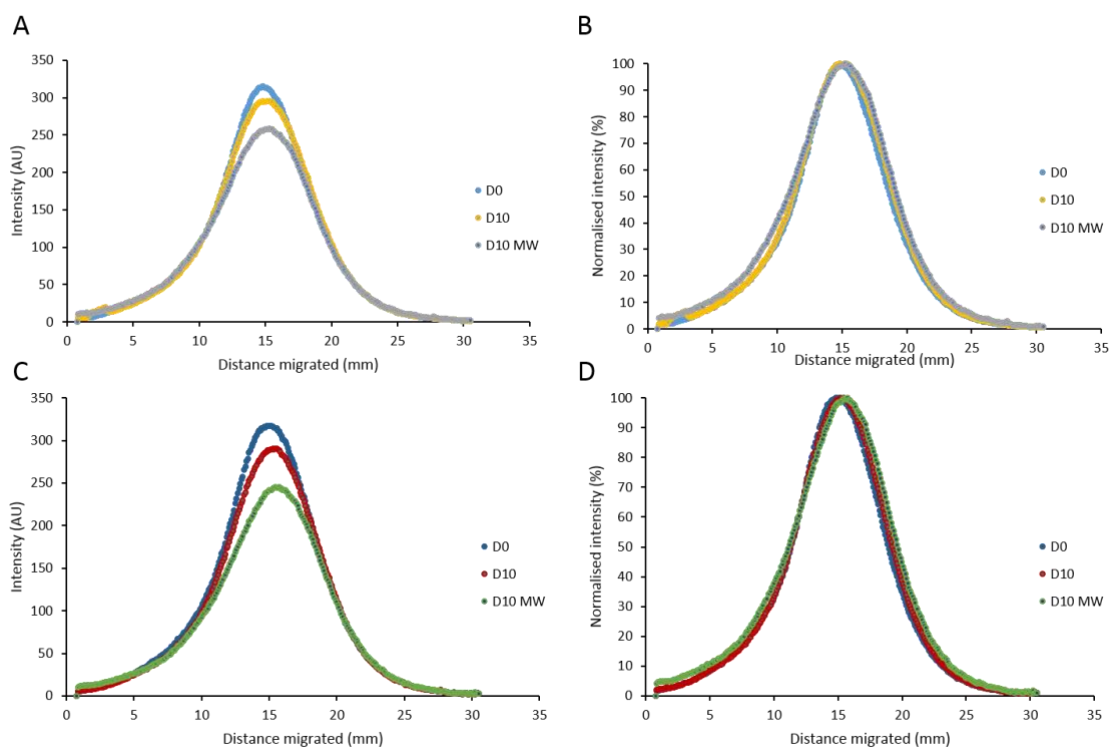


Figure 7-7 Electrophoretic separation of *Rhodococcus jostii* treated and microwaved 1.5 g/L L6 without 0.1 g/L vanillic acid (A and B) and 1.5 g/L L6 with 0.1 g/L vanillic acid (C and D). A and C = raw data B and D = normalised data.

To check this, the microwaving heat treatment procedure was tested. Graph A in Figure 7-7 shows a slight decrease in overall intensity from 0 to 10 days, which is less than the decrease observed in Figure 7-6, this was likely due to the low concentration of lignin leading to high standard deviation. Significantly there was a large decrease in band intensity after microwaving, and a shift to the right, i.e. less mass or higher anionic charge, shown clearly in the normalised graph B. The microwaved sample in graph B also shows a higher band intensity from 0 to 12.5 mm, which was likely due to aggregated proteins that were removed by centrifugation. Similar results are shown for when vanillic acid was present (graph C and D), though there is a more pronounced shift to the right after microwaving

of the sample. These results suggest that protein was present in the *R. jostii* samples after degradation, so there is still ambiguity over whether protein can be removed from the sample without removal of lignin.

7.3.4 Quantification of bacterial lignin degradation

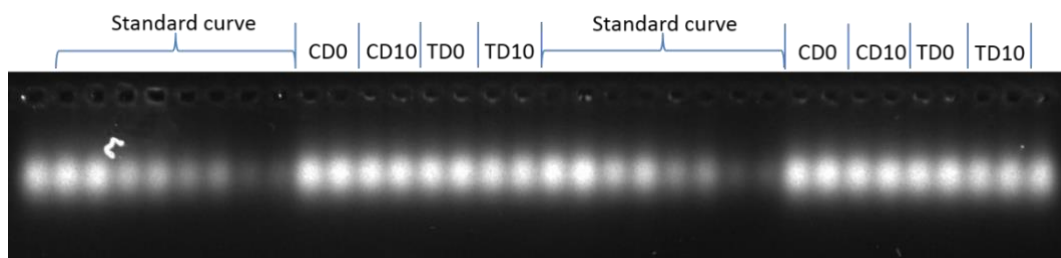


Figure 7-8 Agarose gel containing a lignin concentration gradient, controls and 1.5 g/L *R. jostii* degraded L6 Kraft lignin. Sample order in duplicate: 1.5 g/L, 1.125 g/L, 0.75 g/L, 0.375 g/L, CD0, CD10, TD0 and TD10. The sequence was then repeated so there were 4 repeats for each sample. The 1.5 g/L and 1.125 g/L samples were only in triplicate as a dust particle covers part of the sample in lanes 3 and 4. Control day 0 (CD0), control day 10 (CD10), *R. jostii* degraded lignin day 0 (TD0) and *R. jostii* degraded lignin day 10 (TD10)

Figure 7-8 shows how a lignin concentration gradient, controls and degraded samples can be run on the same gel with four repeats, and highlights the high throughput nature of the technique. One of the issues with the technique is shown by the presence of dust particle over two gel lanes that presumably fell before the agarose had gelled, leading to those samples being omitted from analysis. From the image, a decrease in band intensity with concentration is clearly seen; the control samples are similar and the degraded sample looks slightly less intense.

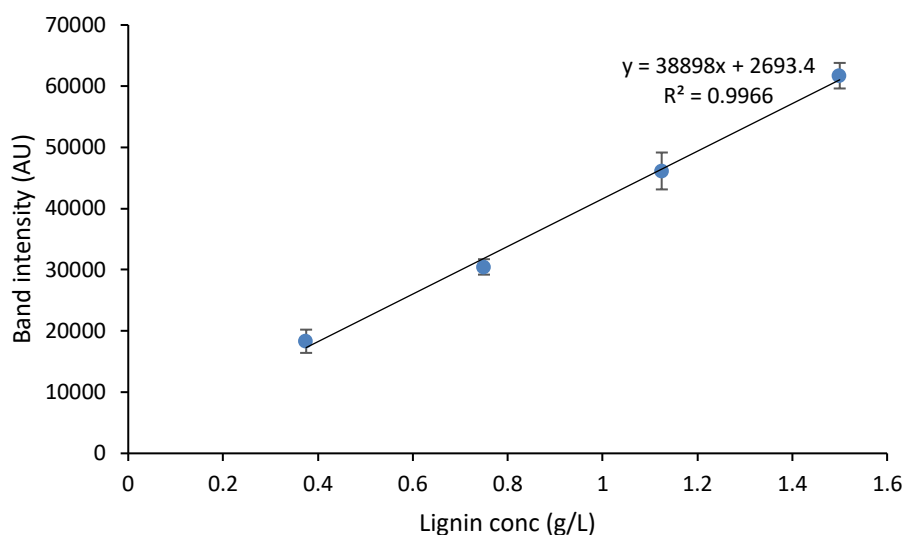


Figure 7-9 Lignin concentration gradient produced using Figure 7-8

After imaging the gel a graph a calibration curve for band intensity vs lignin concentration was obtained, Figure 7-9. There is a low standard deviation showing good reproducibility. This shows it ought to be possible to determine lignin concentration in an unknown sample.

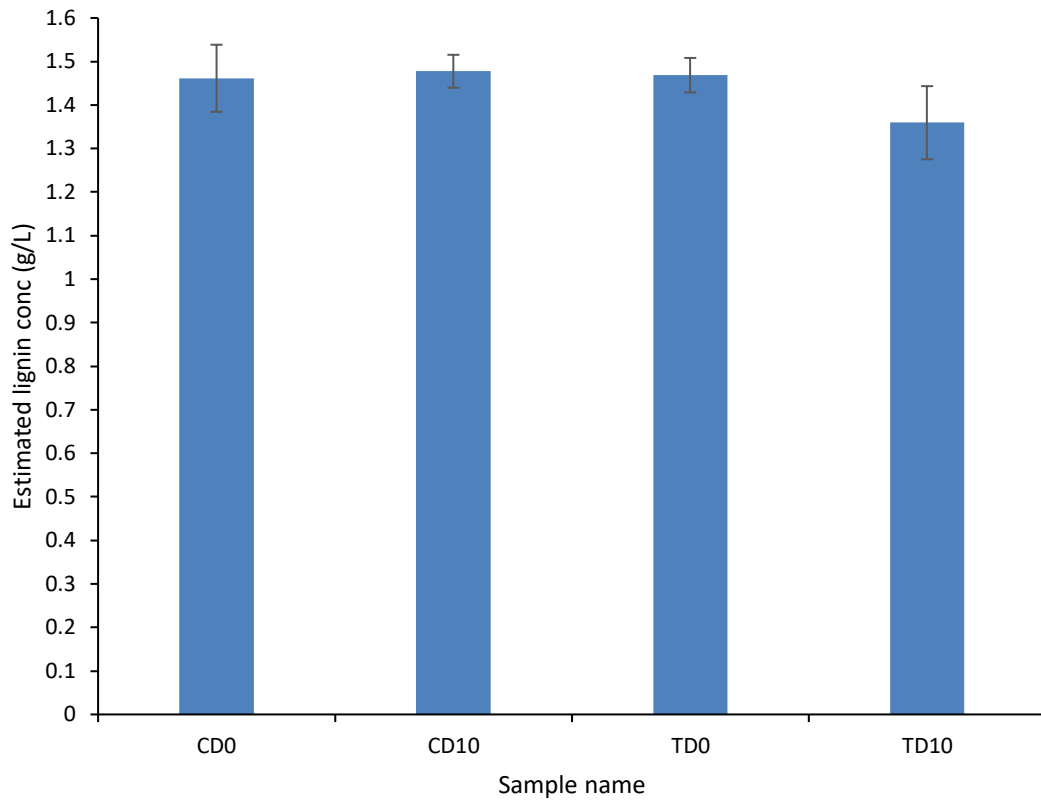


Figure 7-10 Estimated concentration of *R. jostii* degraded lignin and controls samples produced using Figure 7-9

The concentrations of 1.46, 1.48 and 1.47 g/L for the controls CD0, CD10 and TD0, respectively, are very close to the expected 1.5 g/L, Figure 7-10. The lignin concentration in the degraded sample was found to be 1.36 g/L which is a 7.5% reduction in concentration though the error bars in CD0 and TD10 are wide. Kraft lignin is a difficult substrate to metabolise, and is toxic, which may have limited the bacterial growth (Chandra et al., 2007).

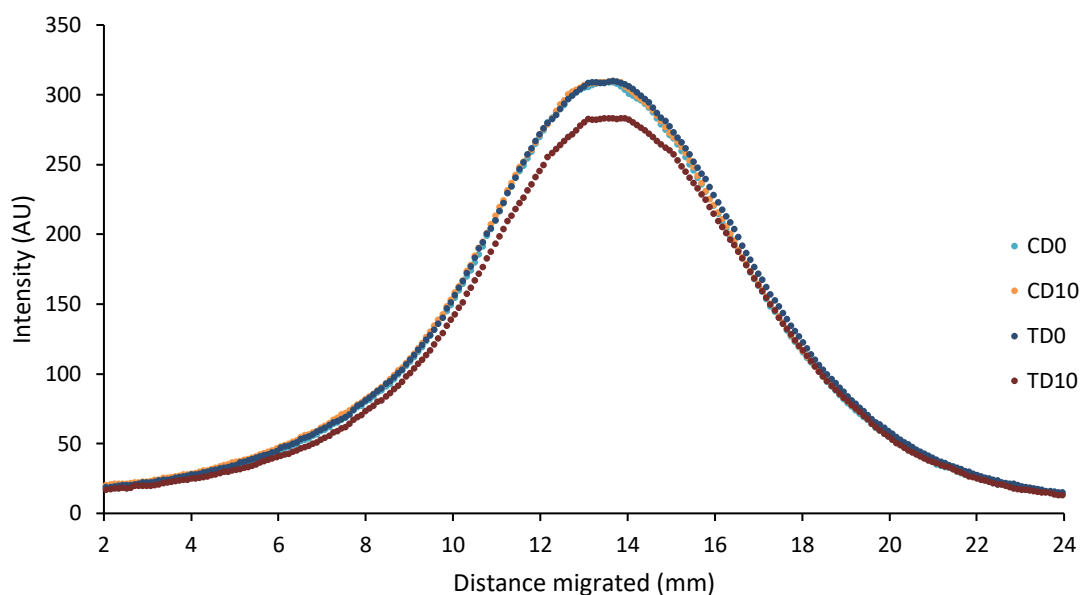


Figure 7-11 Electrophoretic separation of control and *R. jostii* treated samples produced using Figure 7-8

Figure 7-11 shows the electrophoretic separation of the control and *R. jostii* degraded samples run on a single gel. The similarity of the controls and the pre incubation samples is especially clear. A decrease in the band intensity of the bacterially degraded sample can be seen, along with a slight shift to the right, suggesting preferential degradation of high m/z lignin polymers. The result demonstrates that using a single agarose gel, the concentration in an unknown sample can be detected, and changes in the lignin polymer can be assessed.

7.3.5 Quantification and analysis of hydrothermal carbonisation of lignin

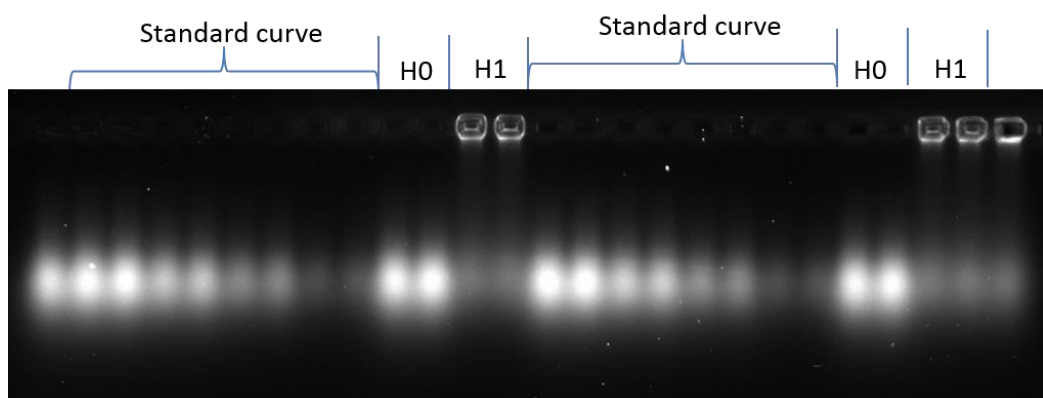


Figure 7-12 Agarose gel containing a lignin concentration gradient, controls and 100 g/L (diluted 20x) Alkali lignin. Sample order in duplicate: 5 g/L, 3.75 g/L, 2.5 g/L, 1.25 g/L, H0 and H1. The sequence was then repeated so there were 4 repeats for each sample. Sample pre-HTC (H0) and sample after 1 hour of HTC treatment (H1)

Alkali lignin samples were hydrothermally treated and the effects upon degradation assessed using electrophoresis. The experiments were run at high lignin concentrations, and whilst 100 g/L samples can be run on the gels, they were diluted 20-fold prior to running to stay within the bounds of the calibration curve. In Figure 7-12 there was a clear decrease in intensity with decreasing lignin concentration. To add to that, the sample taken before HTC also appears to be similar in intensity to the 5 g/L sample. The main band of the HTC treated sample migrates the same distance as the control samples. However, there is an obvious smear above the band and in the pockets which is likely due to polymerisation/carbonisation of lignin that increases the particle size and changes the m/z ratios. Without standards the solid fraction cannot be accurately estimated, preventing a mass balance. In addition, light may not penetrate the solid, so perhaps the intensity was underestimated.

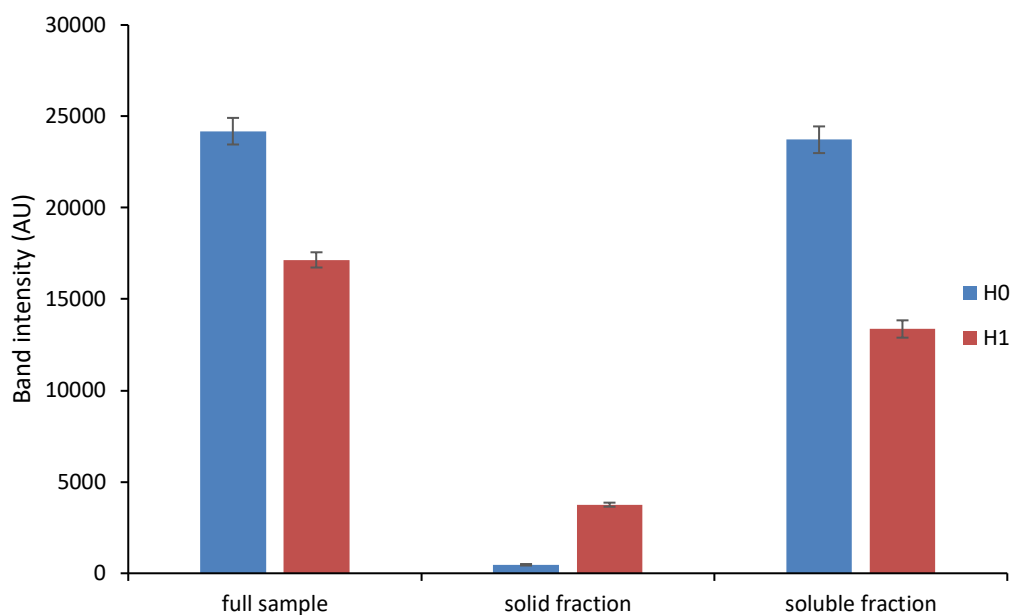


Figure 7-13 Intensity of the solid fraction of lignin in the gel well, the soluble fraction that migrated down the gel and the combined solid and soluble to represent the full sample. This was produced using Figure 7-12.

Figure 7-13 shows attempted analysis of the whole sample: the solid fraction that remained in the well and the soluble fraction that migrated on the gel. The HTC treated sample had significantly lower overall intensity compared to the sample taken before HTC, with tight error bars which suggests the decrease is significant. In the solid fraction, there was a significantly higher intensity observed for the HTC treated sample. Additionally, the band intensity for the soluble HTC fraction was significantly less than the control. The band intensity for the soluble fraction pre-HTC was very similar to the value for the full sample, which implies few solids were present in this sample. Once HTC treatment had taken place, the band intensity of the soluble fraction was much lower, likely due to the conversion of soluble lignin to solids perhaps with gasification during heating (Pińkowska et al., 2012).

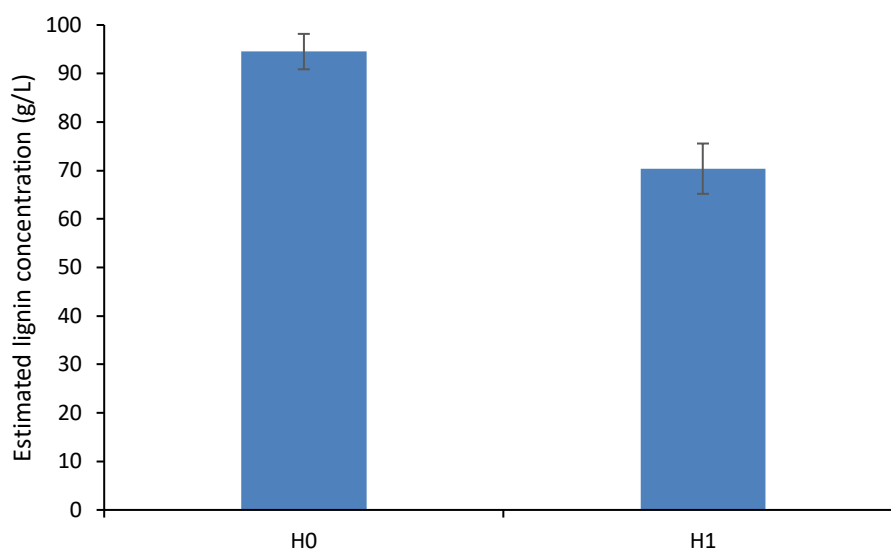


Figure 7-14 Estimated concentration of HTC treated lignin produced using Figure 7-12.

As the lignins were diluted 20x prior to electrophoresis, the estimated lignin concentration was then corrected for this dilution and found to be 94.5 g/L rather than 100 g/L, which could be explained by the error represented by the error bars. The HTC treated sample is considerably lower in and determined to be 70.4 g/L which is around a 25% decrease. The result shows that a complex mixture containing both solids and liquids can be assessed by gel electrophoresis.

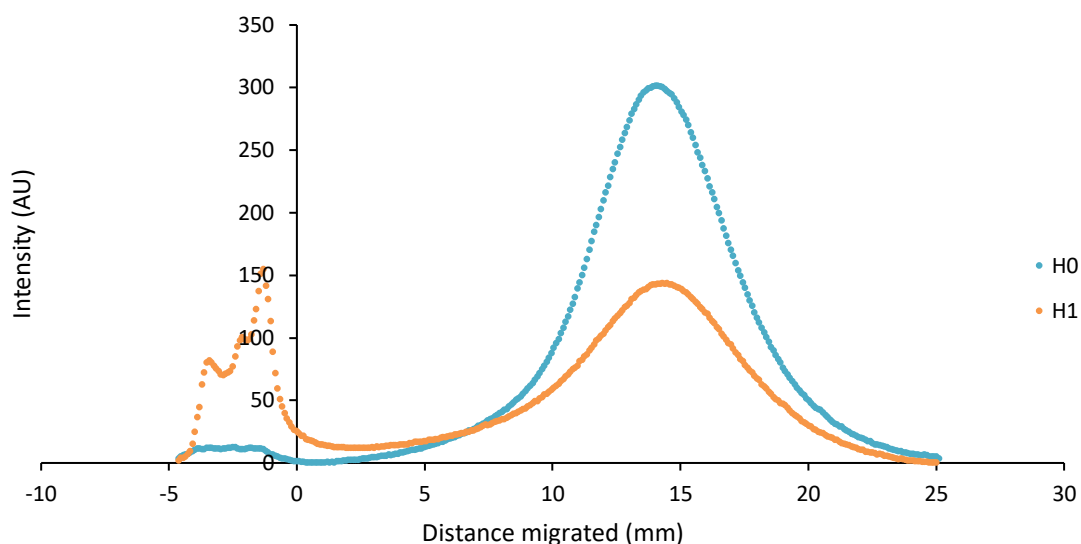


Figure 7-15 Electrophoretic separation of control and HTC treated lignin samples produced using Figure 7-12.

Figure 7-15 shows the electrophoretic separation of the pre-HTC sample and the HTC treated sample and there is a clear difference. For the pre-HTC sample there is small plateau between -5 and 0 mm which corresponds to the gel well, whilst for the HTC treated sample the intensity within this region is much higher with peaks at -5 to 0 mm. The peak at around -3.5 mm most likely corresponds to the gel wall closest to the anode. Lignin migrates towards a cathode so a peak in this area would not be expected. Perhaps this was due to high molecular weight carbonised lignin or solids which do not migrate in agarose electrophoresis or have possibly adsorbed to the agarose gel wall. The peak at 1.5 mm likely represents carbonised lignin that was too high in molecular weight to migrate through the gel matrix but was 'pulled' against the well wall by the cathode at the end of the gel. Higher intensity for the HTC treated sample compared to the pre-HTC sample was observed from 0 to around 7.5 mm, which can likely be assigned to high molecular weight and therefore high m/z species, produced by

carbonisation of lignin. The major peak at around 15 mm was much lower in intensity compared to the pre-HTC sample, which suggests that large amounts of lignin was carbonised or degraded due to the large change. The lack of clear shifts in electrophoretic migration implies that the soluble lignin was carbonised but not degraded. This corresponds to the observations in (Liu et al., 2013) where temperatures over 250 °C were required to degrade lignin. Ideally this experiment would be repeated at higher temperatures but HTC required twenty grams of lignin, which is a large amount for a single test.

Although it appears gel electrophoresis can assess the solid constituent of a sample, it is unclear how accurate this is due to the lack of standards that could then be used to create a standard curve. Additionally it is unclear if just the surface of the solid was measured due to the lack of penetration by the excitation light compared to a liquid, this could have led to an underestimation of the amount of solids present.

7.3.6 Quantification and analysis of enzymatic degradation of lignin

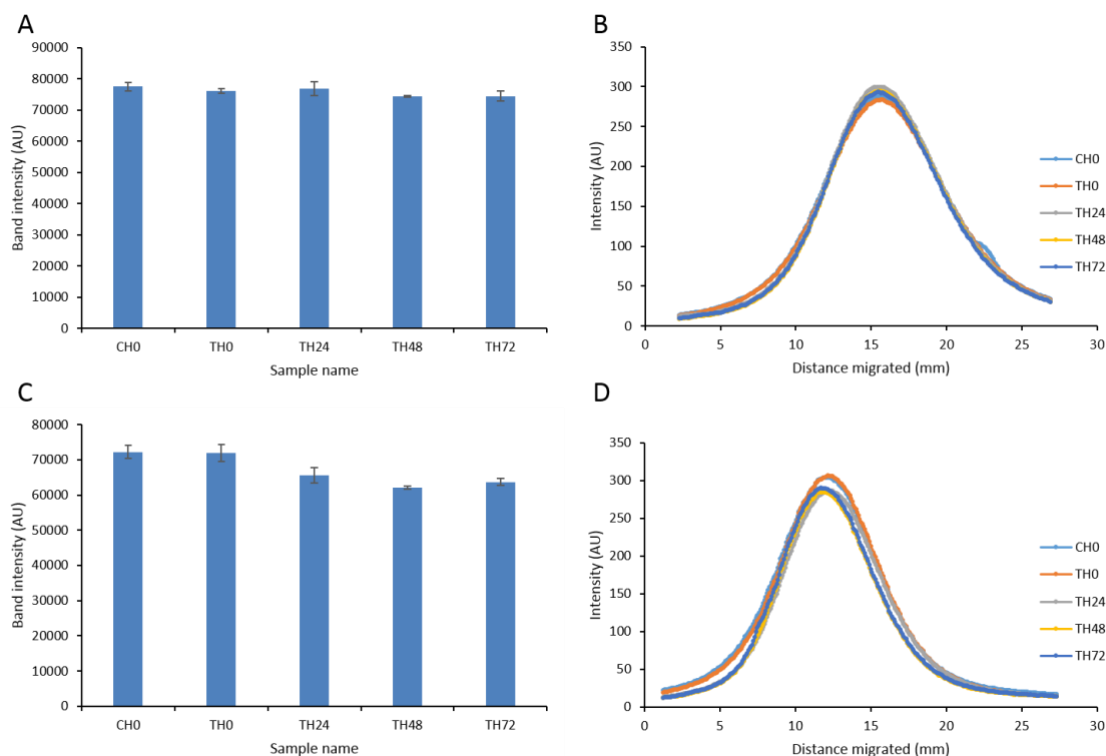


Figure 7-16 Decrease in band intensity (A and C) and electrophoretic separation (B and D) after enzymatic lignin degradation of 5 g/L Alkali lignin (A and B) and 5 g/L L6 Kraft lignin (C and D) over a period of 72 hours. C= control and T= laccase degraded sample. Samples were taken after 0, 24, 48 and 72 hours.

Figure 7-16 shows the band intensity of Alkali lignin and L6 Kraft lignin samples and their electrophoretic separation after treatment with enzymes. The values for band intensity in graph A show no major changes after enzyme treatment, with the values close to that of the control and the pre-incubation sample. However, graph B demonstrates that there were some changes to electrophoretic migration. Firstly the treated samples have lower intensity in the region between 0 and 7.5 mm and secondly there was a small apparent increase in the height of the main peak. Perhaps the region between 0 and 7.5 mm corresponds to high

molecular weight lignin aggregates which move through the gel matrix slowly. After enzyme treatment it is possible that these aggregates were solubilised and migrated with the rest of the lignin sample, leading to an increase in the intensity of the main lignin peak. This fits with the data published by (Hämäläinen et al., 2018) where after enzyme treatment very high molecular weight lignin (corresponding to around 100KDa) was found to be converted to lower molecular weight compounds by analysis via GPC; these high molecular weight compounds could be aggregates. Additionally, in this publication there was a decrease in colloidal particle size and an increase in acid solubility, which all infer that aggregates were removed and/or the solubility of the lignin sample was increased post enzyme treatment. Perhaps the lack of changes in band intensity in graph A was due to the MetZyme® LIGNO™ enzymes being ineffective in depolymerising Alkali lignin, which is highly processed as part of the Kraft process and lacking easily breakable bonds.

Graph C in Figure 7-16 shows that, unlike Alkali lignin, L6 Kraft lignin shows a decrease in band intensity after enzymatic treatment. The values for the intensity of the control and the pre-incubation sample are very similar, which implies that no degradation occurred prior to incubation. After 24 hours there was approximately a 10% decrease in intensity, which increased to around a 15% decrease after 48 hours. However, at 72 hours there was a slight increase in band intensity compared to the sample taken after 48 hours. This could be due to re-polymerisation after degradation but was most likely due to error, and the fact that the sample was loaded next to the control. Previous results showed high fluorescence intensities can illuminate an adjacent pocket causing an over-estimation of the concentration. The decrease in band intensity was large enough

to be outside of error, which infers that it was due to degradation. Graph D shows a similar separation of enzymatically treated samples between 0 and 7.5 mm, except the intensity was lower for the L6 lignin samples. Significantly there was a decrease in intensity of the main peak and also a change in electrophoretic migration, with a shift of the major peak to the left. This could be due to lignin being degraded from the inside out, rather than the outside inwards where a right shift of the peak would have been expected. This suggests that the lignin was quickly degraded to lower molecular weight fragments. This is likely, as syringaldehyde can diffuse into the lignin structure and degrade the lignin in an endo fashion; rather than the enzyme producing radicals that diffuse poorly into the lignin structure. Perhaps this hypothesis could be tested by degrading lignin with and without syringaldehyde. The shift in electrophoretic migration could also be due to enzymatic modification of functional groups, for instance demethylation, leading to a higher m/z ratio. Conversely, this could be due to enhanced degradation of the lower molecular weight fraction of the main peak rather than due to any changes in the m/z ratio as part of enzymatic treatment. Results in the literature show that lignin degradation with laccases such as those from *C. versicolor*, can lead to simultaneous polymerisation and depolymerisation of lignin, which would explain the changes in electrophoretic migration (Youn et al., 1995).

The fact that degradation occurred using L6 Kraft lignin and not Alkali lignin is not surprising, as earlier work showed that L6 Kraft lignin is higher in molecular weight than Alkali lignin so is presumably less processed and has more readily breakable bonds. Although both lignins were produced from the Kraft process they were made using different lignocellulose sources so will have different

compositions. This highlights the benefit of gel electrophoresis as tool to assess the accessibility of different lignin substrates to degradation.

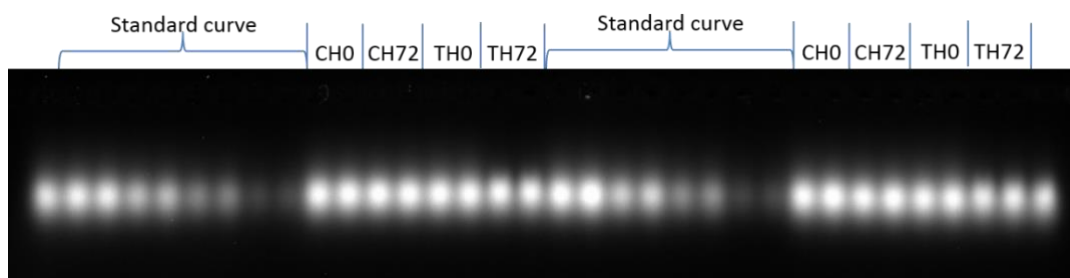


Figure 7-17 Agarose gel containing a lignin concentration gradient, controls and 5 g/L enzymatically degraded L6 Kraft lignin. Sample order in duplicate: 5 g/L, 3.75 g/L, 2.5 g/L, 1.25 g/L, CH0, CH72, TH0 and TH72. The sequence was then repeated so there were 4 repeats for each sample. Control hour 0 (CH0), control hour 72 (CH72), enzymatically degraded lignin hour 0 (TH0) and enzymatically degraded lignin hour 72 (TH72)

The enzymatically degraded sample, TH72 was of similar band intensity, but there was a difference in electrophoretic migration, Figure 7-19. There was a reduction in the smear above the main band, which gives the band a 'blunted' appearance.

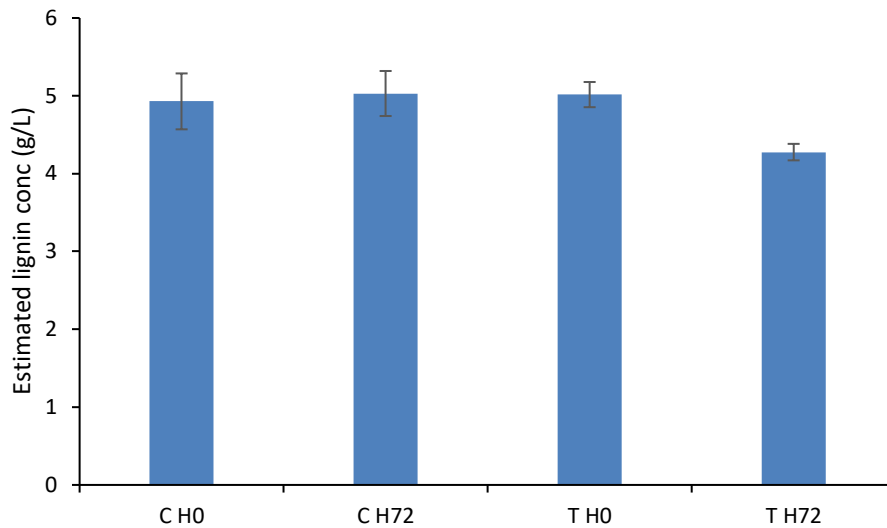


Figure 7-18 Estimated concentration of enzymatically degraded lignin samples produced using Figure 7-17.

The controls and the pre-incubation sample in Figure 7-18 show remarkable similarity and are all at the expected 5 g/L of lignin. The control sample taken pre-incubation has higher standard deviation compared to the other samples. A low standard deviation is shown for the control after 72 hours, and the sample taken pre-incubation with the presence of enzyme. After enzymatic degradation, the concentration of lignin in the sample was determined to be 0.74 g/L lower than before degradation, with a decrease of 15%. The standard deviation of the measurement was low, so the result is significant. This is a large improvement over current analytical techniques and removes the need to carry out convoluted methods, such as the Klason method to estimate lignin concentration (Kirk and Obst, 1988).

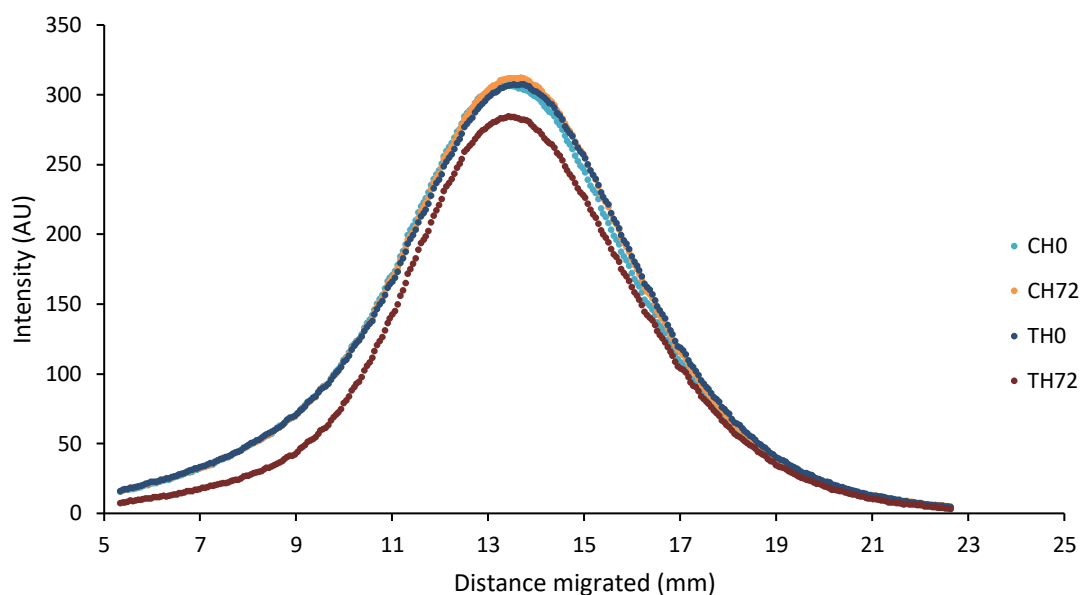


Figure 7-19 Electrophoretic separation enzymatically degraded lignin samples produced using Figure 7-17.

Figure 7-19 shows the changes in electrophoretic separation after treatment using enzymes. The peak was lower in intensity compared to that of the controls, as opposed to only the top of major peak and the region between 0 and 10 mm, seen in Figure 7-16. Nevertheless, the level of degradation was lower between 11 and 15 mm, which is similar to the first experiment. The controls and pre-incubation samples show similar separation and overall intensities, implying that any major changes observed after enzyme treatment were significant. Overall, the level of degradation appears to be higher than the results in Figure 7-16, so future work should be carried out to investigate why the enzymatic degradation can vary in this manner.

7.3.7 Quantification and analysis of hydrogen peroxide degradation of lignin

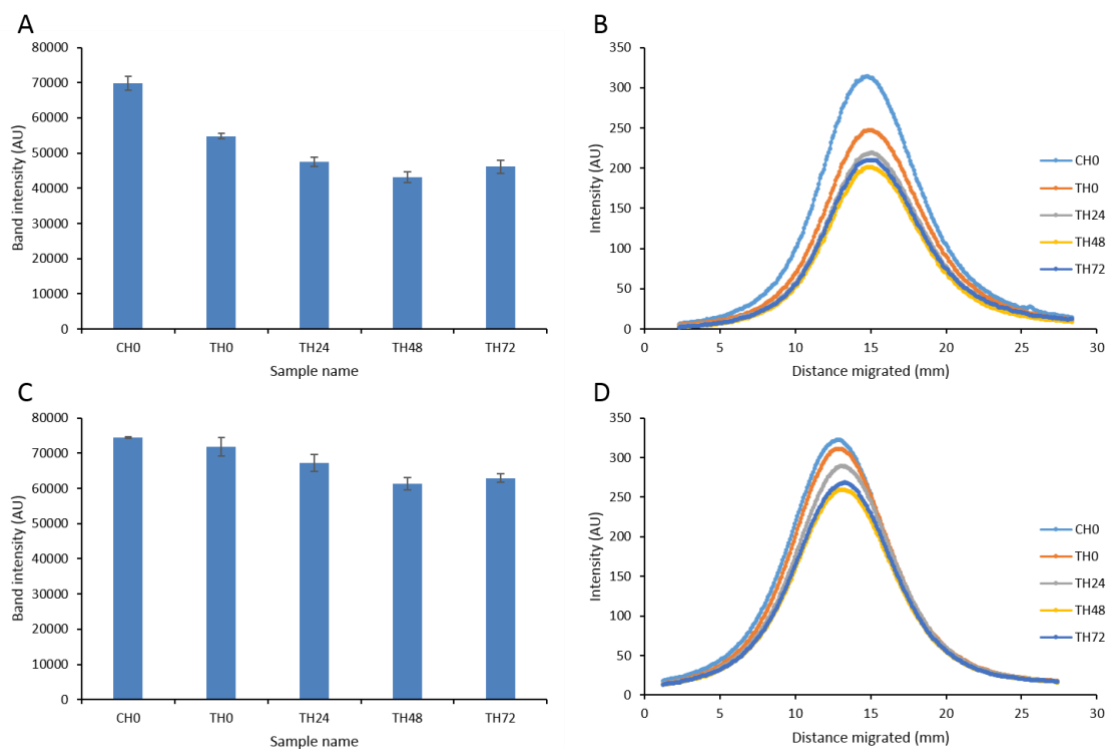


Figure 7-20 Decrease in band intensity (A and C) and electrophoretic separation (B and D) after hydrogen peroxide lignin degradation of 5 g/L Alkali lignin (A and B) and 5 g/L L6 Kraft lignin (C and D) over a period of 72 hours.

Figure 7-20 shows hydrogen peroxide degradation over time for Alkali and L6 Kraft lignin. There was a large difference between the control and pre-incubation, as shown in graph A. It was unexpected that such a large level of degradation would occur in the time from sampling, freezing the sample to sample preparation for electrophoresis. This implies that hydrogen peroxide can readily degrade Alkali lignin at ambient temperatures. The presence of metal ions, such as iron, could have catalysed oxygen radical formation via the Fenton reaction (Zepp et al., 1992). In previous work, the degradation of lignin using Fenton reagent reagents was optimised by (Seesuriyachan et al., 2015). However this was

carried out in view of water treatment, not to produce low molecular weight aromatics, so perhaps there is scope for this in future work. There was a decrease in band intensity of around 10%, from 24 to 48 hours of incubation but the decrease was smaller than the difference between the control and the pre-incubation sample. After 72 hours there was an increase similar to that observed in Figure 7-16, which was likely due to the same reasons discussed above. The difference between the control and the pre-incubation sample with hydrogen peroxide is apparent in graph B, where the intensity values after 24, 48 and 72 hours are close to each other, implying that degradation mostly stopped after 24 hours. This could be due to consumption of the hydrogen peroxide, or that breakable bonds in the lignin structure were already oxidised.

The results for L6 Kraft lignin in graph C of Figure 7-20 are similar to that of the Alkali lignin, however the decrease in band intensity was smaller. There was a noticeable decrease in intensity between the control and the pre-incubation sample containing hydrogen peroxide, which implies a rapid reaction and the need to quench the sample. Addition of sodium bisulfite was tested, however, lignin precipitated (data not shown). Graph D shows less pronounced differences in intensity compared to graph B, but degradation increased after 24 hours, with the maximum occurring after 48 hours. The reaction likely ceased at 48 hours, in contrast to the reaction with Alkali lignin which likely ceased after 24 hours. In graph D there is a slight shift to the right, i.e. faster migration, less m/z , that may indicate degradation from the outside inwards.

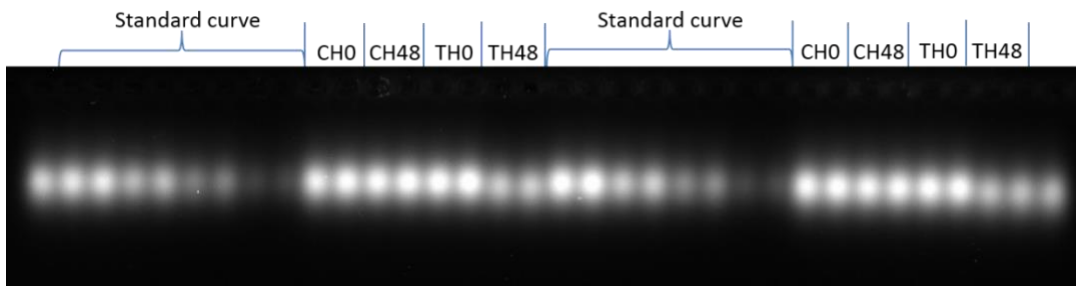


Figure 7-21 Agarose gel containing a lignin concentration gradient, controls and 5 g/L hydrogen peroxide degraded L6 Kraft lignin. Sample order in duplicate: 5 g/L, 3.75 g/L, 2.5 g/L, 1.25 g/L, CH0, CH48, TH0 and TH48. The sequence was then repeated so there were 4 repeats for each sample. Control hour 0 (CH0), control hour 48 (CH48), H₂O₂ degraded lignin hour 0 (TH0) and H₂O₂ degraded lignin hour 48 (TH72)

The gel shown in Figure 7-21 gave a standard curve with R₂ of 0.999. The hydrogen peroxide degraded sample, TH48 is visibly different to the other samples and has clearly migrated further down the gel in comparison to the other samples. The band is less intense, implying that the high molecular weight lignin has experienced modification.

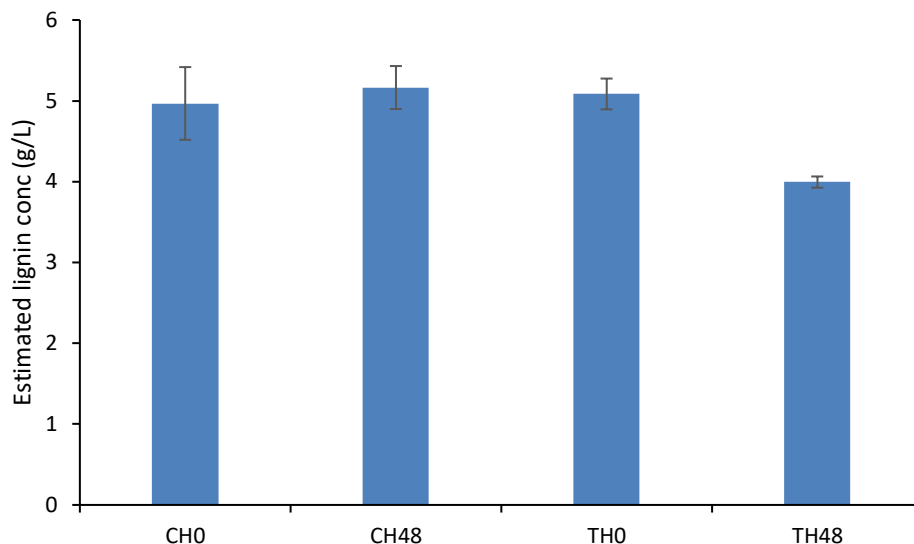


Figure 7-22 Estimated concentration of hydrogen peroxide degraded lignin and controls produced using Figure 7-21.

Using the standard curve the controls and pre-incubation samples were ~5 g/L, Figure 7-22. The pre-incubation control, however, had slightly higher standard deviation than anticipated but the concentration was still at the expected level. After 48 hours of hydrogen peroxide treatment there was a decrease in lignin concentration to 4 g/L, with only a small error bar. This result demonstrates that lignin concentration of chemically degraded samples can be estimated using gel electrophoresis.

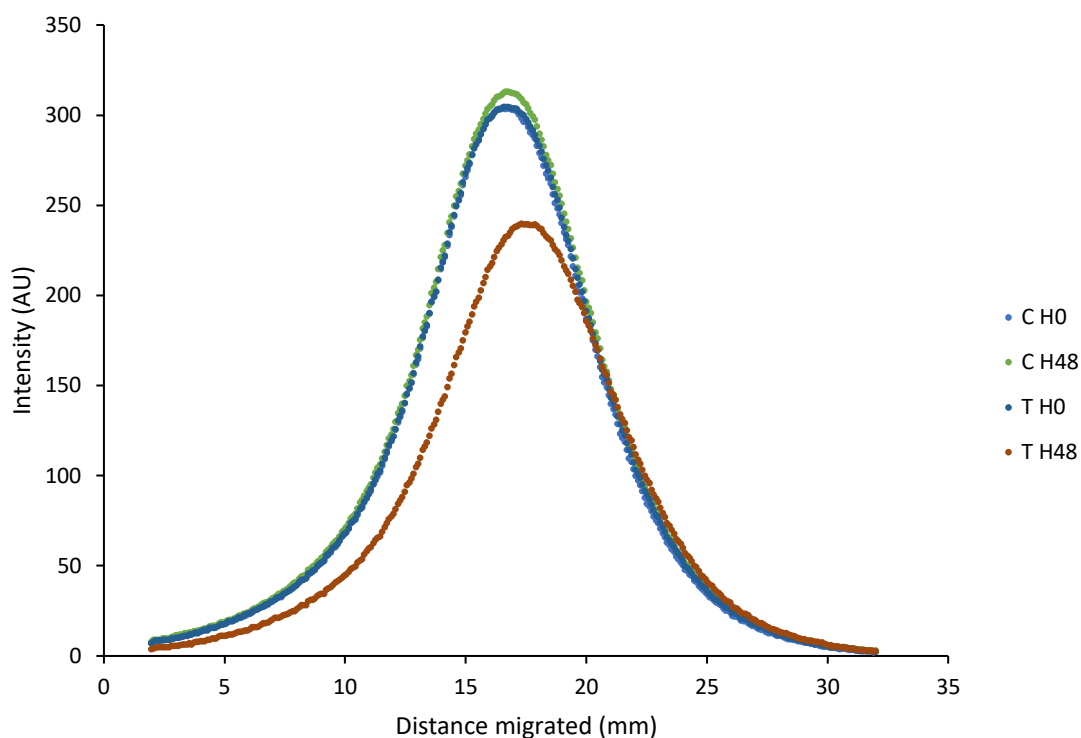


Figure 7-23 Electrophoretic separation of control and hydrogen peroxide degraded lignin samples produced using Figure 7-21.

The controls and pre-incubation samples (CH0, CH48, TH0) in Figure 7-23 showed similar intensities and electrophoretic migration. There was a slight increase in overall intensity for the control sample taken after 48 hours, but this was almost certainly due to error as previous results showed that incubation of control samples does not lead to higher band intensities. The difference between the controls and the degraded sample is significant, and there was an overall increase in electrophoretic migration between 22 to 25 mm. This change in m/z is because of a decrease in molecular weight of the lignin polymer, because the results accord with literature SEC report of chemically degraded lignin (Guizani and Lachenal, 2017). This fits with the suggested mechanism of chemical degradation of lignin, where the lignin polymer is degraded into monomers from

the outside inwards. This therefore suggests that gel electrophoresis can be used to monitor changes in molecular weight as part of chemical degradation of lignin.

7.4 Conclusions

The results in this chapter establish gel electrophoresis as a high throughput method that can be used to estimate lignin concentration in an unknown sample and provide information about changes in m/z ratios as a result of degradation. Changes in concentration and m/z were detected after bacterial degradation. Bacterially treated lignin samples are complex and contain degradation products, proteins, DNA and other contaminating compounds. Therefore, it is impressive that gel electrophoresis is able to analyse lignin samples resulting from *R. jostii* growth. Nevertheless, questions still remain about the influence of proteins on electrophoretic separation. This is an issue with most methods to measure lignin. For example, proteins absorb UV light, especially due to aromatic amino acids, meaning that lignin concentration measurements are inaccurate. This also occurs when using the Klason method for lignin quantification as tyrosine can be problematic (Kirk and Obst, 1988). GPC methods commonly use UV light to monitor elution of lignin and can be affected by bound protein (Salvachúa et al., 2015), where an increase in GPC signal occurred after growth using *Paenibacillus sp* which cannot degrade lignin. Though, this was not observed when *P. putida* was incubated with lignin (alkaline pre-treated liquor produced using corn stover). This group also showed that the presence of monomers produce inaccurate values. Most methods analyse the whole sample, whereas gel electrophoresis separates the low from the high molecular weight polymeric lignin, so is therefore more accurate in this respect. The results obtained with

laccase degradation follow the same trend observed in previous published results, providing evidence that gel electrophoresis can be used to monitor enzymatic degradation of lignin by (Hämäläinen et al., 2018). Another aspect of this work was demonstrating how electrophoresis can be used to compare the accessibility of certain lignins to degradation. This is exemplified by the laccases that degrade L6 Kraft lignin, with limited degradation of Alkali lignin.

The ability to assess the concentration and successfully carry out electrophoresis on HTC and hydrogen peroxide treated lignin fully demonstrates the ability of this method to analyse complex substrates, even in the presence of solids. Methods such as GPC can only handle compounds that are soluble in the column solvent. The shape of the imaged profiles may give some information about the mechanism of degradation, i.e. outside inwards as with hydrogen peroxide breaks off monomers or small fragments, that change the m/z and shape of the main polymers, whilst inside outwards as with laccases causes little change in the shape but may change the charge (demethylation) and fluorescence intensity. More work needs to be done to understand this further.

Using high throughput gel electrophoresis degraded samples were assessed as a function of time, and to enable quantification a concentration gradient, containing 4 samples and 3 controls, each with 4 repeats, was included. The number of repeats could be reduced to accommodate more samples, though there is scope to scale-out further using 7 combs to increase the number of lanes. The multichannel pipette would avoid diffusion and make this possible. As a result, a multitude of different degraded lignin samples using different degradation methods could be compared on a single gel in a high throughput manner, which is unique in the field of lignin research.

Chapter 8

Analysis of low molecular weight components

8.1 Introduction

The primary aim of degrading lignin is to generate valuable products, therefore it is important to understand the formation of low molecular weight products. The ability to do this would assist with the optimisation of processes for monomer production. Pyrolysis GC/MS is used to determine the monomeric component after lignin degradation for example (Abdelaziz et al., 2016). Since the polymer is pyrolysed along with any monomers it fails to inform about the concentration of low molecular weight products. HPLC can separate monomer from polymer and give information about specific compounds such as vanillin, however as complex mixtures are usually present following digestion, these are difficult to analyse by this method. For lignin to be an industrially useful source of aromatics, there need to be multiple product streams, similar to how the petroleum industry has differentiated during its development; therefore it is useful to be able to assess the total low molecular weight production from a degradation process rather than one or two specific products. Other chapters in this thesis present gel electrophoresis as a novel method to quantify and provide information about polymeric lignin. This chapter reports attempts to get a mass balance by assessing the low molecular weight aromatic products that pass through the agarose matrix uninhibited. This raises the possibility of characterising the gel buffer at the electrodes.

8.2 Methods

8.2.1 Samples investigated

The following samples were investigated for low molecular weight products: 100 g/L Alkali lignin, low sulfonate content; 100 g/L HTC processed Alkali lignin; 100 g/L L6 Kraft lignin; H₂O₂ treated Alkali lignin; 10 g/L vanillin and 10 g/L guaiacol. The H₂O₂ treated Alkali lignin was produced by incubating 10 ml solution of 100 g/L Alkali lignin with 70 mM phosphate buffer and 3.53 M hydrogen peroxide in a 50 ml conical flask which was placed in a shaker incubator at 37 °C at 180 rpm for 48 hours. The treated lignin was then used for electrophoresis.

8.2.2 Electrophoresis method

Electrophoresis was carried out in a Clarit-E Mini gel tank at 50 V. 50 µL of the respective sample was mixed with 20 µL of 50% glycerol and 20 µL 0.375M NaOH. 20µL of this mixture was added to 8 of the gel wells (leaving the first and last well empty).

8.2.3 Low molecular weight product sampling and analysis

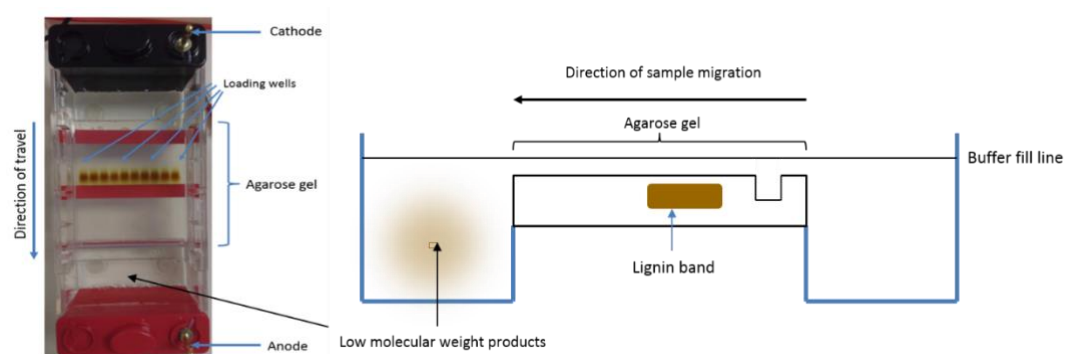


Figure 8-1 Annotated image of gel tank (left) along with diagram of gel electrophoresis equipment (right) (gel shown in figure is only an example and was not used to generate any results)

Samples were taken before electrophoresis, and every 15 minutes (ensuring the current was switched-off), for 60 minutes. The gel tank was filled with 450 ml of SB buffer (filling up to the max fill line on the gel tank). 10 ml samples were taken by the anode section of the gel tank (where the low molecular weight products are shown to be located in Figure 8-1) immediately after electrophoresis ceased, first using a P1000 pipette to gently mix the buffer around the electrode in order to ensure the electrophoresis eluent wasn't specifically concentrated around the electrode. It was deemed important to do this carefully and immediately after electrophoresis in order to limit the diffusion and movement of eluent over the gel and into the cathode section of the gel tank, which could lead to an underestimation of material present and/or unreliable results. The buffer was then measured for absorbance at 280 nm using SB buffer as a blank. 280 nm was selected as aromatic compounds (such as vanillin) absorb strongly in this region (Rind et al., 2009). The mass of vanillin and guaiacol in the buffer were calculated using absorbance readings taken at 274nm. An extinction coefficient of $\epsilon = 2739 \text{ M}^{-1}\cdot\text{cm}^{-1}$ (274 nm, pH 12) and $3488 \text{ M}^{-1}\cdot\text{cm}^{-1}$ (289 nm, pH 12) was used to calculate the mass of vanillin and guaiacol present (Lemon, 1947) using the Beer-Lambert law (absorbance = path length x extinction coefficient x concentration).

8.2.4 Extraction of electrophoresis eluent for NMR

Electrophoresis was carried out as described above, using hydrogen peroxide treated 100 g/L Alkali lignin, to test whether low molecular weight degradation products were present in the gel buffer post electrophoresis. No samples were taken until electrophoresis at 50V was complete in one hour and all the buffer was taken from the gel tank (450ml in total). The buffer was tested using starch

paper to confirm the absence of hydrogen peroxide. Compounds present in the buffer were purified using ethyl acetate before then extracting the compounds in vacuo. The solids produced were then dissolved in CDCl_3 , and $^1\text{H NMR}$ was carried out by colleague Calum Birch.

8.3 Results and discussion

8.3.1 Low molecular weight product UV analysis

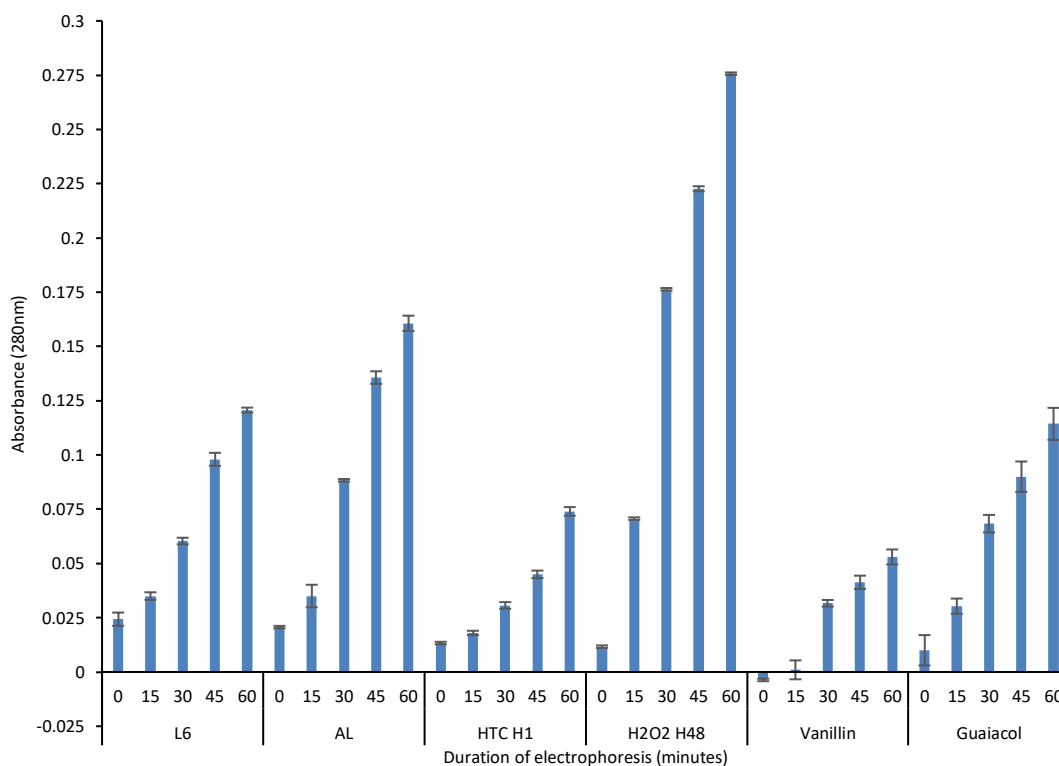


Figure 8-2 UV absorbance of gel buffer taken every 15 minutes for 1 hour after running lignin standards, treated lignin and low molecular weight compounds. Sample description from left to right: 100 g/L L6 lignin; 100 g/L Alkali lignin; HTC treated Alkali lignin; hydrogen peroxide treated Alkali lignin; 10 g/L vanillin and 10 g/L guaiacol.

Figure 8-2 shows the absorbance data over time in the gel buffer for a wide range of sample, encompassing lignin standards, treated lignin and low molecular weight compounds. The low molecular weight compounds can be produced by degradation of lignin so are a test to see if it is possible to detect low molecular weight aromatic compounds in the gel buffer post-electrophoresis (Obst, 1983). The results for L6 start with an absorbance reading around 0.025 which rises to a final reading of just under 0.125. For the Alkali lignin sample the same trend

and similar intensities are observed between 0 and 15 minutes, however there is a large increase observed at 30 minutes, another large rise from 30 to 45 minutes, then a much smaller rise to around 0.16 after 60 minutes. This implies that Alkali lignin has more low molecular weight compounds than L6 lignin. L6 lignin is membrane separated so should contain a lower proportion of low molecular weight compounds.

The results for the HTC treated lignin were surprising due to the low values for absorbance, with a maximum of around 0.075 observed after 60 minutes. This implies that instead of producing low molecular weight products, HTC has actually decreased the concentration. This is perhaps due to polymerisation/carbonisation of these compounds or gasification during heating. This is supported by (Pińkowska et al., 2012) where a decrease in certain aromatic compounds was observed post HTC and was suggested to be due to gasification. The same increasing absorbance trend is shown for the hydrogen peroxide degraded lignin, however significantly higher readings were observed. A final absorbance reading of 0.275 is most likely due to the production of low molecular weight aromatic compounds as part of hydrogen peroxide degradation.

When 10g/L vanillin was run on the gel no increase in absorbance was observed between 0 and 15 minutes, implying that the vanillin (if migrating) was in the agarose gel matrix. However at 30 minutes there is a larger increase to around 0.03, this then rises to around 0.05; this increase in UV absorbance suggests the vanillin had eluted out of the gel matrix and into the gel buffer. The absorption equates to 3.6 μM of vanillin, with 5.8 μM charged to the gel in total. For guaiacol a slightly different overall trend was observed then for vanillin, at time zero there is a reading of 0.012, however this could be due to error, highlighted by the large

error bars. The reading at 60 minutes for guaiacol is 0.115 which equates to 6.3 μM compared to 7.2 μM charged to the gel. The absorbance is comparable to the reading for L6 Kraft lignin. Conversely around 7.16 μM of guaiacol was loaded onto the gel compared to around 5.84 μM of vanillin and this difference is not as significant as the difference between the readings. An HPLC unit could be connected to the gel tank with a continuous auto sampler which takes samples the gel buffer during electrophoresis; the times at which different compounds appear could then be assessed.

8.3.2 NMR of extracted low molecular weight products

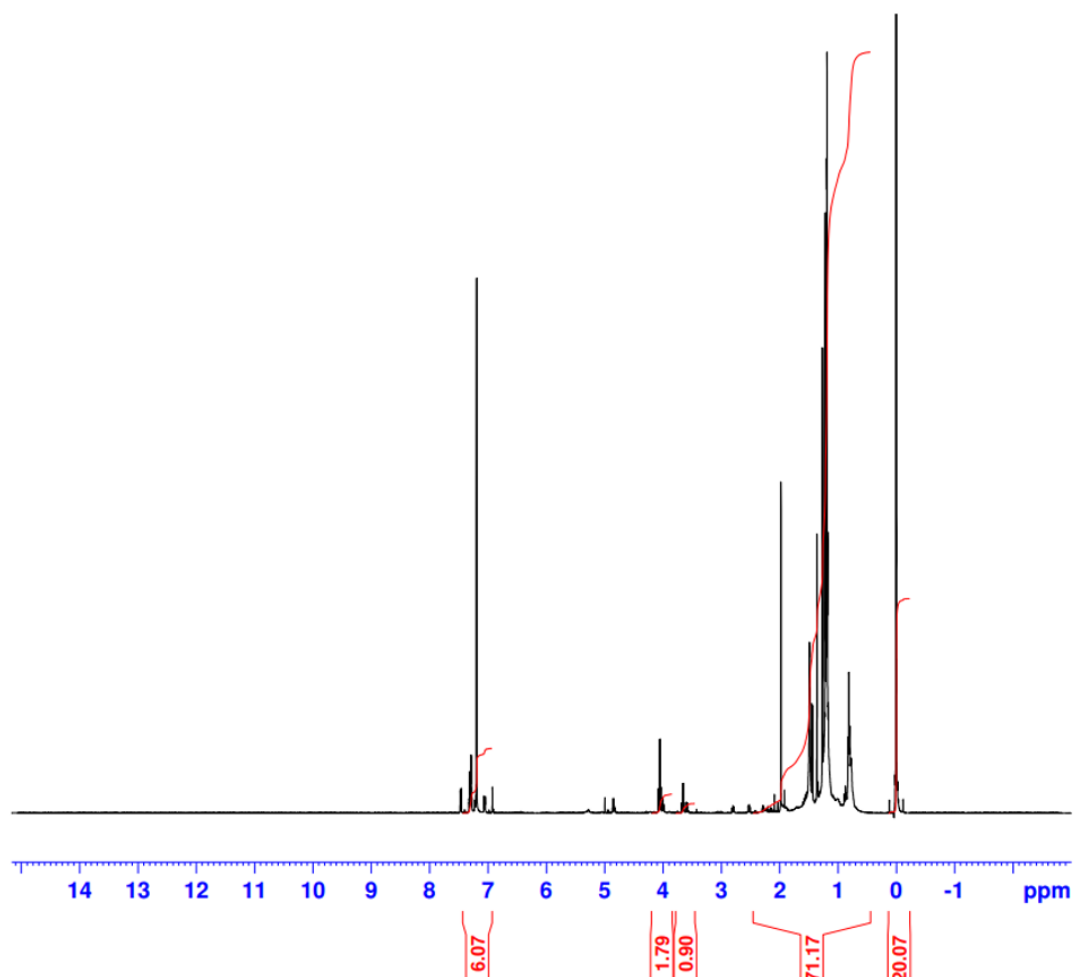


Figure 8-3 Full ¹H NMR spectra of extracted compounds from the gel electrophoresis buffer eluent

Figure 8-3 shows a full ^1H NMR spectrum in CDCl_3 of the compounds reconstituted into dichloromethane from electrophoresis buffer. It is clear that multiple different compounds were extracted, but critically there are peaks in the aromatic region that can only have come from the digested lignin, as the sample has not been in contact with any contaminating aromatic (solvent etc). There are more aliphatic than aromatic compounds in the degraded sample which fits with hydrogen peroxide degradation (Gierer and Jansbo, 1993). The appearance of aliphatic compounds in the spectra demonstrates the ability of gel electrophoresis to not only separate low molecular weight compounds from lignin but low molecular weight aliphatic compounds.

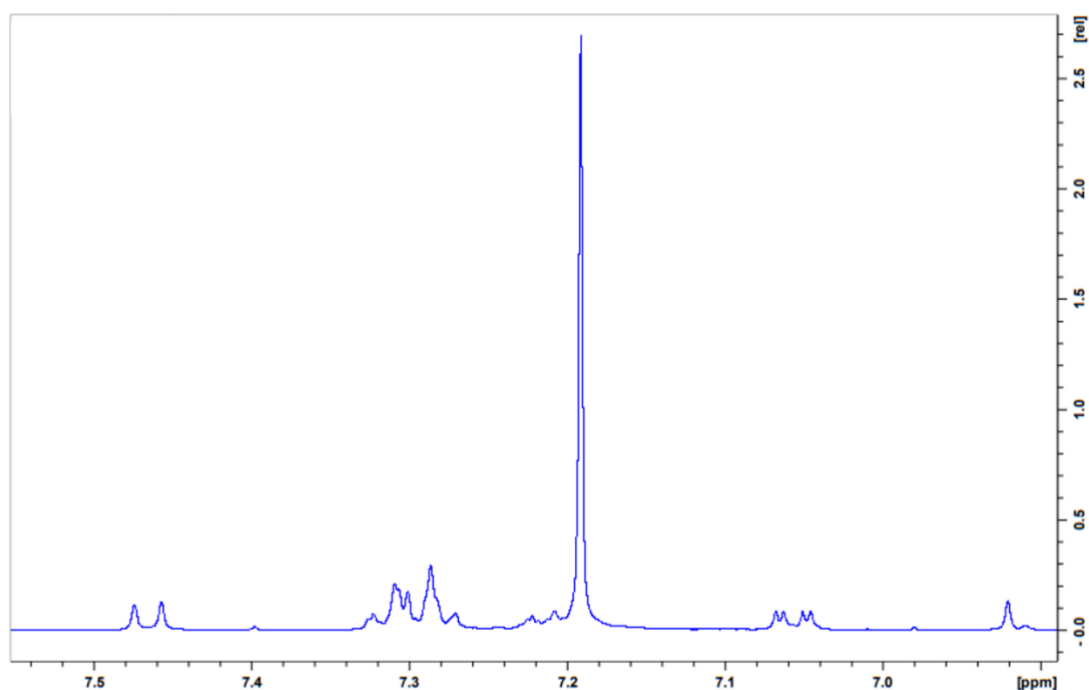


Figure 8-4 Aromatic region on the ^1H NMR spectra of the extracted compounds from the gel buffer eluent

Figure 8-4 shows the aromatic part of spectrum. Several peaks are observable that from the coupling pattern match those of a 1,3,4-trisubstituted aromatic tentatively identified as 3,4-dihydroxybenzoate. If correct, this would be promising as 3,4-dihydroxybenzoate is a platform chemical that can be converted to pyridine 2,4-dicarboxylic acid or pyridine 2,5-dicarboxylic acid which can be used to produce bioplastics (Mycroft Z. et al, 2015). With the help of gel electrophoresis monitoring, a process could be developed to optimise the formation of monomers and could be used to purify the compound of interest.

8.4 Conclusions

This work provides evidence that gel electrophoresis can be used to assess the production and presence of low molecular weight compounds. However additional work needs to be carried out in order to accurately quantify the amount of low molecular weight compounds in a sample; due to different compounds having different extinction coefficients which is problem when lignin degrades to produce a complex mixture. There was a clear difference between lignin standards and hydrogen peroxide degraded lignin, which suggests that this method can be used to monitor produce of low molecular weight compounds from lignin. The presence of aromatic compounds was confirmed using ^1H NMR. Several challenges still remain and using a gel electrophoresis tank is not the ideal equipment to assessment of low molecular weight products. Several problems exist such as the risk of missing the gel lane and loading lignin sample into the gel buffer, leading to inaccurate readings. Therefore an enclosed capillary type vessel such as the one shown in Figure 8-5 could help resolve this.

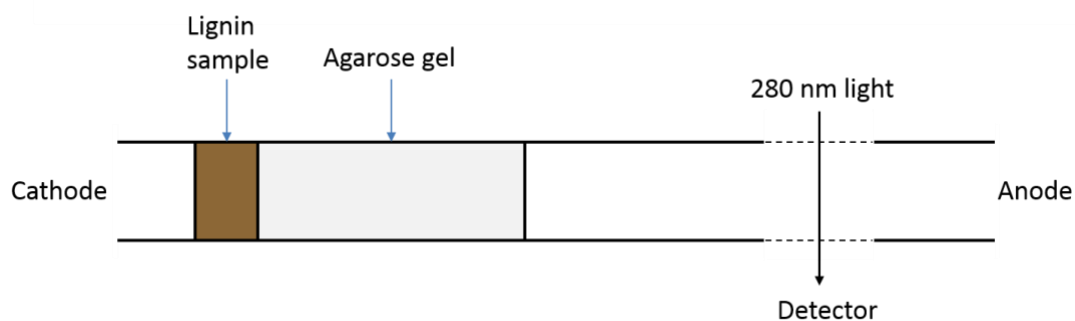


Figure 8-5 Diagram of proposed capillary electrophoresis method for the assessment of low molecular weight products

Another problem is that the tank needs to be switched-off before manually taking a sample, but use of a capillary with an online UV-vis spectrometer could allow measurement of the compounds as they elute. If this is combined with a HPLC it could be investigated when these compounds elute. The use of a capillary reactor means that more sample can be tested, whereas using the gels the amount of sample is limited by the volume of the gel wells. The ability to load more sample could mean that much more dilute samples could be investigated, potentially allowing the investigation of low molecular weight products after bacterial degradation for example. Overall this work is extremely promising and suggests that if further work is carried out, this method could be used to optimise production of valuable low molecular weight compounds from lignin.

Chapter 9

Discussion, future work and summary

9.1 Discussion of research outcomes

9.1.1 Need for a high throughput technique to analyse lignin

Lignin represents the sole bulk source of sustainable aromatic chemicals and has the potential to replace aromatic platform chemicals derived from oil (Gillet et al., 2017). This readily available feedstock is currently underutilised and is mostly burnt for energy as a low grade fuel (Patil et al., 2016). A factor leading to underutilisation of lignin is the lack of a high throughput technique to analyse polymeric lignin. This is a crucial gap in the field, as in order to develop a process it is important to understand the starting material and product to give a mass balance. Techniques exist to analyse lignin but are often not specific to the polymeric fraction, so can give inaccurate results. Furthermore these techniques are often low in throughput and require specialist equipment, for instance GPC columns. Agarose gel electrophoresis of lignin has only been mentioned briefly in one paper and is completely uncharacterised for this application. It was selected for its low-cost, high throughput and is readily available in most research organisations due to its frequent use in DNA and protein analysis.

9.1.2 Electrophoresis to analyse lignin

Electrophoresis of lignin produced a brown smeared band which was hypothesised to be lignin. AL extraction method was designed in order to successfully isolate lignin from the agarose gel post electrophoresis. These samples were confirmed to be lignin using techniques such as GPC, pyrolysis

GC/MS and NMR. Critically, GPC demonstrated that the band on the gel encompassed the entirety of the polymeric lignin sample. Furthermore, pyrolysis GC/MS confirmed that there was no residual presence of sugars from the agarose gel or sugars from hemicellulose for instance. These results show that lignin can be extracted and indicate how lignin can be purified.

It is challenging to confirm whether bacterial strains can degrade lignin, as growth alone is insufficient to confirm whether the microbe can do this. This is due to the fact that lignin samples are often contaminated with hemicellulose or low molecular weight aromatics. If pure lignin is extracted post-electrophoresis then microbial growth itself would be sufficient to confirm the capacity to degrade lignin, which would lead to much faster and effective screening of potential lignin-degrading microbes. This is demonstrated by (Taylor et al., 2012) where several methods were utilised to confirm whether isolated microbes could degrade lignin. Purification of lignin prior to degradation would remove contaminating and potentially toxic compounds, which would lead to improve lignin degradation rates and reduced downstream purification costs.

Samples ranging from 0.25 and 250 g/L were shown to run successfully on agarose gels, demonstrating the preparative aspect of the method. GPC does not support such a broad range of analysis. Furthermore, when using GPC it was impossible to characterise Alkali lignin, as it did not dissolve in THF, whereas it was possible to run Alkali lignin on an agarose gel.

Protein electrophoresis utilises detergents such as SDS in order to remove charge as a variable, and separate based on mass (Weber et al., 1972). We wondered whether this could be used to improve the separation of lignin. The addition of SDS led to a single band for different Kraft lignins, which co-migrated

with SDS micelles, that surprisingly fluoresce. SDS has been found to complex with carbon nanotubes and migrate as a complex under electrophoretic conditions (Kastrisianaki-Guyton et al., 2016), so complexation with lignin is unsurprising. Unfortunately, the co-migration of SDS with lignin prevents using electrophoresis to determine molecular weight. The study also showed that low pH samples could be analysed in the presence of SDS, so in specific scenarios it may be useful. Furthermore, SDS could aid analysis of otherwise insoluble lignins.

9.1.3 Electrophoresis to measure lignin concentration

The Klason method or FT-IR are unable to measure lignin concentration and confusing results are obtained when degradation products are included in the analysis (Nuopponen et al., 2005). Absorption and fluorescence experiments confirmed that lignin absorbs and emits at wavelengths corresponding to the Coomassie blue imaging setting in the gel imager, making it possible to measure lignin using fluorescence. Agarose does not fluoresce at these wavelengths enabling high resolution and precise images that can be quantified using image analysis.

The optimal pH was determined as 8.75 using sodium borate (SB) buffer and the addition of NaOH to samples prior to loading increased the lignin migration rate which is due to phenoxide formation and solubilisation of lignin aggregates. SB buffer was shown to facilitate effective electrophoresis using a range of different lignin types and concentrations, without the agarose gel melting and optimal voltage settings were identified. The fluorescence intensity was increased at Alkali pH, allowing lignin samples of lower concentrations can be analysed with

increased accuracy. This is especially relevant to bacterial degradation of lignin where it is not possible to add high concentrations of lignin due to its toxicity (Libralato et al., 2011). When different types of lignin: protobind, Kraft and organosolv lignins were analysed on the same gel, different fluorescent intensities were observed; demonstrating they cannot be compared directly. The functional groups and level of ionisation vary in lignin type, and this affects the structure and aggregation all which affect the photometric properties (Gordobil et al., 2018). It was shown that serially diluting lignin samples and electrophoresing these, the bands can be imaged, measured and the fluorescence intensities measured to give a calibration curve to accurately determine the concentration of a related lignin, for example one that has been partially digested. Using Kraft lignin it was possible to create concentration calibration curves with an R^2 value of around 0.99. However, a limitation is when the lignin associates with proteins, for example during digestion or in extracellular bacterial breakdown as this can change the lignin's fluorescence and migration properties (Venkatesagowda, 2019).

Gel electrophoresis was effective in quantifying the degradation of lignin using hydrogen peroxide. There were visually apparent changes in fluorescence intensity compared to the controls. However, it is possible that part of this decrease could be due to the bleaching properties of hydrogen peroxide reducing the aromaticity of the lignin polymer (Doshi and Dyer, 2001). Importantly, the standard deviation of measurements was low, meaning that the concentration of a degraded lignin sample can be determined with a level of certainty. The work shows that gel electrophoresis is a useful method to assess concentration changes that occur as part of chemical degradation.

Hydrothermal degradation produces a mixture of solid, liquid and gaseous products (He et al., 2013). It is not possible for electrophoresis to measure the gaseous products, however, the gaseous phase is not relevant for production of aromatic platform chemicals. The mixture produced after hydrothermal carbonisation (HTC) is highly complex (Xiao et al., 2012), nonetheless, the soluble lignin was able to pass through the mixture of solid and aggregated lignin in the gel pocket and enter the agarose gel matrix allowing for effective quantification. The solids produced were unable to pass into the agarose gel matrix, so resided in the wells where their concentration was estimated. A limitation of the estimation of solids in the agarose pocket is that the excitation light was not able to pass through the solid sample, and a lower fluorescence intensity may have led to a underestimation of the concentration. Electrophoresis could be carried using a high mass sample of HTC treated lignin, with the collection and weighing of solids after electrophoresis to estimate the quantity of solids produced. This would however dramatically reduce the throughput due to the need of an extraction step to remove the solids. The carbonised lignin is not easily convertible to aromatic platform chemicals, so has little relevance in lignin valorisation (Wikberg et al., 2015).

Similar to hydrogen peroxide and HTC treatment of lignin, there was a clear decrease in lignin fluorescence compared to the controls after enzymatic treatment. This infers that gel electrophoresis can be used to detect changes in lignin concentration after enzymatic degradation. The laccase enzyme used in this work not only acts to degrade lignin, but can also carry out functional group modification as it has been shown to demethylate lignin. It catalyses oxidative demethylation, which occurs by cleaving an aryl ether to form two phenolic groups

(Hämäläinen et al., 2018). These changes could lead to higher fluorescence intensity and increased charge (more phenoxide), giving faster migration at apparently higher concentration. However, if the enzyme associates with the lignin without bond breakage this could also give a change in fluorescence intensity, and therefore an inaccurate assessment of lignin degradation/polymerisation.

It was impossible to quantify lignin digestion after *Pseudomonas putida* treatment, as the lignin fluorescence intensity increased. This could be due to protein association discussed above. However, after microwave treatment, the bacterially treated lignin behaved differently to the native lignin sample, with the fluorescence intensity decreasing and the apparent presence of aggregates. This may be due to proteins in the sample denaturing and aggregating due to the high temperature, and suggests that high protein concentration can decrease the accuracy of the technique. The same problems are seen with other techniques such as UV spectroscopy and Klason analysis of lignin. Conversely, this could have been caused by polymerisation of low molecular weight products already present in the lignin sample (Ohta et al., 2017).

Changes in lignin concentration were successfully detected using *Rhodococcus jostii*, which was grown on comparably nutrient poor media, likely leading to lower levels of protein expression, meaning there was less protein present to bind to lignin and interfere with the results. However, similar results to *P. putida* were seen, implying that residual proteins in the sample led to an underestimation of lignin concentration. Future work is required to resolve this issue.

9.1.4 Electrophoresis to assess lignin mass to charge changes

To confirm whether agarose gel electrophoresis can separate lignin based on molecular weight, protobind, organosolv and Kraft lignin samples were analysed, and compared by GPC and gel electrophoresis. The aim was to compare mass to charge separation in electrophoresis to molecular weight separation of acetylated, THF soluble lignin in GPC, and also the quality of the resolution. The separation of several Kraft lignins were very comparable by both methods, and the resolution similarly high. It was possible to characterise an Alkali lignin sample by electrophoresis, not possible using GPC. The protobind lignin samples were shown to have similar separation by GPC and agarose gel electrophoresis. Minor differences were detected using gel electrophoresis but the resolution was slightly lower than GPC, as individual peaks were not resolved. Differences in separation were seen in organosolv samples. The peak shapes varied between both methods, as aggregates formed in the organosolv sample in water, that did not in THF used in GPC. The aggregation caused the organosolv lignin to migrate more slowly in electrophoresis than higher molecular weight, unaggregated, Kraft lignin. This is due to the lower water solubility of the organosolv lignin compared to the Kraft lignin polymers, which are likely ionised to a greater extent and are able to migrate further due to lower m/z . The fact that electrophoresis works effectively for Kraft lignin is important, as Kraft lignin is significantly more commercially available than organosolv and protobind lignins.

The gel electrophoresis method was assessed for monitoring changes in lignin structure as a result of different degradation methods and treatments. The results show that it is effective in assessing changes after chemical degradation, with an

increase in migration, which corresponds to literature GPC results (Guizani and Lachenal, 2017).

Due to issues of protein contamination it was impossible to determine whether gel electrophoresis can assess m/z changes due to bacterial degradation. Since proteins can also influence GPC results, it is also challenging to confirm bacterial degradation using this technique. To test effective removal of protein without removal of lignin, perhaps the suspected protein pellet produced after microwaving and centrifugation could be analysed via pyrolysis GC/MS. If no phenolic compounds are detected then this would confirm that protein has been extracted without removing any lignin.

9.1.5 Quantification of low molecular weight compounds from lignin degradation

Agarose gel electrophoresis was shown to be a useful tool to quantify the low molecular weight compounds produced following chemical degradation, presenting an opportunity to produce a complete mass balance. The conversion rate of lignin to low molecular weight aromatics is a crucial piece of information for the valorisation of lignin. Nevertheless, further work needs to be done to relate absorbance readings to the total concentration of aromatic degradation products. This was briefly explored by quantifying the concentration of vanillin and guaiacol charged to a gel and recovered in the gel tank, and the results were surprisingly close given the small quantities and inaccuracies. The complex mixture produced after lignin degradation have different absorptions and extinction coefficients, which presents challenges in accurate quantification. The combination of (capillary)electrophoresis and HPLC may be able to overcome this problem.

9.2 Originality and overall impact of this work

High throughput techniques that can provide specific information about polymeric lignin structure and concentration have not been reported in the literature. Agarose gel electrophoresis has the potential to be the first choice technique for analysis of polymeric lignin, as the equipment used is low cost and available or accessible to biochemistry laboratories. Furthermore, the ability of electrophoresis to provide information about polymeric lignin as well as the amount of low molecular weight products, makes this an outstanding method compared to others. A laboratory with electrophoresis equipment can readily carry out electrophoresis of lignin, making this an accessible and high throughput technique for the quantification and analysis of polymeric lignin and its degradation products. Furthermore, the availability of a low cost technique will help drive research and innovation in the field of lignin process development.

9.3 Future research

There is an opportunity to scale-up the gel electrophoresis further to accommodate more samples. Up to 280 samples could be run on a single gel. Differences in gel thickness could affect sample comparison, so pre-made gels could be purchased to increase reproducibility.

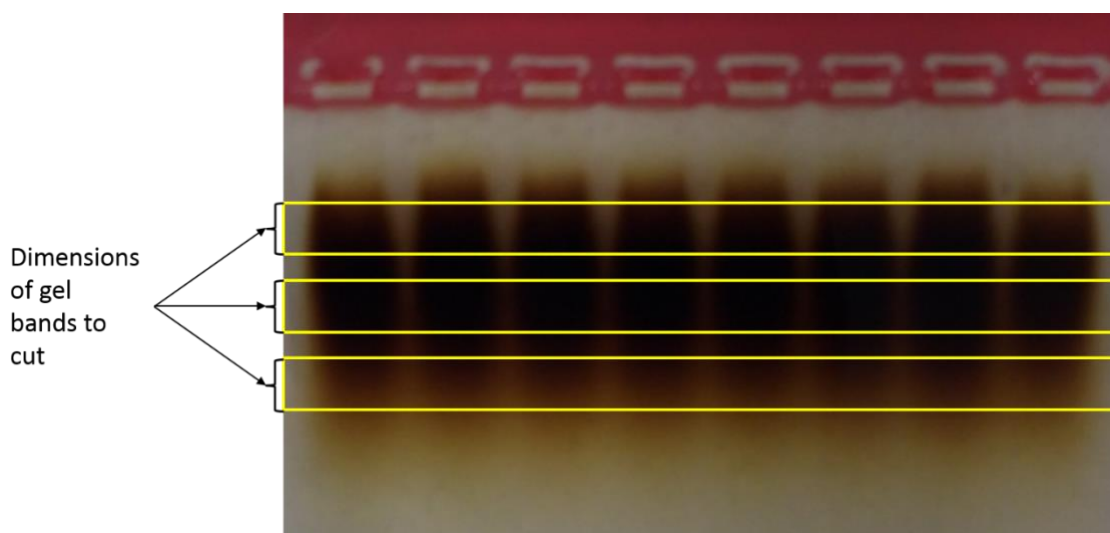


Figure 9-1 Proposed experiment to create molecular weight standards

Further evidence that electrophoretic migration is directly comparable to molecular weight could be obtained by extraction and purification of fractions of the lignin band as shown in Figure 9-1. These samples could then be analysed by GPC to determine their molecular weights. The lignin fractions could be purified in sufficient quantities to use as molecular weight markers on the gel. Future work should include determining the efficiency of lignin extraction from an agarose gel which is important if standard technical lignins are to be produced.

A critical step in validating electrophoresis as a method to assess lignin degradation is providing certainty that it can be used to assess biological methods. If proteins are responsible for the problems in assessing this, more work needs to be done to fully characterise the complexes. Further work should be carried out to assess whether low molecular weight products eluting from the gel can be characterised.

Future work might explore the analysis and quantification of lignin from lignocellulose, for instance to determine types and sources of wood to assist in

identification of illegal sources. In this regard some discussions have been held with an expert in Kew Gardens. FT-IR is used to estimate the amount of lignin in a sample of wood, however, it is unable to measure lignin degradation, as the products will be measured alongside the lignin (Rana et al., 2010). An extraction method could be designed to remove the lignin from the wood, as in the Kraft process, allowing for electrophoresis. Higher pH buffers could aid solubilisation of poorly soluble lignins that could then be analysed by electrophoresis. Kraft lignin represents one of the largest waste sources of lignin and more than 107 tonnes of Kraft lignin are burnt for fuel within the EU every year. As a result, Kraft lignin is feedstock that is yet to be fully utilised (Saidane et al., 2010). The main reason soluble lignin is used is that reactor design and operation is much simpler. The use of a solid feedstock would lead to poor mixing, poor mass transfer and complicate the reaction by adding another phase. Additional expensive pre-treatment options such as milling and steam explosion would be required to increase the accessibility of lignin, further increasing the costs (Duque et al., 2016) (Baruah et al., 2018). Therefore, soluble lignins are the substrate of choice in developing a process to degrade lignin, whose breakdown can be monitored by agarose gel electrophoresis.

An application that would establish agarose gel electrophoresis as a technique for lignin analysis would be to aid development a process to degrade lignin to produce platform chemicals. This work has shown it is successful in analysing chemically degraded lignin, implying that it would be an appropriate tool for process development using chemical methods. In terms of throughput, chemical methods have the advantage over biological treatments, although they produce a complex mixture after degradation (Prado et al., 2016). This could be mitigated

by using chemical degradation as a pre-treatment step and utilising a genetically modified bacteria to metabolise the lignin degradation products, which can in turn export specific low molecular weight aromatic products. There was limited success in assessing biological degradation. Nevertheless, in this proposed process it would not be necessary to assess lignin degradation by bacteria, as the lignin will already be degraded. Electrophoresis could instead be utilised to assess the quantity of low molecular weight products before each degradation and treatment step to determine product yield and conversion. Conversely, if few products are produced then orthogonal techniques such as HPLC would be more favourable. In the bio refinery model, multiple product streams need to be created, electrophoresis can be used to provide mass balance information, and might even be considered for at-line measurement and control.

9.4 Overall Conclusions

Agarose gel electrophoresis has been characterised as a flexible, high throughput technique to analyse lignin. This technique is unique in the field as it provides high throughput information about the concentration and structure of polymeric lignin while also providing information about the concentration of low molecular weight products. Agarose gel electrophoresis was shown to work extremely well for chemical degradation and also provided important information about polymeric lignin after enzymatic and HTC treatment. Further investigations need to be carried out to determine whether this technique can accurately assess bacterial degradation of lignin in its current form. Nevertheless, agarose gel electrophoresis has huge potential in its current form and there are opportunities for future work to further develop the versatility and throughput of this technique.

In summary, agarose gel electrophoresis has the potential to become the standard technique for lignin analysis, and in its current form, has the capacity to be used to develop a process to chemically degrade lignin.

References

- Abdelaziz, O.Y. et al. 2016. Biological valorization of low molecular weight lignin. *Biotechnology Advances*. **34**(8), pp.1318-1346.
- Agrawal, K. et al. 2018. Fungal laccase discovered but yet undiscovered. *Bioresources and Bioprocessing*. **5**(1), p4.
- Ahmad, M. et al. 2011. Identification of DypB from *Rhodococcus jostii* RHA1 as a Lignin Peroxidase. *Biochemistry*. **50**(23), pp.5096-5107.
- Akiba, T. et al. 2017. Induction of lignin solubility for a series of polar ionic liquids by the addition of a small amount of water. *Green Chemistry*. **19**(9), pp.2260-2265.
- Arantes, V. et al. 2012. Peculiarities of brown-rot fungi and biochemical Fenton reaction with regard to their potential as a model for bioprocessing biomass. *Applied Microbiology and Biotechnology*. **94**(2), pp.323-338.
- Armisen R. 1991. Agar and agarose biotechnological applications. *Hydrobiologia*. **221**(1), pp.157-166.
- Asikkala, J. et al. 2012. Accurate and Reproducible Determination of Lignin Molar Mass by Acetobromination. *Journal of Agricultural and Food Chemistry*. **60**(36), pp.8968-8973.
- Bajpai P. et al, . 1993. Decolorization of kraft bleach plant effluent with the white rot fungus *Trametes versicolor*. *Process Biochemistry*. **28**(6), pp.377-384.
- Bartzoka, E.D. et al. 2016. Coordination Complexes and One-Step Assembly of Lignin for Versatile Nanocapsule Engineering. *ACS Sustainable Chemistry & Engineering*. **4**(10), pp.5194-5203.
- Baruah, J. et al. 2018. Recent Trends in the Pretreatment of Lignocellulosic Biomass for Value-Added Products. *Frontiers in Energy Research*. **6**(141).
- Baumberger S. et al. 2007. Molar mass determination of lignins by size-exclusion chromatography: Towards standardisation of the method. *Holzforschung*. **61**(4), pp.459-468.
- BBC News, . 2011. *Fire crews tackle wooden pellets blaze at Port of Tyne*. [Online]. [Accessed 19/01/2019].
- Beckham, G.T. et al. 2016. Opportunities and challenges in biological lignin valorization. *Current Opinion in Biotechnology*. **42**, pp.40-53.
- Biller P. et al. 2014. Pyrolysis GC-MS as a novel analysis technique to determine the biochemical composition of microalgae. *Algal Research*. **6**(1), pp.91-97.
- Borregaard ASA, . 2014. *Borregaard ASA* [Online]. [Accessed 30/01/2019]. Available from: <http://www.fondsfinans.no/wp-content/blogs.dir/4/files/2014/04/BRG1Q14PreviewInitialCoverage010420141.pdf>.
- Brandt A et al. 2013. Deconstruction of lignocellulosic biomass with ionic liquids. *Green Chemistry*. **15**(1), pp.550-583.
- Brody J. R. et al, . 2004. Sodium boric acid: a Tris-free, cooler conductive medium for DNA electrophoresis. *BioTechniques*. **36**(2), pp.214-216.
- Bugg T.D.H et al. 2011. The emerging role for bacteria in lignin degradation and bio-product formation. *Current Opinion in Biotechnology*. **22**(3), pp.394-400.
- Bugg T.D.H et al, . 2016. *Bacterial Enzymes for Lignin Oxidation and Conversion to Renewable Chemicals*. Springer Singapore.

- Chakar F S et al. 2004. Review of current and future softwood kraft lignin process chemistry. *Industrial Crops and Products*. **20**(2), pp.131-141.
- Chandra, R. et al. 2007. Characterisation and optimisation of three potential aerobic bacterial strains for kraft lignin degradation from pulp paper waste. *Chemosphere*. **67**(4), pp.839-846.
- Chandra, R. et al. 2008. Isolation and characterization of bacterial strains *Paenibacillus* sp. and *Bacillus* sp. for kraft lignin decolorization from pulp paper mill waste. *The Journal of General and Applied Microbiology*. **54**(6), pp.399-407.
- Cheng, S. et al. 2012. Hydrothermal degradation of Alkali lignin to bio-phenolic compounds in sub/supercritical ethanol and water–ethanol co-solvent. *Polymer Degradation and Stability*. **97**(6), pp.839-848.
- Cherr G. N. et al. 1993. Electrophoretic separation, characterization, and quantification of biologically active lignin-derived macromolecules. *Analytical Biochemistry*. **214**(2), pp.521-527.
- Contreras, S. et al. 2008. Propensity of Lignin to Associate: Light Scattering Photometry Study with Native Lignins. *Biomacromolecules*. **9**(12), pp.3362-3369.
- Da Re, V. and Papinutti, L. 2011. Black Liquor Decolorization by Selected White-Rot Fungi. *Applied Biochemistry and Biotechnology*. **165**(2), pp.406-415.
- Dalton R. et al, ,. 1974. *Purification of aromatic hydrocarbons*.
- Das, L. et al. 2016. Selective oxidation of lignin into aromatic aldehydes using niobium oxalate. *Transactions of the ASABE*. **59**(2), pp.727-735.
- Dashtban M. et al, ,. 2010. Fungal biodegradation and enzymatic modification of lignin. *International Journal of Biochemistry and Molecular Biology*. **1**(1), pp.36-50.
- Daylan, B. and Ciliz, N. 2016. Life cycle assessment and environmental life cycle costing analysis of lignocellulosic bioethanol as an alternative transportation fuel. *Renewable Energy*. **89**, pp.578-587.
- Doshi, M.R. and Dyer, J.M. 2001. Paper: Recycling and Recycled Materials. In: Buschow, K.H.J., et al. eds. *Encyclopedia of Materials: Science and Technology*. Oxford: Elsevier, pp.6711-6720.
- Drabik A. et al. 2016. 7- Gel Electrophoresis. In: Ciborowski P. et al ed. *Proteomic profiling and analytical chemistry (second edition)*. Elsevier, pp.115-143.
- Duan W. H. et al. 2011. Dispersion of carbon nanotubes with SDS surfactants: a study from a binding energy perspective. *Chemical Science*. **7**(1).
- Duque, A. et al. 2016. Chapter 15 - Steam Explosion as Lignocellulosic Biomass Pretreatment. In: Mussatto, S.I. ed. *Biomass Fractionation Technologies for a Lignocellulosic Feedstock Based Biorefinery*. Amsterdam: Elsevier, pp.349-368.
- Dutta, T. et al. 2018. Characterization of Lignin Streams during Bionic Liquid-Based Pretreatment from Grass, Hardwood, and Softwood. *ACS Sustainable Chemistry & Engineering*. **6**(3), pp.3079-3090.
- Eastwood D. C. et al, ,. 2011. The Plant Cell Wall–Decomposing Machinery Underlies the Functional Diversity of Forest Fungi. *Science*. **333**(1), pp.762-765.
- Ebringerova A et al. 2000. Naturally occurring xylans structures, isolation procedures and properties. *Macromolecular Rapid Communications*. **21**(1), pp.542-556.
- Esposito L J et al, ,. 2000. Vanillin. *Encyclopedia of Chemical Technology*.

- Fackler K. et al. 2011. *GreenValue*.
- Florin Ciolacu D C et al. 2011. Amorphous cellulose - structure and characterization *cellulose chemistry and technology*. **45**(1), pp.13-21.
- Forchheim D. et al, ,. 2012. Modeling the lignin degradation kinetics in an ethanol/formic acid solvolysis approach. Part 2. Validation and transfer to variable conditions. *Industrial and Engineering Chemistry Research*. **51**(32), pp.15053-15063.
- Gianfreda L et al, ,. 1999. Laccases: A Useful Group of Oxidoreductive Enzymes. *Bioremediation Journal*. **3**(1), pp.1-26.
- Gierer, J. and Jansbo, K. 1993. Formation of Hydroxyl Radicals from Hydrogen Peroxide and their Effect on Bleaching of Mechanical Pulps. *Journal of Wood Chemistry and Technology*. **13**(4), pp.561-581.
- Gilland, B. 2002. World population and food supply: can food production keep pace with population growth in the next half-century? *Food Policy*. **27**(1), pp.47-63.
- Gillet, S. et al. 2017. Lignin transformations for high value applications: towards targeted modifications using green chemistry. *Green Chemistry*. **19**(18), pp.4200-4233.
- Glasser, W.G. et al. 1993. Molecular Weight Distribution of (Semi-) Commercial Lignin Derivatives. *Journal of Wood Chemistry and Technology*. **13**(4), pp.545-559.
- Glazer A N et al. 2007. *Microbial biotechnology: fundamentals of applied microbiology*. Cambridge: Cambridge University Press.
- Gomaa, O.M. and Momtaz, O.A. 2015. Copper induction and differential expression of laccase in *Aspergillus flavus*. *Brazilian journal of microbiology : [publication of the Brazilian Society for Microbiology]*. **46**(1), pp.285-292.
- Gonzalo G. et al, ,. 2016. Bacterial enzymes involved in lignin degradation. *Journal of Biotechnology*. **236**(1), pp.110-119.
- Gordobil, O. et al. 2018. Potential use of kraft and organosolv lignins as a natural additive for healthcare products. *RSC Advances*. **8**(43), pp.24525-24533.
- Gosselink, R.J.A. et al. 2012. Lignin depolymerisation in supercritical carbon dioxide/acetone/water fluid for the production of aromatic chemicals. *Bioresource Technology*. **106**, pp.173-177.
- Goujon, T. et al. 2003. Genes involved in the biosynthesis of lignin precursors in *Arabidopsis thaliana*. *Plant Physiology and Biochemistry*. **41**(8), pp.677-687.
- Graichen, F.H.M. et al. 2017. Yes, we can make money out of lignin and other bio-based resources. *Industrial Crops and Products*. **106**, pp.74-85.
- Guizani, C. and Lachenal, D. 2017. Controlling the Molecular Weight of Lignosulfonates by an Alkaline Oxidative Treatment at Moderate Temperatures and Atmospheric Pressure: A Size-Exclusion and Reverse-Phase Chromatography Study. *International Journal of Molecular Sciences*. **18**(12).
- Hämäläinen, V. et al. 2018. Enzymatic Processes to Unlock the Lignin Value. *Frontiers in bioengineering and biotechnology*. **6**, pp.20-20.
- Hatfield, R. and Fukushima, R.S. 2005. Can Lignin Be Accurately Measured? This paper was originally presented at the Lignin and Forage Digestibility Symposium, 2003 CSSA Annual Meeting, Denver, CO. *Crop Science*. **45**(3), pp.832-839.

- He, C. et al. 2013. Conversion of sewage sludge to clean solid fuel using hydrothermal carbonization: Hydrochar fuel characteristics and combustion behavior. *Applied Energy*. **111**, pp.257-266.
- Helleur R. J. et al. 1985. Analysis of polysaccharid pyrolysate of red algae by capillary gas chromatography-mass spectrometry. *Journal of Analytical and Applied Pyrolysis*. **8**(1), pp.333-347.
- Heuer D. M. et al. 2003. Topological effects on the electrophoretic mobility of rigid rodlike DNA in polyacrylamide gels. *Biopolymers*. **70**(4), pp.471-481.
- Holker U. et al, , 2005. Solid-state fermentation — are there any biotechnological advantages? *Current Opinion in Microbiology*. **8**(3), pp.301-306.
- Ikeda, S. and Okamoto, A. 2007. pH-dependent fluorescence of uncharged benzothiazole-based dyes binding to DNA. *Photochemical & Photobiological Sciences*. **6**(11), pp.1197-1201.
- Gasson, J. R. et al, , 2012. Modeling the lignin degradation kinetics in an ethanol/formic acid solvolysis approach. Part 1. Kinetic model development. *Industrial and Engineering Chemistry Research*. **51**(32), pp.10595-10606.
- Jankowska D. et al. 2018. Enzymatic synthesis of lignin-based concrete dispersing agents. *ChemBioChem*. **19**(13), pp.1365-1369.
- Joffres B. et al, , 2013. Thermochemical Conversion of Lignin for Fuels and Chemicals: A Review. *Oil and Gas Science and Technology*. **68**(4), pp.753-763.
- Jokela, J. and Salkinoja-Salonen, M. 1992. Molecular weight distributions of organic halogens in bleached kraft pulp mill effluents. *Environmental science & technology*. **26**(6), pp.1190-1197.
- Jones SM et al, , 2015. Electron transfer and reaction mechanism of laccases. *Cellular and Molecular Life Sciences* **72**(5), pp.869-883.
- Kaar, W.E. and Brink, D.L. 1991. Simplified Analysis of Acid Soluble Lignin. *Journal of Wood Chemistry and Technology*. **11**(4), pp.465-477.
- Kadla, J.F. et al. 2002. Lignin-based carbon fibers for composite fiber applications. *Carbon*. **40**(15), pp.2913-2920.
- Kang S et al, , 2013. Hydrothermal conversion of lignin: A review. *Renewable and Sustainable Energy Reviews*. **27**(1), pp.546-558.
- Kastrisianaki-Guyton, E.S. et al. 2016. Adsorption of sodium dodecylsulfate on single-walled carbon nanotubes characterised using small-angle neutron scattering. *Journal of Colloid and Interface Science*. **472**, pp.1-7.
- Key, R.E. and Bozell, J.J. 2016. Progress toward Lignin Valorization via Selective Catalytic Technologies and the Tailoring of Biosynthetic Pathways. *ACS Sustainable Chemistry & Engineering*. **4**(10), pp.5123-5135.
- Kirk, T.K. and Obst, J.R. 1988. Lignin determination. *Methods in Enzymology*. Academic Press, pp.87-101.
- Košíková, B. et al. 2002. Reduction of carcinogenesis by bio-based lignin derivatives. *Biomass and Bioenergy*. **23**(2), pp.153-159.
- Kostanski, L.K. et al. 2004. Size-exclusion chromatography—a review of calibration methodologies. *Journal of Biochemical and Biophysical Methods*. **58**(2), pp.159-186.
- Kumar, L. et al. 2012. The lignin present in steam pretreated softwood binds enzymes and limits cellulose accessibility. *Bioresource Technology*. **103**(1), pp.201-208.

- Lange, H. et al. 2013. Oxidative upgrade of lignin – Recent routes reviewed. *European Polymer Journal*. **49**(6), pp.1151-1173.
- Lange, H. et al. 2016. Gel Permeation Chromatography in Determining Molecular Weights of Lignins: Critical Aspects Revisited for Improved Utility in the Development of Novel Materials. *ACS Sustainable Chemistry & Engineering*. **4**(10), pp.5167-5180.
- Lavoie J. M. et al, ,. 2011. Depolymerization of steam-treated lignin for the production of green chemicals. *Bioresource Technology*. **102**(7), pp.4917-4920.
- Lazaridis P. A. et al. 2018. Catalytic fast pyrolysis of kraft lignin with conventional, mesoporous and nanosized ZSM-5 zeolite for the production of alkylphenols and aromatics. *Frontiers in Chemistry* **6**(1), p295.
- Lee, R.A. et al. 2013. UV–Vis as quantification tool for solubilized lignin following a single-shot steam process. *Bioresource Technology*. **144**, pp.658-663.
- Lemon, H.W. 1947. The Effect of Alkali on the Ultraviolet Absorption Spectra of Hydroxylaldehydes, Hydroxyketones and other Phenolic Compounds. *Journal of the American Chemical Society*. **69**(12), pp.2998-3000.
- Li, J. et al. 2007. Lignin depolymerization/repolymerization and its critical role for delignification of aspen wood by steam explosion. *Bioresource Technology*. **98**(16), pp.3061-3068.
- Libralato, G. et al. 2011. Lignin and tannin toxicity to *Phaeodactylum tricornutum* (Bohlin). *Journal of Hazardous Materials*. **194**, pp.435-439.
- Liu, Z. et al. 2013. Production of solid biochar fuel from waste biomass by hydrothermal carbonization. *Fuel*. **103**, pp.943-949.
- Maaloum M. et al. 1998. Agarose gel structure using atomic force microscopy: Gel concentration and ionic strength effects. *Electrophoresis*. **19**(10), pp.1606-1610.
- Magasanik B., ,. 1961. Catabolite repression *Cold Spring Harbor Symposia on Quantitative Biology*. **26**(1), pp.249-256.
- Marra, M.A. et al. 1997. High throughput fingerprint analysis of large-insert clones. *Genome Research*. **7**(11), pp.1072-1084.
- Mathews J. A. et al, ,. 2014. Manufacture renewables to build energy security. *Nature*. pp.166-168.
- MetGen. 2019. *MetZyme® LIGNO™*. [Online]. [Accessed 30/07/2019]. Available from: <http://www.metgen.com/products/metzyme-ligno/metzyme-ligno-v1/>.
- Mod R R et al. 1978. Hemicellulose Composition of Dietary Fiber of Milled Rice and Rice Bran *Nutrients and Flavour Quality of Plant Foods*. **26**(5), pp.1031-1035.
- Mycroft Z. et al, ,. 2015. Biocatalytic Conversion of Lignin to Aromatic Dicarboxylic Acids in *Rhodococcus jostii* RHA1 by Re-Routing Aromatic Degradation Pathways. *Green Chemistry*. **17**(1), pp.4974-4979.
- Nagy, M. et al. 2010. Characterization of CO₂ precipitated Kraft lignin to promote its utilization. *Green Chemistry*. **12**(1), pp.31-34.
- Neuhoff, V. et al. 1985. Clear background and highly sensitive protein staining with Coomassie Blue dyes in polyacrylamide gels: A systematic analysis. *Electrophoresis*. **6**(9), pp.427-448.
- Nuopponen, M. et al. 2005. Thermal Modifications in Softwood Studied by FT-IR and UV Resonance Raman Spectroscopies. *Journal of Wood Chemistry and Technology*. **24**(1), pp.13-26.

- Obst, J.R. 1983. Analytical Pyrolysis of Hardwood and Softwood Lignins and Its use in Lignin-Type Determination of Hardwood Vessel Elements. *Journal of Wood Chemistry and Technology*. **3**(4), pp.377-397.
- Ohta, Y. et al. 2017. Enzymatic Specific Production and Chemical Functionalization of Phenylpropanone Platform Monomers from Lignin. *ChemSusChem*. **10**(2), pp.425-433.
- Pal K. S. et al, ,. 1998. Photophysical Processes of Ethidium Bromide in Micelles and Reverse Micelles. *Journal of Physical Chemistry B*. **102**(1), pp.11017-11023.
- Pandey M. P. et al, ,. 2010. Lignin Depolymerization and Conversion:A Review of Thermochemical Methods. *Chemical Engineering Technology*. **34**(1), pp.29-41.
- Parker W. et al. 1992. Protein structures in SDS micelle-protein complexes *Biophysical Journal*. **61**(5), pp.1435-1439.
- Patil, N.D. et al. 2016. 3 - Lignin Interunit Linkages and Model Compounds. In: Faruk, O. and Sain, M. eds. *Lignin in Polymer Composites*. William Andrew Publishing, pp.27-47.
- Perez J et al, ,. 2002. Biodegradation and biological treatments of cellulose, hemicellulose and lignin: an overview. *International Microbiology*. **5**(1), pp.53-63.
- Pińkowska, H. et al. 2012. Hydrothermal decomposition of Alkali lignin in sub- and supercritical water. *Chemical Engineering Journal*. **187**, pp.410-414.
- Pinto, P.C. et al. 2002. Behavior of Eucalyptus Globulus Lignin During Kraft Pulping. II. Analysis by NMR, ESI/MS, and GPC. *Journal of Wood Chemistry and Technology*. **22**(2-3), pp.109-125.
- Prado, R. et al. 2016. Lignin oxidation and depolymerisation in ionic liquids. *Green Chemistry*. **18**(3), pp.834-841.
- Quere C. Le et al. 2015. Global Carbon Budget 2015. *Earth System Science Data*. **7**(1), pp.349-396.
- Ragauskas, A.J. et al. 2014. Lignin Valorization: Improving Lignin Processing in the Biorefinery. *Science*. **344**(6185), p1246843.
- Ragnar M. et al. 2000. pKa values of guaiacyl and syringyl phenols related to lignins. *Journal of Wood Chemistry and Technology* **20**(3), pp.277-305.
- Rakhmatullin, I.Z. et al. 2016. Structural studies of pravastatin and simvastatin and their complexes with SDS micelles by NMR spectroscopy. *Journal of Molecular Structure*. **1105**, pp.25-29.
- Rana, R. et al. 2010. FTIR spectroscopy, chemical and histochemical characterisation of wood and lignin of five tropical timber wood species of the family of Dipterocarpaceae. *Wood Science and Technology*. **44**(2), pp.225-242.
- Rentizelas A. A. et al, ,. 2009. Logistics issues of biomass: The storage problem and the multi-biomass supply chain. *Renewable and Sustainable Energy Reviews*. **13**(1), pp.887-894.
- Rind, F.M.A. et al. 2009. Spectrophotometric Analysis of Vanillin from Natural and Synthetic Sources. *Asian Journal of Chemistry*. **21**, pp.2849-2856.
- Saidane, D. et al. 2010. Preparation of functionalized Kraft lignin beads. *Journal of Applied Polymer Science*. **116**(2), pp.1184-1189.
- Sainsbury P. D. et al, ,. 2013. Breaking Down Lignin to High-Value Chemicals: The Conversion of Lignocellulose to Vanillin in a Gene Deletion Mutant of *Rhodococcus jostii* RHA1. *ACS Chemical Biology*. **8**(1), pp.2151-2156.

- Saiz-Jimenez C. et al. 1999. Polyacrylamide gel electrophoresis of soil humic acids, lignins and model phenolic polymers, and fungal melanins *Communications in Soil Science and Plant Analysis*. **30**(3-4), pp.345-352.
- Salvachúa, D. et al. 2015. Towards lignin consolidated bioprocessing: simultaneous lignin depolymerization and product generation by bacteria. *Green Chemistry*. **17**(11), pp.4951-4967.
- Sangchoom, W. and Mokaya, R. 2015. Valorization of Lignin Waste: Carbons from Hydrothermal Carbonization of Renewable Lignin as Superior Sorbents for CO₂ and Hydrogen Storage. *ACS Sustainable Chemistry & Engineering*. **3**(7), pp.1658-1667.
- Sannigrahi P. et al, . 2013. *Fundamentals of Biomass Pretreatment by Fractionation*. John Wiley and Sons Ltd.
- Santos, R.B. et al. 2012. Lignin Structural Variation in Hardwood Species. *Journal of Agricultural and Food Chemistry*. **60**(19), pp.4923-4930.
- Seesuriyachan, P. et al. 2015. Improvement in efficiency of lignin degradation by Fenton reaction using synergistic catalytic action. *Ecological Engineering*. **85**, pp.283-287.
- Sigma-Aldrich. 2019. *Lignin, alkali*. [Online]. [Accessed 06/09/2019]. Available from:
https://www.sigmaaldrich.com/catalog/product/aldrich/471003?lang=en®ion=GB&cm_sp=Insite-_-prodRecCold_xviews-_-prodRecCold10-10.
- Sipponen, M.H. et al. 2018. Understanding Lignin Aggregation Processes. A Case Study: Budesonide Entrapment and Stimuli Controlled Release from Lignin Nanoparticles. *ACS Sustainable Chemistry & Engineering*. **6**(7), pp.9342-9351.
- Sluiter, J.B. et al. 2010. Compositional Analysis of Lignocellulosic Feedstocks. 1. Review and Description of Methods. *Journal of Agricultural and Food Chemistry*. **58**(16), pp.9043-9053.
- Southern, E.M. 1979. Measurement of DNA length by gel electrophoresis. *Analytical Biochemistry*. **100**(2), pp.319-323.
- Stoll V. S. et al. 1990. [4] Buffers: Principles and practice *Methods in Enzymology*. **182**(1), pp.24-38.
- Subramaniyam R. et al, . 2012. Solid state and submerged fermentation for the production of bioactive substances: a comparative study. *International Journal of Science and Nature*. **3**(3), pp.480-486.
- Sun, R.C. et al. 2000. Delignification of rye straw using hydrogen peroxide. *Industrial Crops and Products*. **12**(2), pp.71-83.
- Tanaka K. et al. 1999. Photocatalyzed degradation of lignin on TiO₂. *Journal of Molecular Catalysis A: Chemical*. **138**(2-3), pp.287-294.
- Taylor, C.R. et al. 2012. Isolation of bacterial strains able to metabolize lignin from screening of environmental samples. *Journal of Applied Microbiology*. **113**(3), pp.521-530.
- Tian, J.-H. et al. 2016. Isolation of bacterial strains able to metabolize lignin and lignin-related compounds. *Letters in Applied Microbiology*. **63**(1), pp.30-37.
- Toledano, A. et al. 2010. Lignin separation and fractionation by ultrafiltration. *Separation and Purification Technology*. **71**(1), pp.38-43.
- Tweedie J. W. et al. 2005. Quantification of DNA by agarose gel electrophoresis and analysis of the topoisomers of plasmid and M13 DNA following

- treatment with restriction endonuclease or DNA topoisomerase I. *Biochemistry and Molecular Biology Education*. **33**(1), pp.28-33.
- Valdes R H et al, . 2004. Production of L-DOPA under heterogeneous asymmetric catalysis. *Catalysis Communications*. **5**(10), pp.631-634.
- Vanholme R et al. 2010. Lignin biosynthesis and structure. *American Society of Plant Biologists*. **153**(2), pp.895-905.
- Venkatesagowda, B. 2019. Enzymatic demethylation of lignin for potential biobased polymer applications. *Fungal Biology Reviews*. **33**(3), pp.190-224.
- Walton, N.J. et al. 2003. Vanillin. *Phytochemistry*. **63**(5), pp.505-515.
- Wang H. et al, . 2013. Recent Development in Chemical Depolymerization of Lignin: A Review. *Journal of Applied Chemistry*. **2013**.
- Wang Y. et al, . 2013. A novel lignin degradation bacterial consortium for efficient pulping. *Bioresource Technology*. **139**(1), pp.113-119.
- Warren C. M. et al. 2003. Vertical agarose gel electrophoresis and electroblotting of high-molecular-weight proteins. *Electrophoresis*. **24**(11), pp.1695-1702.
- Weber, K. et al. 1972. [1] Measurement of molecular weights by electrophoresis on SDS-acrylamide gel. *Methods in Enzymology*. Academic Press, pp.3-27.
- Whetten, R. and Sederoff, R. 1995. Lignin Biosynthesis. *The Plant Cell*. **7**(7), pp.1001-1013.
- Wikberg, H. et al. 2015. Structural and Morphological Changes in Kraft Lignin during Hydrothermal Carbonization. *ACS Sustainable Chemistry & Engineering*. **3**(11), pp.2737-2745.
- Xiao, L.-P. et al. 2012. Hydrothermal carbonization of lignocellulosic biomass. *Bioresource Technology*. **118**, pp.619-623.
- Xu, Z. et al. 2019. Recent advances in lignin valorization with bacterial cultures: microorganisms, metabolic pathways, and bio-products. *Biotechnology for Biofuels*. **12**(1), p32.
- Youn, H.-D. et al. 1995. Role of laccase in lignin degradation by white-rot fungi. *FEMS Microbiology Letters*. **132**(3), pp.183-188.
- Zepp, R.G. et al. 1992. Hydroxyl radical formation in aqueous reactions (pH 3-8) of iron(II) with hydrogen peroxide: the photo-Fenton reaction. *Environmental Science & Technology*. **26**(2), pp.313-319.
- Zhang, M. et al. 2012. Pyrolysis of lignin extracted from prairie cordgrass, aspen, and Kraft lignin by Py-GC/MS and TGA/FTIR. *Journal of Analytical and Applied Pyrolysis*. **98**, pp.65-71.
- Zhong, R. and Ye, Z.-H. 2009. Transcriptional regulation of lignin biosynthesis. *Plant signaling & behavior*. **4**(11), pp.1028-1034.